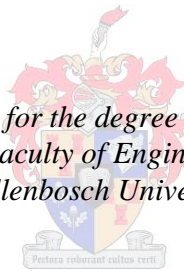


Risk based dam safety in Namibia: a quantitative approach

by
Gert Christiaan Cloete

*Dissertation presented for the degree of Doctor of Philosophy
in the Faculty of Engineering at
Stellenbosch University*



Supervisor: Prof. Gerrit Roux Basson
Co-supervisor: Prof. Johannes Verster Retief
Co-supervisor: Dr. Celeste Barnardo-Viljoen

March 2015

Declaration

I, Gert Christiaan Cloete, declare that the entire body of work contained in this dissertation is my own, original work; that I am the sole author thereof (save to the extent explicitly otherwise stated), that reproduction and publication thereof by Stellenbosch University will not infringe any third party rights and that I have not previously in its entirety or in part submitted it for obtaining any qualification.

Signature:

Date:

Copyright © 2015 Stellenbosch University of Stellenbosch

All rights reserved

Abstract

A flood event in the town of Mariental, in 2006, raised a sudden awareness regarding the state of dam safety in Namibia. Although damage was caused at the town, the flood was not extreme; it was approximately a one in fifty year event. The concern, however, was the increase in risk imposed on the town due to the temporary malfunctioning of the back-up power system: should the secondary back-up system also have failed, the embankment could have overtopped with subsequent failure; a catastrophe.

The Rational Quantitative Optimal (RQO) approach, presented in this dissertation, provides a robust risk evaluation model which produces a definitive result for the reduction of risk from the overtopping of earth-fill dams. The model is based on principles of risk, but an assessment of a portfolio of dams provides discrete optimal results, not expressed in terms of probability. All the steps that the methodology comprises have been developed exhaustively and propose to address concerns raised by dam owners and decision makers regarding risk-based dam safety: a transparent framework for decision making related to public safety, which will also appeal to the technically minded portfolio manager looking for a purely quantitative procedure to assist in the decision making process. The RQO process is applied mechanistically, not requiring judgement from the decision maker. It thus addresses the concern raised by dam owners regarding the probability of risk assessment being judgmental.

Risk in this dissertation is associated with embankment dams and concomitant external erosion, which globally is the single largest cause of failure of these dams. This specific failure mechanism, in particular, is a threat in Namibia, since other mechanisms, such as internal erosion, poses very little risk to the type of embankment dams typically found in Namibia. Therefore, for practical purposes, the extreme flood hydrology in Namibia is revisited and applied to real dams in the RQO model.

Extreme flood hydrology in Namibia has, for the past thirty years, largely been based on the South African Department of Water Affairs Technical Report 137 (TR 137) of 1988; This report proposes an empirically established upper limit of flood peaks, called the Regional Maximum Flood (RMF), which is associated with an annual recurrence interval of 10 000 years, as shown in this study from probabilistic analysis which included palaeoflood data.

The updated flood model incorporates thirty years of additional systematic data, as well as palaeoflood data that has resulted from a new approach. The new data have provided an increase in the K-value boundaries for some of the regional flood zones. A revised graphical

distribution of the K-value zones for Namibia is presented and is proposed as a replacement for the current model.

Opsomming

‘n Vloed in die dorp Mariental, in 2006, het belangstelling in damveiligheid in Namibia aangewakker. Alhoewel skade aangerig is aan die dorp, was dit nie ‘n besonderse groot vloed nie; dit was ‘n vloed met ongeveer ‘n vyftig jaar herhalingsperiode. Kommer met betrekking tot die voorval spruit uit die toename in risiko weens die bystand kragaanleg wat gefaal het toe dit nodig was. Indien die tweede bystand stelsel ook nie gewerk het nie, kon die dam se wal oorstrom het, wat tot katastrofiese faling van die dam kon gelei het.

Die Rationele Kwantitatiewe Optimale benadering (RQO) vir damveiligheid, wat verlaging in risiko teen oorstroming van grondvul damme teweegbring word hier voorgestel. Die model is gebaseer op beginsels van risiko analise, maar die resultaat vir ‘n portefeulje van damme word uitgedruk nie in waarskynlikheidssterme nie, maar in terme van ‘n diskrete optimale antwoord.

Die metode is in diepte ontwikkel en spreek onsekerhede aan waarvoor dam-eienaars en besluitnemers te staan gekom het; ‘n deursigtige besluitnemings proses wat die veiligheid van die publiek eerste stel, en wat ook aanklank sal vind by ‘n tegniese georiënteerde bestuurder wat ‘n kwantitatiewe oplossing soek vir besluitneming by ‘n portefeulje van damme.

Die RQO proses is meganisties in sy toepassing; dit verg geen oordeel van die besluitnemer nie. Sodoende spreek dit ‘n bekommernis aan wat menige dam-eienaars het oor die onpartydigheid of onbevooroordeeldheid in risiko besluitneming.

Risiko word in hierdie studie geassosiëer met grondvul damme en eksterne erosie. Eksterne erosie is op internasionale vlak die grootste enkele oorsaak van faling van grondvuldamme. Hierdie falingsmeganisme is ook die grootste risiko van faling wat in Namibia voorkom, aangesien interne erosie nie by rotsvul damme, wat tipies in Namibia gebou word, ‘n groot risiko inhou nie.

Dus, vir die praktiese toepassing van die RQO metode, word die ekstreme vloedhidrologie van Namibië ook onder oënskou geneem.

Die afgelope dertig jaar is vloedhidrologie in Namibië hoofsaaklik gebaseer op die streekmaksimum vloed metode wat deur Kovács (1988), van die destydse Suid Afrikaanse Departement van Waterwese, opgestel is vir lande in suidelike Afrika. Dit is beskryf in die tegniese verslag, die TR 137 van 1988, van die Departement van Waterwese, Suid Afrika.

TR 137 stel ‘n streeksverbonde empiries-gebaseerde boonste limiet vir vloede voor, die sogenaamde Streeks Maksimum Vloed (SMV). Hierdie studie het gevind dat die SMV vloede

tipies 'n 10 000 jaar herhalingsperiode het deur 'n waarskynlikheidsontleding te doen van die vloeirekords en palaeovloeddata.

Die opgedateerde SMV vloedmodel vir Namibie sluit in dertig jaar se addisionele aaneenlopend-gemete data, asook nuwe palaeovloed data. Die nuwe data vergroot die areas van sommige van die die K-sones, wat die streeksvloed sones voorstel. 'n Hersiene kaart met die nuwe K-sone grense daarop aangedui word deur hierdie navorsing aangebied en word voorgestel as 'n vervanging van die Kovács-SMV-kaart van Namibië van 1988.

Acknowledgements

I wish to thank Prof Basson, Prof Retief and Dr Barnardo-Viljoen, my promoters, for their guidance, assistance and support throughout the duration of this work.

I wish to thank the late Mr. Guido van Langenhove of the Namibia Department of Water Affairs and also Ms. Siglande Somses of the Namibia Meteorological Office in Windhoek for making available the flood peak data and the rain gauge data, respectively, which was used in this research. Thanks to Mr. Campbell Abrahamson of Knight Piesold, South Africa, for making available the descriptions of work and associated costs for the rehabilitation of five embankment dams in South Africa. Also thanks to staff from the Namibia Water Corporation, in particular Ms. Janine Vorster and Mr. Sabbat Hauwanga, for assisting in data processing for this research. I would also like to thank Messrs Danie van der Spuy and Pieter Rademeyer of the Flood Studies division of the South African Department of Water Affairs for their guidance and assistance regarding the probabilistic analysis of the data.

A special expression of thanks goes to Profs Enzel and Dr Grodek of the Hebrew University of Jerusalem, as well as Dr Benito of the Spanish CSIC, for the significant contribution of their time and resources to assist me in the palaeoflood study in the Fish River. They introduced me to the interesting field of palaeoflood hydrology, and how to open the stratigraphic vaults holding evidence of ancient floods, which could be used to populate remote and arid areas of Namibia, and elsewhere, with flood peak data.

Thanks to the Husselmann brothers, of the farm The Analyst, as well as Mr Mannie Goldberg of the Gondwana Collection, for permitting me to do palaeoflood studies on their properties in the upper and lower Fish River respectively.

Thanks also to the many people who supported, assisted and encouraged me along the way; Dr Shivuti, Dr Tjipangandjara, Martin Harris, Piet du Pisani, Ferdi Brinkman, Pastors Cas Becker, Leon Visser and Johan Burger; Leon Furstenburg of Knight Piésold, Fanie Becker, Andre de Klerk and, last but not least my family.

From the findings of this dissertation, a paper has been published on the revision of the Namibia Regional Maximum Flood, in the journal *Water SA*, Vol. 40 No. 3, July 2014; ISSN 0378-4738 (Print).

With some minor variations, the same paper on Namibia's extreme flood hydrology was presented at the SANCOLD Annual Conference in Johannesburg in November 2014, and, also published in the proceedings of the conference.

This dissertation has been edited by Anita van der Spuy, a member of the Professional Editors' Group.

Dedications

I dedicate this dissertation to my wife, Hannelie Cloete, and our three children, Marí-Daleen, Johan and Lené who supported me, though sometimes not of their own free will. Precious family time has been lost through the hours I have spent at my desk; however, I trust that God will restore the friendship, love and companionship that got bruised along the way; in the name of Jesus Christ.

Table of Contents

Declaration	ii
Abstract	iii
Opsomming	v
Acknowledgements	vii
Dedications.....	ix
Table of Contents	x
List of Figures	xv
List of Tables.....	xviii
List of Abbreviations/Glossary	xix
List of Symbols	xxi
Definitions.....	xxii
1 Introduction	1
1.1. Background	2
1.1.1 <i>Namibia Legislation regarding Dam Safety</i>	2
1.1.2 <i>Flood Hydrology in Namibia</i>	3
1.2. Dam Safety in General	4
1.2.1 <i>The Standards Based Approach to Dam Safety</i>	5
1.2.2 <i>Risk Based Dam Safety</i>	6
1.3. Problem Statement	7
1.4. The Method Statement	8
1.5. Brief overview of chapters	10
2 Literature Review	12
2.1. Inception.....	12
2.2. Extreme flood hydrology of Namibia.....	13
2.2.1 <i>Flood models</i>	13
2.2.2 <i>Palaeoflood hydrology</i>	15
2.2.3 <i>Upperbound evidence for palaeoflood</i>	17
2.2.4 <i>Applying palaeoflood hydrology</i>	18

2.2.5	<i>Topographic and geologic features in Namibia which affect run-off</i>	18
2.3	Dam safety in Namibia.....	19
2.3.1	<i>Legislation regarding dam safety in Namibia</i>	19
2.3.2	<i>Current practice of dam safety in Namibia</i>	20
2.4	Risk based dam safety	20
2.4.1	<i>General risk approach (Icold bulletins)</i>	22
2.4.2	<i>Consequences translating to risk</i>	23
2.4.3	<i>Current practice in risk based dam safety</i>	24
2.4.4	<i>Qualitative and quantitative risk</i>	26
2.5	The Life Quality Index and marginal life-saving costs	27
2.5.1	<i>The LQI method</i>	28
2.5.2	<i>The technology curve</i>	29
2.6	Detailed discussion of authors pertinent to the research.	30
2.7	Observations from the literature review	31
3	Data collection.....	34
3.1	Rain gauge data	35
3.1.1.	<i>Missing rainfall data</i>	36
3.1.2.	<i>The three-day maximum rainfall data</i>	36
3.2.	Systematic flow gauging data.....	39
3.2.1.	<i>The raw data</i>	39
3.2.2.	<i>Validation of the new data</i>	41
3.2.3.	<i>Data quality</i>	41
3.2.4.	<i>Verifying flood peaks as large floods</i>	42
3.2.5.	<i>Completeness of the data set</i>	44
3.3.	Palaeoflood hydrology: extending the extreme flood data base.....	44
3.3.1.	<i>Suitable topography for palaeoflood studies</i>	45
3.3.2.	<i>The palaeoflood method</i>	46
3.3.3.	<i>The hydraulic model</i>	49
3.3.4.	<i>An upper bound flood indicator</i>	49
3.3.5.	<i>Palaeoflood fieldwork</i>	50

3.3.5.1.	<i>The palaeoflood study team and the equipment</i>	50
3.3.5.2.	<i>The selected time for the fieldwork</i>	51
3.3.5.3.	<i>Identifying suitable palaeoflood sites</i>	52
3.3.5.4.	<i>Vogelkrantz site, upper Fish River</i>	52
3.3.5.5.	<i>Camp Echo site, lower Fish River</i>	57
3.3.5.6.	<i>Results of the palaeoflood study</i>	61
3.3.5.7.	<i>Confidence levels in Palaeoflood data</i>	61
3.3.6	<i>Comparing the upper bound flood peak with systematic data</i>	62
3.4.	Data on the earthfill-unit cost for embankment dam rehabilitation and raising	64
3.4.1.	<i>The earthfill-unit cost approach</i>	64
3.4.2.	<i>Determining the earthfill unit rate cost for rehabilitation of embankment dams</i>	64
4.	Updating the Namibia Regional Maximum Flood model	66
4.1.	Alternative extreme flood models	67
4.1.1.	<i>Extreme flood models</i>	67
4.1.2.	<i>Concerns regarding the extreme models</i>	68
4.2.	The study area	69
4.3.	Palaeoflood peaks.....	69
4.4.	Data sources and approach	70
4.4.1.	<i>The recorded data</i>	71
4.4.2.	<i>The natural indicators</i>	71
4.5.	The Francou-Rodier K-values	71
4.5.1.	<i>K-value results</i>	72
4.6.	Delimitation of maximum flood peak regions.....	73
4.6.1.	<i>The Uhlenhorst anomaly</i>	73
4.6.2.	<i>Delimitation of the maximum flood peak regions</i>	74
4.7.	Results of delineated hydrology regions	85
4.8.	Francou-Rodier curves and the highest recorded flood peaks in the various flood zones.....	87
4.9.	Annual recurrence interval of the RMF flood	90
4.10.	Discussion of delineated flood regions.....	93
4.11.	Observations on the new flood data	94

5.	Quantitative risk in dam safety.....	95
5.1.	Dam safety in general.....	95
5.1.1.	<i>Dam safety performance</i>	96
5.1.2.	<i>Design standards</i>	96
5.1.3.	<i>Safety standards</i>	97
5.1.4.	<i>Risk assessment in dam safety</i>	97
5.1.5.	<i>Quantifiable risk</i>	98
5.2.	Probability issues in dam safety.....	99
5.3.	Flood models.....	99
5.3.1	<i>Updating flood models</i>	100
5.3.2	<i>Design floods and safety check floods</i>	101
5.3.3	<i>Flood frequency analysis for extreme events</i>	102
5.4.	Methodology.....	103
5.4.1	<i>The structure of the Rational Quantitative Optimal approach</i>	103
5.4.1.1	<i>Assumptions</i>	104
5.4.1.2	<i>Flood hydrology: Constructing a flood frequency model</i>	105
5.4.1.3	<i>Probability of dam failure</i>	109
5.4.1.4	<i>Increasing the flood discharge capacity of the dam</i>	110
5.4.1.5	<i>The cost of life safety investments</i>	110
5.4.1.6	<i>The Loss of Life</i>	112
5.4.1.7	<i>The risk</i>	113
5.4.2	<i>The Technology Curve</i>	114
5.4.2.1	<i>Constructing the Technology Curve</i>	114
5.4.2.2	<i>The Inverted Technology Curve</i>	115
5.4.3	<i>Reducing risk over a portfolio of dams</i>	117
5.4.3.1	<i>The starting point and sequence of rehabilitation</i>	117
5.4.3.2	<i>Optimising the investment</i>	118
5.4.3.3	<i>The transition point of expenditure</i>	118
5.5	Decision making in RQO process: a hypothetical case.....	120
5.6	Observations regarding the RQO method.....	121

6.	Applying the RQO process to real dams in Namibia	123
6.1.	The selection of dams for the trial-run	123
6.2.	Constructing the inverted technology curves	124
6.2.1.	<i>The Avis Dam inverted technology curve</i>	125
6.2.2.	<i>The Hardap Dam inverted technology curve</i>	132
6.2.3.	<i>The Von Bach Dam inverted technology curve</i>	134
6.2.4.	<i>The inverted technology curves</i>	136
6.3.	Constructing the combined inverted technology curves.....	136
6.4.	The decision making process.....	138
6.5.	Reviewing the RQO model	139
7.	Findings and Analysis	139
7.1	Flood hydrology of Namibia	139
7.2	Risk based dam safety	140
8	Conclusions	142
8.1	Flood hydrology in Namibia	142
8.2	The RQO portfolio risk assessment process.....	143
9	Recommendations	145
	References	146
	Appendices	153

List of Figures

Figure 3.1: The distribution of the 180 rain gauge stations used in this study.	35
Figure 3.2: The distribution of the 3-day maximum rainfall from North to South in Namibia, as well as the average annual rainfall	37
Figure 3.3: Isolines for the annual maximum 3-day rainfall measured at rain gauging stations with record lengths exceeding 30 years	38
Figure 3.4: Distribution of recorded flood peak points, obtained from either river flow gauging stations, palaeoflood sites or indirect flood peak measurements	40
Figure 3.5: Distribution of annual flood peaks for the entire data set provided by the Namibia Department of Water Affairs	41
Figure 3.6: The bankfull width of the Kuiseb River at Us	43
Figure 3.7: Site Echo Camp-4 (EC-4) in the lower Fish River. A vertical excavation in a flood sediment bank, indicating the stratigraphy of the flood units	48
Figure 3.8: An aerial view of Vogelkranz palaeoflood site in the upper Fish River	54
Figure 3.9: Palaeoflood stratigraphy at Vogelkranz in the upper Fish River	55
Figure 3.10: An aerial view of Echo Camp palaeoflood site in the lower Fish River.	58
Figure 3.11: Palaeoflood stratigraphy at Camp Echo in the lower Fish River;	59
Figure 3.12: Various probabilistic distribution models for the 50 years of systematic data recorded at Seeheim in the Fish River	63
Figure 3.13: Various probabilistic distribution models for the 30 years of systematic data recorded at Ais-Ais weir in the Fish River	63
Figure 4.1: K-value isolines for the available floodpeak data	75
Figure 4.2: Geology of Namibia: Rock Types	76
Figure 4.3: A Google image of the Omatako River approximately 31 km upstream of its confluence with the Kavango River	77
Figure 4.4: The isolines for the 3-day maximum rainfall	78
Figure 4.5: The preliminary K-zone lines overlaid on the Namibian rivers	79

Figure 4.6: The topography of the country and some adjustments to K-zones in the north	80
Figure 4.7: The geology of Namibia	81
Figure 4.8: Revisit the river systems of Namibia	82
Figure 4.9: The K-value lines generally follow the vegetation regions of Namibia	83
Figure 4.10: The K-value lines generally follow the vegetation regions of Namibia.	84
Figure 4.11: The new RMF flood zones based on new flood peak and palaeoflood data.	86
Figure 4.12: The TR 137 RMF flood zones constructed in 1988	86
Figure 4.13: The Franco-Rodier curves for the RMF applicable to Namibia	88
Figure 4.14: The highest recorded flood peaks for Region 4.6.	98
Figure 4.15: Swakop River at Westfaler in central Namibia: P-distribution	92
Figure 4.16: Hutub River at Rietkuil in southern Namibia: P-distribution	92
Figure 4.17: Ugab River at Vingerklip in northwest Namibia: P-distribution	93
Figure 5.1: The cross-section of a typical embankment dam depicting the basic freeboard components	102
Figure 5.2: Various probabilistic models represent the annual flood peaks of the Fish River at Seeheim	106
Figure 5.3: Various probabilistic models represent annual flood peaks of the Fish River at Ais-Ais	107
Figure 5.4: The fitted functions representing the fractions of the RMF and PMF against annual recurrence interval	108
Figure 5.5: The cross-section of a typical embankment dam illustrating incremental raising of the embankment NOC	111
Figure 5.6: The typical technology curve; investment in life saving activities brings about a reduction in risk to life	114
Figure 5.7: The Invert Technology Curve (ITC) for a dam	116

Figure 5.8: Inverted Technology Curves representing polynomial functions for two hypothetical dams in a portfolio of dams	117
Figure 5.9: The combined ITC for two dams (ITC1+2); starting with the dam with the steepest initial slope (ITC1)	119
Figure 5.10: A third, smaller dam is added to the two existing dams	120
Figure 6.1: Construction work underway at the Avis Dam in central Namibia during 1931	124
Figure 6.2: The Avis Dam several years after construction in the 1930's	126
Figure 6.3: The technology curve for the Avis Dam	130
Figure 6.4: The inverted Technology Curve for the Avis Dam	131
Figure 6.5: The Hardap Dam spillway structure during the 2006 flood release	132
Figure 6.6: The inverted Technology Curve for the Hardap Dam	133
Figure 6.7: The Von Bach Dam main embankment upstream face	134
Figure 6.8: The inverted Technology Curve for the Von Bach Dam	135
Figure 6.9: The inverted technology curves for the Von Bach, Hardap, and Avis Dams	136
Figure 6.10: The combined inverted technology curves for the Hardap, Von Bach and Avis Dams	138

List of Tables

Table 3.1: Distribution of the data according to the NDWA Quality Code Index	42
Table 3.2: The Legend for the various symbols used to describe the stratigraphic layers	48
Table 3.3: The Legend for the various symbols related to the finer sediment in the description of the sequence of layers	49
Table 3.4: Summarised results for the palaeoflood study in the upper Fish River at Vogelkranz, on the farm “The Analyst”	56
Table 3.5: Summarised results for the palaeoflood study in the lower Fish River in the Gondwana Nature Reserve at Camp Echo	60
Table 3.6: The unit rate cost per cubic metre of placed soil for rehabilitation and raising of earth embankment dams.	65
Table 4.1: The RMF equations for the various K-regions in Namibia, applicable to the Transition Zone as well as the Flood Zone	89
Table 5.1: The components of incremental rehabilitation, associated cost and risk are presented	115
Table 6.1: Avis Dam AEP for various height increments above the NOC	127
Table 6.2: The Avis Dam cumulative cost table for each increment height with which the NOC is raised	128
Table 6.3: Avis Dam risk associated with the probability of failure for each increment with which the dam is raised	129
Table 6.4: Marginal Lives Saved which is the inverse of Risk	130

List of Abbreviations/Glossary

ALARP	As Low As Reasonably Practicle
AP	Annual Probability
AEP	Annual Exceedence Probability
ANCOLD	Australian National Committee on Large Dams
BP	Before present; number of years before the present, associated with OSL dating
DEFRA	Department for Environment, Food and Rural Affairs; UK
DWAF	South African former Department of Water Affairs and Forestry
DWS	South African Department of Water and Sanitation
DSO	Dam Safety Office of the DWS
FSL	Full Supply Level
GEV	Generalised Extreme Value probability distribution
GEVpwm	Generalised Extreme Value probability weighted moments distribution
ICOLD	International Commission on Large Dams
ITC	Invert technology curve
LLOL	Likely Loss of Life
LN	Log-normal probability distribution
LOL	Loss of Life
LP3	Log-Pearson type 3 probability distribution
mAMSL	metres above mean sea level
MAP	Mean annual precipitation
NOC	Non-Overspill Crest (a dam crest)
OSL	Optically stimulated luminescence
PAR	Population at Risk
PMF	Probable Maximum Flood
PMP	Probable Maximum Precipitation

QRA	Quantitative Risk Assessment
RMF	Regional Maximum Flood
SEF	Safety Evaluation Flood for dam safety in South Africa
SED	Safety Evaluation Discharge over the spillway structure of a dam
SANCOLD	South African National Committee on Large Dams
SWD	Slack water deposit
TC	Technology curve
TR 105	South African Department of Environmental Affairs Technical Report 105 of 1980
TR 137	South African Department of Water Affairs Technical Report 137 of 1988
USBR	United States Bureau of Reclamation
USCOLD	United States Committee on Large Dams
WRM	Water Resource Management

List of Symbols

A	drainage area (km^2)
c	consequence in terms of lives lost
ft	foot
g	gravitational acceleration
K	regional coefficient expressing relative flood peak magnitude
m	metres
N	number of fatalities
n	number of events (leading to dam failure)
p	probability of an event occurring
P	wetted perimeter of the bankfull river channel in feet
Q_b	bankfull discharge in cusec (ft^3/s)
Q	discharge rate (m^3/s)
s	second
S_o	bed slope of an open channel stream/river
S_f	friction slope of a stream/river
v	velocity in metres per second

Definitions

Definitions relevant to this research are discussed below:

- i. Abandoned gravel bar: a gravel bar in a river which has been abandoned by the river; the river has incised next to the gravel bar to such a depth that the upper bound floods do not flow over it.
- ii. Aeolian deposits: wind driven sediment deposits
- iii. Alluvial deposits: water driven sediment deposits
- iv. Bioturbid: the stratigraphy of sediment layers so disturbed by burrowing animals and plant roots that they are no longer easily distinguishable.
- v. Colluvium: This term is also used to refer specifically to sediment deposited at the base of a hill-slope by non-concentrated surface runoff, usually mechanically eroded rock.
- vi. Dam raising: increasing the elevation of the non-overspill crest so that either the freeboard is increased or the dam storage capacity is increased.
- vii. Desert Varnish: Dark lustrous coating, mainly of silica coloured by manganese or iron oxide, which forms on desert rocks over millennia.
- viii. Freeboard: The distance between the full supply level and the non-overspill crest of a dam, which is required to accommodate the flood surge, wave action and wind-setup.
- ix. Frequentist approach: The measure of likelihood expressed as the number of occurrences of an event in a given number of trials.
- x. Gravel bar: a large deposit of gravel (100 to 500 mm diameter boulders) found in the slack water area of a river channel. It could be active or abandoned. It looks like a river terrace and vice versa.
- xi. K-value: a regional coefficient expressing flood peak magnitude
- xii. Marginal life saving cost: the investments necessary for a small increase in life safety.
- xiii. Old surface: relating to Palaeofloods, this refers to a gravel bar or similar exposed surface next to a river which has not been flooded in thousands of years.
- xiv. Pediment: gradual slopes over large areas covered with weathered material
- xv. Reach: a reach in the context of flow modelling in rivers refers to a portion of the length of a river, which could be several hundred to several thousand metres long, which is modelled for discharge elevation and flow conditions in the river channel.

- xvi. Ripple marks: wavelet deposit of sand usually indicating the flow direction of the water during deposition.
- xvii. Sandveld: wide expanses of dry sandy soil.
- xviii. Terrace: bedrock which was once the river basin, covered in alluvium, but inactive (old surface).

1 Introduction

Dams have been and still are being built for various purposes and in many cases for multiple purposes. These include, among others, water supply for domestic and industrial use, generation of hydropower, irrigation purposes, for flood protection, or for the improvement of river navigation (SU, 2009:4). The first dam of which any record exists was built around 4000 BC in Egypt (SU, 2002:1).

Dams are not constructed to be indestructible; therefore all dams carry a risk of failure, and decision making regarding dam safety inherently takes place under conditions of uncertainty (Kreuzer, 2000:769). This risk is mitigated by applying best practice design standards during the design and construction of the dam, and also by monitoring and maintaining the dam to extend its life and keep the risk of failure as low as practically possible.

Dam safety in Namibia, as in other countries, needs to be constantly reviewed, since flood models are updated and risk conditions change over time. To reduce the risk to existing dams, particularly for a portfolio of dams, the efficient distribution of limited resources could be achieved by considering the risk to each dam, and not merely limiting this to design standards.

This research investigates the risk of failure of embankment dams due to external erosion based on floods which would overtop the non-overspill crest of a dam. Assuming that the embankment dam will fail if overtopped, the size and recurrence interval of these floods are determinable, hence the probability of failure is known.

Large embankment dams in Namibia are more susceptible to external than internal erosion. Construction material in an arid country like Namibia, is usually coarse and without cohesion, a product of the mechanical erosion processes of the landscape. Typically, embankment dams constructed with this kind of material are concrete-faced rockfill dams (CFRD), which characteristically have a resistance against internal erosion. This research therefore focusses on extreme flood events which could lead to external erosion, dam failure and subsequent loss of life.

The research culminates in an innovative quantitative approach to risk analysis for existing dams, the Rational Quantitative Optimal (RQO) approach, which evaluates risk, prioritises rehabilitation and optimises expenditure over a portfolio of dams in a transparent way. It achieves the objective of using the ‘worst first’ management approach, i.e. to start maintenance work on the dam that is at highest risk first, and also to apply the ‘greatest risk

reduction' over the whole portfolio of dams, in the shortest period of time and within the funds available, an objective proposed by Charlwood *et al.* (2007:27), Bowles (2013:48), ICOLD (2005:181) and Snorteland (2013:5).

1.1. Background

The flooding of the town of Mariental in the year 2006 focused attention on the topic of dam safety in Namibia, and more specifically on the Hardap Dam which lies in the Fish River approximately 20 km upstream of the town Mariental. Mostert (2007) indicated that during the flood the power supply to the dam was cut off, the back-up power generator failed to start, and the secondary back-up source had to be employed to open the flood gates for the incoming flood to pass through. Fortunately no lives were lost during the Mariental flood, but significant damage to infrastructure and private property occurred. The flood damage was caused by development encroachment on the flood plains alongside the river, and was not caused by, nor associated with the dam or any delay in the opening of the flood gates. In fact, the incoming flood was estimated as being approximately a one in fifty year flood, and the dam attenuated the flood peak fractionally, hence reducing flood damage. The point of concern here is the risk of failure due to overtopping had the flood gates not been opened. The one in fifty year flood could have caused significantly more damage had the dam overtopped its non-overspill crest.

A state owned enterprise called the Namibia Water Corporation (NamWater), owns and operates the large water supply dams in Namibia, including the Hardap Dam. The company was established in 1998 to supply water in bulk to cities, towns and settlements within Namibia. Sixty percent of all bulk water supplied in Namibia comes from large storage dams (Cullis, 2006:1). Until the occurrence of the Mariental flood, none of the dams in NamWater's control had received a formal "First dam safety evaluation", although periodic maintenance inspections were performed.

However since the Mariental flood event, dam safety in general has been addressed by NamWater and several large dams have received their first dam safety evaluations. The flood attenuation capacity of the Hardap Dam has also been increased, by reducing its operational full supply capacity.

1.1.1 *Namibia Legislation regarding Dam Safety*

As custodian of the majority of the large dams in Namibia, NamWater has a social responsibility toward the people of Namibia: NamWater needs to manage these water

resources in a sustainable way in a country where water is scarce, and NamWater has a social responsibility to limit the risk to the public through the operation and management of its dams (Cullis, 2006:1). Guidance in this regard comes from legislation.

The Namibian Water Resources Management Act No 24 of 2004, section 79(1), requires that the owner of a dam(s), shall upon request of the Minister, make available information on the dam and/or appoint a professional engineer to evaluate the safety of a dam, and if it is found to be a dam with a safety risk, the Minister may, by notice in the Gazette, categorise dams to be dams with a safety risk, or declare a dam to be a dam with a safety risk (WRM Act 24 of 2004:41).

Therefore until such a request has been submitted, the owner of a dam is not obligated to comply with the requirements of the WRM Act regarding dam safety. According to Clause 81(1) of the Act (2004:42), the Minister must keep a register of dams with a safety risk. However, in discussion, Van Langenhove (2008) mentioned that such a register did not exist at the time (in 2008).

The new Namibian WRM Act, Act 11 of 2013 still does not provide risk classification such as height of the dam, or storage capacity, but in Clause 94 it states that risk categories will be gazetted.

This approach to the law does not bind the owner of a dam by fixed safety standards, but it does allow the Minister to follow the latest international developments in dam safety and hence gazette the best practice regarding dam safety as it develops. Currently dam safety practitioners still embrace the tried and tested Standards-Based Approach (SBA) but, due to economic considerations, the practice is leaning toward a risk based approach; aiming to address risk issues as priority opposed to compliance with a rigid standard.

1.1.2. Flood Hydrology in Namibia

Dam failures due to overtopping of the Non-Overspill Crest (NOC) is the single largest cause of embankment dams failing internationally (ICOLD, 1995:22). Even more so in Namibia, where the larger embankment dams are constructed in a way which gives them an inherent resistance against internal erosion; the second highest cause of dam failure, according to ICOLD.

Overtopping of the embankment is usually due to insufficient spillway capacity; a product of the short hydrological records available and flood models at the time of design. This is a global problem, especially with the older dams which were built early in the 20th century, or

even earlier. As new flood data becomes available, current flood models are updated to incorporate the newer information, and in many cases the probability of the previous extreme floods increase.

One method of obtaining more data is by constructing more river gauging stations and over time collecting more data on discharge and annual flood peaks. It may, however, take several decades of data capturing before any significant flood peaks are measured. An alternative, which is especially well suited for a semi-arid country like Namibia, is palaeoflood studies.

Palaeoflood studies utilise stratified sediment deposits in sheltered areas within an active river channel. These quartz or feldspar grains of sand, within the strata, are sampled and by means of a dating process the time of deposition, in number of years before the present, is determined.

Also, in the arid regions of Namibia, geomorphological evidence such as desert varnish, a dark lustrous layer which forms on rock, provides a clear indicator of the upper bounds of floods in selected rivers. Due to the slow accretion rate of desert varnish, this indicator provides the maximum level of discharge over several thousand years.

Together with extended systematic flood recording, additional river gauging stations and the palaeoflood studies, the flood model of Namibia is reviewed in this dissertation and updated to provide a new model.

1.2. Dam Safety in General

Dam safety is not an absolute condition, but it is a tolerated situation, with low levels of residual risk ever present (ICOLD, 2005:17; Charlwood *et al.*, 2007:36). The practice of dam safety aims at reducing the risk of failure of new and existing dams to acceptable levels; as discussed in the International Commission on Large Dams (ICOLD) Bulletin 99 (ICOLD, 1995:13), dam failure means the ‘Collapse or movement of a part of the dam or its foundation, so that the dam cannot retain water. In general a failure results in the release of large quantities of water, imposing risks on the people or property downstream’ (ICOLD, 1995:13).

By the year 2000 there were approximately 40,000 risk bearing dams in the world, of which at least 20,000 were older than 50 years (Sims, 2009:127). According to Sims many of these older dams were built under difficult circumstances with inadequate resources. ICOLD Bulletin 99 (ICOLD, 1995:17) states that 2.2% of dams constructed before 1950 had failed,

while the number of failures for dams constructed after 1950 had been reduced to below 0.5%.

ICOLD (2010:13) also mentions that, since 1950, the annual worldwide investments in dams have been in the range of USD 30 or 40 billion (2008 value) and presently the investment total is about USD 2,000 billion. A loss of 0.5% in an annual investment of USD 40 billion is a significant loss in infrastructure, not even considering the loss in lives, the environmental impact and the economic losses.

According to ICOLD (1995:22) the failure of embankment dams contributes to 80% of all dam failures. The most common cause of failure of embankment dams is overtopping of the non-overspill crest, which leads to subsequent external erosion and failure. ICOLD provides the figure for overtopping as the primary cause of failure at 31%.

For various historical reasons and some technical reasons, the safety of dams has been controlled by an engineering Standards-based Approach. This research, however, investigates an approach to dam safety which addresses risk quantitatively and, within budget constraints, optimally reduces risk over a portfolio of dams without employing design standards.

1.2.1 The Standards Based Approach to Dam Safety

Accidents in industry have always been a spur to human progress (ICOLD, 1995:9); so also in dam safety. Due to failures, design guidelines are improved and enforced by regulators to ensure that risk to the public, as well as other risks are reduced.

Over time, as these guidelines evolved, best practice standards were developed for the design of new dams, incorporating specialist input from various countries. This design approach became known as the Standards-based Approach (SBA) to dam design; ‘the traditional approach to dams engineering, in which risks are controlled by following established rules as to design events and loads, structural capacity, safety coefficients and defensive design measures.’ (ANCOLD, 2003b:15) (ICOLD, 2005:17).

The Standards-based Approach to mitigating risk has served dam safety well, reducing the rate of dam failures from 2.2% in the early part of the 20th century to less than 0.5% in the second half (ICOLD, 1995:17). The SBA, however, does not differentiate between high and low risk, either the dam complies with the standard or it does not.

Therefore, the SBA is impracticable if the cost of achieving the standard is grossly disproportionate to the improvement gained. A risk-based approach is required which will

optimise the ratio of expenditure vs improvement gained (or risk reduced), so that more dams within a portfolio can benefit from a limited budget.

1.2.2 Risk Based Dam Safety

Risk based dam safety is a wide-ranging topic within the domain of dams. Human error associated with the operation and maintenance of a dam induces risk, so do natural events such as earthquakes or extreme floods. Sometimes a complex linking of circumstances or errors, natural and human, can lead to a dam failure, as expressed by Equation 1.1.

For example, the 2006 flood event at Mariental, routed through the Hardap Dam, was a rather insignificant flood with an annual recurrence interval of 50 years. The primary power supply, which is required to open the dam flood gates, failed, and then the first back-up power supply also failed. Had the second back-up power source also failed, the dam could have overtopped its embankment and failed with significant consequences: a combination of natural events and human error.

In engineering, risk is usually defined as the product of probability and consequence (Hartford & Baecher, 2004:252). Bedford and Cooke (2001:10) state that risk analysis requires knowledge of three things; (1) what can happen, (2) how likely it is to happen, and (3) what the consequences are should it happen. The 'what' question could be a combination or set of scenarios, each with their own probability and consequence. When more than one event may lead to an adverse outcome, the definition of risk is extended to be the expected value of the consequence over the set of events (Hartford & Baecher, 2004:252):

$$Risk = \sum p_i.c_i \quad \text{for } i = 1, n \quad (1.1)$$

where p_i is the probability of event i

c_i is the consequence of event i

n is the number of events leading to dam failure

In this dissertation, the 'what' event is failure of an embankment dam due to external erosion. This occurs when the flood discharge exceeds the capacity of the spillway and water starts flowing over the non-overspill crest. The consequence in this case is related to loss of life if the dam fails. Such a flood is a singular event with a determinate probability which is amenable to risk calculation as indicated in Equation (1.2).

$$Risk = p.c \quad (1.2)$$

where $Risk =$ the product of probability and consequence, or expected consequence

$p =$ the annual probability of the flood that overtops the embankment

$c =$ the consequence in terms of lives lost if the dam were to fail during overtopping

Current practice permits an individual dam owner the choice of managing commercial risk on the basis of engineering judgment and experience. This process should, however, be as objective as possible, although there will always be subjectivity present. In general, those responsible for making decisions concerning risk will decide on the extent to which they will be fair and equitable, transparent, comprehensive, and it will vary from owner to owner and within the owners portfolio of risks to be managed (Hartford & Baecher, 2004:23). Removing risk at all cost is not practicable. DEFRA (2002:44) therefore proposes that risk be reduced to As Low As Reasonably Possible (ALARP).

Risk based dam safety is gaining popularity, specifically where a portfolio of dams requires the owner to prioritise rehabilitation activities. In these cases, however, the standards based approach is still used as a guide for the extent of the rehabilitation required at each dam (ICOLD, 2005:181).

In the standards based approach, risks are controlled by following established rules related to design events and loads (ANCOLD, 2003b:15). The SBA requires rehabilitation up to the set standard for each dam in a portfolio, irrespective of the gain in risk-reduction. In such a case full rehabilitation over the portfolio could exhaust a limited budget within the first dam or two. An optimal risk based approach, which is proposed here, on the other hand utilizes the budget and based on the result of the risk model, spreads the resources over several dams. This will produce a greater gain in lives saved than by following the standards based approach.

1.3. Problem Statement

The flood incident in the town of Mariental, discussed above, raised concern regarding dam safety in Namibia and it focused attention on flood events and risk associated with dam safety. The problem faced in general by dam owners is that the current Standards Based Approach (SBA) to dam safety is a blunt instrument which does not evaluate risk, but only indicates whether a dam complies with preset standards; a 'yes' or 'no' tick box. Irrespective

of whether an investment is disproportionate to the reduction in risk, the SBA requires that all standards be met.

For dam owners in Namibia, with a portfolio of large dams, guidance in the allocation of scarce resources over the portfolio will not come from the SBA. A risk based approach is required which optimises the investment with regard to the reduction of risk. To address this, a quantitative risk model, which prioritises investments within a portfolio of dams and optimises the budget with regard to a reduction in risk, needs to be developed to suit Namibian conditions. Under public scrutiny, this model will have to be quantitative and transparent, and not be based on judgmental inputs.

A critical input to the quantitative risk model is the probability of extreme floods in Namibia. Van Langenhove (2006) mentioned that the current Namibian flood model was compiled in the 1980s with limited data, and its reliability today is questioned. The quantitative risk model is based on the probability of extreme flood events, hence the flood model will directly impact the outcome of the risk model. The flood model needs to be reviewed and updated to include the latest systematic flood data, as well as palaeo flood data, which brings new depth to hydrological flood records.

This dissertation will deliver an updated and more reliable extreme flood model, and a risk based model which will quantitatively evaluate the risk, while the analysis of a portfolio of dams will provide discrete optimal results, and not be expressed in terms of probability. This approach can be used by dam owners with a portfolio of dams in Namibia, and elsewhere.

1.4. The Method Statement

This dissertation takes a limited risk approach by expressing extreme flood magnitude probabilistically, and consequence and cost deterministically. Extreme flood events are the critical driver of the probability of dam failure, failure with subsequent consequences due to overtopping of the non-overspill crest of the dam.

The general approach followed is to take the magnitude of the flood that would cause overtopping to represent the probability of the critical event, whilst the consequences, consisting of failure of the wall and subsequent lives lost, could be treated deterministically, in the conventional manner. In this way the risk can be expressed without the need for judgment and, because the assumptions made will be clearly defined, resulting in transparency.

Since the probability of extreme floods is based on the flood hydrology model, these models need to be updated as significant contributions to data are made. This comes from additional recorded flow data, and also by investigating the use of palaeoflood hydrology for determining those events with high return periods, which are expected to dominate the risk of overtopping.

The flood peak data required for the flood model is determined from available systematic data records collected and kept by the Department of Water Affairs. Other sources of distinct flood peaks are the records of ancient flood events kept in the Namibia National Archives, as well as the flood peak evidence locked up in the stratigraphic sequences of sedimentary layers along river banks. Palaeoflood techniques and fieldwork are required to unlock this information and produce ancient flood peak data and upper bound flood peaks.

Procedures are devised to make a reasonable, but simplified, estimate of the consequences of overtopping of the embankment, in accordance with standard procedures. This would require first, an evaluation of embankment failure due to external erosion. Secondly, the procedure of estimating life safety as the result of dam failure would need to be considered.

Remediation would comprise modifying the spillway capacity to reduce the probability of overtopping. A procedure needs to be devised to estimate the cost of such remedial work. A short outline will be provided of a process consisting of deriving the unit costs of earthworks, according to which cost estimates could be made for increasing the NOC level of an embankment.

A procedure is devised to relate the expenditure on increasing the spillway capacity to the change in expected lives lost due to the reduced probability of the flood magnitude causing overtopping, based on the revised flood hydrology model.

This procedure is then extended to compare and combine the characteristics in terms of expenditure and marginal life safety, in order to be able to make decisions on prioritisation of remedial work, including the option of switching at an optimal stage to the rehabilitation of another dam.

The procedure is investigated further and demonstrated by applying it to a selection of three dams in Namibia.

The degree to which the initial objectives of the investigation could be achieved, the utility, merit and limitations of the method is finally considered; with consideration of ways in which it could be improved by additional research.

1.5. Brief overview of chapters

Chapter 1 provides a brief background to the development and practice of dam safety in Namibia and internationally. It discusses the current legislation in Namibia which relates to dam safety, and also extreme flood hydrology, which is one of the main risk components threatening the safety of dams. It presents a problem faced by dam owners, how to optimize investment over a portfolio of dams.

Chapter 2 presents an overview of the relevant literature related to dam safety, extreme flood hydrology and risk based dam safety.

Chapter 3 discusses the processes of data collection, and the validation thereof, to update the extreme flood model of Namibia. The data required is that of the latest systematic flood peaks, the latest rainfall data, fieldwork investigations of palaeoflood data on recent and ancient floods, and also the rehabilitation cost, in order to determine a unit rate for the construction cost of raising the non-overspill crest of an embankment dam.

In Chapter 4 the extreme flood hydrology models which are currently used in Namibia are discussed and the Regional Maximum Flood (RMF) model is updated with the latest data. This updated flood model provides probability input to the risk model presented in this study.

Chapter 5 explores risk based dam safety and the challenges and reservations that dam engineers have over this approach. Taking into account the updated flood hydrology of Namibia and rehabilitation costs, technology curves area developed for a portfolio of dams which assists the decision maker in applying and optimizing resources for life-safety. This chapter presents a novel approach to risk based dam safety; the Rational Quantitative Optimal approach, which addresses risk within a portfolio of dams in a transparent way, and which reduces risk optimally over the portfolio.

Chapter 6 applies the RQO process to three dams in Namibia; presenting a case study to quantify portfolio risk over the three dams and assist the decision maker in reducing the risk, optimally.

Chapter 7 discusses the findings of the dissertation; extreme flood models and the benefits of applying palaeoflood data. It also discusses the development of the RQO process and its application in real life situations.

Chapter 8 presents conclusions of the dissertation regarding palaeoflood studies and its contribution to extreme flood models in Namibia, and elsewhere, also regarding the RQO process and its applicability as a quantitative risk based tool to rank and optimally reduce risk over a portfolio of dams given budget constraints.

Chapter 9 proposes recommendations regarding the use of palaeoflood hydrology, further developments in the extreme flood model for Namibia and on the RQO process, as well as future research opportunities in decision making related to the RQO process.

2 Literature Review

This chapter discusses the literature reviewed for the various phases of this research, from the inception to the flood hydrology in Namibia and lastly the aim of this research, risk based dam safety. The chapter concludes with an overview of the literature pertinent to the problem statement.

2.1. Inception

Discussions with Van Langenhove (2006) after the 2006 Mariental flood had exposed a gap in the field of dam safety in Namibia; which had proved to be the reliability of the Namibia flood model. Hattingh's (2007:11) safety evaluation report indicated that the discharge capacity of the Hardap Dam spillway underestimates the Safety Evaluation Flood (SEF) by approximately 30%. Notably, design standards have evolved since the late 1950's when the dam was designed, and limited data on systems or flood peaks may have been available during the design phase, hence an underestimation of the design flood could easily have occurred.

Reviewing the legislation regarding dams at risk, it became evident that owners of dams in Namibia were not, by law, obliged to perform dam safety evaluations on their dams unless instructed to do so by the Minister. Clause number 79 of the Water Resources Management Act (2004), Act No. 24 of 2004, states that the owner of a dam shall, upon request from the Minister, provide the Minister with information on the dam, and also provide access to any person appointed by the Minister to determine whether the dam is a dam with a safety risk.

Therefore the risk of dam failure, with flood hydrology as a major risk component, presented an opportunity to research and propose a risk model for Namibia, which would include updating of the current flood model for Namibia.

Since floods have a major influence on the risk of dams, as demonstrated by the Mariental Flood incident in 2006, a risk model for dams in Namibia would also require a revision of extreme flood hydrology. Based on the latest research and methods available, such as palaeoflood data, and the latest systematic data, a flood model can be updated which would be current and applicable and used to assess the flood risk imposed on dams in Namibia.

The literature review looks at the current flood hydrology model of Namibia, other models and the latest methods that could be employed to update or improve on the model. It also looks at the standards based as well as risk based dam safety practices applied in southern Africa and abroad.

2.2. Extreme flood hydrology of Namibia

The Mariental flood event raised public awareness of the threat and exposure to risk. Questions about public safety, early warning of flood release from the dam and flood mitigation were raised by those affected. The safety of the dam and the risk it held were of utmost concern to the public and of the dam owners.

The flood model used by Hattingh to determine the size of the expected design discharge in 2007 was developed by Kovács in the 1980s (1988:16). Van Langenhove (2006) suggested that with nearly 30 years of additional systematic flow data in Namibia, the current flood model needed to be updated.

Sims (2009:127) proposed that new hydrological studies might suggest an increase in spillway capacity. This is confirmed by the dam safety investigation of Hardap Dam near Mariental (Hattingh, 2007:5), where the original design floods were approximately 30% lower than the present day recommended floods. A similar exercise in Spain, where the hydrology model was updated for the Valdeinferno Reservoir in the Gaudalentin River, it was found that the spillway capacity significantly underestimated the required design discharge of the spillway, in fact by approximately 76% (the spillway capacity of 550 m³/s is significantly less than the recommended design flood of 2 350 m³/s) (Benito, 2006:2113).

2.2.1 Flood models

Three basic methods are available for the estimation of maximum flood peaks: empirical, probabilistic and deterministic methods.

- In the empirical approach, maximum flood peaks observed in a hydrologically homogeneous region are plotted against catchment area and an envelope curve is drawn for the points. This curve is then considered as the upper limit of expected flood peaks; Q_{\max} (Kovács, 1988:1). The popularity of this method dwindled from the 1930s to the 1960s with the development of probabilistic and deterministic methods. However, in 1967 the empirical approach was revived by Francou and Rodier (Kovács, 1988:3) with their regional maximum flood (RMF) peak envelope curves. A common shortcoming of the empirical approach is the uncertainty of the boundaries of the homogeneous regions. Kovács proposed that the return period for the RMF should not be 10 000 years because of the erratic character of the flood peaks. However, van der Spuy (2009) mentioned that, after analysing 30 to 40 years of additional data, that the annual recurrence interval of the RMF flood peak generally exceeds 10 000 years.

- Probabilistic models are based on extrapolation, which estimates a 100 or a 10 000 year flood based on 20 years of data, which begs the question of the form of the tail of this distribution (Hartford & Beacher, 2004:324). The probabilistic method predicts flood peaks based on the extrapolation of a theoretical probability distribution, fitted to annual maximum flood peak records in the same river or region. The maximum peak is associated with a very low probability, most often $P = 0.0001$ i.e. an annual recurrence interval of 10 000 years, which is entirely arbitrary (Kovács, 1988:2). The representativeness of a relatively short data sample period is unknown, therefore distribution periods longer than two to three times the sample length cannot be justified without supporting evidence, such as palaeoflood data (Kovács, 1988:2).
- The deterministic method predicts a hydrograph and an associated flood peak based on storm rainfall input and estimated storm losses. For extreme flood peaks, the presumption is that the Probable Maximum Precipitation (PMP) is falling on a saturated catchment area, and this produces the Probable Maximum Flood (PMF) (Kovács, 1988:3). By definition the PMF has no annual recurrence interval, but arbitrarily it was assigned a return period of 10 000 to 1 000 000 years at the upper and lower confidence limits for flood frequency analysis (National Research Council, 1985:241; Brown & Gosden, 2004:30). Yevjevich (1987:1) questions the possibility of attaching a probability value to the PMF.

From palaeoflood data obtained at various rivers in the USA, Benito (2006:2119) extrapolated the discharge rates for 10 000 flood events in these rivers. He found these discharge rates to be between 5% and 20% of the calculated PMF value. This finding supports a comment by Enzel *et al.* (1993:2294) that the inconsistency between PMF estimates and the actual regional data (gauged, historic, and palaeofloods) is a cause for concern; ‘It may indicate, for this hydrological region, either that the understanding of extreme rainfall events used in constructing the PMP and the subsequent basin responses is deficient, or failure in the model construction’.

Kovács (1981:3) states that a great number of assumptions are employed in the PMF method, which can lead to a serious cumulative error, providing flood estimates which are generally too high. This overestimation is also questioned by some committee members of the National Research Council (NRC, 1985:7) in the USA, who inferred that it leads to the extravagant use of resources. However, they also recognised that, in the USA, an adequate substitute design basis was not available at that time.

2.2.2 Palaeoflood hydrology

Yevjevich and Harmancioglu (1987:2) said that the reliability of the flood model cannot be better than the level of information available on flood characteristics. In that regard, Kovács (1988:2) also mentions that the representativeness of short-period sample data is unknown. Therefore supporting evidence is required to extrapolate the probability for longer than two or three times the length of the record.

According to Tasker and Stedinger (1987:256) one of the best future research opportunities in flood-frequency analysis is the incorporation of palaeoflood data in regionalised flood frequency analysis; providing useful flood information for the pre-gauged period and, in so doing, supplementing the systematic gauge record at a site (Benito, 2006:2115; Kovács, 1988:2). This statement supports the remark by Klemes (1993:168) that if more light is to be shed on the probabilities of hydrological extremes, then it will have to come from more information on the physics of the phenomena involved, not from the mathematics.

Benito (2006:2117) states that the value of palaeoflood data is the potential to include physical evidence of large floods, or limits on flood magnitude, over long time periods. The basic hypothesis in the statistical modelling of palaeoflood information is that a certain threshold of water level exists and that, over a specified time interval (from one year to thousands of years), all exceedances of this level have been recorded in the form of geological palaeoflood evidence left along the river channels, such as sediment deposits. A stationary long term incidence of floods is also assumed.

It is not the time scale of flooding that defines palaeoflood hydrology, but the fact that flood evidence derives from the lasting effects of floods on natural recording indicators (palaeostage indicators) (Benito *et al.*, 2004:15). Hence palaeoflood hydrology is a reconstruction of the magnitude and frequency of recent, past, and ancient floods (approximately 50, 500 and 5 000 years ago, respectively) using geological evidence (Baker *et al.*, 2002:1; Benito *et al.*, 2004:15).

Boshoff *et al.* (1993:25) refer to it simply as the study of floods that occurred before there were historical or direct (systematic) hydrologic measurements.

Critics of palaeoflood hydrology discredit it due to the indirect approach of determining the flood peak of floods which occurred long ago. Enzel (2009) mentioned that even in this modern age extreme floods may damage or wash away stage recorder instruments, and in these cases the indirect approach is also used by hydrologists to determine the flood peak. There is no difference in the indirect approach as applied to a modern day flood or applied to

a flood which occurred several hundred years ago; the stage indicator must simply be clearly defined.

According to Baker (2008:7) early work in palaeoflood hydrology relied almost exclusively on conventional radiocarbon dating for its geochronology. Since the 1980s, however, spectacular advances have been made in geochronological techniques for precisely determining the ages of ancient palaeofloods. Most important has been the optically stimulated luminescence (OSL) technique, which is used to date sedimentary deposits, deposited in stratigraphic sequences (Benito *et al.*, 2004:21).

Since it acquired its formal name in 1992, the most productive approach in palaeoflood hydrology has become energy-based inverse hydraulic modelling of discrete palaeoflood events, recorded in appropriate settings as sedimentary deposits and other palaeo stage indicators (Baker, 2008:1).

In hyperarid regions flood evidence is well preserved in the form of sediment deposits. These sediment deposits, also known as slack-water flood deposits, are stage indicators of floods and can be preserved in stratigraphic sequences (Benito *et al.*, 2003a:110). These sedimentary deposits commonly collect in environments such as (i) areas of channel widening, (ii) severe channel bends, (iii) the hydraulic shadow of obstacles where flow separation causes eddies, (iv) alcoves and caves in bedrock walls, (v) back-flooded tributary mouths and valleys, and (vi) on top of high alluvial or bedrock surfaces that flank the channel (Kochel and Baker, 1982:355; Baker and Kochel, 1988:126; Benito *et al.*, 2003b:170).

Benito & O'Connor (2013:469), and Fernandez *et al.* (2010:1129) noted that historical and palaeohydrologic information on floods is usually of the censored type, being either upper bounded (UB), or lower bounded (LB), or double-bounded (DB), as corresponds to the limiting water levels (or discharges) associated with the individual floods that occurred in a given time period. In any situation, the exact value of the water level (or the exact value of the maximum discharge) reached during a particular flood is unknown.

Benito *et al.* had addressed this in 2004 in their discussion on two principal sources of error in palaeohydrology: (a) an underestimation of the palaeodischarge due to the level of the flood waters above the deposited sediments being unknown and (b) changes in the valley cross section. The first can be approached by the study of sedimentology of the flood deposits, which has shown that the top of the deposit is very close to the flood stage. The second can be dealt with by conducting the palaeoflood study in a bedrock channel which is significantly more stable than alluvial floodplain channels, for example, and will not have been

substantially altered over the past centuries or even millennia; as incision of a river into the bedrock is very slow and occurs over geological time (Enzel, 2009; Benito *et al.*, 2004:23).

2.2.3 *Upperbound evidence for palaeoflood*

According to Benito & O'Conner (2013:469) it is known that no floods exceeded a certain discharge over a specific time period. Surfaces or features known not to have been flooded are referred to as an upper bound. Some of these include gravel and boulder bars, silt lines, and erosion features.

Another upper bound indicator is called desert varnish. Desert or rock varnish dating provides an age for the last erosion or deposit of a rock surface (Dorn, 1989:561). If the underlying rock or the varnish has experienced mechanical (flooding) or biochemical erosion, the varnish clock would reset, and any CR (cation ratio) obtained would reflect the time of last erosion and hence the time when the rock was last disturbed by flooding, for example.

Rock varnish is slow accreting (1–40 micron/ky) Mn- and Fe rich dark coating on subaerially exposed rock surfaces in drylands. Because of its sedimentary origin, varnish often contains a layered microstratigraphy that records past climatic changes (Lui, 2013:39). Hooke, in 1969, analysed varnish through an electron microscope, revealing layering within varnish and defining the relative quantities of elements at various depths within the varnish film (Dorn & Oberlander, 1982:317). Therefore varnish research is, in fact, a stratigraphic problem on the micron scale (Dorn & Oberlander, 1982:360).

Rock varnish is usually 10 to 30 microns thick, but depths ranging from two to over 500 microns have been observed. The constituents of all rock varnishes are derived from sources external to the underlying rock (Dorn & Oberlander, 1982:317).

According to Dorn & Oberlander (1982:324) varnish formation under dry (alkaline) altithermal conditions is by deposition of mostly airborne ambient material, suggesting that 3 000 to 5 000 years is required to produce a discernable varnish and much longer to form a solid coat.

In a similar vein, Lui suggests that varnish is a slow accreting (1–40 micron/ky) Mn- and Fe rich dark coating on subaerially exposed rock surfaces in drylands. According to his writing, Varnish Microlamination (VML) has been calibrated and climatically correlated to date surficial geomorphic and geoarchaeological features of the Holocene (0–12 ka), and millennial-scale to late glacial time (12–18 ka), and dating potentially to the late Quaternary (85–300 ka) (Lui, 2013:39).

Any age estimate for the varnish is only a minimum-limiting date for the exposure of that rock surface (Dorn,1989:562).

2.2.4 *Applying palaeoflood hydrology*

Understanding the magnitude and frequency of extreme floods is critical for the design of hydraulic structures such as dams (Benito *et al.*, 2006:2113). England (2003:1) proposes using peak discharge frequency curves that include palaeoflood data as a basis to develop probabilistic extreme flood hydrographs.

Fernandez *et al.* (2010:1129) indicated that there is frequently a situation of complete absence of systematic information on extreme floods, hence it seems more pragmatic not to dismiss and ignore palaeoflood data, but instead at least to see what these data have to tell the investigator about extreme flood phenomena. Grodek (2013:3) confirms that where flood records do exist in hyperarid desert regions, the data is either partial or limited. Also usually missing from such records are crucial data on large floods, since the monitoring instruments are usually destroyed by them.

England (2003:1) proposed that extreme flood hydrographs, using palaeoflood data, are needed to evaluate dam safety issues for situations where the reservoir inflow peak discharge is greater than the maximum spillway capacity. Such a case is discussed by Benito *et al.* (2006:2113) with reference to the Valdeinfierno Dam in south eastern Spain; the design capacity of the dam spillway was of 550 m³/s. Then, after combining palaeoflood data with the gauge station records, a new design discharge of 2350 m³/s was recommended, which is a significant increase from the original design.

Boshoff *et al.* (1993:25) emphasised the need to revisit the Orange River flood model since a palaeoflood study in the lower Orange River in 1993 had determined that approximately 550 years before present a flood peak of 28 000 m³/s passed down the river, increasing the RMF K-value in the Orange River from 2.8 (TR 137) to 3.18.

2.2.5 *Topographic and geologic features in Namibia which affect run-off*

The great escarpment running from north to south divides much of Namibia into two general landscapes: the low lying coastal plain to the west and the higher inland plateau to the east (Mendelsohn *et al.*, 2002:15).

Goudie (2007:19) describes four main landform types in the desert regions of Namibia; the sand dunes of the Cunene erg in northern Namibia, yardangs in the southern and northern Namib Desert, aligned drainage on calcrete in the western Kalahari, and banded vegetation strips (*brousse tigrée*) in southern Namibia.

The central part of northern Namibia is the Owambo Basin from where most drainage flows toward a series of salt pans, of which the Etosha is the largest. South of the area lies the Karstveld. The rocks are dominated by limestone, which easily dissolves in water, forming large underground caverns, lakes and aquifers. There is little surface water runoff from the karstveld and no major rivers drain it (Mendelsohn, 2002:17).

Much of northern and eastern Namibia, the Kalahari Sandveld, is dominated by savanna woodlands. The whole landscape slopes gently down to the east and south. Several rivers cut through the sandveld, but those that drain out of Namibia very seldom flow any distance (Mendelsohn, 2002:16). The western part of the Kalahari, called the Weissrand, is underlain with calcretes of considerable thickness; over 30 metres at places. These thick pure calcretes may be susceptible to karstification (Goudie, 2007:27). A significant rainfall event over the western Kalahari Desert, at the Uhlenhorst settlement, precipitated between 400 and 489 mm in 12 hours. An estimated 230 million cubic metres of rain fell, of which 50% infiltrated into the ground during the rain storm, and the remainder was caught up in pans and between dunes and evaporated over the following three months (Schalk, 1961:445). Karstification could have been the main cause of the rapid infiltration, no surface run-off reached the nearby Auob River.

2.3 Dam safety in Namibia

Pandey *et al.* (2004:181) stated that the engineering and management of human safety is an important societal objective that includes extensive efforts by governments, both legislative and administrative, to enhance the health and safety of the public.

2.3.1 *Legislation regarding dam safety in Namibia*

In the WRM Act (2004:41, 2013:65), powers are given to the Minister who may, at his discretion, appoint a suitably experienced professional engineer to determine the safety risk of a dam or to perform a safety evaluation on an existing dam. The evaluation shall be done in accordance with acceptable engineering practices. These ‘practices’, however, are not defined in the Act.

The 2004 WRM Act (2004:43) as well as the 2013 WRM Act (2013:63) gives wide-ranging powers to the Minister of Water Affairs, including the power to adopt standard regulations or any code of practice. However, until such regulations or codes have been adopted, it will not be possible to enforce the act (Cullis, 2006:6).

According to the 2004 (41) WRM Act the Minister may request that any dam be inspected regarding its safety risk, and from the results of such inspections, the Minister may declare dams to be dams with a safety risk. As discussed however, a register of such dams does not exist.

2.3.2 *Current practice of dam safety in Namibia*

According to Cullis (2006:1) until 2006, no formal dam safety evaluation, to assess the risk category of a dam, had been performed on any of the large dams in Namibia. Dam inspections, generally for electrical and mechanical maintenance, had been performed on an ad-hoc basis.

From the above it can be seen that Namibia has scope for developing capacity in the field of risk related to dam safety and improving its mechanisms for the classification of dams in terms of risk.

The social responsibility of NamWater, however, stretches beyond its legal responsibility. NamWater has therefore started planning and compiling a programme for safety evaluations. The first two safety evaluations of large NamWater dams first were performed in 2013, prior to the publishing of the new 2013 WRM Act. Another four large dams will have safety evaluations performed in 2014/2015. NamWater however uses the SBA to deal with risks.

2.4 Risk based dam safety

Ammo Hoekstra, the ICOLD chairman of the committee on dam safety (ICOLD, 2005:11), said that it is futile to try and solve tomorrow's challenges with yesterday's technology. 'Risk assessment should be considered as a tool of improvement on the way to tomorrow'.

The broadest goal in managing risk is to serve the public interest, and although knowledge of the extent of the risk can never be complete, decisions must nevertheless be made on behalf of the public (Nathwani *et al.*, 1997:6).

Reservoir safety has traditionally been managed by safety standards (Brown & Gosden, 2004:4; ICOLD, 2005:17), either the dam complies with the standard or it does not, and if it does not, then modifications to meet the standard are warranted (Hartford & Baecher,

2004:27). However, the traditional standards based approach alone, is becoming increasingly inadequate in the management of a portfolio of dams when it comes to allocating limited resources for their operation or improvement in a climate of growing public scrutiny. Risk assessment is one technique which will assist with this type of problem (ICOLD, 2005:29; ANCOLD, 2003b:S2; Charlwood *et al.*, 2007:18).

According to ICOLD Bulletin, 130 of 2005, the ultimate goal of risk assessment is the quantification of the probability and consequence of system failure (system risk), i.e. when the dam can no longer retain water. Other authoritative bodies such as ANCOLD and DEFRA (ANCOLD 2003b:19; Brown & Gosden, 2004:78) further define the ultimate goal as a region of tolerable risk. The bounds of this region are referred to as the ‘limit’ or upper-bound beyond which risk is unacceptable, and the ‘objective’ or lower-bound above which risk is tolerable, given the benefits received from the risk exposure. Within this tolerable risk region, the risk should be ‘As Low As Practicably Possible’ (ALARP).

The USBR (2011:1) oppose the idea of a ‘tolerable risk’ and have chosen not to use the term. This is in recognition of the fact that the risk numbers are only approximate, are produced by a variety of methods (often including expert judgment), and by a variety of individuals and teams. A hard line separating tolerable risk from risks that cannot be tolerated would be difficult to define under these conditions.

Looking beyond the risk of individual dams, another approach has gained popularity. Portfolio Risk Assessment (PRA) is a tool to cost-effectively prioritise remedial measures for a group of dams since resources are limited and ageing dams are increasing in number. The PRA therefore is a guide to the decision maker to prioritise dams for rehabilitation and utilize resources more effectively. The SBA, however, is still used to reduce the risk at these dams. (USCOLD, 1998:2; Hartford & Baecher, 2004:25).

The main purpose of risk analysis is to provide support for decision making (Hartford & Baecher, 2004:4; Oosthuizen and Hattingh, 2007:3). The risk analysis guides the decision maker in prioritising an inventory of dams for improvement, but the standards-based approach is still used as a guide to the extent of rehabilitation (ICOLD, 2005:167; Hartford & Baecher, 2004:28). This is in part due to the fact that there are currently no accepted risk evaluation criteria for dam safety (Hartford & Baecher, 2004:25).

This is particularly true of dam safety where the use of risk assessment is in its infancy and needs to be further developed with more research and more mature understanding. This knowledge will come from experience, research and understanding. (Hartford & Baecher, 2004:26; ICOLD, 2005:17).

According to ICOLD (2005:59), a risk assessment method will be valid if it:

- i. is scientifically valid and appropriate for the system under consideration
- ii. provides results from enhanced understanding of nature of the risk and genuinely informs the decision process
- iii. can be used by variety of practitioners, in a manner that is traceable and repeatable and verifiable.

Key limitations to risk analysis are (ICOLD, 2005:49, ANCOLD, 2003b;22):

- i. Reliability in quantifying the probability of failure or incident, particularly for failure modes, such as internal erosion, that are not amenable to analysis.
- ii. Difficulty in estimating the consequences of dam failure.
- iii. Lack of widely recognised and accepted methodology for determining tolerable risk, particularly for life safety risks.
- iv. Lack of broad societal acceptance of the concept of tolerable risk.

The process of decision making generally starts when there is insufficient knowledge about dam or portfolio of dams.

2.4.1 General risk approach (Icold bulletins)

Risk analysis leads to an understanding of the sources and magnitude of risk. Risk analysis is a structured process aimed at identifying both the likelihood of failure of the dam or dam components, and the extent of the consequences of failure (Hartford & Baecher, 2004:5). Risk assessment, however, is not easy and the approach is not purely quantitative; dam safety engineers have to cross the boundary from the technical world to the more subjective world of values and value judgments (ICOLD, 2005:23).

Intuitive risk management may be appropriate when the risk and the costs are small and when the risk is borne personally. Risk must be analysed carefully when there are major issues and they affect the lives and health of others. This particularly is the case for large dams, both in terms of the value of the infrastructure as well as the risk to society. Tools required for evaluation of the options, as a matter of necessity, rely on quantitative methods. (Nathwani *et al.*, 1997:4).

The three categories of risk analysis (ICOLD, 2005:57) are:

- i. Standards-based approach, which is not actual risk analysis, rather the consideration of risk is implied through the use of classification schemes that reflect the hazardous nature of dams.
- ii. Qualitative approach considers risk more explicitly than SBA, without characterising the uncertainty in mathematical (probabilistic) form. This is a useful screening method. It is used for indexing and ranking a portfolio of dams.
- iii. Quantitative approach includes formal reliability analysis methods such as First Order Second Moment (FOSM) and full integration - also quantitative event tree and fault tree.

A semi-quantitative alternative is to rank severity and probability descriptors on numerical scales of, say, one to five and then to combine them by multiplication. This approach is recognised as overly simplistic and overlooks many complex issues of system behaviour (Hartford & Baecher, 2004:45).

To produce quantitative numbers, a process including statistical estimates, reliability models, fault tree analysis and expert opinions is relied upon. Such processes will produce precise numbers associated with risk, but still relies on techniques of deduction and the subjectiveness of human input (Hartford & Baecher, 2004:66). However, that does not suggest that the risk guidelines should be taken lightly. Indeed, every effort should be made to meet them (USBR, 2011:1).

Pandey *et al.* (2004:182) suggested that risk can always be reduced, but at some cost. However, demands for absolute safety, implying zero risk, can do more harm than good. If the costs of risk reduction are disproportionate to the benefits derived, then it diverts societal resources away from critical areas such as health care, education and social services that also enhance quality of life.

2.4.2 *Consequences translating to risk*

Understanding the consequences of dam failures is fundamental to the assessment of risk (Hartford & Baecher, 2004:81).

Three direct consequences are:

- Life safety
- Economical and financial
- Environmental impact

Predictions of loss of life (LOL) will necessarily have very large bounds of uncertainty (Hartford & Baecher, 2004:97). A draft of 178 case history accounts of flood disasters carried out at Utah State University indicates that LOL in dam breach flood events is determined by a very large number of factors. Bowles and McClelland have identified at least 100 variables that they consider to be determining factors in the probability of survival. This research demonstrates that analytical determination of human response to impending flooding is presently extremely difficult, and in many cases impossible (Hartford & Baecher, 2004:98).

Robin Fell (ANCOLD, 2003b:S2) proposes that if consistent methods are used to determine loss of life, then one will generally be able to rank the possible outcomes and compare them in scale with others, an approach adopted in this dissertation.

Modelling the risk to human life using regression analysis from historic databases has met with limited success (Hartford & Baecher, 2004:100). The number of people at risk, due to a dam break, and the warning time before the flood wave reaches a city/town are the most important numbers correlated with the loss of life. For a better fit of the data, DeKay & McClelland (1993:200) introduced a distinction between ‘high lethality’, or deep swift water flowing down a canyon, and ‘low lethality’, i.e. on a plain where the flood waters are likely to be more shallow and slower.

2.4.3 Current practice in risk based dam safety

The ALARP principle, short for ‘as low as reasonably practicable’, was established in Britain in a court case in 1949, involving the National Coal Board. The outcome indicated that if there is a gross disproportion between the risk and the cost of reducing it, in which case the risk is insignificant in relation to the cost, then compliance with risk reduction is considered not reasonably practicable (DEFRA, 2002a:46). This principle is applied today in dam safety to define a state of tolerable risk; if the risk is greater than a limit, there is an indicated need for risk reduction. If the risk falls below the limit, then ALARP needs to be applied to reach a conclusion on tolerability (ANCOLD, 2003b:16, Hartford & Baecher, 2004:27).

Brown & Gosden (2004:3) developed an interim guideline to quantitative risk assessment (QRA) for United Kingdom reservoirs. This guide proposes assigning an annual probability of failure of a dam due to four core threats: extreme rainfall, upstream reservoir, internal erosion of embankment dams and, lastly, internal instability of appurtenant works. This UK guide evaluates whether the risk is tolerable; in compliance with the ALARP principles.

Mason (2008:1) commented, in a questionnaire to UK users of the Guide, that the QRA Guide is full of disclaimers which emphasise that the whole process, and the numbers quoted, are really for preliminary approximations and screening purposes. In his opinion the current guide is more a work-in-progress than a definitive answer.

Huges (2009:2) also commented that one must be very careful when using the UK QRA Guide, ‘because you can get any answer you want, really’.

According to Oosthuizen and Hattingh (2007:4), a qualitative risk approach is applied for dam safety in South Africa. The South Africa Dam Safety Office (DSO) of the DWS has developed a simplified probabilistic method to identify dams which should receive priority for remedial work. It compares relative risk ranked according to two criteria, expected loss of life and expected economic loss (Oosthuisen & Hattingh, 2007:3).

Charlwood *et al.* (2007:13), however, have a different view, they propose that, even when fully developed, risk analysis cannot be used as a substitute for the sound professional judgement of engineers, contractors and review boards.

Since the 1980s-event tree analysis (ETA) has emerged as the most common approach to risk analysis for dams. It pertains to cause and effect, requiring an initiating event. ETA is a deterministic model of a binary functional state (events occur or do not occur) of the system where probabilities are assigned in a conventional (statistical frequency) way. (Hartford & Baecher, 2004:47).

According the Hartford and Baecher (2004:66) the best (or only) probability assignments are based on statistical prediction.

The ICOLD Bulletin 130 (2005:39) asks ‘how safe is safe enough, what level of risk is tolerable?’ However, according to this 2005 risk assessment survey, certain risk assessment activities around the world have been abandoned by knowledgeable dam owners or professionals with good descriptions of the reasons why. These include:

- The abandonment of tolerable life safety assessment by BC Hydro in 1997.

- The use of embankment dam piping statistics from a limited population of dams to derive the probability of failure of an individual dam.
- The use of subjective probabilities within event trees.

Implying that the uncertainties and subjectiveness of the process disqualify it as purely quantitative.

2.4.4 *Qualitative and quantitative risk*

Hartford and Baecher (2004:7) stated that risk analysis can be either qualitative or quantitative and to various levels of detail. Risk evaluation, the process of understanding and judging the significance of risk, is fundamental to risk assessment and risk based decision making.

Nathwani *et al.* (1997:4) suggest that quantitative risk methods are a hallmark of professional quality in risk management, and used not just for academic reasons to improve our often ‘meagre and unsatisfactory’ understanding of the processes managed, and certainly not to replace judgement in management. Quantitative risk analysis will aid the judgement of a decision maker faced with complex issues, to foster consistency among risk management decisions, and to support accountability.

A study by ICOLD (2005:135) revealed that 50% of the responding countries used only the SBA. Their opinion is that quantitative risk assessment will not produce reliable results ‘as each dam is an individual case’ and there is skepticism about ‘quantitative risk determination for some failure mechanisms’.

A fully quantitative risk analysis is a measure of the risk that includes complete mathematical specification of the uncertainty in the estimate. For example, the risk associated with internal erosion is not a fully quantitative risk in a scientific sense, as many of the uncertainties are unknown (Hartford & Baecher, 2004:209; ICOLD, 2005:59). Oosthuisen & Hattingh (2006:5) concur that internal erosion and other secondary modes of failure such as liquefaction, sabotage and failure of the outlet works are generally not calculated, but are accounted for by using relative probabilities. Similar opinions are found in the ICOLD survey of 2005.

Regulators in Sweden feel it is not possible to ‘sign off’ a dam to be ‘safe enough’ by using quantitative risk assessments for failure modes such as internal erosion, nor to compare the results with possible acceptable criteria, since there is a high likelihood that internal erosion induced failures would not be detected in advance (ICOLD, 2005:157).

Mason (2008:2) said that extensive investigations carried out on old Austrian dams revealed some filters met some acceptance criteria but not others. This is not surprising given the range of criteria available. However, the investigators noted that no significant migration of fines was taking place. In other words, detailed site investigations indicated that the dams were performing well with regard to potential internal erosion problems. How would one therefore assign a failure-risk to such dams?

California, like South Africa, uses qualitative risk assessment for ranking dams in priority for risk reduction measures (ICOLD, 2005:139). A qualitative approach is often based on expert opinion, when in some cases there is no data at all, only the judgement of experts. According to Hartford and Baecher (2004:149), the tacit knowledge of experts is based on intuition, unenumerated past experience, and subjective theory, and qualitative beliefs.

No Canadian dam owner, or regulator, has expressed sufficient confidence in the scientific validity, or robustness, of judgmentally quantified probabilities to make life safety decisions using these techniques (ICOLD, 2005:147).

Methods are not yet available to enable fully quantitative and rigorous risk assessment for dams. Currently, quantitative assessment is still partly scientific and partly subjective (ICOLD, 2005:69). Presently risk assessment frameworks are used for index type characterisation of risk.

The topic of risk evaluation is not an easy one, especially for the technically minded person looking for a straightforward and purely quantitative approach (ICOLD, 2005:91).

Experience has shown that the use of detailed event- and fault tree analyses to calculate the probabilities of a series of consequences, is not defensible when applying confidence limits to the data. Uncertainties in the data dominate the process and little or no significant advantage could be gained by these calculations (Oosthuisen & Hattingh, 2006:3).

People tend to overestimate the probability of events that have a favourable consequence, and to underestimate the probability of those with an unfavourable consequence (Hartford & Baecher, 2004:160).

2.5 The Life Quality Index and marginal life-saving costs

The concept of risk acceptance raises ethical concerns, as human life is regarded as being of inestimable value (Nathwani *et al.*, 1997:18). A way out of this dilemma is established by the marginal life-saving costs principle which is based on the recognition that societal resources

for life saving activities are scarce and need to be invested in the most efficient risk reduction measures available (Kraemer *et al.*, 2010:1). Quantitative risk acceptance criteria help to achieve a consistent level of safety in different areas.

In this approach, absolute criteria for the risk magnitude define whether a specific activity lies in the ‘acceptable’, the ‘non-acceptable’ or the so-called ALARP region. In the latter region, an activity is termed ‘tolerable’ if all reasonable risk reduction measures available have been implemented. While the ALARP approach is intuitively sensible, from an ethical point of view the application of absolute risk acceptance criteria is highly problematic. (Kraemer *et al.*, 2010:1)

According to Schubert *et al.* (2007: 2), decision makers are often in the spotlight and, as a consequence thereof, may over-commit societal resources for reasons other than serving the general public. In such cases resources are not used in an optimal way; the decision maker is buying personal insurance by using the resources of society. Due to this, the rational consideration of risk aversion has taken on renewed significance.

Nathwani *et al.* (1997:7) proposes that where new or additional risk is to be imposed on the public, the Kaldor-Hics Compensation Principle be applied, by which a policy is judged to be socially beneficial if the gainers receive enough benefits that they can compensate the losers fully, and still have some gain left over. If the losers are, in fact, compensated fully, they are by definition transformed into non-losers and the policy is Pareto optimal: i.e. optimal for all or at least neutral.

Modern society’s fundamental value settings, however, tell us that the value of human life is immeasurable. Taking this perspective, the so-called ‘vision zero’, i.e. aiming at a zero probability of death, is the only risk management principle that can be seen as ethically justifiable. Yet, from a practical point of view, it is well-known that a certain risk to life and limb can never be avoided (Kraemer *et al.*, 2010:1).

2.5.1 *The LQI method*

Nathwani *et al.* (1997:1) have developed a tool, the Life Quality Index (LQI), for managing risk in the public interest, the aim being guidance to decision makers who have the responsibility for managing safety. The LQI is a social indicator composed of the part of the GDP per capita available for risk reduction, the life expectancy at birth and the fraction of total lifetime spent for work. (Kraemer *et al.*, 2010:3; Nathwani *et al.*, 1997:19)

The balancing of impacts on the quality of life and health against the economic costs of risk reduction, although controversial, is an essential professional obligation (Pandey *et al.*, 2003:66). The LQI can be used to quantify the societal willingness to pay for a marginal increase in life safety. (Fischer *et al.*, 2013:37).

The LQI is determined from societal indicators; an active process, whereas the ALARP criterion is determined from the SBA; an inactive process. Hence both methods define a certain level of tolerability towards risk, however, the drivers of the processes differ.

It could be noted that the LQI process is in contrast to absolute probabilistic risk criteria such as “the probability of death shall not exceed 1/1 000 000 per year for the person most at risk. (Nathwani *et al.*, 1997:12)

For the derivation of quantitative risk acceptance criteria, the marginal life-saving costs have to be compared to the societal willingness to pay (SWTP) for a marginal increase in life safety, which can be determined with the aid of the Life Quality Index (LQI). (Fischer *et al.*, 2013:37; Pandey *et al.*, 2003:65).

The LQI aggregates the various important components of life: life, health, money and environment, into a single quantity. It is proposed as a summary index of the net benefit (Nathwani *et al.*, 1997:13). Therefore although risk is present, the benefits to those affected outweigh the risks.

2.5.2 *The technology curve*

Our ability to allocate scarce resources wisely is the central problem in managing risk. A simple and meaningful test of the effectiveness of a risk management allocation is: how much life-saving does it buy, and could the same resource, if directed elsewhere, result in better gain for society as a whole? (Pandey *et al.*, 2003:67).

Fischer (2012a:22) noted that the LQI net benefit criterion has to be understood as a criterion for the efficiency of life-saving measures. The Societal Willingness to Pay (SWTP) denotes the maximum amount society is willing to pay for a marginal increase in life safety.

Schubert (2009:112) reasoned that if all available measures were sorted by their efficiency, the resulting curve will show the available technology or best praxis (the practical side and application of something such as professional skill, as opposed to its theory) for risk reduction.

The shape of the curve can be explained as follows: If we did not invest any resources at all into life safety and survival, the life expectancy would be equal to zero. The first measures are very efficient and require only small investments for significant increase in life expectancy. Examples for this are food and hygiene. The efficiency then decreases more and more as investment increases (Schubert, 2009:112).

In principle the use of risk aversion factors, which contain a very high degree of subjectivism poses the problem that the basis for the decision making is not transparent and further that the model cannot be scrutinized nor verified – a prerequisite for any engineering model (Schubert et al., 2007:5).

2.6 Detailed discussion of authors pertinent to the research.

Organisations and regulating authorities such as ICOLD, ANCOLD and DEFRA indicate that dam practitioners have low confidence in risk based dam safety, due to the unknown probabilities of failure by internal erosion or failure of appurtenant works.

The review and updating of the flood hydrology of Namibia builds upon the original work of Kovács (1988:3) regarding the Francou-Rodier K-values and delineation of flood zones.

Utilizing the palaeoflood approach and fieldwork methodology as described by Baker (1993), Enzel (2005), and Grodek (2007), additional extreme flood peaks were determined and added to the list of systematic annual flood peaks. Palaeoflood data provides flood magnitude and frequency for recent floods (50 years), as well as ancient floods (several thousand years). Enzel (2009) indicated that the method of determining ancient flood peaks is exactly the same as for modern flood peaks, as long as the stage indicators are clearly defined.

Dorn's work (1982:1989) on desert varnish contributed to the estimation of upper bound flood peaks at the palaeoflood sites, which contributed in delineating the Francou-Rodier K-regions.

Klemeš (1993:168) proposed that flood modelling should not be based on more mathematical rigour but rather on more information on the phenomenon of flooding. This proposal supports the use of palaeoflood hydrology, which provides evidence on actual flood peaks for a sequence of floods as well as upper bound flood peaks.

Globally, dam specialists are agreeing that the traditional standards-based approach to dealing with risk is becoming increasingly inadequate, especially for the management of a portfolio of

dams where the budget is limited (ICOLD, 2005:11; ANCOLD, 2003b:S9). Therefore risk assessment could assist with this type of decision making process.

The work of Brown & Gosden (2004) addresses quantitative risk based dam safety in the UK. However, several years after implementation, UK dam safety practitioners proposed that Brown & Gosden's work should be used as a screening tool only, and not to produce quantitative risk results for decision making purposes. Their approach however, on determining the return period of a flood which overtops an embankment dam and causes it to fail, was used in this research.

ICOLD bulletins 99 and 130 (1995:2005) contributed to the safety of dams in general and more specifically to the application of risk based dam safety and the concerns of users internationally who took part in the survey.

ANCOLD, SANCOLD and SPANCOLD provided inputs regarding current day practice of dam safety. Charlwood, Bowles and the USBR provided a North American view of dam safety which still relies on the standards based approach, but uses RA as a tool to rank individual dams according to priority.

DeKay & McClelland (1993:200) and Serrano (2011:1001) provided valuable input to populations at risk and the concept of likely loss of life due to a dam failure.

The work of Schubert (2009), Kraemer (2010) and Fischer (2012a) discussed marginal life-saving cost and its application in the technology curve. This, however, led to the development of the inverted technology curve and the ranking of dams for rehabilitation.

2.7 Observations from the literature review

From the literature reviewed, the following observations are made:

- Nearly all references to quantitative risk based dam safety mention that the process is not yet fully supported; the bone of contention is internal erosion which is referred to by all as the reason for the low level of confidence in the process.
- Risk based dam safety, however, is gaining interest internationally as a tool for prioritising rehabilitation over a portfolio of dams. In this case the SBA would still be used to determine the extent of rehabilitation.
- The literature reviewed does not discuss risk evaluation based on single components of risk; it refers to risk as a whole, whereby all risk components contribute to the total risk of a dam. This dissertation presents a new view on risk based dam safety by

evaluating only the risk based on extreme flood. The probability of the flood and the loss of life upon failure of the embankment are the two variables for the risk calculation.

- The flood estimates which have been used in designing dam spillways in Namibia since the early 1900s, may have overestimated the annual recurrence interval of design floods.
- The earlier work of Kovács (1988:52) proposes that the RMF has an annual recurrence interval of less than 10 000 years. Recently Van der Spuy (2009), after analysing 30 to 40 years of additional floodpeak data, proposed that the RMF flood generally exceeds the 10 000 year return period.
- Approximately 30 years have elapsed since the last Namibia flood model was updated. With the aspirations of applying risk based dam safety in Namibia, updating the flood model, with the incorporation of palaeoflood hydrology, will play a vital role.
- Palaeoflood hydrology can provide evidence of extreme flood events in the past, thereby increasing the data on general floods, as well as upper bound floods. In so doing, valuable information is added for the updating of flood models.
- The probability of overtopping a dam is amenable to risk estimation, since it is based on flood frequency analysis of systematic data and also palaeoflood data. A conservative assumption is made that the dam will fail catastrophically if it is overtopped. For a portfolio of dams, if the flood model and consequences of failure are dealt with consistently, the resultant risk will be comparable.
- The probabilities of dam failure events such as internal erosion, or failure of the appurtenant works, depends on a frequentist approach. Regulating authorities in several countries are not comfortable with this approach of probability estimation when lives are at risk.
- Quantitative risk based dam safety, based on the probability of actual events and not on a frequentist approach (purely quantitative as some call it), is the only approach which would be accepted by some countries.
- A general feeling among some practitioners of risk based dam safety is that allocation of resources to reduce risk should not be based on a fixed standard but rather on an acceptable level of risk, thereby effectively optimising expenditure based on risk.
- The technology curve indicates the rate and quantity of risk reduction for the investment of resources. This curve could be used as a tool in risk based dam safety, to optimise expenditure over risk reduction.

The risk based dam safety model proposed in this dissertation concentrates on external erosion only, which is quantifiable.

3 Data collection

The data required for this research consists of rain gauge data, annual flood peak data, palaeoflood data, and information on the cost of raising an embankment. These four sources of data are discussed individually in the following four sections.

The flood hydrology model of Namibia was last updated in 1988 (Kovács, 1988). Nearly three decades of additional systematic flow data has subsequently been collected as well as rainfall data which is required for the three day maximum precipitation; a mechanism for generating extreme floods.

Non-systematic flood peaks were also collected. Since the early 1990s developments in palaeoflood hydrology opened new avenues in determining flood peaks that occurred long before historical or systematic flood recording commenced. For this research, discrete flood peaks were determined in the field as a part of palaeoflood studies which were performed in the Fish-, Kuiseb-, and Kahn Rivers.

Other sources of non-systematic flood peaks are found in historically documented flood records. The archives of the Namibia Department of Water Affairs has notes compiled by Stengel (undated) on historical flood events, however many of these flood peaks had been incorporated in the work of Kovács. Some were only qualitatively described, such as a big flood on 8 December 1954 in the Stamp River at Gaab: ‘Water tot by huis’ (translated from Afrikaans: ‘the flood waters reached the house’). Another flood description for the Kuiseb River, noted by staff at the Gobabeb Research Station in November 1963: ‘The flood reached the sea’. These two descriptions had not been quantified in the notes of Stengel, and although they could be quantified if the aforesaid house could be located and the elevations surveyed, or if the flood peak could be estimated for the flood required to breach the natural sand bar at the Kuiseb River mouth, the scope of such fieldwork would require significant time and resources. Hence these qualitative sources were not further pursued.

Other relevant data included information on the cost of rehabilitation of dams for the improvement of dam safety. Information on the rehabilitation costs of several dams in South Africa was used to develop an empirically based unit rate cost for raising the non-overspill crest of an earth embankment dam. This unit-rate was used in the process of developing a risk reduction method, as described later in this dissertation.

The sequence of the types of data collected and their preparation, which is discussed in this section, starts with rainfall data, followed by the systematic flood hydrology data, then

palaeoflood fieldwork and data processing and, lastly, the data used for determining the unit rate for rehabilitation of embankment dams.

3.1 Rain gauge data

The Namibia Meteorological Office in Windhoek made available daily rainfall data from 434 rain gauge stations spread throughout Namibia. The total number of recorded years of data is 14 100 years. After a process of removing several gauge stations with incomplete geo-referencing, and also reducing the list to only the stations with more than 30 years of recorded data, the list shrank to 180 rain gauge stations with a combined data record of 10 343 years. Refer to Appendix A for the list of rainfall stations with records lengths of 30 years or longer. Figure 3.1 shows the distribution of the 180 rain gauge stations that were used in this study.

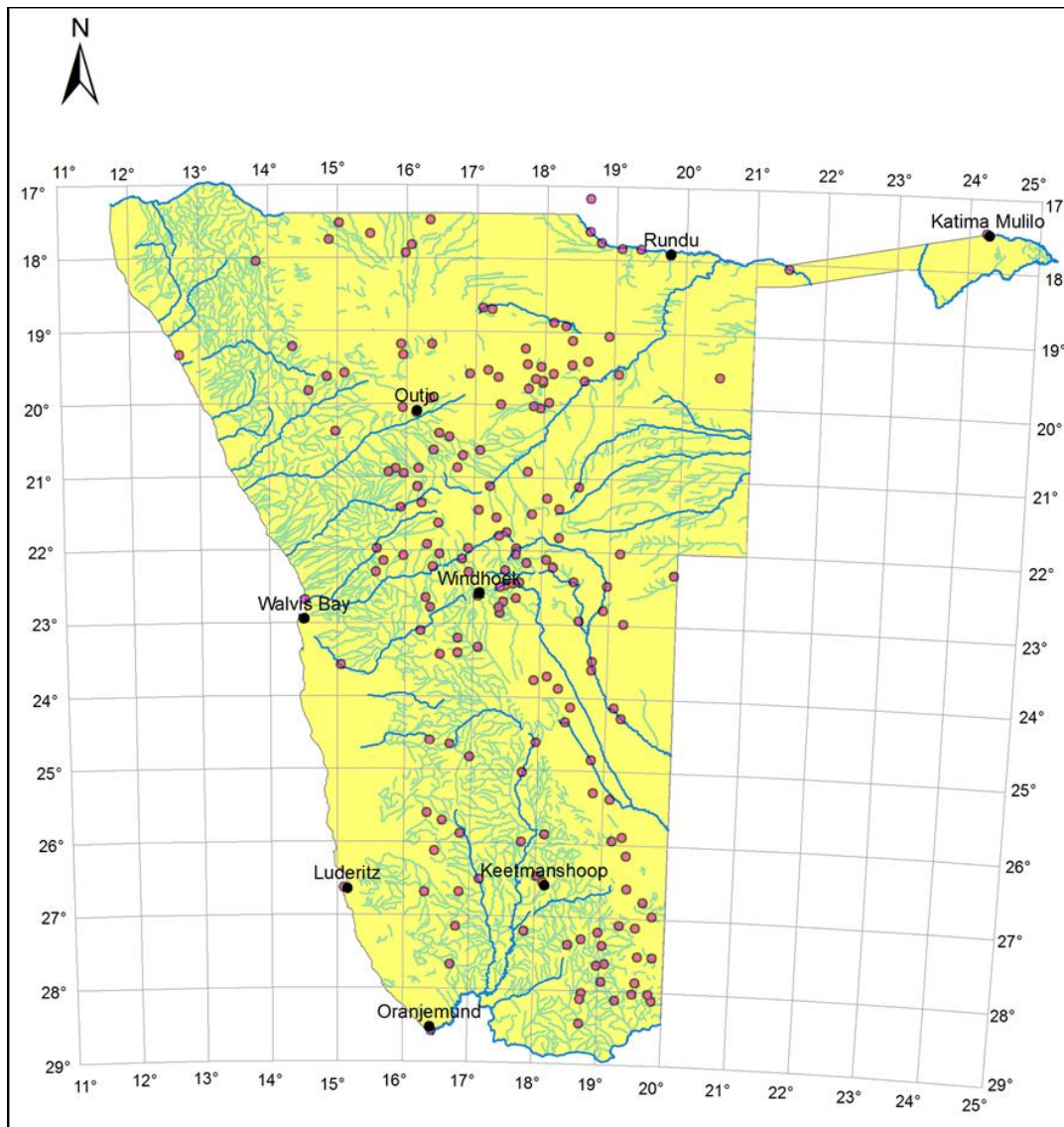


Figure 3.1: The distribution of the 180 rain gauge stations used in this study

In TR 137, Kovács (1988) used approximately 110 rain gauge stations. However the combined data record length of these stations is unknown.

3.1.1. Missing rainfall data

In the data set there are missing days as well as missing months, where either the data was most likely never recorded, for example where on one or several days the person responsible did not take readings or, in the case of an entire month of missing data, probably the entire recorded data sheet for the month went missing. To resolve the two cases of missing rain gauge data, the following approach was followed:

- The missing daily data, represented by a star (*) in the original record, was replaced with a zero rainfall value. This was required for the algorithm to determine the three-day maxima. In most of the cases of missing daily data, the rain gauge data before and after the day(s) with gaps was zero. No cases were found where there was missing data with significantly high rainfall recorded in the days before and after the missing data. Therefore this approach, i.e., to replace missing data with zero rainfall, is deemed to have provided realistic results and the three-day maxima are not expected to be underestimated because of this approach.
- In the case of the missing months, those data were omitted in further calculations. The occurrence of missing months is only a small fraction of all the data, and in many cases falls outside the rainy season. Generally, when significant rainfall occurs, the individuals recording the data are more attentive to properly recording the data and, therefore, it is expected that the results of the three-day maxima are representative of the actual events.

3.1.2. The three-day maximum rainfall data

The sum of three consecutive days of rainfall was calculated for each day of the 14 100 years of data. This was done by summing the total precipitation on the day before the reference day, on the reference day itself, and on the day after.

For each rain gauge station, having obtained the three-day sum of rainfall for every day of recorded data (approximately 5 million days), the three-day maximum for the recorded history of the station could be determined. As a comparison, a distribution of the three-day maxima, as well as the distribution of the average annual rainfall, as indicated in the NDWA

Technician's Manual (1988:16), from the south to the north of Namibia, is indicated in Figure 3.2.

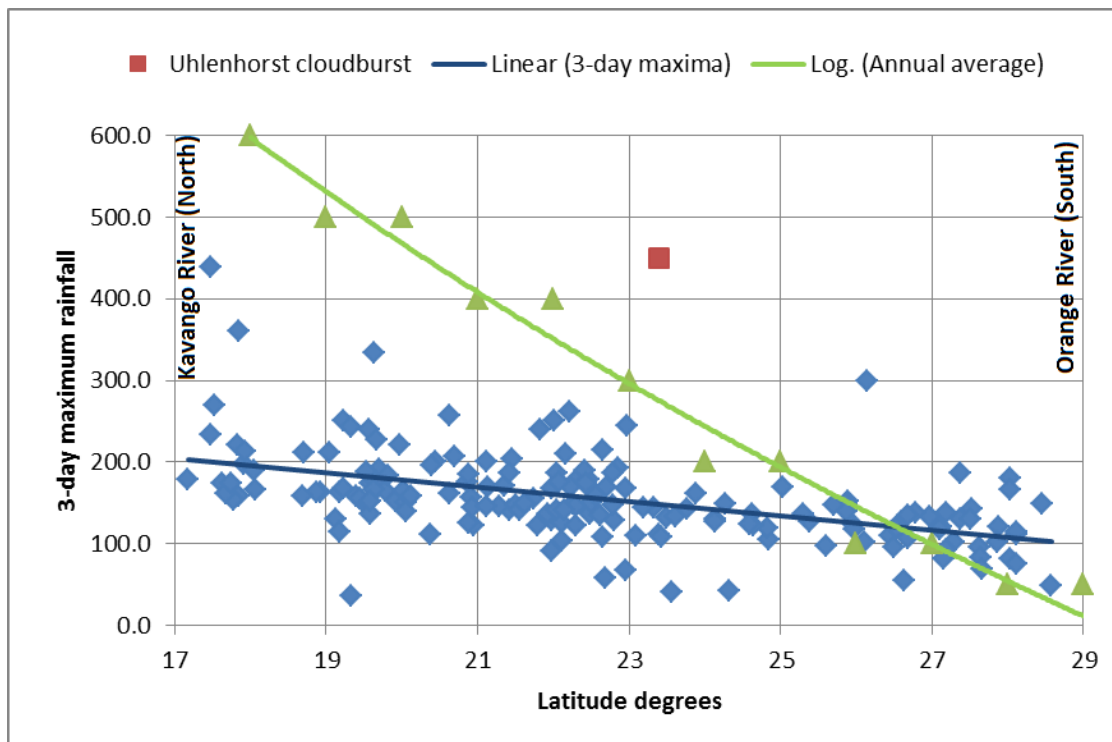


Figure 3.2: The distribution of the 3-day maximum rainfall from North to South in Namibia, as well as the average annual rainfall. For comparison, Uhlenhorst extreme rainfall event is also included.

Notice that the average annual rainfall has a more rapid increase from south to north, when compared to the three-day maximum rainfall. The rainfall measured for an extreme rainfall event, which occurred at the Uhlenhorst settlement area in the Kalahari (Schalk, 1961:443), is significantly higher than the three-day maximums. The Uhlenhorst 12 hour rainfall event however was not included in the Namibia Meteorological Office list; possibly at the time it was not registered as an official rain gauge station with the Meteorological office. The Uhlenhorst anomaly is discussed in more detail in Chapter 4: Updating the Namibia Regional Maximum Flood.

Having determined the three-day maximums, the data is plotted on their geographic positions and isolines are generated to join points of equal rainfall depth. Refer to Figure 3.3.

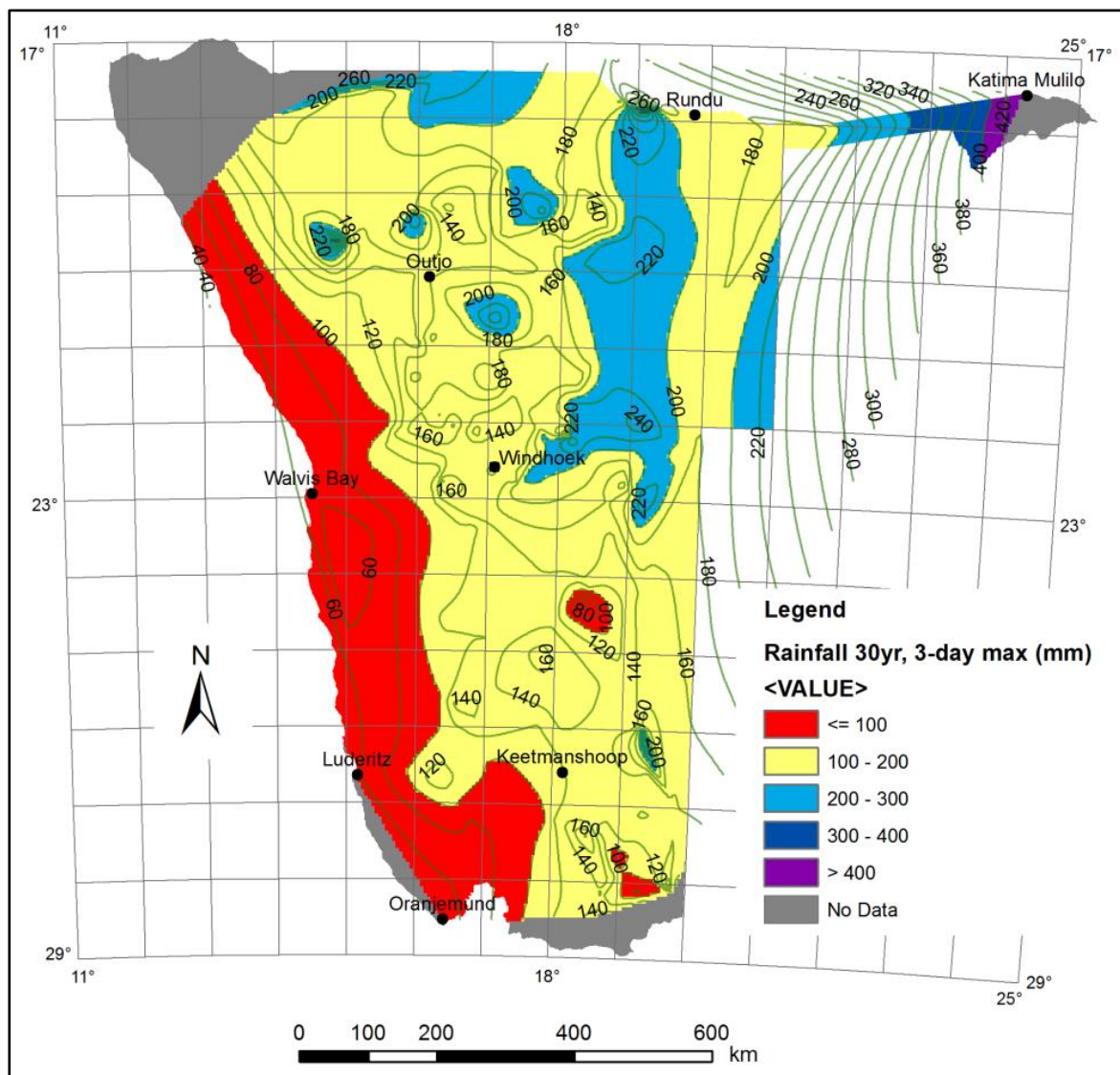


Figure 3.3: Isolines for the annual maximum three-day rainfall measured at rain gauge stations with records of a length exceeding 30 years.

The predominant rainfall generating mechanism, which causes higher rainfall in the northeast of Namibia, is the Intertropical Convergence Zone, and particularly its extension over southern Africa known as the Zaire Air Boundary (Grodek, 2013:259). Moist air masses from the tropical north-east move toward central Namibia. The semi-permanent Angola low-pressure cell directs moisture to the north and eastern parts of Namibia, resulting in higher rainfall in the northeast. And as the air masses move further south and less moisture is available, the mean annual rainfall decreases to 200 mm at the north-south escarpment and down to 10 mm along the Atlantic Ocean coastline.

3.2. Systematic flow gauging data

The Namibia Department of Water Affairs (NDWA) provided maximum monthly instantaneous flood peak data for 55 river gauging stations throughout Namibia. From these 55 stations a total of 1 887 station years of recorded data are available. On average, each of these stations has been operational for 33 years. This corresponds to the age of most of the stations which were commissioned in the late 1970s to the early 1980s. Exceptions are the Kavango and Zambezi Rivers in the north, which have records exceeding 60 years, and the Fish River in the South at Seeheim, with more than 50 years of data.

In TR 137, there are a total of 64 gauging stations with recorded flood peaks which were used to calculate K-values for Namibia. Eighteen of these gauging stations are duplicated in the latest NDWA list of 55 gauging stations. Of these 18 gauging stations, four had recorded newer flood peaks which exceeded those used in TR 137. The other 14 recorded in TR 137 are still the largest recorded floods. Therefore, after omitting the 4 flood peaks which have remained the same, duplicating those in TR 137, the latest NDWA list of gauging stations is reduced to 41.

The TR 137 data set was reduced from 64 to 60 by omitting the four stations which are also found in the new data set, with larger floods recorded. Therefore a systematic gauging station data set of 101 flood peaks was used in this study; 60 flood peaks from the TR 137 and 41 flood peaks from the latest NDWA list. Refer to Appendix B for a list of all the flood peak data.

3.2.1. *The raw data*

The data record for each individual river gauging station or flood-recording site consisted of the year and month, and the size of the recorded peak discharge in cubic metres per second for each month, as well as the NDWA Quality Code for each month's peak. Some months have zero discharge, so the peak for the month is zero. The NDWA Quality Code indicates whether the recorded flood peak was obtained from a good continuous record (Code 1), good quality edited data (Code 2), or generated recession (Code 10), etc.

A separate file was provided by NDWA which indicated the geographical position of the gauge station in degrees and minutes, and also the size of the catchment area of each of the gauging sites. Refer to Figure 3.4 for the distribution of flood peak sites in Namibia used in this study.

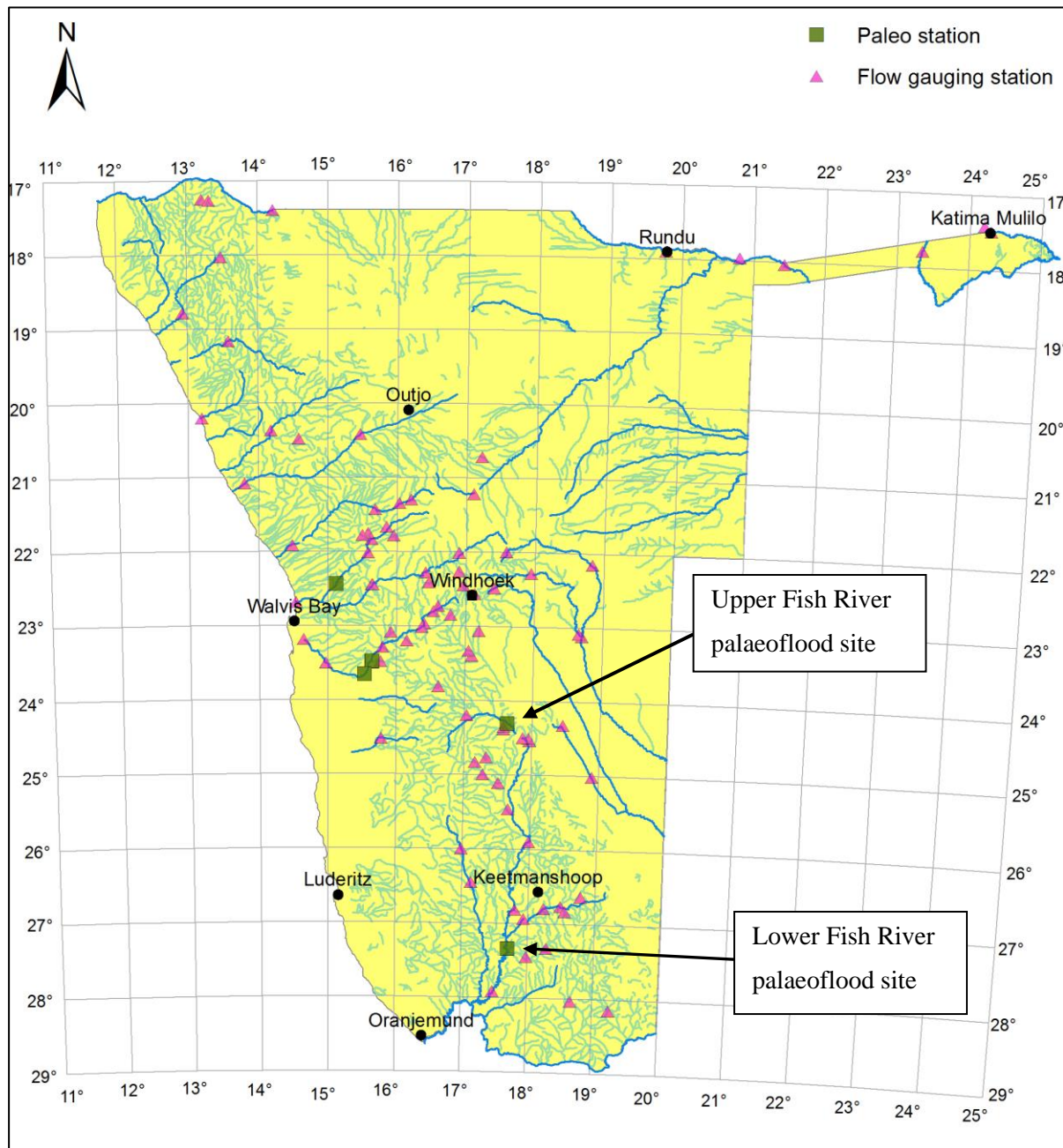


Figure 3.4: Distribution of recorded flood peak points, obtained from either river flow gauging stations, palaeoflood sites or indirect flood peak measurements at remote sites.

For the duration of the recorded data, the maximum peak discharge was selected for hydrological year cycles, 1 October to 30 September. From all the selected annual peaks, the highest peak was then selected for each specific station as the maximum flood peak. The quality code for that specific peak was also attached for later evaluation of the data quality.

This process could have been simplified by selecting only the largest peak from the bulk of the data for each station. However, from the approach followed here, other valuable

information is made available such as distribution of the peak months; refer to Figure 3.5 below for the monthly distribution of the flood peaks.

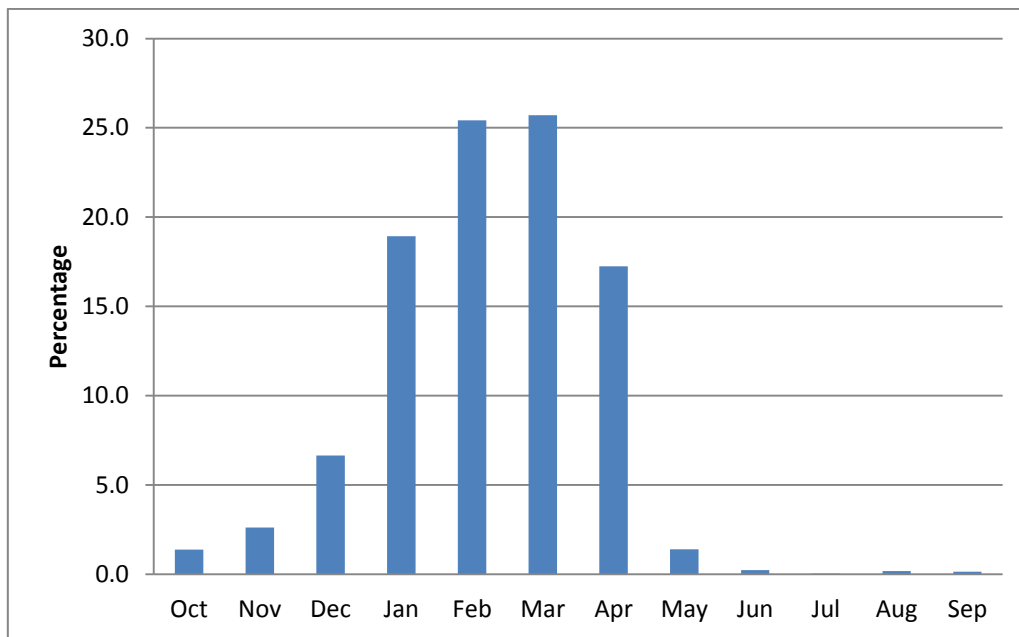


Figure 3.5: Distribution of annual flood peaks for the entire data set provided by the Namibia Department of Water Affairs: 55 gauging stations with a total of 1 887 years of recorded data

It is interesting to note that of the 1887 recorded years of newer data, 369 hydrological years recorded zero flow. This is equal to approximately 20% of the time. Refer to the annual data per station in Appendix O.

3.2.2. Validation of the new data

Validation of the 41 additional flood peaks consisted of two checks; the first was the NDWA Quality Code for each flood peak, discussed in section 3.2.3. The second was a comparison of the gauged flood peak with the calculated 10-year flood peak for each specific gauge point. This was to ensure that the flood peak would have a significant contribution to determining the K-value. Refer to discussion in section 3.2.4.

3.2.3. Data quality

Refer to Table 3.1 for the distribution of the data quality. The quality of the data received from NDWA is not questioned since, at the least, a quality control process applied to

measured data is indicative of a mature data collection system and is commendable. This discussion focuses attention on the distribution of the quality of the data; 61% of all the flood peaks are from a good continuous record; 23% of the flood peaks are estimated records; less than 1% of the data is questionable; and 6% is missing. The NDWA quality code guide extends further than the nine codes indicated in Table 3.1; these were the only ones applicable to the selected flood peaks of the 41 new stations used in this research.

Table 3.1: Distribution of the data according to the NDWA Quality Code Index

Quality Code	Description	Percentage of data
1	Good continuous record	61%
2	Good quality edited data	1%
10	Generated Recession	7%
104	Records estimated	23%
105	Doubtful data	0.7%
106	Missing data, peaks preserved	0.4%
130	Estimated	0.7%
150	Rating table extrapolated	0.6%
151	Data missing	5.6%
		100%

3.2.4. Verifying flood peaks as large floods

In order to validate that the magnitude of the floods used in this study is larger than the 1 in 10-year flood, the measured flood peaks were compared with flood peaks estimated from the river channel parameters which are indicators of the 1 in 10-year flood, i.e., the width of the natural stream measured between the riparian vegetation on the left and right banks of the river. The 1 in 10-year flood is the discharge that has the dominant impact on river channel fluvial morphology, as described by Beck & Basson (2003:3-2).

Several regime equations for calculating the river width are available and are based on parameters such as the channel width between the riparian vegetation. One of these equations, the Lacey regime method, as described in the work of Beck & Basson (2003:3-6), is applicable to bankfull discharge in rivers with sandy or silty beds. The units in the equation are in feet (ft); the equation reads as follows:

$$P = 2.667 \cdot Q_b^{0.5} \quad (3.1)$$

where: P = the wetted perimeter of the bankfull river channel in feet (ft). For this exercise the wetted perimeter is assumed to approximate the width of the bankfull channel; ephemeral river channels in Namibia are relatively flat and shallow.

Q_b = the bankfull discharge in cusec (ft^3/s)

Satellite images (Google Earth) were used to determine the bankfull width of the river for each of the gauging stations used. If a weir was detected at the site of the flood peak, then the width of the river was measured several hundred metres upstream or downstream, away from the influence on stream width, caused by the weir. Applying Eq. (5.1), the estimated 10-year flood peak for each site could be determined, and could be compared with the flood peak data received from NDWA. Refer to Figure 3.6 for the estimation of the bankfull width of the Kuiseb River at the farm, Us. The 10-year flood peak determined from the bankfull width of 60 m is estimated at $130 \text{ m}^3/\text{s}$, using Equation 3.1 (Beck & Basson, 2003:3-6). It can be noted that the maximum flood peak at the nearby weir was recorded as $333 \text{ m}^3/\text{s}$.



Figure 3.6: The bankfull width of the Kuiseb River at Us, 1 km upstream of the weir.

In all cases the NDWA flood peak discharge rates were larger than the calculated 10-year discharge, and were therefore suitable to be included in this study. Alternatively, where systematic data is available, one can probabilistically also determine whether the selected maximum flood peak has an AEP exceeding 10-years. Refer to Appendix N.

3.2.5. *Completeness of the data set*

It should be noted that there are large areas in Namibia without any gauging stations or recorded flood peaks. Refer to Figure 3.4. These are the southern low lying coastal plains, the Kalahari in the north-east and east where runoff very seldom occurs, and the northern Cuvelai area, where drainage occurs overland and not in well-defined river systems. Where possible, flood peak data should be gathered in these areas to get a better representation of flood data over the whole country. Palaeoflood techniques can be employed to gather this data, however only well-defined river systems, carved into the surface, provide evidence of significant runoff and are likely to contain palaeostage indicators.

3.3. Palaeoflood hydrology: extending the extreme flood data base

A common major problem in acquiring hydrological information in hyper-arid desert regions, such as in Namibia, is the lack of flood monitoring. In the very few locations where flood records do exist, the data are either partial or limited to a short period, whereas the mean recurrence interval of large floods could be longer than the record period (Grodek *et al.*, 2013:258).

Hence there is a critical need specifically to extend the recorded period of extreme floods (the systematic period). Information on hydrological variability and extreme floods can be completed using either or both palaeoflood hydrology and written chronicles of historical floods (Benito, 2006:2115).

Palaeoflood techniques are well suited to determine a series of flood peaks and/or upperbound flood peaks in ungauged river basins. The following methodology proposed by Benito *et al.* (2004:15) can be applied to locate and develop palaeoflood sites and process the results:

- i. Source topographical maps and aerial photos for an initial interpretation of potential palaeoflood sites.
- ii. Perform field inspections of the selected site/s (several if available). Search for and identify suitable flood indicators; flood deposits and other geomorphological evidence.
- iii. Excavate perpendicularly into the sediment banks, exposing the stratigraphy of sediment deposits.
- iv. Describe the stratigraphy with emphasis on identifying flood units.
- v. Collect samples for age dating.

- vi. Perform a topographical survey of the river reach, far enough upstream and downstream of the palaeoflood sites to record the bed slope as accurately as possible. Also survey the elevations of the strata at the various palaeo sites.
- vii. Perform hydraulic river modelling for the surveyed section and determine the discharges for the various flood deposits in the stratigraphy.
- viii. Compare the data with available historical data.
- ix. Perform a flood frequency analysis

3.3.1. Suitable topography for palaeoflood studies

Bedrock channels are the most suitable geomorphologic settings for reconstructing palaeoflood discharges because of their stable geometry (Benito *et al.*, 2004:16). As mentioned by Enzel (2009), incision of a river into the bedrock is very slow and occurs over geological time, therefore the cross-sectional profile of a bedrock river is assumed to have remained stable since the time when the flood occurred. The accuracy of the discharge estimations depends on the stability of the cross-section geometry through time. In stable, bedrock-confined channels, the channel geometry at the maximum stage of the flood is known.

Western Namibia's topography is dominated by the north-south Great Escarpment. To the east, the elevated semi-arid inland high plateau reaches elevations of 1000–2000 metres above sea level (masl), where mean annual rainfall reaches 350 mm. To the west, below the escarpment at an elevation of 0–1000 masl, is a low-lying arid to hyper-arid pediment and coastal plain along the Atlantic Ocean, which encompasses the Namib Desert (Grodek *et al.*, 2013:259).

Suitable bedrock canyons, for palaeoflood studies are found along the escarpment, incised by rivers en route to the low lying coastal regions. All of these are likely to have stable river channels with sediment deposits at suitable slackwater sites. Stable canyons are also found in most of the mountainous parts in the central and southern regions. For example, the Fish River has several rocky sections spread along its entire length.

The central northern parts and the eastern parts of Namibia are relatively flat, with less prominent bedrock channels. The Omatako River in the north and the Nossob River in the east has flat sandy meandering river channels, not suitable for palaeoflood studies.

The central highlands of Namibia, has a relatively high mean annual precipitation (MAP) of 350mm per annum. This relates to the rapid local erosion of sedimentary deposits, and it also

supports the vegetation of these sedimentary deposits. Burrowing animals, together with the roots of plants, cause bio-turbidity within the stratigraphy, which makes it less suitable for sampling.

Better sites for palaeoflood studies are found along the arid coastal region, west of the great escarpment. The arid southern parts are also likely to have suitable sites for the containment of slack water deposits and less bio-turbidity.

3.3.2. *The palaeoflood method*

The palaeoflood sites which were investigated in Namibia were selected in river channels incised into bedrock, in mountainous areas and canyons. The resulting slack-water flood deposits found in these sites commonly contain sedimentary structures and textures reflecting flow, energy, direction and velocities. Slack-water depositional environments commonly include: (i) areas of channel widening, (ii) severe channel bends, (iii) obstacle hydraulic shadows where flow separation causes eddies, (iv) alcoves and caves in bedrock walls, (v) back-flooded tributary mouths and valleys, and (vi) on top of high alluvial or bedrock surfaces that flank the channel (Kochel and Baker, 1982:355; Benito *et al.*, 2003b:1740).

Vertical excavations in the flood sediment bench in the tributaries expose the stratigraphic layers associated with individual flood events: refer to Figure 3.7, a photograph taken at an excavated sediment deposit site in the lower Fish River near the wilderness campsite, Echo Camp. The stratigraphic layers, numbered on the photograph, are definable by close inspection and tell-tale signs for the experienced eye; stratigraphical breaks separating individual floods are frequently represented by fine drapes of silt and clay (Benito & Thorndycraft, 2004:20). The textures of the layers are commonly dominated by sand and silt deposits. The description of the stratigraphy in Figure 3.7, in the column to the left of the photograph, displays thick dark horizontal lines between layers 5 and 6, and 6 and 7. These lines represent finer clayey deposits left behind by the subsiding flood. These thin clayey layers form a part of the flood unit beneath them. Refer to Table 3.3 for the legend depicting the finer sediments in the sequence of layers.

On top of sediment layers 5, 6, 7 and 8, aeolian, or wind driven, sand forms a cover layer. Refer to Table 3.2 for the legend depicting the descriptions of the stratigraphy. The layers are usually discernable by the homogeneous grading of the sand within these layers; wind driven sand usually has a constant size, which depends on the velocity of the wind: the grading takes

place naturally, since the finer particles are lighter and are blown away, and the larger and heavier particles do not become airborne.

Compare this with the alluvial particles in the strata, which are graded larger at the bottom and finer at the top (i.e. the clayey layers on top): the rising leg of the flood hydrograph has a higher velocity than the subsiding part of the wave, hence larger sedimentary particles are picked up and remain in suspension until the velocity and turbulence reduces, such as in a tributary alongside the main stream. At this point the coarser sediment is deposited on top of a previous flood bench (assuming that this flood is higher than a previous flood). During the flood peak and the subsiding leg of the flood wave, the water which flowed upstream into the tributary starts flowing out again and, after having deposited the larger sediment particles elsewhere in the tributary, only the finer silts remain in the water and settle out in a thin layer before the water level drops below the deposited layer.

One must be careful not to confuse the aeolian with the alluvial layers, since the dating of aeolian layers will not provide any useful result.

Flood chronology can be obtained from optical stimulated luminescence dating. Samples are collected by hammering opaque PVC cylinders (diameter at least 10 mm and length approximately 300 mm) into a clean vertical exposure until completely filled with sediment.

Figure 3.7 shows a vertical excavation in a flood sediment bank, indicating the stratigraphy of the flood units, as well as the sediment sample points. The description of the stratigraphy describes flood unit thickness, the material properties, the numbering and the grading of the sedimentary deposits. The ruler is graded in centimetres, showing an excavation depth of approximately 2.4 metres.

By means of a topographical survey, the elevation of the top of each layer is determined relative to the river channel, and is used as an indication of minimum flood stage and discharge associated with the stratigraphic unit. The age of the flood deposit and discharges that have been determined from hydraulic modelling of the river channel are then the basis for flood frequency analysis.

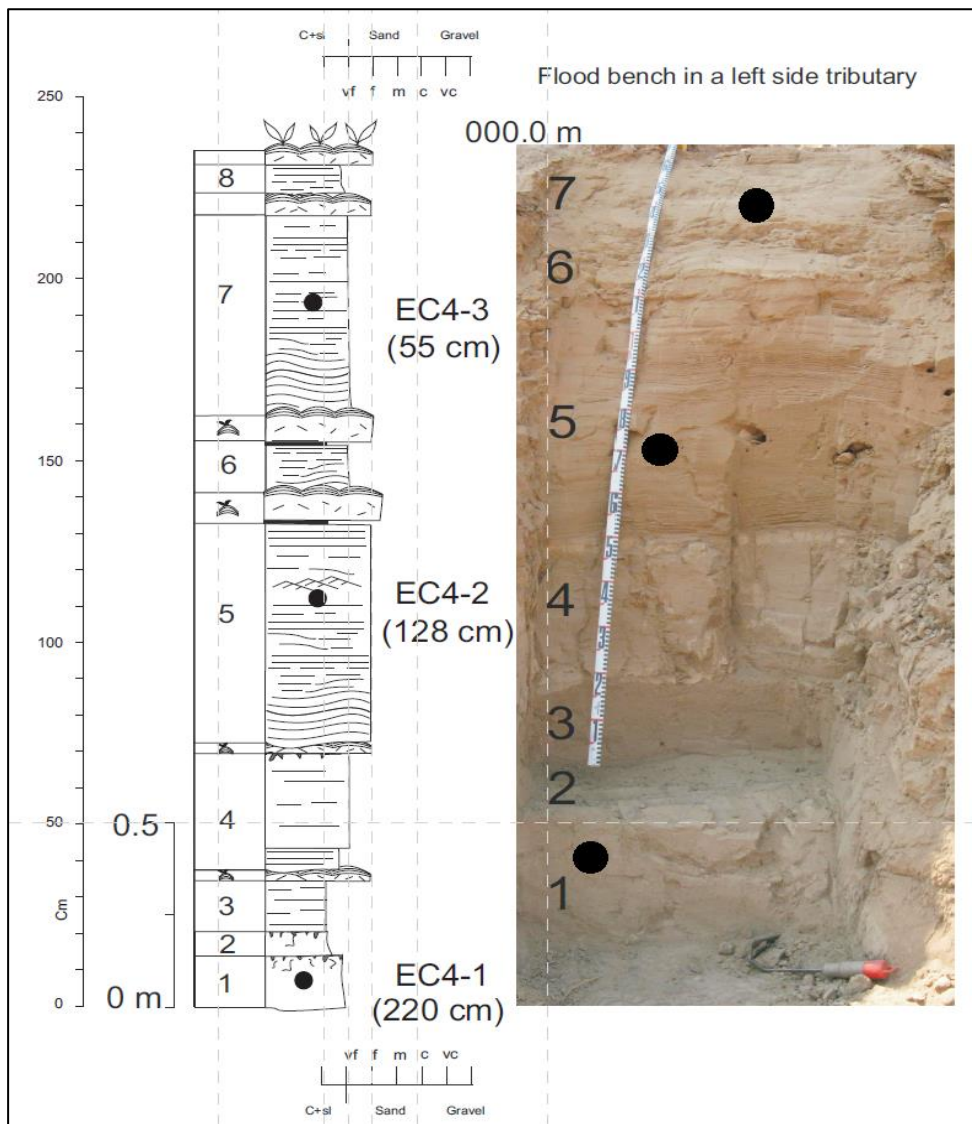


Figure 3.7. A stratigraphic column at a palaeo site at Echo Camp-4 (EC-4) in the lower Fish River.

Table 3.2. The Legend for the various symbols used to describe the stratigraphic layers.

LEGEND					
	Parallel lamination		Slope washflow		Charcoal
	Climbing ripples		Gravel levels		OSL sample
	Climbing ripples In phase		Aeolian sand		Bioturbation
	Ripples lamination		Carbonates		Bedrock
	Wavy Cross bedding		Mud cracks		Small aeolian coppice dunes
	Planar (2d) Cross bedding		Roots		Rip-up clast
	Trough (3d) Cross bedding				

Table 3.3. The Legend for the various symbols related to the finer sediment in the description of the sequence of layers.

<u>GRAIN SIZE</u>	
■	Clayed silt
C+sl	= Clay-Silt
S	= NUMBER OF SEQUENCE (each represents one flood only)

3.3.3. *The hydraulic model*

It is necessary to convert ancient flood levels (palaeo stage indicators) into flood discharge in order to produce hydrological data series which are representative of the flood regime (Lang *et al.*, 2004:43). The discharge estimates associated with the palaeoflood slack water deposits are calculated using the energy equation applied in a one-dimensional flow model. Flood stage indicators are surveyed, as well as several cross-sections in the river channel upstream and downstream of the palaeo stage-indicator sites. At each cross-section, signs of upper bound flood marks are searched for and also surveyed. In so doing one can determine the size of these floods and apply the findings in extreme flood hydrology models.

Applying the step backwater HECRAS model (Hydrologic Engineering Centre, 2001), with the bed slope and the discharge area of the river channel being known for each of the various stage indicators, the roughness coefficients are selected which best represent the upper bound flood marks along the river channel. These roughness coefficients are then applied to the model for lower stage indicators as well. The computation procedure of the HECRAS model is based on the solution of the one dimensional energy equation, derived from the Bernoulli equation

3.3.4. *An upper bound flood indicator*

In arid regions, such as the drier parts of Namibia, desert varnish, which forms on rock, is a common indicator of upper bound floods. Dorn (1989:561) indicated that rock varnish dating provides the time in the past for when a rock surface was last eroded or deposited.

The varnish is composed of clay minerals, oxides and hydroxides of manganese and/or iron. It appears as a blackish-brown layer on the top surface of a rock or stone on desert pavements.

When such a stone is rolled or displaced due to the flowing water, the varnish erodes off or the stone is turned upside down. In these cases varnish formation begins anew and the varnish ‘clock’ starts from zero.

Most other researchers agree that arid rock varnish formation is extremely slow, being barely perceptible after a few thousand years. Dorn & Oberlander’s (1982:321) observations point towards a very slow rate of formation, with many thousands of years required to develop a complete coat of the manganese-rich type; 3 000 to 5 000 years for a discernable coat, and much longer to form a solid coat.

Lui (2013:39) proposes that Varnish Microlamination (VML) is suitable for dating various desert landforms and archaeological features on which rock varnish has formed. He also stated that VML can be used as a technique for determining climate-based correlative age; to correlate and date various geomorphic features in deserts. Refer to Appendix D for an image of microstratigraphy under a light microscope, as well as an estimation of the ages associated with the separate stratigraphic layers (Lui, 2013:40).

3.3.5. *Palaeoflood fieldwork*

Identifying a relevant river for palaeoflood studies would require evaluating the suitable options against the criteria discussed earlier in this section; a bedrock channel for stable channel geometry, an arid to semi-arid area which would better preserve the stratigraphy of the sediment deposits (having less bioturbation), and site accessibility.

The more arid parts of Namibia are the west coast and the southern parts of Namibia, where the rainfall is as low as 50 mm per annum. Recent palaeoflood studies in the Kuiseb and Gaub Rivers (Grodek *et al.*, 2013) and Kahn River (Greenbaum *et al.*, 2014) deal with three prominent western flowing rivers. Looking toward the south, however, the most prominent south flowing river is the Fish River; its upper reaches lie within the central highlands of Namibia and it flows through the more arid parts of the country. It also has several canyon sections where the channel has been incised through mountainous areas. These provide suitable bedrock channels and tributaries for the settlement and preservation of flood sediment deposits.

3.3.5.1. *The palaeoflood study team and the equipment*

The author was granted the opportunity in 2009 to work together with a team of geomorphologists on the palaeoflood studies in the Kuiseb- and Gaub Rivers (Grodek *et al.*, 2013). This was the author’s first exposure to palaeoflood hydrology and the new techniques

used by these specialists: techniques in identifying suitable sample sites, exposing the preserved sediment stratigraphy, describing the stratigraphic profiles and surveying the river channel, as well as the sample site, to perform hydraulic calculations for the various flood units identified in the stages.

Through subsequent discussions and from a keen interest in extending palaeoflood studies in Namibia, particularly as regards the Fish River, a team of three geomorphologists who had also been involved in the Kuiseb study, agreed to assist the author. These were Professor Yehouda Enzel and Dr Tamir Grodek from the Hebrew University in Jerusalem, and Dr Gerardo Benito of the Spanish Science Research Centre; ‘Museo Nacional de Ciencias Naturales, CSIC’.

Refer to Appendix E for a picture of the team, taken at a Wilderness Campsite in the Gondwana Reserve, near the Fish River Canyon.

Aside from the surveying equipment, no special tools were required for the fieldwork. Basic equipment such as a small hand shovel, a regular paint brush, a straight edge tool, measuring tape, a hand levelling instrument, a notepad and pencil sufficed as well as organic sample containers, in case organic debris was found within the stratigraphic layers. The age of these organic samples could also be dated using carbon dating methods. A handheld water mist sprayer was used to wet the surface when describing the layer profile: a wet surface brings out better definition for assessing.

The survey equipment was a Trimble 5700 GPS instrument which works with satellite signals, a temporary base station and a handheld roving unit to pick up spot shots with which to generate the cross sections in geo-referenced space. Since no national survey benchmarks or trigonometric beacons were available in the immediate area for the exact calibration of the instrument position, the instrument reference position and height were determined from satellite data, which might differ fractionally from that of the national survey grid.

3.3.5.2. The selected time for the fieldwork

For practical reasons the most suitable time for a palaeo study in the Lower Fish River, or any part of Namibia, would be during the winter when temperatures are cooler and the ephemeral rivers are dry.

The planned study took place at the end of September 2010, on the turn of the season, however conditions were still favourable: the Fish River was not flowing which simplified the fieldwork and surveying.

3.3.5.3. *Identifying suitable palaeoflood sites*

Due to the size of the Fish River catchment area, two sites were selected, one in its upper reaches, upstream of the Hardap Dam, and one in the vicinity of the Fish River Canyon in the lower parts of the river.

These sites, specifically, would be used to determine upper bound flood peaks which could be used to update the flood hydrology model of Namibia. This would also be particularly relevant to existing and proposed future dams in the upper and lower reaches of the river.

Two sites were initially identified from Google-Earth images and topographical maps. These sites were discussed with the specialist team and agreed upon as a starting point. Refer to Figure 3.4 for the two sites.

The proposed upper site was identified on the farm Cimarron, 10 km upstream of the highest flood silt deposits at full supply capacity. However, discussion with a local farmer regarding the flood levels of the Hardap Dam added to the concerns regarding the influence of the back water action caused by the Hardap Dam during floods. Therefore a site further upstream was found on the farm 'The Analyst', owned by the Husselman brothers. The site on the topographical map is called Vogelkrantz. It lies approximately 30 km upstream of the FSL water line of the Hardap Dam, and 40 metres higher than the FSL of the dam. Several narrow sections were identified in the reach of river between Vogelkranz and Hardap Dam, which are likely to act as control points in the river: restrictions creating supercritical flow. Therefore the influence of the backwater effect of the Hardap Dam is not likely to reach the selected palaeoflood site.

The initial lower site was identified in the Gondwana Wilderness game reserve, which lies directly upstream of the Fish River Canyon. The site was initially proposed to be at the Horseshoe campsite but, after scouting the river further downstream, a better site was found at the Echo Campsite. Due to time constraints, the investigation focussed on this site without searching any further.

3.3.5.4. *Vogelkrantz site, upper Fish River*

The river- reach has exposed rocky ridges on the upstream as well as the downstream side: these ridges are approximately two kilometres apart, with a gravel bar and shallow sand bars in between. The rocky ridges indicate likely control points and hence a stable geometry. Refer

to Figure 3.8 for an aerial view of the site. The river reach has a right bend in it, with clear indication that the main channel flows along the outside of the bend and, typically, on the inside of the bend there is a gravel bar. A straight channel is preferable for one dimensional modelling; however the well-defined river channel, together with the stable channel geometry, provided good results.

The river reach has three small tributaries joining from the left bank side, which all contain alluvial sediment deposits. The gravel bar also contains sandy deposits in shallow depressions on top of the bar. During the survey of the cross sections, signs of upper bound floods were searched for and surveyed, to derive maximum flood peaks for the hydraulic model. One of the geomorphologists identified several probable upper bound flood markings at the different cross sections. However, upon entering these flood-indicator elevations into the flood model, it was found that not all of them are upper bounds; some of them turned out to be similar to large floods which had occurred in the past 50 years.

Profiles of five sediment deposit sites were excavated, of which three were found to have well defined stratigraphy, and only these three were developed, described and sampled. These were VK1, VK2 and VK4. VK is an abbreviation for the name 'Vogelkranz', a name on a 1:50000 topographical map allocated to the infrastructure site on the left bank of the river; a wind pump and watering point for livestock. VK1 and VK2 are on top of an old gravel bar, at least 300 years old, and VK4 is in a tributary on the left bank of the river. These sites are clearly marked on Figure 3.8. Figure 3.9 describes the stratigraphy profile of VK1 and also the discharges allocated to each layer: the discharge associated with the 1955 flood is $3\,610\text{ m}^3/\text{s}$, and the 1845 flood is $3,530\text{ m}^3/\text{s}$. (The profile description was done by Benito in 2010, and the discharge rates by the author).

Figure 3.9 shows a thin clayey layer which typically settles out during the subsiding leg of a flood; as the flood peak passes, a drop in flow velocity is experienced in the river, only finer material remains in suspension, since higher velocities are required for the coarser material to remain in suspension along the edges of the flood plain. The finer material then starts to settle and forms a cap on the coarser material which had been deposited during the rising leg of the flood.

The stratigraphy of VK2 and VK4 are presented in Appendix C.

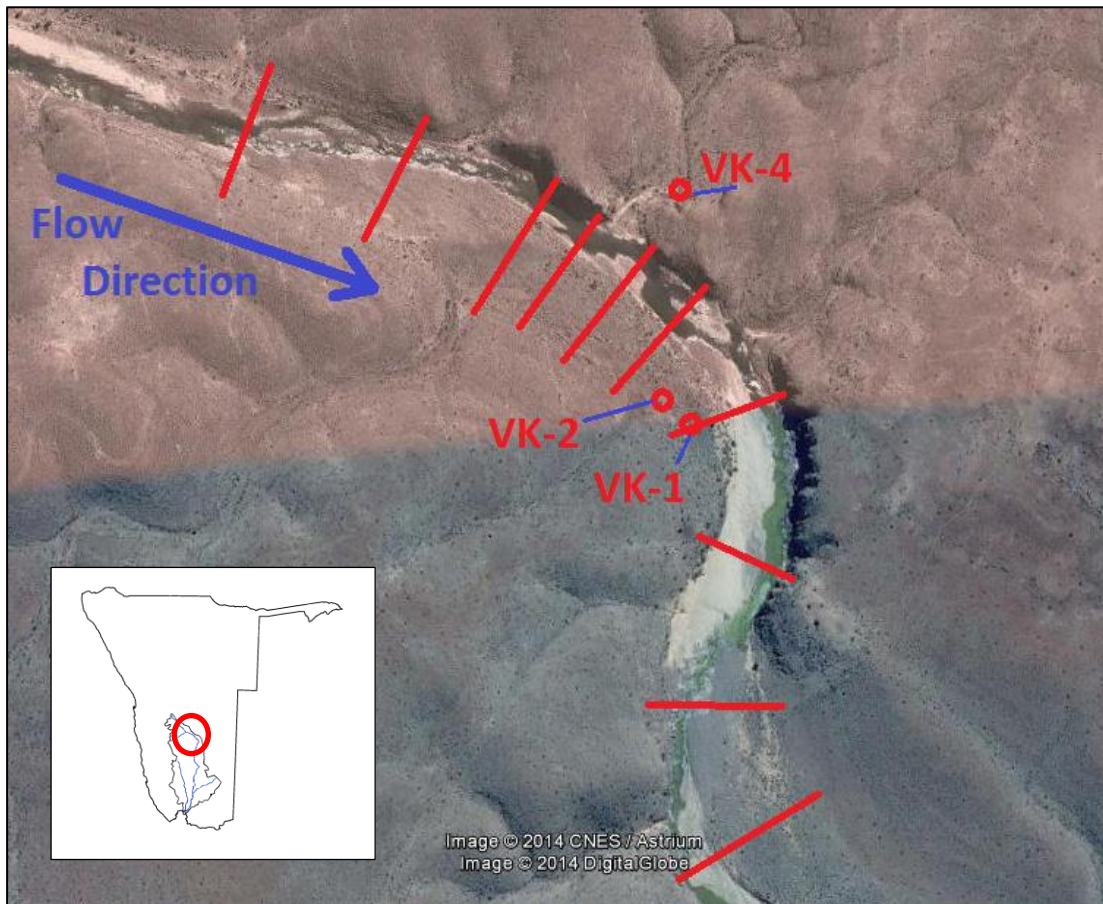


Figure 3.8: An aerial view of Vogelkranz palaeoflood site in the upper Fish River. Ten cross sections, as indicated, were surveyed to set up a hydraulic model. The distance from the upstream cross section to the downstream cross section is 1.8 km. VK1, VK2 and VK4 are three palaeoflood sampling sites.

Due to stretched resources, not all flood units within the stratigraphy were sampled, also not all of the samples that were taken were analysed. Table 3.4 indicates the identified layers in the stratigraphy at each site, the flood associated with each layer, and where determined, the year in which the flood took place. The flood units within the stratigraphy at each site, VK1, VK2 and VK4, are included in Appendix C.

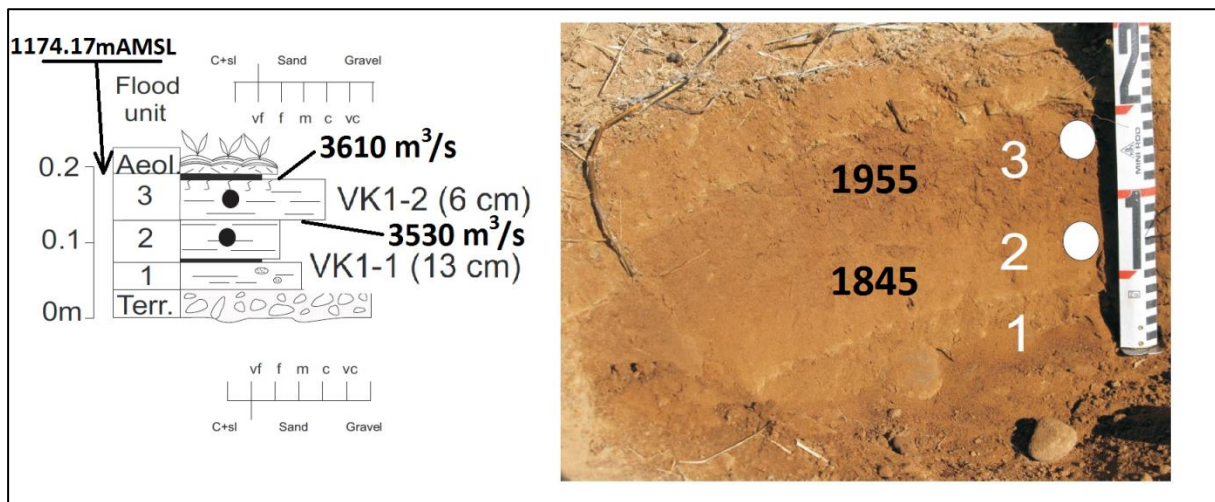


Figure 3.9: Palaeoflood stratigraphy at Vogelkranz in the upper Fish River; site VK1 on top of a gravel bar. The dates for samples VK1-2 and VK1-3 are 1845 and 1955 respectively.

A tree log was found wedged into a crack in the rock face of a cliff within the river reach investigated. The height of the log was approximately 13 metres above the adjacent lowest point in the river. This was thought to be an upper bound marking of floods at this point in the river. A carbon sample of the tree was taken and analysed in an analytical lab in the USA (refer to Appendix G for carbon dating results). The hydraulic model allocates a flood discharge rate of $4\,800\text{ m}^3/\text{s}$ to the flood which forced the log into the crack. The age of the log was found to be very young, at approximately 30 years before present; the test was performed in 2010, and the estimated date would therefore be 1980.

Upon reviewing corresponding flood peaks recorded at the Hardap Dam, it was found that an exceptionally large flood was routed through the dam in 1972. This flood caused flooding in the town Mariental. The discharge rate of the 1972 flood peak flowing into the Hardap Dam was estimated at $6\,100\text{ m}^3/\text{s}$ (Kovács, 1989:82).

Table 3.4: Summarised results for the palaeoflood study in the upper Fish River at Vogelkranz, on the farm ‘The Analyst’.

Profile	Flood unit	Discharge	OSL Date
		(m³/s)	
VK1	1	3 460	
VK1	2	3 530	1845
VK1	3	3 610	1955
VK2	1	2 260	
VK2	2	2 330	1700
VK2	3	2 370	
VK2	4	2 420	
VK2	5	2 480	1775
VK2	6	2 500	
VK4	1	1 410	
VK4	2	1 460	
VK4	3	1 490	
VK4	4	1 520	
VK4	5	1 560	
VK4	6	1 590	
VK4	7	1 630	
Upper bound floods in the reach			
Cross section 10			
	Colluvium	4 700	m ³ /s
Cross section 8			
	Tree log stuck in rock	4 800	m ³ /s
Cross section 3			
	Old surface	6 400	m ³ /s

By applying the square root method, the Vogelkranz floodpeak can be translated to the Hardap Dam; based on the difference in catchment areas, the flood peak at one point in a river can be translated upstream or downstream to another point, as follows:

$$Q_I = Q_0 \cdot (A_I/A_0)^{0.5} \quad (3.2)$$

where: Q_I = the transposed flood peak at the Hardap Dam

Q_0 = the flood peak at Vogelkranz

A_I = the catchment area at Hardap Dam

A_0 = the catchment area at Vogelkranz palaeoflood site

At Vogelkranz the catchment area is 11 200 km² and at Hardap Dam it is 13 600 km². Therefore, by applying the square root method the Vogelkranz flood of 4 800 m³/s is increased to 5 300 m³/s at the Hardap Dam. This approximates the recorded 1972 flood. The difference, however, could be attributed to various factors; a likely one being the time at which the log was wedged into the crevice; this could have occurred either before or after the time that the flood peak passed by Vogelkranz.

3.3.5.5. Camp Echo site, lower Fish River

In this lower part of the river, incision of the river into the surrounding countryside has cut two to three hundred metres deep, creating canyons similar to the renowned Fish River Canyon which is approximately 40 kilometres further downstream with incision depths of five to six hundred metres.

Numerous tributaries are found in the several kilometres upstream and downstream of the selected river reach, however the smaller ones are relatively steep with low storage potential for alluvial sediments. This phenomenon is due to the slower incision rate of local streams compared to the main river channel which gets more frequent discharge from the central highlands of Namibia: the local annual rainfall is much less than the rainfall in the upper reaches of the river.

From the 1:50 000 map several possible sites for sediment deposits were identified. Central to these sites was the Horseshoe Camp in the Gondwana Nature Reserve. The hut at this camp was used as a base station and the group split into two; one team to search the river upstream and the other to search the downstream sites for suitable sediment deposits. Refer to

Appendix F for a copy of the 1:50 000 map indicating the Horseshoe Camp as well as the routes walked to search for potential palaeoflood sites.

The scouting work took a full day and a hike of approximately 27 km over rough terrain. The route south passed by the Echo Camp which had several potential palaeoflood sites. This area was later selected as the most suitable site mostly due to its accessibility. A jeep trail used only by game rangers led up to the Echo Camp which was convenient for the transport of survey and other equipment.

The stratigraphy of several deposition sites was excavated and exposed, however, only four selected sites were developed, described and sampled. These were EC1, EC4 and EC6 where EC refers to Echo Camp. As with the Vogelkranz site, not all of the flood units within the stratigraphy were sampled, also not all of the samples that were taken were analysed. Refer to Figure 3.10 for the palaeoflood sampling points and cross sections.

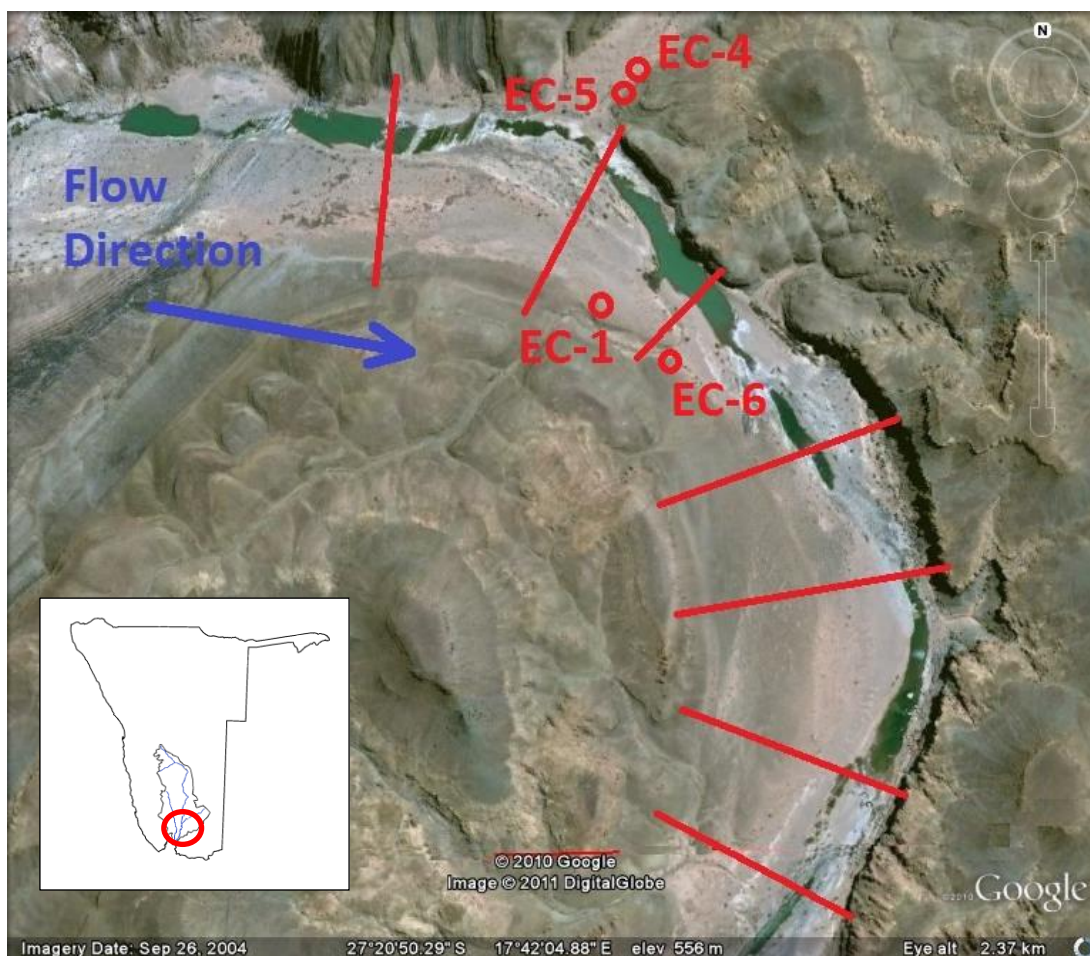


Figure 3.10: An aerial view of Echo Camp palaeoflood site in the lower Fish River. Seven cross sections, as indicated, were surveyed to set up a hydraulic model. The

distance from the upstream cross section to the downstream cross section is 2.1 km. EC1, EC4, EC5 and EC6 are the four palaeoflood sampling sites.

Figure 3.11 shows the stratigraphy of a sand bar at EC-6. The gravel on the surface of the sand bar which indicates stationarity of the sand bar despite flood waters passing over it; stones and pebbles were deposited on top of it during larger floods without washing it away. The samples in this stratigraphic unit were not dated. The discharge associated with flood unit 9 at the top of the sand bar is $3\,330\text{ m}^3/\text{s}$. The stratigraphy profile description was performed by Benito in 2010, and the associated river discharge rates were modelled by the author.

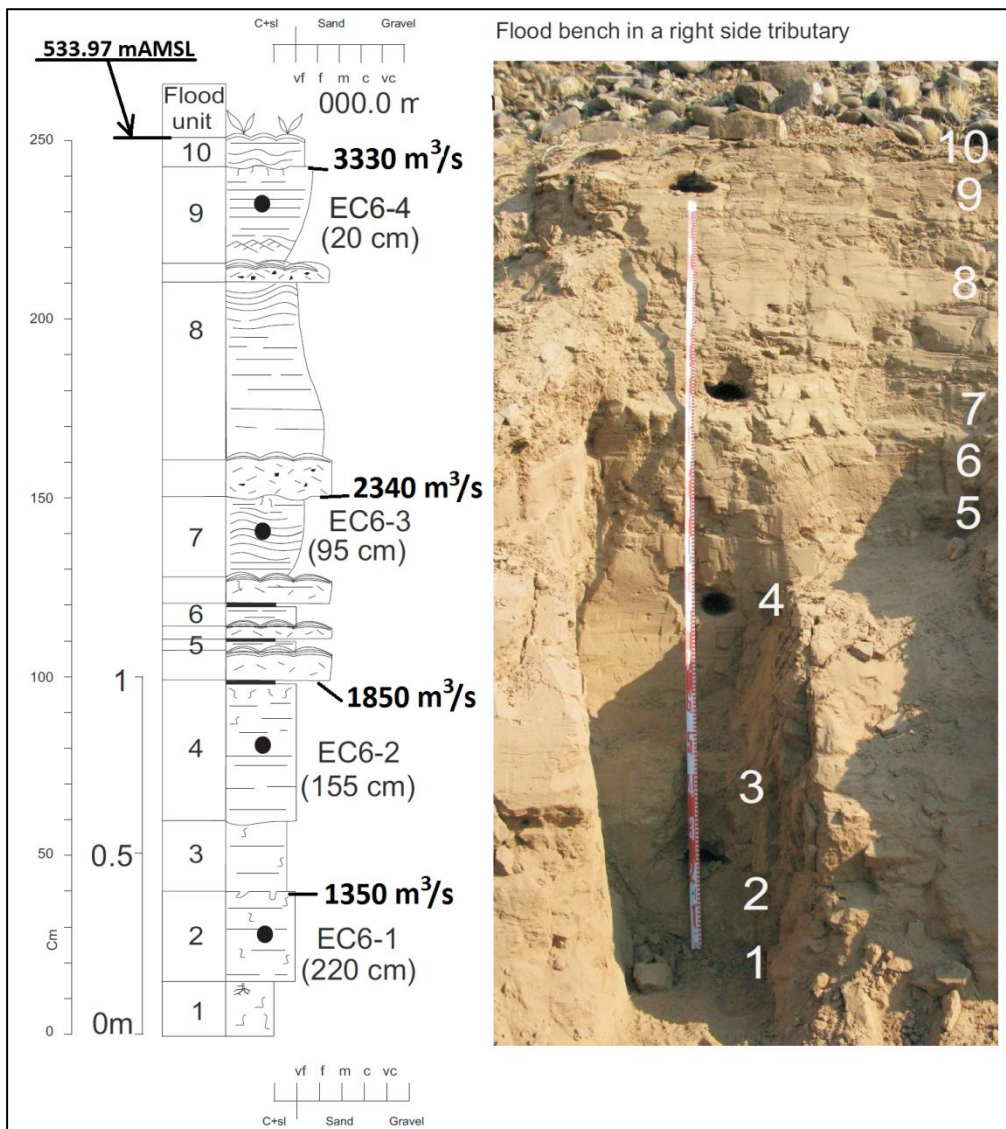


Figure 3.11: Palaeoflood stratigraphy at Camp Echo in the lower Fish River; site EC6 is situated on the side of a sand bar.

Table 3.5 indicates the layers identified in the stratigraphy at each site, the flood associated with each layer, and where determined, the year in which the flood took place. The flood units within the stratigraphy at each site EC1, EC4, and EC6 are included in Appendix C.

Table 3.5: Summarised results for the palaeoflood study in the lower Fish River in the Gondwana Nature Reserve at Camp Echo.

Profile	Flood unit	Discharge	OSL Date
		(m³/s)	
EC1	1	8 690	1640
EC4	1	510	1865
EC4	2	550	
EC4	3	590	
EC4	4	720	
EC4	5	970	
EC4	6	1 090	
EC4	7	1 450	1895
EC6	1	1 180	
EC6	2	1 350	
EC6	3	1 490	
EC6	4	1 850	
EC6	5	1 950	
EC6	6	2 100	
EC6	7	2 340	
EC6	8	2 950	
EC6	9	3 330	
EC6	10	3 400	
Upper bound floods estimated in the reach			
Cross section 6			
	Old surface	16 140	m ³ /s
Cross section 6			
	Flooded surface	15 900	m ³ /s
Cross section 4			
	Old surface	14 900	m ³ /s

At EC4, over a period of 30 years, seven flood units were deposited ranging from 510 m³/s at flood unit 1, up to 1 450 m³/s for flood unit 7 which is at the top. Floods of this size are quite common for the Fish River, which has a catchment size of approximately 60 000 km². This data could provide valuable information regarding the climate for the period from 1865 to 1895. However for the purposes of this research the focus was on extreme flood events and, therefore, upper bound flood indicators were also searched for and surveyed. These produced flood peak discharges of 14 900, 15 900 and 16 140 m³/s.

3.3.5.6. Results of the palaeoflood study

The palaeoflood study produced extreme flood information in the upper and lower Fish River. At both locations these upper bound floods increased the previous maximum historical floods recorded in the upper Fish River; the largest recorded flood at the Hardap Dam, upper river area, is presently 6 100 m³/s measured in 1972 (Kovács, 1988:82). This has been increased to beyond 6 400 m³/s. At Ais-Ais, which lies downstream of Echo Camp, the maximum recorded flood peak is 5 460 m³/s measured in 1972 (Kovács, 1988:82). The upper bound peak at Echo Camp is 16 140 m³/s.

The smaller flood peaks, determined from the sediment captured in the stratigraphy of sediment deposits, also provided insight to the value of palaeoflood hydrology. The results of the stratigraphic study, discharge rate and years before present of the floods, provide only censored data regarding a series of floods over a time span. This is due to the threshold of flood recording, which is raised after every subsequent larger flood. These results could, however, be used to improve flood risk estimation by lengthening the flood record beyond that of the instrumental gauging station data.

However, the results of the smaller floods were not analysed further for this study.

3.3.5.7. Confidence levels in Palaeoflood data

Confidence levels in the age of upperbound floods, based on observation of Old Surfaces, has been fixed at approximately 3 000 to 5 000 years by Dorn and Oberlander (1982:321). This is the time required for a discernable coat desert varnish to form. Based on these findings, the author allocated the average age of 4000 years to the upperbound floods of the palaeoflood study at the Vogelkranz and Echo sites.

When calculating the discharge associated with extreme flood peaks, Enzel (1994:308) found that changes of up to +20% in Mannings n-value produced less than 5% change in corresponding flood discharge, this however was for sub-critical flow conditions in a specific river.

The author checked the Vogelkranz and Echo discharge calculations using Manning's n-values ranging from 0.025 for a relatively smooth channel, and increasing the n-value in steps of 0.005 up to 0.030, 0.035 and 0.040.

The Manning values of 0.025 and 0.030 produced discharge figures differing by less than one percent. Mannings n-value between 0.03 and 0.035 produced discharges differing on average by 7%, and between 0.03 and 0.04 the average difference is 9%. For the upperbound flood peak results, the n-value which produced the best correlation between the different cross sections at Vogelkranz was determined at 0.030, and at Echo Camp was 0.035.

The selected n-values at Vogelkranz and Echo Camp are similar to a figure generally used by the DWS; from discussion with Wessels (2014), the DWS Flood Studies division found that generally a Manning n-value of 0.032 provides the most suitable results for extreme flood calculations in large rivers.

3.3.6 *Comparing the upper bound flood peak with systematic data*

The Echo Camp palaeo site lies approximately 60 km south of the Seeheim flow gauging station in the Fish River, and the Ais-Ais flow gauging station lies a further 70 km south. Using Equation 3.2, the Echo Camp upper bound flood peak is converted to the Seeheim, as well as to the Ais-Ais flow gauging sites. The catchment area at Echo Camp is 57 000 km². At Seeheim the catchment area is 46 400 km² and at Ais-Ais weir it is 63 300 km². With the peak discharge at Echo Camp determined 16 140 m³/s, the peak discharges translated to Seeheim and Ais-Ais are 14 500 m³/s and 16 970 m³/s respectively.

Figure 3.12 and Figure 3.13 shows various probabilistic distribution models plotted for the recorded systematic data in the Fish River at Seeheim and at Ais-Ais. Indicated in both is also the plot position of the palaeo upper bound flood peak translated to these sites. The 'Proposed' line, which follows the LP3 distribution, represents the systematic data. This line passes in close proximity to the palaeoflood point, which strengthens the hypothesis that the RMF is approximately a 10 000 year flood. From the work of Dorn & Oberlander (refer to Section 3.3.4) the upper bound flood peaks occurred approximately 4 000 years ago, which is the time required for a discernable coat of Desert Varnish to form.

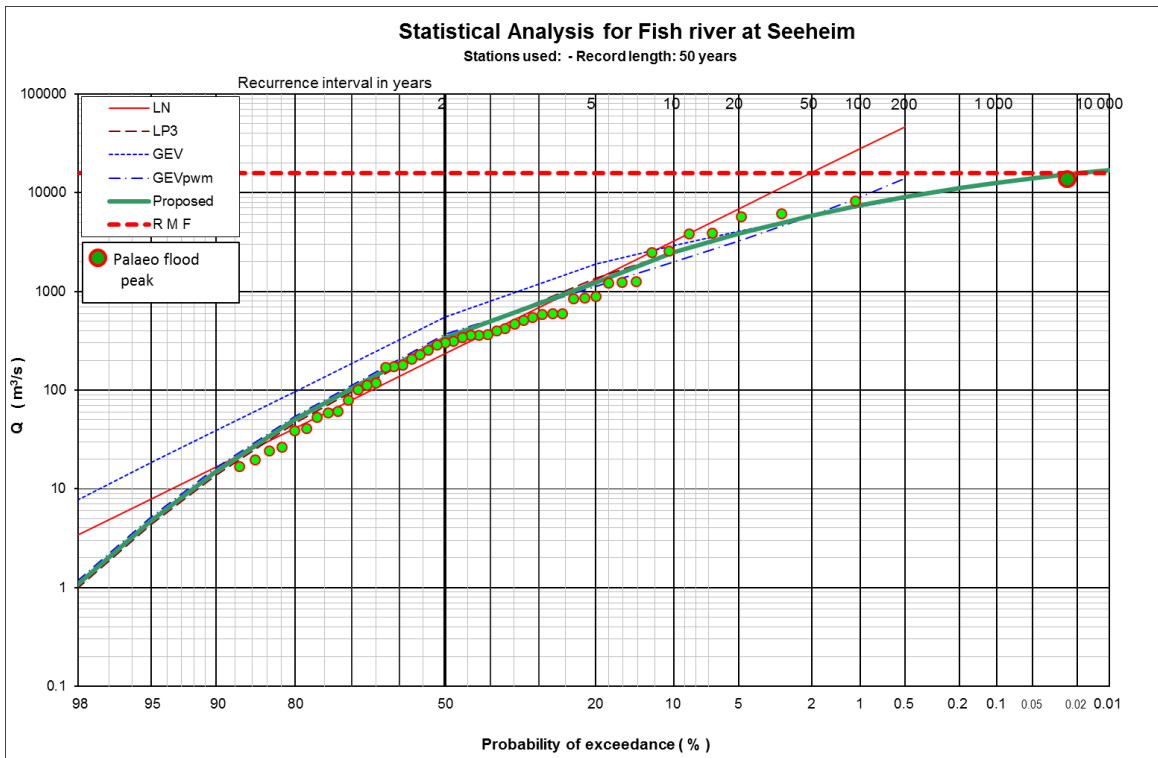


Figure 3.12: The palaeoflood point and various probabilistic distribution models are plotted for the 50 years of systematic data recorded at Seeheim in the Fish River, upstream of the palaeoflood site at Echo Camp.

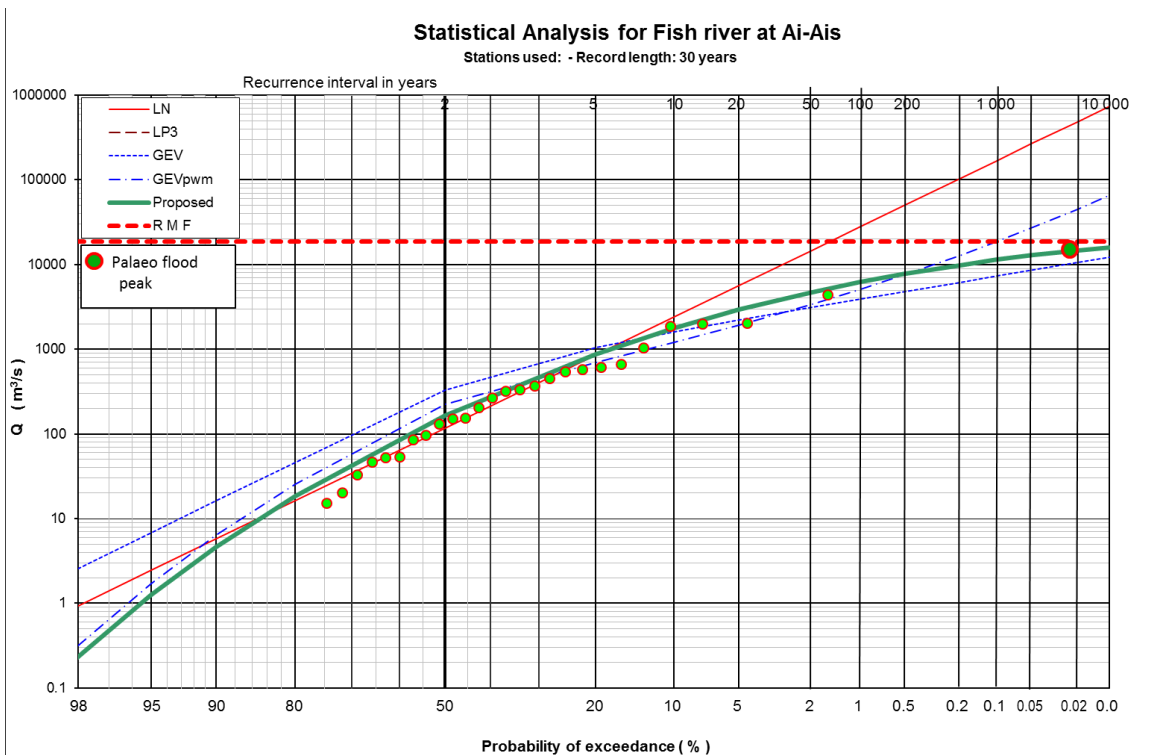


Figure 3.13: The palaeoflood point and various probabilistic distribution models are plotted for the 30 years of systematic data recorded at Ais-Ais weir in the Fish River, downstream of the palaeoflood site at Echo Camp.

3.4. Data on the earthfill-unit cost for embankment dam rehabilitation and raising

The process of optimising risk reduction activities over a portfolio of dams requires an evaluation of the increase in the flood discharge capacity of a dam versus the reduction in risk associated with this increase.

This principle is discussed in more detail in Chapter 5; however, the data required to evaluate this increase in discharge capacity is the cost associated with modifications to the dam to accommodate a larger discharge capacity. These modifications, or rehabilitation, involve full scale construction activities, from site establishment to large scale earthworks, as well as upgrading of appurtenant structures.

3.4.1. The earthfill-unit cost approach

A simplistic approach to determine a unit cost for the rehabilitation of embankment dams, specifically the raising of an embankment dam NOC, is to determine a unit-rate average, based on the rehabilitation cost of several dams. This approach includes judgmental decision making by the author and is considered a first attempt to obtain real figures on the unit cost of earthfill material.

This empirical approach includes all the costs associated with the rehabilitation of a dam, within the unit cost of earthworks. These are the cost of site establishment, the cost of appurtenant structures associated with the raising, as well as the cost of the earthworks. Little data was used and the result is likely to differ as more data becomes available.

Since the result is used as a constant for all dam cases investigated in this research work, a slight variation up or down in the cost is unlikely to have an impact on the outcome.

3.4.2. Determining the earthfill unit rate cost for rehabilitation of embankment dams

With the permission of the DWS of South Africa, a consultant involved in the rehabilitation of several state owned dams in South Africa, provided the author with the priced schedules of quantities for the rehabilitation of these dams.

These dams, ranging from 20 to 49 metres high, are Makazana-, Glenbrock-, Grassridge, Cata and Mnyameni dams. All of these dams had earth embankments which were raised or modified to either accommodate larger floods or improve structural stability.

Of these five dams, three had significant earthworks components while the other two had relatively small volume earthworks. These two dams distort the unit rate cost of the dams relative to the earthworks, since their costs per cubic meter of compacted soil is very high in relation to the others. Therefore they were not included in the average cost calculation. Refer to Table 3.6 for the cost of the dam rehabilitation, as well as the average unit rate per cubic metre of placed soil. The costs of the works are 2010 value. Appendix H provides a description of the work undertaken at each of the dams, as received from the consultancy firm involved in the rehabilitation process.

Table 3.6: The unit rate cost per cubic metre of placed soil for rehabilitation and raising of earth embankment dams. The project costs are 2010 values, excluding VAT.

	Project Name	Volume of earthworks undertaken	Total cost of the project excl. VAT	Unit cost of earthworks related to the project	Average unit cost per cubic metre of earthfill
		(m3)	(R Million)	(R)	(R)
1	Makazana Dam rehab	25 800	20 .1	778.29	839.67
2	Glenbrock Dam rehab	66 000	33.2	503.75	
3	Grassridge Dam rehab	86 000	106.4	1 236.99	
4	Cata Dam rehab	15 300	23.2	1 514.24	Excluded from average
5	Mnyameni Dam rehab	3 500	22.5	6 426.82	Excluded from average

The unit cost of rehabilitation was escalated to 2013 costs to adjust for inflation. The escalation rate was estimated at 8% per annum.

Therefore the final, all inclusive, unit cost per cubic meter of earthworks for dam raising and rehabilitation is R 1 057.00 excluding VAT. This value will be used in Chapter 5 to determine the cost of raising embankment dams to increase the flood surge component of dam freeboard.

4. Updating the Namibia Regional Maximum Flood model

Extreme flood hydrology forms a significant input to the risk model presented in this dissertation: the probability of extreme flood events directly relates to the risk associated with this model.

In Namibia extreme flood hydrology has been based on the empirically established upper limit of flood peaks, namely the Regional Maximum Flood (RMF), however other models have also been applied. The RMF for Namibia is described in the Technical Report 137 (TR 137); '*Regional Maximum Flood Peaks in Southern Africa*', of the South African Department of Water Affairs (Kovács, 1988), which was updated in 2014 for Namibia only (Cloete *et al.*, 2014). Practitioners of the RMF method consider these floods to have annual recurrence intervals of up to 10 000 years, as mentioned by Van der Spuy (2008).

In the TR 137 Kovács mentions that the K-value boundaries for Namibia are tentative due to the relatively small data base at the time, the short representative periods, and less accessible hydrologic parameters such as the three-day maximum storm rainfall.

Since the compilation of the TR 137, nearly 30 years of additional data have been gathered, and several new gauging stations have been added to the list.

According to Tasker and Stedinger (1987:256), 'one of the best future research opportunities in flood-frequency analysis is the incorporation of palaeoflood data in regionalised flood frequency analysis'. Palaeoflood hydrology is a reconstruction of the magnitude and frequency of recent, past, and ancient floods (approximately 50, 500 and 5 000 years ago, respectively) using geological evidence (Baker *et al.*, 2002:1). In hyper-arid regions such as the drier parts of Namibia, flood evidence is well preserved in the form of sediment deposits. These sediment deposits, also known as slack water flood deposits, are stage indicators of floods and can be preserved in stratigraphic sequences (Benito *et al.*, 2003a:108).

In this dissertation, the concerns of Kovács are addressed by adding 38 additional flood peak sites to the existing 64 flood peaks which were used in the TR 137, and also by increasing the flood peaks of three of the 64 floods listed in the TR 137. The flood peak data increased from 2 759 years of recorded data used in the TR 137, to 4 169 years, taking into account the additional 38 stations as well as the longer recording period for several of the original stations.

Six palaeofloods are also included in the data: two in the south flowing Fish River (unpublished), two in the Kuiseb, one in the Gaub (Grodek *et al.*, 2013:260) and one in the Khan River (Greenbaum *et al.*, 2014:155), all of which are west flowing rivers. The Fish

River flood peaks and one of the Kuiseb River floods are considered upper bound floods for these rivers; floods which had not been exceeded in a very long time, at the scale of thousands of years (Grodek *et al.*, 2013:261).

The Kovács K-values were revisited with the new data- and, taking into consideration the maximum three day rainfall peaks, the topography and geology, new K-zones were delineated and are presented in this dissertation.

The K-value zone boundaries are likely to increase as data records are extended over time: recorded extreme flood peaks have a low probability of being exceeded; however, if they are exceeded, the regional K-value will move upwards. By employing palaeoflood hydrology at more of the remote river systems in Namibia, a significant contribution can be made to flood data and extreme flood values and will assist future researchers in populating the open spaces of Namibia for which no flood data is presently available.

4.1. Alternative extreme flood models

Dams engineers in other countries, which do not have a RMF model developed in their respective countries, could still use the quantitative risk approach discussed in this dissertation. They could apply an alternative extreme flood model, however alternative models must be used consistently throughout a portfolio of dams to obtain comparative results.

Three basic methods available for the estimation of maximum flood peaks are the empirical, the probabilistic and the deterministic methods. Having been discussed in more detail in Section 2.2.1., these are only discussed briefly here, together with concerns related to the validity of the models.

4.1.1. Extreme flood models

- The empirical method

This approach considers maximum observed flood peaks and associated catchment areas in hydrologically homogeneous regions. From a graphical presentation of the data, envelope curves are drawn for the points which is then form an upper limit of expected flood peaks; Q_{\max} (Kovács, 1988:1). If the observations cover relatively large areas and periods, the chances of including extraordinary events in the database are fair. This, in particular, makes

palaeoflood hydrology attractive for the further development of the empirical method, by adding regional extreme flood peaks to the body of data.

- The probabilistic method

This approach predicts flood peaks based on the extrapolation of a theoretical probability distribution fitted to annual maximum flood peak records in the same river or region. A low probability of 0.0001 is allocated to extreme flood events.

- The deterministic method

This approach predicts a hydrograph and an associated flood peak based on storm rainfall input and estimated storm losses. For extreme flood peaks, the presumption is that the Probable Maximum Precipitation (PMP) is falling on a saturated catchment area, and this produces the Probable Maximum Flood (PMF). By definition the PMF has no annual recurrence interval, but arbitrarily it was assigned a return period of 10 000 to 1 000 000 years at the upper and lower confidence limits for flood frequency analysis (National Research Council, 1985:241).

4.1.2. *Concerns regarding the extreme models*

- The empirical method

There is an uncertainty regarding the boundaries of the homogeneous regions. Very small catchment areas cannot be accounted for because of unusual hydrological features (Kovács, 1988:1).

- The probabilistic model

The maximum peak is associated with a very low probability, most often $P = 0.0001$ i.e. an annual recurrence interval of 10 000 years, which is entirely arbitrary. Also the estimate is obtained from extrapolation of a theoretical probability distribution fitted to annual maximum flood peaks. The extrapolated period is usually 100 to 500 times longer than the period of the record. The representativeness of such a short period sample is unknown (Kovács, 1988:2).

- The deterministic model

A remark by Enzel *et al.* (1993:2294) regarding the PMF is worth noting: ‘The inconsistency between PMF estimates and the actual regional data (gauged, historic, and palaeofloods) is a cause for concern’. It may indicate that for this hydrological region, either the understanding

of extreme rainfall events used in constructing the PMP and the subsequent basin responses is deficient, or is a result of failure in the model construction.

Kovács (1988:3) proposed that the cumulative error made in the PMF flood peak estimation may reach the magnitude of the PMF itself.

Benito *et al.* (2006:2120) commented on the reliability of the PMF methodology: ‘In the USA the extrapolated discharges of the 10 000 year palaeoflood annual recurrence interval are between 5% and 20% of the calculated PMF’.

4.2. The study area

The study area discussed in this research is limited to the national boundaries of Namibia and does not include neighbouring countries. The RMF K-values for rivers shared with neighbours need to be revisited, taking into consideration the hydrology of the entire catchment area. Co-operation and data sharing with these neighbouring countries will assist in this regard. For example, a palaeoflood study by Boshoff and Kovács in 1993 in the lower Orange River determined that approximately 550 years before present (in 1450) a flood peak of 32 000 m³/s passed down the river (Boshoff *et al.*, 1993:26). Upon review, Boshoff recalculated the flood peak at 28 000 m³/s. This finding could increase the K-value for the Lower Orange River from 2.8 to 3.18. Further studies to verify these results, using newer palaeoflood techniques, will assist in updating TR 137 for this shared river, which will benefit both neighbouring countries.

Some areas within Namibia such as the Namib Desert, the northwest and parts of the Kalahari are poorly represented regarding flood peaks and rainfall data. Data capturing in these remote areas will assist in increasing the reliability of flood modelling in Namibia.

This study considers only catchment areas in the Transition Zone (from 1 to 100 km²), and the Flood Zone (larger than 100 km²). The 'Storm Zone' for areas smaller than 1 km² is not included and can be used as described in TR 137 (Kovács, 1988). Refer to further discussion in section 4.8.

4.3. Palaeoflood peaks

Several palaeoflood studies have recently been conducted in Namibia; the WADE study (Flood Water Recharge of Alluvial Aquifers in Dryland Environments) in the Kuiseb and Gaub Rivers from 2006 to 2009, as well as studies in the upper and lower Fish River in 2010 (discussed in section 3.3), and in the Khan River in 2006 (Greenbaum *et al.*, 2014:163). Six

high flood peaks were estimated at these sites with evidence indicating that four of these peaks are upper bounds, i.e., the highest floods in possibly thousands of years.

Two of the upper-bound peaks were estimated in the upper and lower Fish River with discharges estimated at 6 400 m³/s at Vogelkranz upstream of Hardap Dam, and 16 140 m³/s at Echo campsite in the Gondwana Wilderness Park near the Fish River Canyon. One upper bound flood peak of 1 600 m³/s was estimated at Khan Mine downstream of Usakos (Greenbaum *et al.*, 2014:163). Two flood peaks in the Kuiseb River, of which one is an upper-bound flood, were estimated at a site approximately 2 km upstream of its confluence with the Gaub River. The two remaining floods were not considered upper bounds but were still seen as significant; one in the Kuiseb River approximately 35 km downstream from its confluence with the Gaub River, with a peak of 800 m³/s and the other in the Gaub River just upstream of its confluence with the Kuiseb River estimated at 400 m³/s (Grodek & Enzel, 2007:31).

4.4. Data sources and approach

First flood peak data is required to determine the updated Francou-Rodier K-values for Namibia. These K-values provide a first step in delineating homogeneous regions, based on the K-values. However since flood data is incomplete, in most cases less than 50 years of recorded flood peaks, it could take several hundreds or even thousands of years to obtain a complete set of data.

Therefore a second and third step are required, such as three-day rainfall, topography, geology, etc. to provide better definition of the hydrologically homogeneous regions over which these K-values apply.

If, however, a complete data set of flood peaks were available, one would find that all catchments within a homogeneous region are likely to have the same K-values. For example, for two catchment areas within a region, one may have recorded an abnormal extreme flood event while the other did not experience that abnormal event. Therefore one cannot draw a line between the two catchments and differentiate between them based on short term recorded history. Other natural indicators also contribute to the delineation of flood zones, such as the geology and topography since these were formed over geological time. Hence, if these indicators are similar for the two catchments, then the nature of extreme flood events is also likely to be similar for the two catchments.

The approach therefore would not be simply to join points of equal height, like ‘contour’ lines, but rather to use a broad brush approach which favours delineation along lines of topography, geology and even vegetation types, which are indicators of climate and basin characteristics.

4.4.1. The recorded data

The first set of data, required to determine the latest K-values, are the flood peaks which are discussed in sections 3.2 and 3.3; these flood peaks were taken from systematic flow gauging stations provided by NDWA, as well as palaeoflood peaks. Another source of flood peaks is found in Kovács’ (1988) report, which he used to determine K-values. Many of these Kovács flood peaks do not appear in the 2010 DWA data set, hence some of the TR 137 report data are still valid and record the dominant floods to this day.

Historical writings in national archives are also a source of data for flood peaks; however, an attempt by the author to tap from this source proved not to be useful, since very few of these writings were quantified. The majority of them were just qualitative descriptions such as ‘a big flood’ or ‘the flood reached the house’. Until such descriptions are quantified they will not add value to flood peak data in Namibia.

Rainfall data, specifically the three-day rainfall data, is also an indicator of events which potentially lead to extreme flood events (Kovács, 1988:9).

4.4.2. The natural indicators

Additional information required to delineate regional flood regions is related to the physical characteristics of the country. These characteristics include the topography, the geology and vegetation types which relate to soil types as well as climate conditions. These are discussed further in section 4.6.

4.5. The Francou-Rodier K-values

Franco and Rodier (Kovács, 1988:3) found that when flood peaks were plotted against corresponding catchment areas, then the envelope curves for hydrologically homogeneous regions were straight lines, specifically for catchment areas larger than about 100 km². Refer to Equation (4.1), and also to Figure 4.14 for the Franco Rodier curves applicable to Namibia.

$$\text{Francou-Rodier equation} \quad Q = 10^6 \left(\frac{A}{10^8} \right)^{1-0.1K} \quad (4.1)$$

where

- Q = flood peak (m³/s)
- 10⁶ = mean annual discharge from all drained land on earth (m³/s)
- A = the drainage area (km²)
- 10⁸ = the total drained land surface on earth (km²)
- K = the regional coefficient expressing relative flood peak magnitude

Kovács proposed in the TR 137 that the gross catchment area should be changed to the effective catchment area, the part which actually contributes to flood generation. Hence in Equation (4.1), the area (A) in km² is replaced with effective area (A_e) in km².

$$\text{Kovács equation} \quad RMF = 10^6 \left(\frac{A_e}{10^8} \right)^{1-0.1K} \quad (4.2)$$

Assuming that the $RMF = Q_{max}$ for the maximum flood peak measured/estimated at each gauging site, then the equation can be rewritten to find the K -value for a flood peak:

$$K = \frac{1}{0.1} \left(1 - \frac{\log\left(\frac{Q_{max}}{10^6}\right)}{\log\left(\frac{A}{10^8}\right)} \right) \quad (4.3)$$

The K -value was calculated for each flood peak; refer to Appendix B.

4.5.1. K -value results

As calculated in the TR 137, the highest K -values of 5 occurred near Windhoek in Central Namibia. The lower Fish River, however, has a higher K -value of 4.6 which was previously indicated as 4.0 in the TR 137. This has resulted from the palaeoflood study performed there. Values were generally the same as in the TR 137; however, the additional flood peaks extended the flood zone boundaries in the central Kalahari, in northern and southern Namibia.

As discussed in the TR 137, negative K-values do occur where the catchments are very flat, permeable, dry or large and swampy. Such cases were encountered with the Black Nossob River which runs through the Kalahari. It has a dry flat catchment area of 8 160 km² measured upstream of gauging station Mentz, with a maximum measured flood of only 33.6 m³/s. In this case the K-value equalled -0.93. Another case is the Kwando River which flows from Angola, crosses the Caprivi Strip at Kongola, and passes on into Botswana. Upstream of Kongola, the catchment area is 170 000 km², with flat marshland in Angola, and the maximum flood peak measured is only 120 m³/s. This produces a K-value of -4.15.

4.6. Delimitation of maximum flood peak regions

The parameters which govern the delimitation of the regional flood boundaries are the calculated Franco-Rodier K-values, the maximum recorded three-day storm rainfall depths, the topography, geological features (soil permeability) and, to a lesser extent, the vegetation types. Of these factors the K value is the most important, followed by the three-day rainfall.

The three-day rainfall is relatively high in the east and north-eastern part of the country, however the K-values are not. This can be attributed to the unconsolidated sediments of the Kalahari Dessert: vegetation in the central and north Kalahari is tree savannah and woodland, which indicates significant rainfall, but the small slope (1:4 000) and high infiltration significantly reduce the flood peak discharge.

4.6.1. The Uhlenhorst anomaly

Before delineating the flood zones, an event worth noting occurred near the Uhlenhorst settlement which lies on the western rim of the Kalahari, roughly 100 km northeast of the town Mariental. The average rainfall in this area is 250 mm per annum. However, in 1960 a significant rainstorm, with precipitation measuring between 400 mm and 489 mm, fell over a period of 12 hours on several neighbouring farms, an area of approximately 115 km² (Schalk, 1961:444).

The storm started on 24 February 1960 at approximately 23h00 and ended at 11h00 the next morning. In the 24 hours prior to this downpour, approximately 35 mm of rain had fallen in the same area. Hence the soil was already drenched before the large rainstorm.

A larger area of approximately 1 000 km² surrounding the Uhlenhorst area received at least 100 mm of rainfall. Schalk (1961:444) estimated that approximately 230 million cubic meters of water had precipitated. He also determined by measurement that approximately half of the water infiltrated into ground water reserves or aquifers and the balance was lost through evapo-transpiration. After three months, all the pans and wetlands were dry again.

Overland flow occurred where water collected in the natural pans commonly found in the area, and also in depressions between the dunes. As the pans filled up, they started spilling toward the southeast in the direction of natural drainage. The flowing water, however, was stopped by dunes and could not reach the Auob River channel several kilometres south of the flood area (Schalk, 1961:444).

The sudden infiltration of a large portion of the rainwater can be attributed to seepage underground through aligned karstic hollows (Goudie, 2007:32). There are numerous depressions and pans in the area. According to Goudie (2007:27), the south western part of the Kalahari, called the Weissrand, is underlain with calcretes with considerable thickness; over 30 metres at places. These thick, pure calcretes may be susceptible to karstification (Goudie, 2007:27). Karst is highly permeable and hence would have contributed significantly to a loss of surface run-off.

This event indicates that after considerable rainstorms in the Kalahari, surface discharge could be significantly reduced or absorbed by the barren sandy landscape. Hence a low K-value is associated with the sandveld dessert areas.

4.6.2. Delimitation of the maximum flood peak regions

Several steps were taken to determine the boundaries for the K-value isolines. These were followed in a step by step order from most important parameter, the K-values, to the least influential parameter, the vegetation distribution. Some fine-tuning was done by revisiting the initial parameters after the delimitation process was completed. The flood zones are grouped similarly to the TR 137, starting at 2.8 and increasing incrementally in steps of $\Delta K = 0.6$ up to $K = 4.6$ and then with $\Delta K = 0.4$ up to $K = 5$. The highest K-value for Namibia is five (5).

The construction process for the TR 137 map is not available; therefore, this demarcation process was performed blind with respect to the previous work by Kovács. His work was not used as a guideline or a goal. The Kovács map is included in Figure 4.12.

The steps for the demarcation of the flood zones are as follows:

Step 1 The K-value isolines: The K-values were plotted using GIS, and isolines connected the points of equal value. Refer to Figure 4.1. The grey spaces indicate areas where no flood peak data is available. These are typical areas where flood peak data should be collected using techniques such as palaeoflood hydrology. Initially the raw calculated K-values were used, but the negative K-values created large variations over short distances in some cases. This cluttered the workspace with unnecessary lines and subsequently all negative values and values smaller than one (1) were replaced with a one (1). Refer to Figure I1 of Appendix I for a full page map indicating K-value isolines.

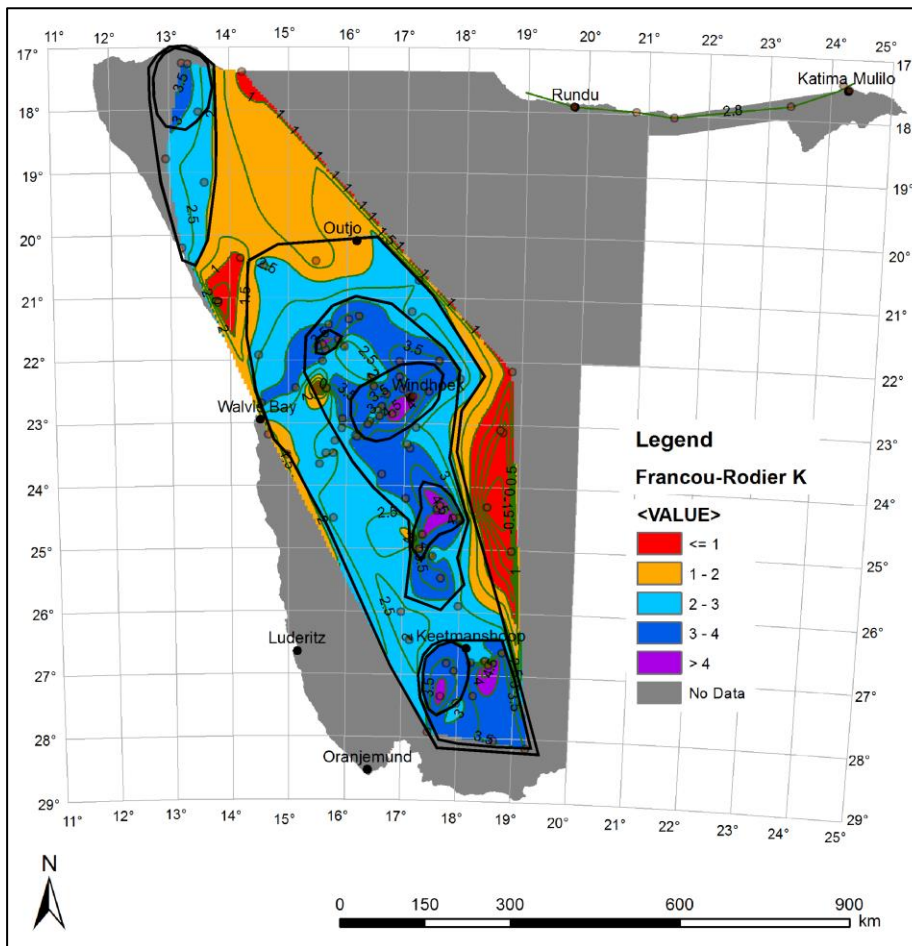


Figure 4.1: K-value isolines for the available floodpeak data, indicating areas of higher and lower K-values. The black lines indicate preliminary K-value boundaries. Grey areas indicate areas without any flood peak information.

A large flood event in a tributary of the Lowen River at Uachanaris in 1954 is mentioned in the TR 137. Kovács (1988:81) however mentions that this floodpeak is unreliable data. The

K-value for this flood peak is calculated at 5.3, the highest in the country. This flood peak, however, is not reflected in the NDWA data, neither is it mentioned in the work of Stengel (1974). Therefore, since it was included in the TR 137 data list, it is also included in the K-value plot. However, it is not considered in the demarcation of the K-zones. Refer to Figure 4.1, the southeastern corner.

Step 2 The geology map of Namibia: although the geology in general does not significantly influence boundary lines of flood zones, it does provide a clear indicator where water does not flow, or where significant loss of surface run-off is expected. These are sandy desert areas, such as the Namib sand sea, the dolomitic area southwest of Etosha pan in the north and also the karst areas in the Kalahari Desert.

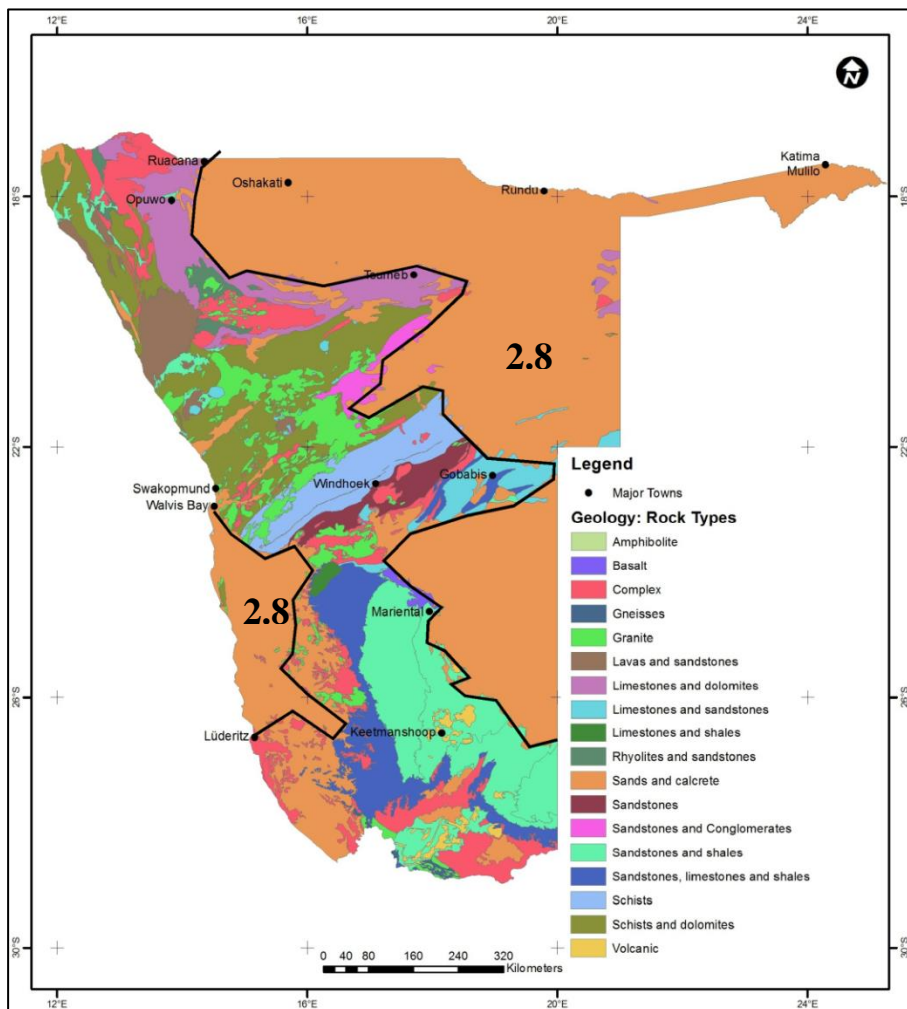


Figure 4.2: Geology of Namibia: Rock Types. The figure reference is the “Atlas of Namibia Project, 2002; the Directorate of Environmental affairs, Ministry of Environment and Tourism”. Refer to the black boundary line demarcating desert and other zero or low-runoff areas.

With specific reference to the Uhenhorst cloudburst which produced no significant flooding of any rivers, it is quite obvious that relatively high 3-day rainfall in the Kalahari will not produce as much run-off as a similar rainfall event in the mountainous central parts of Namibia. Refer to Figure 4.2 for the boundary line demarcating the sandy and karst areas of Namibia where very few river channels are found.

Step 3 The 3-day maximum rainfall isolines: initially the 3-day rainfall was assumed to contribute significantly to the delimitation of the K-value zones. The highest 3-day rainfall occurrences are over the Kalahari Desert in the northeast (Refer to Figure 3.3). Yet no flow gauging stations are found in this area as discharges are significantly low. An analysis of the 10-year flood peak discharge in the lower Omatako River, using the Lacey regime method as described by Beck & Basson (2003:3-6) and in sub-section 3.2.4., indicates a bank full width of 104 m which relates to a 10-year peak discharge of $463 \text{ m}^3/\text{s}$. Refer to Figure 4.3. This discharge is surprisingly low for a catchment area of approximately $59\,000 \text{ km}^2$. Refer to Figure 4.3.

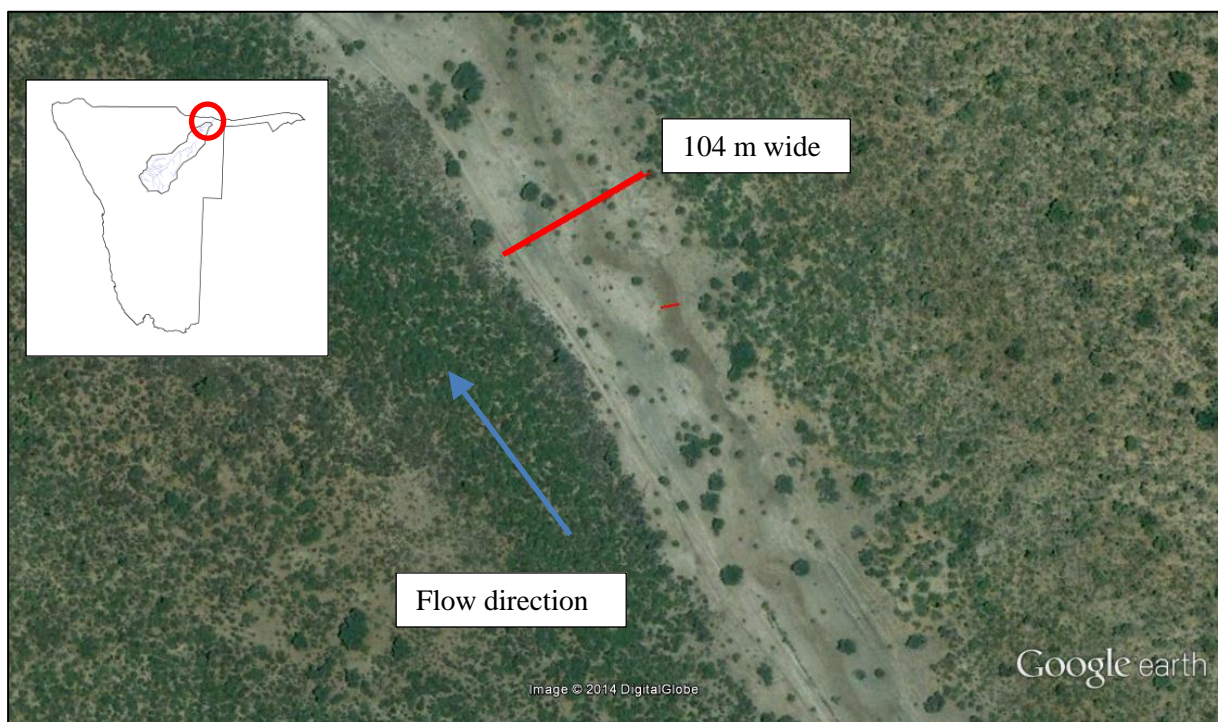


Figure 4.3. A Google image shows the Omatako River approximately 31 km upstream of its confluence with the Kavango River. The inset shows the catchment area as well as the position of the selected point relative to Namibia.

This illustration above indicates that the 3-day maximum rainfall will not dominate or influence the boundaries of the K-zones over highly permeable areas, such as the Kalahari Desert. Figure 4.4 shows altered K- value lines, mostly due to the geology map and to a lesser extent the 3-day maximum lines along the southwest Namib Desert.

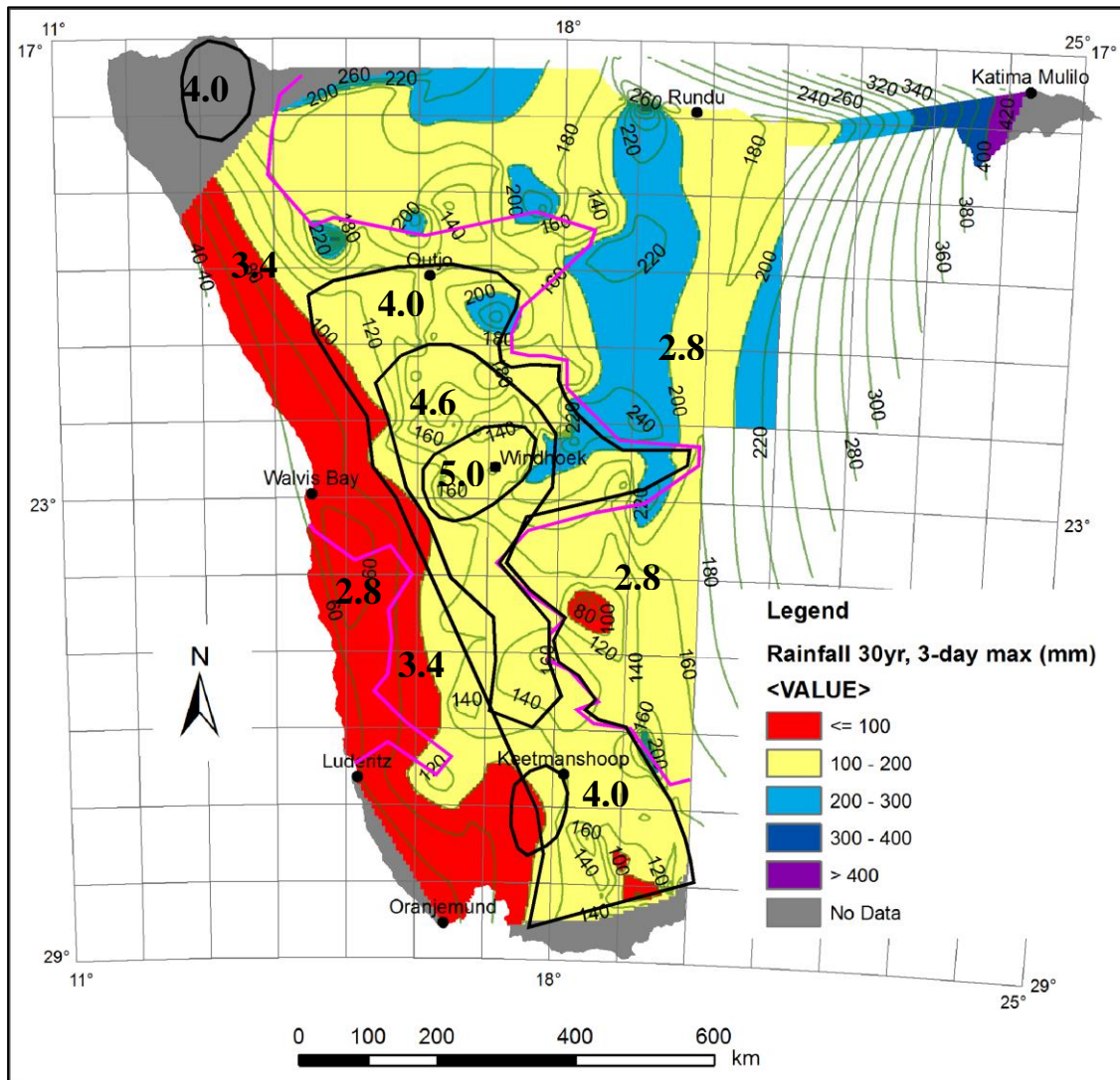


Figure 4.4: The isolines for the 3-day maximum rainfall. K-values are entered into their likely representative regions. The magenta lines demarcate the desert regions with low surface run-off, as indicated in Figure 4.2, while the black lines are carried over from the K-value zones in Figure 4.1.

Step 4 Existing river drainage routes: several large river channels had K-values relatively higher than the K-values of surrounding areas, or larger than the local rainfall depths would tend to predict. These are the rivers originating in the central highlands with high rainfall and hence high flood generating potential.

These rivers then flow through the drier southern or coastal parts of the country. In these cases the local flood zone K-value will be controlled by the local K-values/rainfall, while the river channel would receive a unique K-value. This is the case for the lower Fish River where the local K-value is 4, however the river channel receives a K-value of 4.6 due to the palaeoflood evidence of larger floods. Refer to Figure 4.5.

Two other rivers, which have higher K-values than the local value, are the Tsondab and Tsauchab Rivers. The Tsondab flows into the dunes of the Naukluft National Park, never reaching the sea. The Tsauchab River also flows into the desert, further south, at Sesriem. These two rivers were allocated K-values of 3.4 while the surrounding Namib Desert has a K - value of <2.8 . Refer to Figure 4.5 for the various rivers.

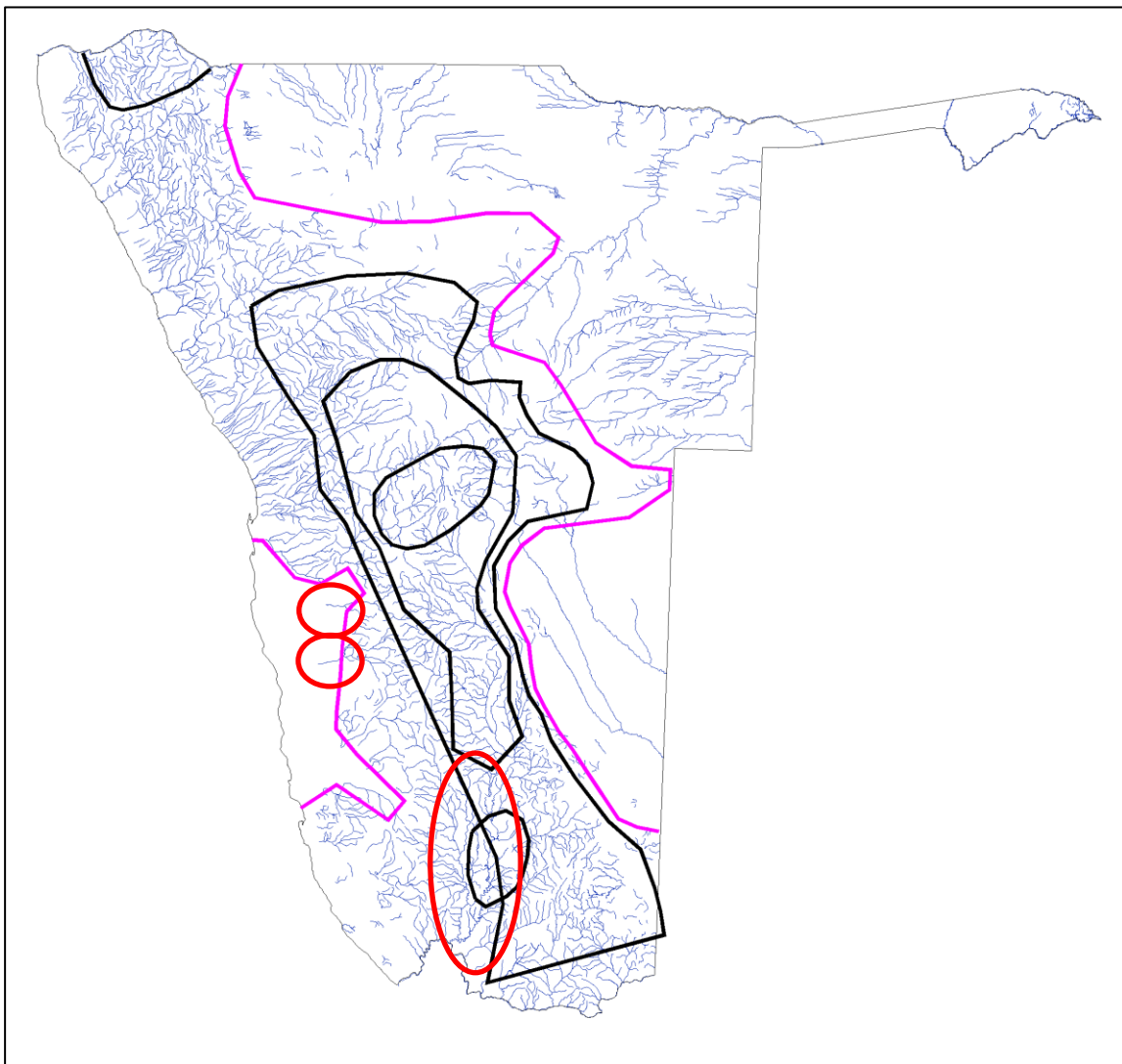


Figure 4.5: The preliminary K-zone lines overlaid on the Namibian rivers. The magenta lines indicate the desert boundaries determined from the geology map in Figure 4.2. The red oval shapes indicate river systems that have been allocated K-values higher than the local values.

Step 5 Topography: The flood zone lines generated in the previous step are then placed on a contour map of Namibia. The coastal escarpment plays a dominant role regarding rainfall patterns; therefore this escarpment line provided a guideline for nearby flood zone lines to follow. The topography also provides guidance regarding the edge of the flat Oshona region in the north which drains into the Etosha Pan, which delineates the higher run-off potential to the south and the lower run-off potential to the north for the same 3-day rainfall figures. Refer to Figure 4.6.

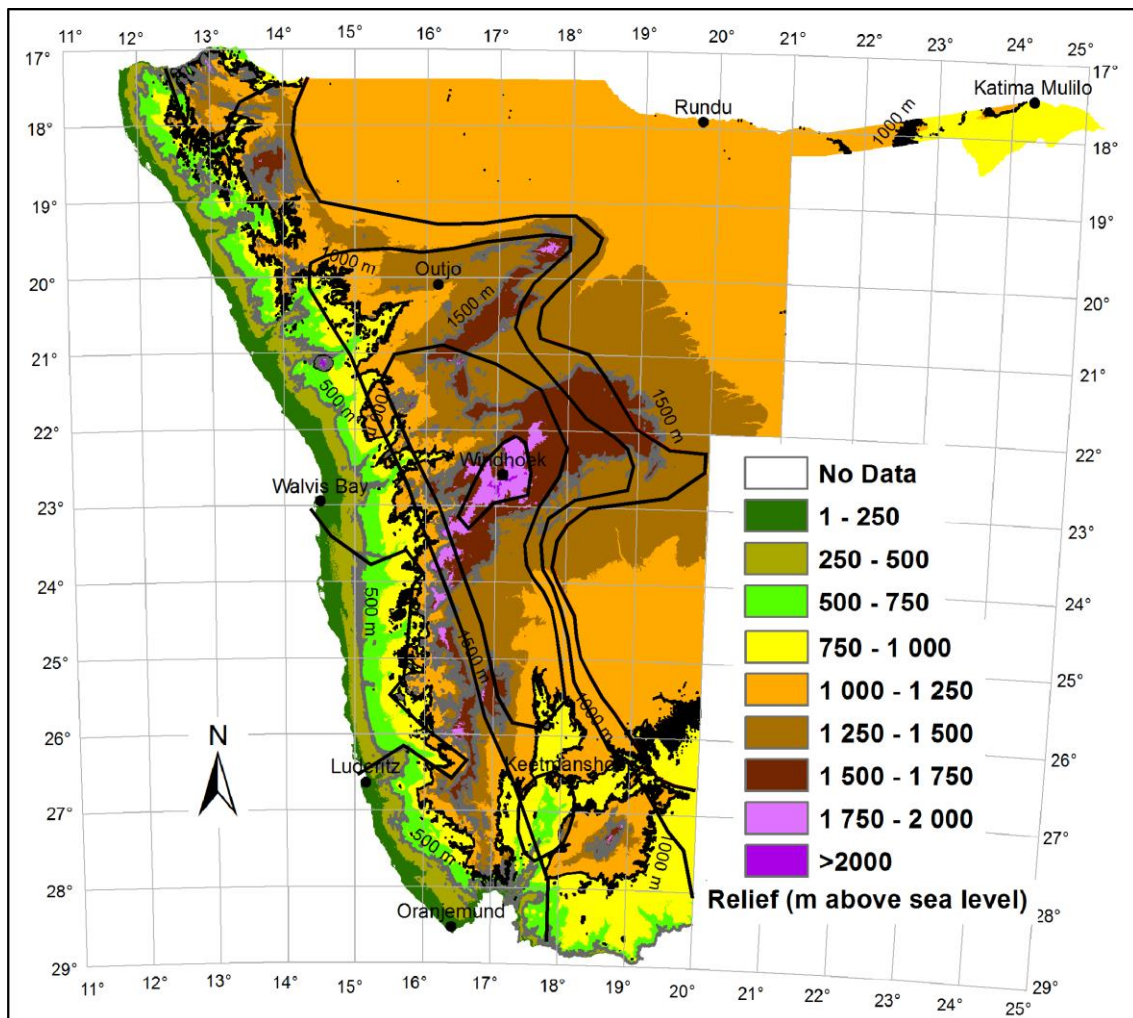


Figure 4.6: The topography of the country and some adjustments to K-zones in the north to follow topography lines.

Step 6 Revisit geology: The central Kalahari Desert, east of Windhoek to the town Gobabis, has a limestone and sandstone protrusion which is also clearly visible on contour maps. This elevated stretch of land also forms the watershed between the north flowing and south flowing rivers of the Kalahari. This area is not covered with sand and has numerous

river channels incised into the rock. The low Kalahari K-value line was moved around this area, making this flood zone $K = 3.4$. This K-value better suites the rainfall patterns and geology of the central Kalahari.

Also visible in the geology is the dolomitic area to the south-west of the Etosha pan. Although the elevation and rainfall predict high run-off potential, this area has few river streams flowing out of it. Therefore this area receives a low K-value. Refer to Figure 4.7.

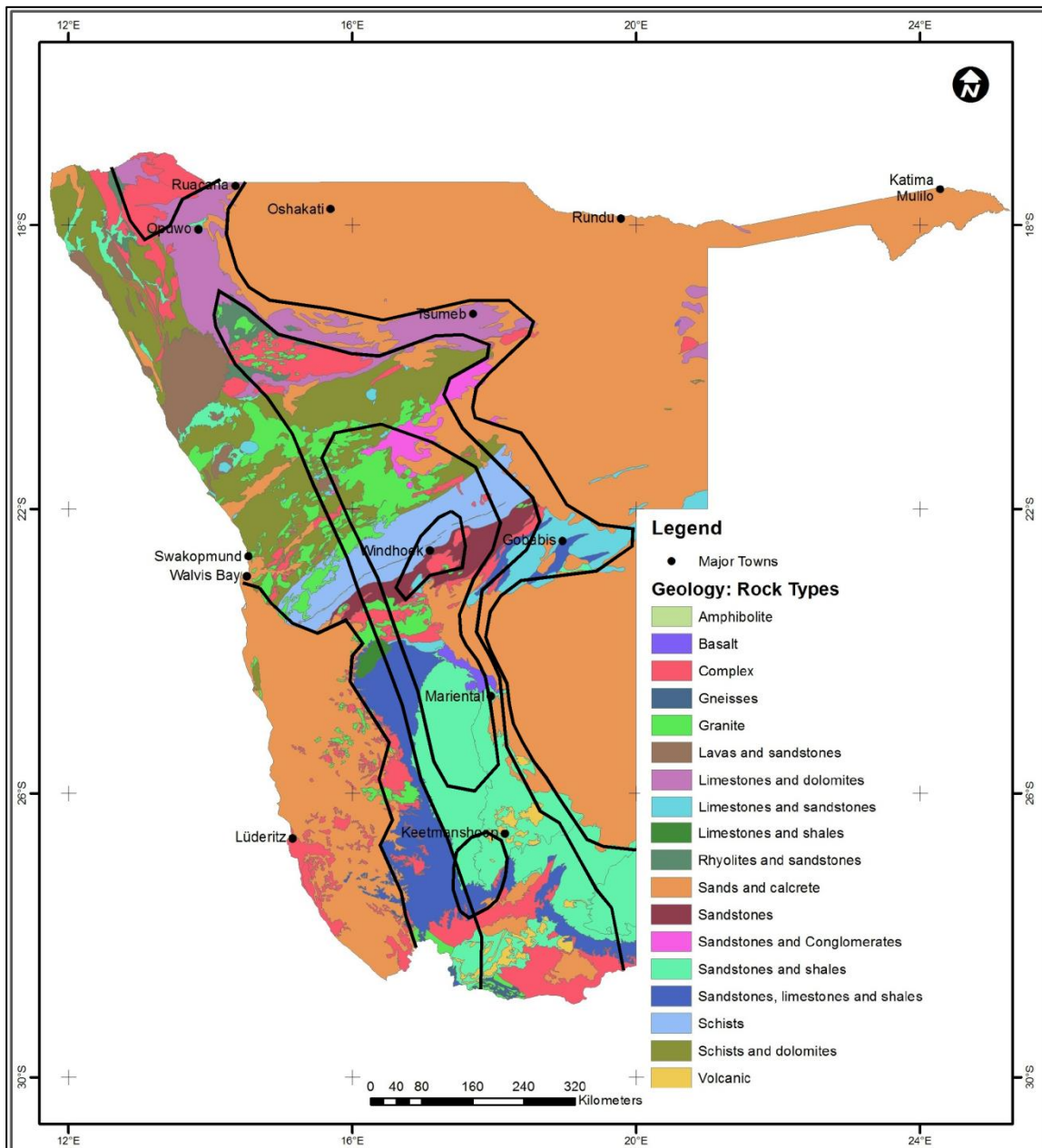


Figure 4.7: The geology of the country and some adjustments to the dolomitic areas in the north. The figure reference is the “Atlas of Namibia Project, 2002; the Directorate of Environmental affairs, Ministry of Environment and Tourism”.

Step 7 The river systems: After the delineated lines had received a second geology-map pass, the newly altered flood zones lines were placed on top of a map indicating all river channels. This check was only done to increase the flood zone boundaries where required, and not to reduce them. This allowed some adjustment around the edges of the dolomitic area in the north as well as the limestone/sandstone zone in the east through the central Kalahari. Refer to Figure 4.8.



Figure 4.8: Revisit the river systems: alter lines along the south east and south west of Namibia.

Step 8 Vegetation map: at this stage the flood zone lines were well defined and delineated with the data available. The flood zone lines were superimposed on the vegetation map just as a check for any possible anomalies. It was found, however, that the flood zone lines and areas corresponded well with the vegetation types, since the vegetation boundaries

are closely linked to the topography, the geology and the rainfall patterns. Therefore no changes were made as a result of the vegetation map. See Figure 4.9.

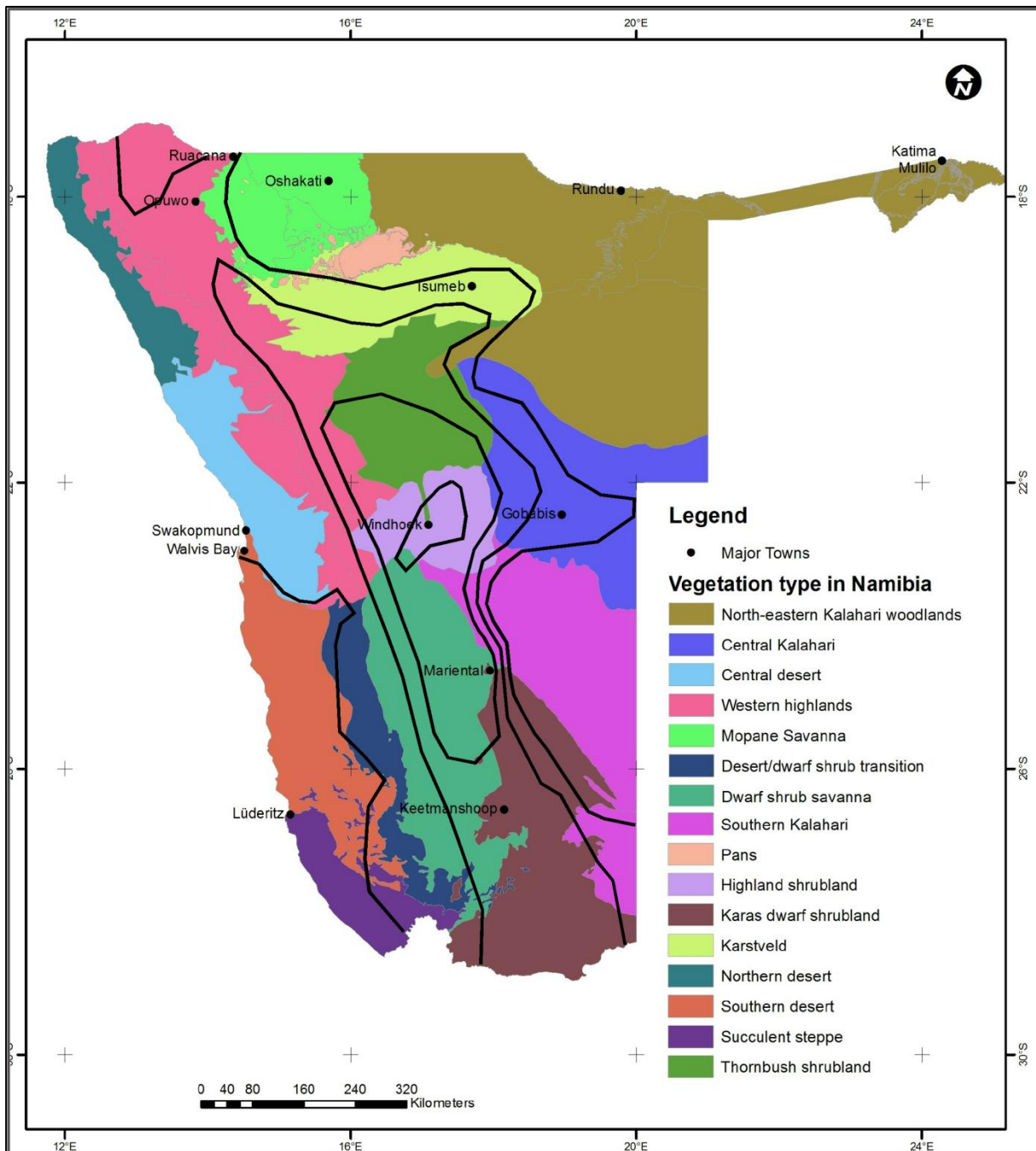


Figure 4.9: The K-value lines generally follow the vegetation regions of Namibia. The figure reference is the “Atlas of Namibia Project, 2002; the Directorate of Environmental affairs, Ministry of Environment and Tourism”.

Step 9 Sparse or no data: As a last check, the areas with sparse or no data regarding rainfall or flood peaks were revisited. Such areas are found in the south and southwest part of

Namibia where low rainfall predicts low run-off. However, the uncertainty of actual K-values forces higher K-value flood zones to include these uncharted regions in the southwestern part of the country. See Figure 4.10.

Other areas requiring floodpeak information is the western parts of the Lower Fish River catchment area, the region between latitude 27° and the Orange River, and the new K = 4.0 flood zone in the Northwest.

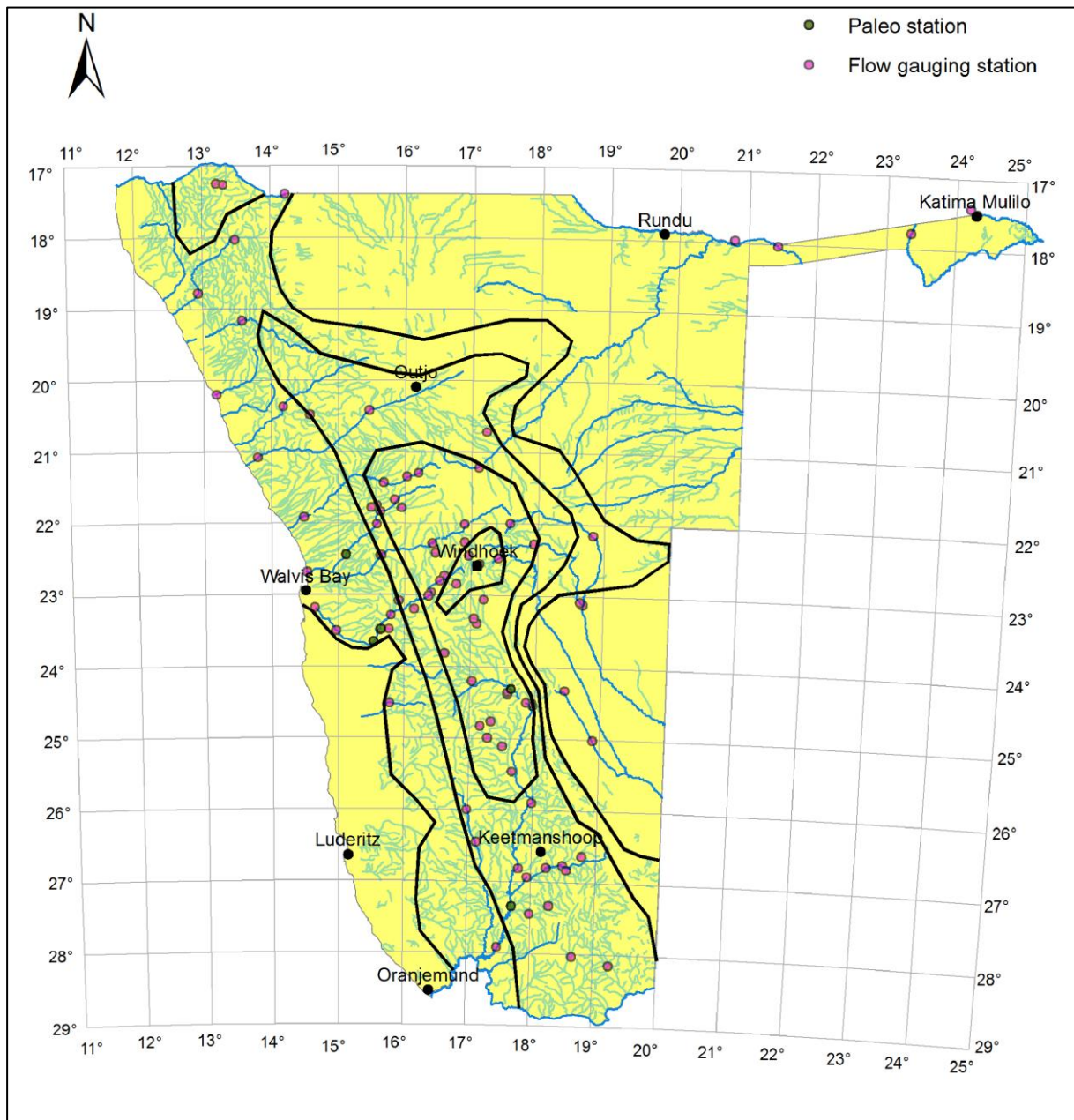


Figure 4.10: Sparse data in the east and south-western part of Namibia highlight areas of uncertainty regarding the regional flood zones.

4.7. Results of delineated hydrology regions

The flood zones delimited in this dissertation correspond reasonably well with the zones indicated in the TR 137, which would be expected since many of the same flood peaks used in the TR 137 are still dominant peaks today. The additional data points however have expanded the boundaries of the flood zones in some parts. This can be expected since the previous data set which generated the TR 137 flood zones will remain dominant unless a larger flood or K-value forces the zone line to enclose a larger area.

Four of the TR 137 list of flood peaks were exceeded in the past 30 years. One of these is the Tsauchab River at Sesriem (on the eastern edge of the Namib Desert) which increased in flood size from 222 m³/s to 360 m³/s. This changed the K-value from 2.44 to 2.87. These were incorporated in the delimitation of the new zones.

The palaeoflood data also made a significant contribution, not only in providing upper bound flood peak data, but also because it populated remote areas with new data. The new upper bound palaeoflood data most likely represents the actual RMF for that region. The RMF flood zones were increased due to the contributions made by the palaeoflood data.

Refer to Figure 4.11 for the new flood zones of Namibia. The lines had been smoothed out in the final drawing.

Comparing the new homogeneous flood zones to those of Kovács (1988), the major differences include the following:

- The lower Kuiseb river now falls entirely in the K=3.4 zone; the boundary line runs directly south of the river. This can be attributed to the palaeoflood study by Grodek *et al.* (2013:1).
- The K-value of the Namib Desert, in the south western part of Namibia, which previously was indicated as <3.4, now falls below the 2.8 K-value. This can be attributed to sandy desert landscapes which have a large capacity for absorbing precipitation, with reference to the significant Uhlenhorst rainfall event in the Kalahari Desert which produced no discharge down a river. Also, the Tsauchab and Tsondeb rivers, which originate in the escarpment east of the Namib Desert, flow into the dunes of Namib Desert; they have well defined river channels upstream of the Namib Dessert. However where they enter the sand dunes of the Namib, the streams lose their water and disappear entirely several kilometres further downstream.

Therefore the Tsauchab River, which has a calculated K-value of 2.87 before it enters the sands of the Namib Desert, will rapidly reduce its K-value as it flows through the sandy landscape. Therefore any streams originating in the sands of the Namib are unlikely to have K-values exceeding 2.8.

- The 4.6 zone which follows the Fish River and stops upstream of the Lowen River (near Keetmanshoop), is shifted back upstream along the river up to a point where regional data also is 4.6. Palaeoflood evidence shows that the Lower Fish River experiences $K = 4.6$ flood events, however, the surrounding regions have K-values equal to 4.0.
- Two new flood peaks recorded in the northwestern corner of Namibia indicate that a small area there has a K value of 4.0 which is higher than the surrounding 3.6 value.
- The $K = 3.4$ zone in the east includes the slightly elevated limestone/sandstone region towards the town of Gobabis. Given rainfall events similar to those of central Namibia, streams over the rocky areas are likely to have significant run-off. Flood information, however, is required in this area to verify this assumption, hence the broken boundary line, which indicates that it is not final.

4.8. Franco-Rodier curves and the highest recorded flood peaks in the various flood zones

The Franco-Rodier flood peak classification consists of three zones; the Flood Zone which refers to catchment areas larger than 100 km^2 . The Storm Zone which refers to catchment areas smaller than 1 km^2 , in which floods are generated by rainfall intensity only (Kovacs, 1988:4). The third zone, which falls between the 1 and 100 km^2 , is called the Transition Zone where the envelope lines provide a smooth transition from the Storm Zone to the Flood Zone.

As per the TR 137, the RMF flood model makes provision for the Flood Zone discharges, which have catchment areas larger than 100 km^2 , and for the Transition Zone discharges, which have catchment areas between 1 km^2 and 100 km^2 .

The Storm Zone discharges, for catchment areas smaller than 1 km^2 , as presented by Kovács (1988:4), are based on world record rainfall intensities for 15 minutes at the upper limit of the envelope, and, for the lower limit, rainfall intensities just capable of generating a flood. The author adopts this approach by Kovacs in this dissertation.

The flood peak data recorded in Namibia since the 1980s does not support the proposal by Kovacs (1988:14) to increase the Transition Zone to 300 km² for the regions K = 4.0 and K = 3.4, and to increase the Transition Zone to 500 km² for the region K = 2.8. Therefore the catchment area for transition from the Transition Zone to the Flood Zone is fixed at 100 km² for all the regions from 2.8 to 5.0.

By reducing the Flood Zone effective area to the 100 km², for regions 4.0, 3.4 and 2.8, the slope of the transition zone lines are changed and new power functions for these lines are determined.

Figure 4.13. indicates the Franco-Rodier K-regions for Namibia. Table 4.1. shows the RMF-equations applicable to the Transition Zone as well as the Flood Zone for the various regions.

The highest recorded flood peak data for each flood region, as well as the applicable RMF flood equation for Namibia, are presented in Appendix J. As an example, Figure 4.14 shows the highest recorded flood data for region K = 4.6. For the region of K = 4.6 the Fish River palaeoflood data, which is considered to be upper bound, are shown near the limit of the regional boundary.

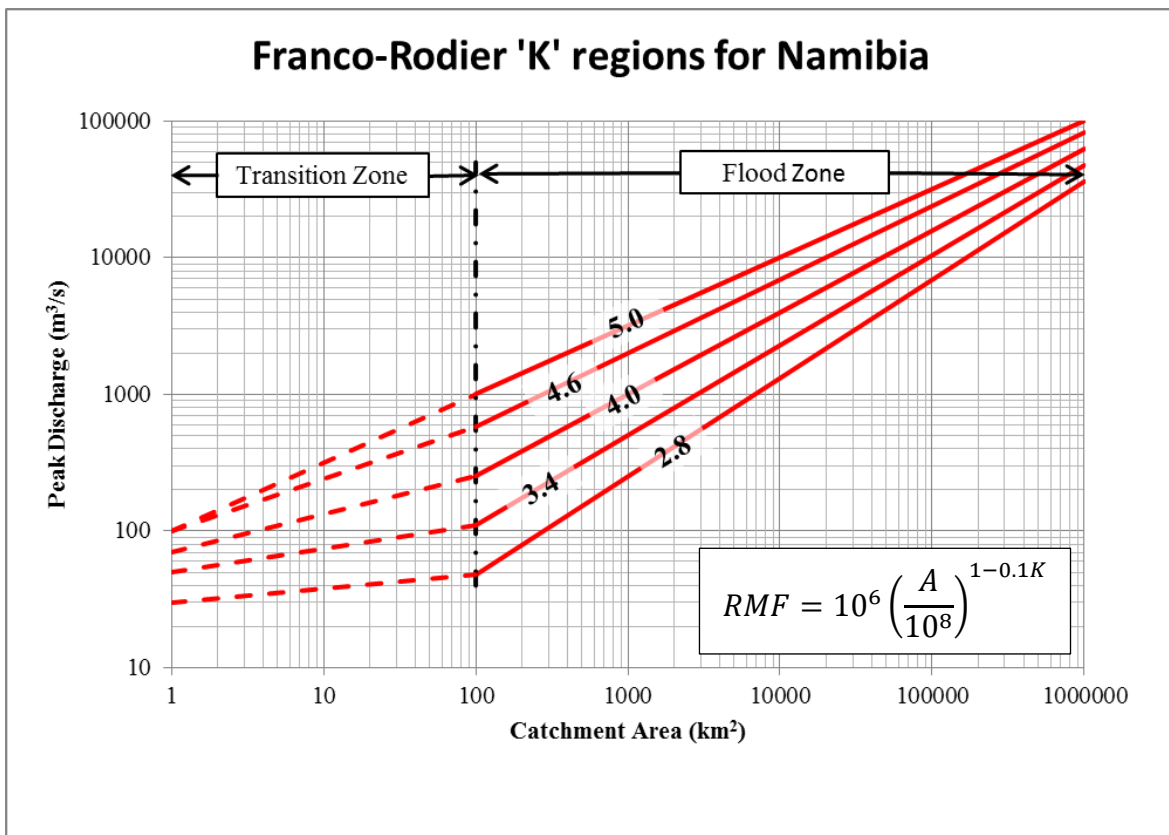


Figure 4.13. The Franco-Rodier curves for the RMF applicable to Namibia.

Table 4.1: The RMF equations for the various K-regions in Namibia, applicable to the Transition Zone as well as the Flood Zone.

K-region	Transition Zone RMF equation	Flood Zone RMF equation
2.8	$30 A_e^{0.102}$	$1.74 A_e^{0.72}$
3.4	$50 A_e^{0.171}$	$5.25 A_e^{0.66}$
4.0	$70 A_e^{0.28}$	$15.9 A_e^{0.60}$
4.6	$100 A_e^{0.38}$	$47.9 A_e^{0.54}$
5.0	$100 A_e^{0.5}$	$100 A_e^{0.50}$

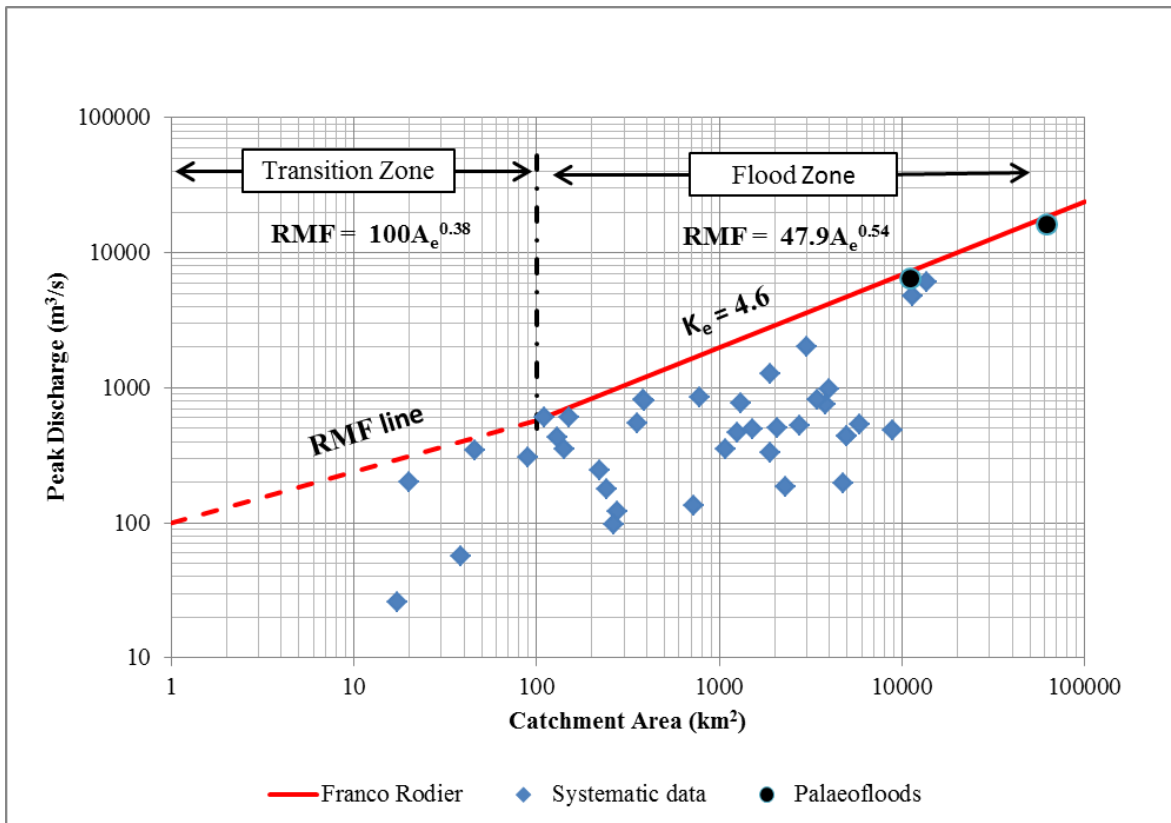


Figure 4.14: The highest recorded flood peaks for Region 4.6. The Equations for calculating the RMF in each of the two zones are included.

4.9. Annual recurrence interval of the RMF flood

By utilising probabilistic methods one can estimate the annual recurrence interval of extreme events and the RMF. The maximum instantaneous flood peak of each year is selected to represent the random behaviour of the stream (Görgens; 2000:19). Although the high end tails of frequency distributions are not well defined, using mathematical probability distribution functions which are known to have appropriate high-end tails one can quantify the magnitude of design floods.

The best-fit distribution was selected from the Log Normal, the Log Pearson 3, and the General Extreme Value models. By adopting the approach used by Van der Spuy (2009) of the DWS Flood Studies Division, in some cases the average of two or three of the distributions were used if it produced a better representation. A problem, however, encountered with the probabilistic approach in an arid country is the many zero flood peaks; years with zero flow. Refer to the number of zero flow years in the annual data presented in Appendix O.

Dealing with zero annual discharges:

At some gauging stations the annual zero flow data occurs 30% of the recorded time. During a discussion with the Flood Hydrology Division of the South African Department of Water Affairs and Sanitation, Rademeyer (2013) pointed out that zero flow lies on the lower end of the distribution and one could allocate very small discharge figures to these without interfering too much with the upper tail of the distribution. However in the probabilistic distribution of the systematic NDWA data, the zero's were included in the distributions. In Appendix N the lower tail of several of the distributions with zero data is found to bend down to annual exceedance probabilities ranging from 50% to 90%.

An alternative approach proposed by Fischer (2012b) in dealing with zero's is to perform a probability distribution by excluding the zero's from a dataset, hence reducing the number of observations as well: $(n_{\text{total}} - n_{\text{zero}})$. Thereafter reapply the probability of a non-zero year back to the distribution data: the probability of a non-zero year is $(n_{\text{total}} - n_{\text{zero}})/(n_{\text{total}})$. This would create a right-shift in the lower end of the distribution, crossing the probability axis at annual exceedance probabilities similar to the range previously discussed.

Fischer's approach (2012b) is applied to three stations with zero data. Refer to Figures 4.15, 4.16 and 4.17. After applying the non-zero probabilities to distributions, the new distribution crosses the probability axis at 50% for the Swakop River at Westfaler, at 60% for the Hutub River at Rietkuil and at 85% for the Ugab River at Vingerklip. The results indicate that the

lower tail of the flood differs significantly, depending on the number of zeros in the dataset, but the upper tails of the distributions converge.

A Partial Duration Series was also considered as an approach to deal with the zero data. Applying this approach to the Seeheim gauging station in the lower Fish River, where 6% of the annual peaks are zero, it was found that the probabilistic distribution experiences a significant reduction in the AEP of the RMF, shifting the distribution curve upwards. Refer to Appendix P for the partial duration curve of the Seeheim gauging station in the lower Fish River, and also to Appendix N, page 214, for the normal distribution of the Seeheim data. The partial duration series was not applied further to gauging station data.

The recurrence interval of the RMF:

The recurrence of the RMF is where the magnitude of the RMF crosses the best-fit distribution of the data. The recurrence interval of the RMF can then be estimated from the graph. Refer to Appendix B for data on the river gauging points, as well as the estimated annual recurrence interval for the RMF's as determined above.

For the 50 river gauging stations with systematic data, which were used in this study, 42 (84%) of the RMF floods have annual recurrence intervals equal to or exceeding 10 000 years. One (2%) has a recurrence interval exceeding 5 000 years but not exceeding 10 000 years. Six (12%) have recurrence intervals exceeding 1 000 years but not exceeding 5 000 years.

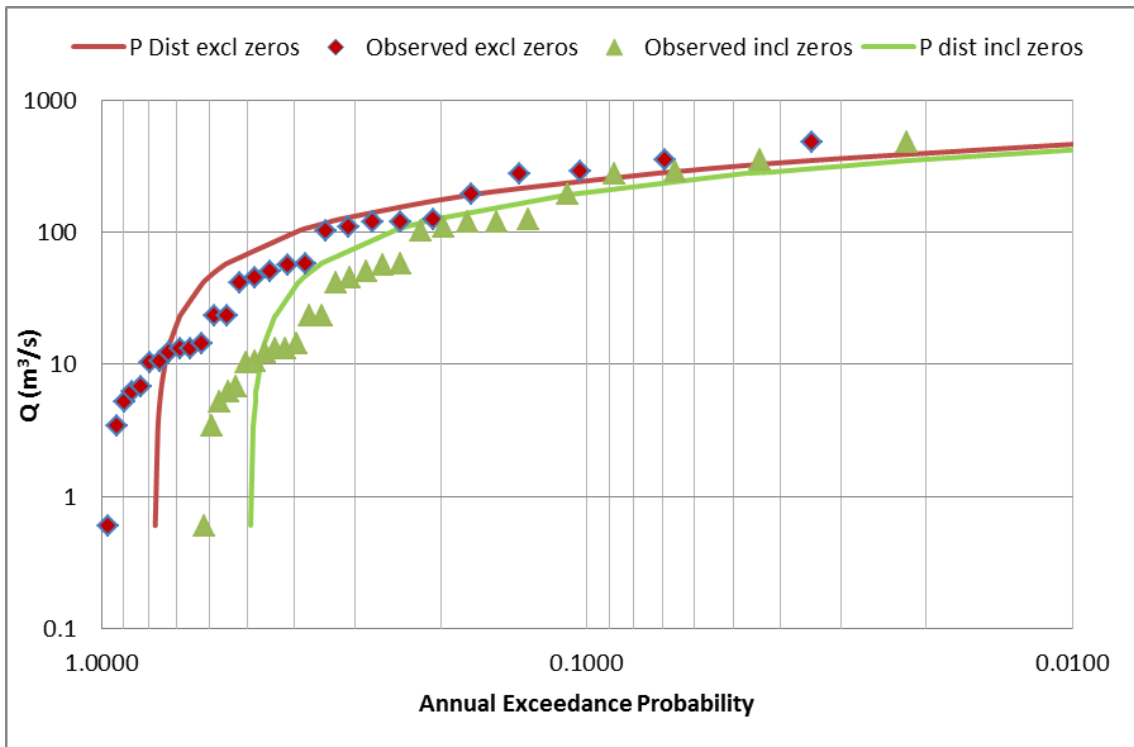


Figure 4.15. Swakop River at Westfaler in central Namibia. 36% of the annual data is zero. The red line produces a probabilistic distribution excluding the zero flood years, the green line includes the zero data.

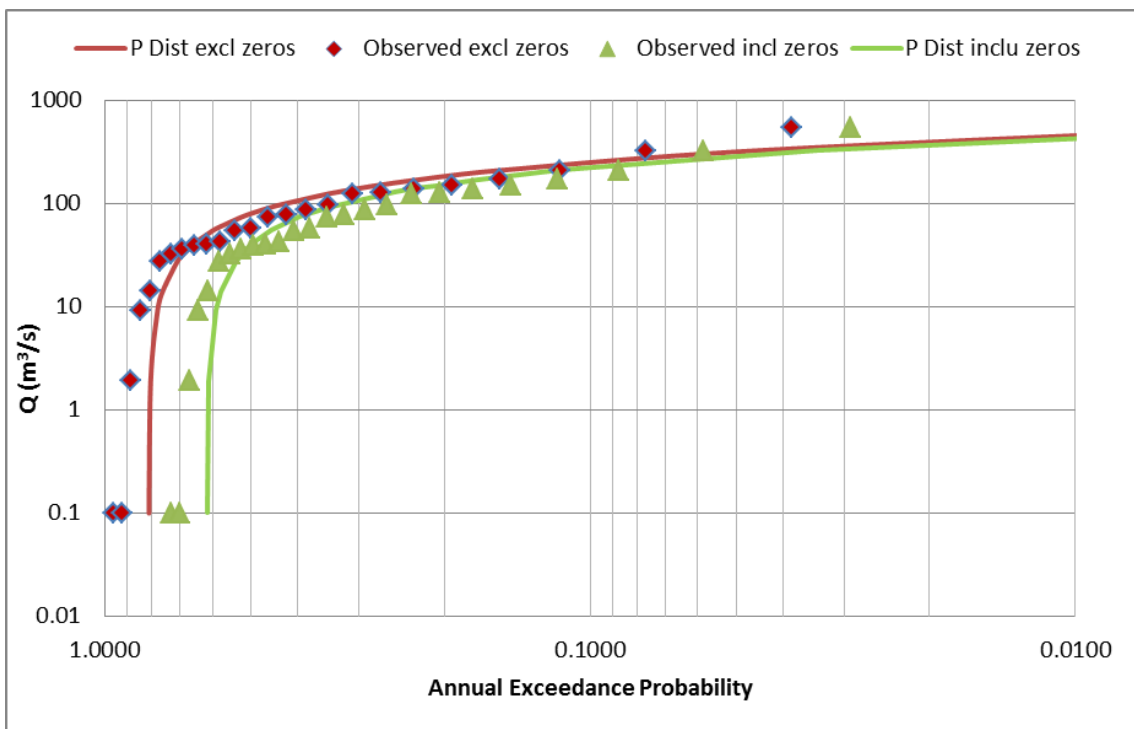


Figure 4.16. Hutub River at Rietkuil in southern Namibia. 24% of the annual data is zero. The red line produces a probabilistic distribution excluding the zero flood years, the green line includes the zero data.

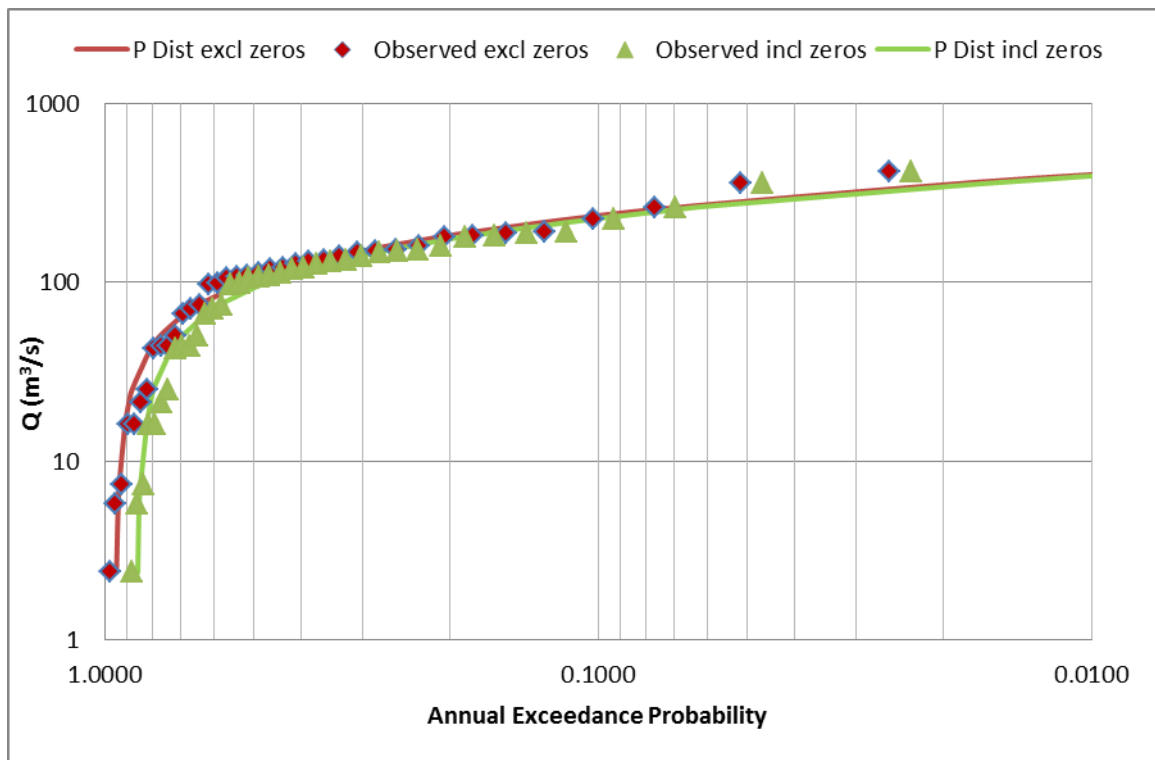


Figure 4.17. Ugab River at Vingerklip in northwest Namibia. 10% of the annual data is zero. The red line produces a probabilistic distribution excluding the zero flood years, the green line includes the zero data.

One station, Ondova at Minimahoro in the northwest, has a recurrence interval for the RMF of less than 1 000 years. Upon checking the data it was found that this station has good quality data, but it is one of the younger stations in Namibia. The calculated K-value of the flood peak at the station is 3.92, which is close to the allocated K-value of 4.0. A slightly larger flood peak at this station would produce a K-value exceeding 4.0, which translates to an RMF floodpeak with an AEP of 2 000 years. Hence a palaeoflood study at this river could provide valuable information in this regard.

4.10. Discussion of delineated flood regions

The flood zones as indicated in the TR 137 were extended in several places as a result of the new data presented in this dissertation.

Thirty years of additional flood recording, as well as several new gauging stations increased the systematic data record from 2 759 years of recorded data, which was used to generate the flood zones in the TR 137, to 4 169 years for this present study.

Palaeoflood data, especially the upper bound data, provided flood peak information in remote areas. This helped to populate the surface of Namibia with flood peaks and hence helped to increase or verify the boundaries of the K-value zones. Since the hyper arid regions of Namibia preserve flood stage indicators very well, more palaeoflood studies can be performed which would increase the distribution of flood data in the country. Especially in the arid regions where it is unpractical to build and maintain gauging weirs.

4.11. Observations on the new flood data

From the findings of Chapter 4, the following:

- The extended duration of data records from the TR 137 flood stations, as well as the new flood gauge stations and palaeoflood peaks presented in this dissertation, have significantly increased the available flood peak data and contributed to the new delimitation of RMF flood zones in Namibia.
- Generally, new flood data can only increase the influence area of the RMF flood zones, and not reduce them since the dominant flood peaks control the flood zones. However should a newer larger flood produce a larger K-value, then the newer value dominates and will very likely have an influence on a nearby flood zone line by increasing the zone area.
- Palaeoflood studies provided valuable upper bound flood data and can also provide data in remote areas where it would otherwise be difficult to obtain data.
- More palaeoflood investigations should be done to increase the data base into remote areas where it would take considerable capital expenditure and years of data capturing before any significant flood data were available.
- The newly delineated RMF flood zones may be applied to determine extreme floods in Namibia for catchment areas larger than 1 km².
- Probabilistic analysis of annual recurrence intervals of the predicted RMF's generally exceed 10 000 years, similar to the findings of Van der Spuy (2008). This finding is supported by palaeoflood evidence found in the lower Fish River.

5. Quantitative risk in dam safety

By trial and error, over many years, design standards have developed into the standards-based approach to dam design and dam safety which is applied today.

As discussed previously, the standards-based approach to risk management has served dam safety well, reducing the rate of dam failures from 2.5% in the early part of the 20th century to less than 0.5% in the second half (ICOLD, 1995). However the Standards-based Approach does not differentiate between high or low risk, either the dam complies with the standard or it does not.

Risk based dam safety is gaining popularity, specifically where a portfolio of dams requires the owner to prioritise rehabilitation activities. This approach is being applied in Australia and also by the United States Bureau of Reclamation (ANCOLD, 2003b:11; Charlwood *et al.*, 2007:10). However in these cases the standards-based approach is still used as a guide for the extent of rehabilitation required at each dam (ICOLD, 2005).

This dissertation presents a quantitative risk approach, known as the Rational Quantitative Optimal (RQO) approach, which evaluates risk, prioritises rehabilitation and optimises expenditure over a portfolio of dams in a transparent way. Thereby it achieves the objective of using the ‘worst first’ management approach, which is to start rehabilitation work on the highest risk dam first, and also to apply the ‘greatest risk reduction’ over the whole portfolio of dams in the shortest period of time within the funds available. This is an objective proposed by Charlwood *et al.* (2007:27), ICOLD (2005:181), Bowles (2013:48) and Snorteland (2013:5).

5.1. Dam safety in general

Acceptable dam safety is not an absolute condition, but it is a tolerated situation, with low levels of residual risk ever present (ICOLD, 2005:4). The practice of dam safety aims at reducing the risk of failure of new and existing dams to acceptable levels; as discussed in the International Commission on Large Dams (ICOLD) Bulletin 99 (ICOLD, 1995:13), dam failure means the

“collapse or movement of a part of the dam or its foundation, so that the dam cannot retain water. In general a failure results in the release of large quantities of water, imposing risks on the people or property downstream”.

For various historical reasons, and some technical reasons, the safety of dams has been

controlled by an engineering standards-based approach. This dissertation, however, investigates an approach to dam safety which addresses risk quantitatively and optimally reduces risk over a portfolio of dams without, or complementary to, employing design standards.

5.1.1. Dam safety performance

As discussed previously, the largest component failure experienced by dam owners all over the world is the failure of embankment dams due to overtopping of the Non-Overspill Crest (NOC): according to ICOLD (1995:22) the failure of embankment dams contributed to 80% of all dam failures. Of this 80%, the largest mode of failure is overtopping of the embankment, which leads to subsequent external erosion and failure. ICOLD (1995:17) provided overtopping as the primary cause of failure, at a figure of 31%.

5.1.2. Design standards

Accidents in industry have always been a spur to human progress (ICOLD, 1995:9), and this holds true also for dam safety. Due to failures, design guidelines are improved and enforced by regulators to ensure that public and other risks are reduced.

Standard guidelines for the design of new dams were developed over time, incorporating specialist input from various countries. This design approach became known as the standards-based approach (SBA) to dam design;

‘the traditional approach to dams engineering, in which risks are controlled by following established rules as to the design of events and loads, structural capacity, safety coefficients and defensive design measures.’ (ANCOLD, 2003b; ICOLD, 2005).

Technical guidelines for the SBA are usually found in regulatory codes of practice for individual countries.

The SBA to dam design serves its objective well; it has significantly reduced the number of dam failures since the 1950’s. However, the current annual failure rate of 0.5% is still significant, considering the investment and the risk to public.

It should be noted that the processes which shape the arid landscape of Namibia are mechanically driven, not chemically induced as one would find in wetter more humid

countries or regions. Due to this phenomenon, dams are generally constructed using the available coarse material and then sealed off with an impervious concrete face on the upstream side; these are referred to as Concrete Faced Rock fill (CFRD) dams. These dams have an inherent resistance to failure due to internal erosion, since leakage water can freely pass through the embankment without causing significant damage. However, these dams are at risk when it comes to overtopping of the non-overspill crest. Therefore the risk of overtopping cannot be taken lightly in Namibia.

5.1.3. Safety standards

Traditionally dam safety has been managed by providing guidance to dam owners and managers regarding safety standards, such as the spillway capacity or a minimum safety factor against slope stability failure (Brown & Gosden, 2004:4). Therefore the SBA, which was initially developed for the design of new dams, has in the past few decades increasingly been applied in the management of dams to assess the safety of existing dams (ICOLD, 2005:17).

The provision of a standard implies that a dam either meets the condition or it does not and, if it does not, then modifications to meet that standard are warranted (Hartford & Baecher, 2004:27).

In 2001 ICOLD submitted a questionnaire on risk based dam safety to member countries (ICOLD, 2005:127). Fifty per cent of the responding countries still used only the SBA (ICOLD, 2005:135), the remainder used risk assessment approaches as a tool for the decision-maker, i.e. to prioritise rehabilitation work on a portfolio of dams, but not as a replacement for the traditional approach (ICOLD, 2005:141).

5.1.4. Risk assessment in dam safety

The main purpose of risk analysis is the transparent treatment of the uncertainty of the causes and consequences of dam failure (ANCOLD, 2003b:3), which is something required by society, but also to provide support for decision making regarding the management and rehabilitation of a portfolio of dams (Hartford & Baecher, 2004:28). Most of the countries using risk assessment use it in the context of portfolio risk assessment (PFRA) (ICOLD, 2005:165), as a tool for the decision maker to prioritise rehabilitation activity.

ANCOLD (2003b:14) believed that the use and development of risk assessment, as an enhancement of the traditional SBA, would significantly improve dam safety management. They currently integrate risk assessment with traditional engineering practice for dam safety management. The general consensus from the ICOLD (2005:111) study is that risk assessment should provide inputs to the decision process, but should not be applied mechanistically in decision making.

In the context of this dissertation the risk levels are not calculated as absolute values, which are compared to independent absolute acceptable levels. The risks of different dams are compared; and, therefore, as long as the flood model and the people at risk are dealt with consistently, the distribution of risk within a portfolio of dams will be comparable.

5.1.5. Quantifiable risk

A comprehensive attempt was made by the UK Department for Environment, Food and Rural Affairs (DEFRA), who in 2004 published a guide on Quantitative Risk Assessment (QRA) for UK Reservoirs (Brown & Gosden, 2004:xi). It was compiled as an interim guide which quantified the risk of failure of embankment dams, based on three fundamental modes of failure; external erosion due to overtopping, internal erosion (piping) and slope failure. Within the UK there is, however, strong opposition against using it as a quantitative tool. As discussed by Mason (2008:1) and Hughes (2009:1), the results of the QRA guide are suspect and it should rather be used as a qualitative assessment tool. According to Hughes, the QRA project requires modifications. In 2013 DEFRA published a revised guide on the risk assessment of dams in the United Kingdom which permits a more qualitative approach.

To produce quantitative numbers, a process including statistical estimates, reliability models, fault tree analysis and expert opinions is relied upon. Such processes will produce precise numbers associated with risk, but still rely on techniques of deduction and the subjectiveness of human input (Hartford & Baecher, 2004:66). Within the technical ranks of regulatory bodies and dam engineers, the subjective approach to risk analysis remains questionable;

‘the topic of risk evaluation is not an easy one especially for the technically minded person looking for a straightforward and purely quantitative approach’ (ICOLD, 2005:23).

5.2. Probability issues in dam safety

Traditionally, probability is defined as frequency: a classical definition of probability states that for N different equally likely outcomes, if n of these outcomes correspond exactly with event A , then the probability of event A is $P(A)=n/N$ (Hartford & Baecher, 2004:106). In the case of dam safety, event A being failure of embankment dams, say, due to internal erosion, $N = 111$ being the population of embankment dams which failed (ICOLD, 1995:30) and $n = 18$ being the number which have failed due to event A , then $P(A) = 18/111 = 0.16$.

Some aspects of dam safety lend themselves to reliability analysis, particularly structural safety. Other aspects, such as piping, are not amenable to conventional reliability analysis, although historic performance data, such as the example above, are useful as a guide to the probability of failure (ANCOLD, 2003b:22). The following comment by ANCOLD (2003a:15) motivates the statement above: ‘No two dams are the same. Each has a unique set of hydrological, topographical, geotechnical, geological and environmental characteristics; as such an appropriate solution for one dam may not be so for another.’

5.3. Flood models

A flood frequency analysis is the probabilistic, deterministic and empirical evaluation of the catchment, rainfall and flow data for the estimation of flood peak probabilities for the site under investigation. Therefore, depending on what approach is used, a flood model estimates flood peaks for different exceedance probabilities.

Typically flood models are compiled from regional data, since usually little data is available on extreme flood events at specific sites. Drawing from a larger body of data allows one to determine upper bound discharges for homogeneous regions, a type of umbrella approach: for any size catchment area within such a region, a typical extreme flood can be estimated.

Alternatively, when sufficient flow data is available for a specific river system, one could do a probabilistic evaluation of the flow data for the estimation of flood peak probabilities. However, this approach is not always possible, since a good distribution of flood events (long continuous record length) is seldom available. Hence the regional models are most often used.

5.3.1 *Updating flood models*

Flood models require updating over time, as more flood data becomes available. More data could increase the size of the expected flood peak with the same probability of occurrence.

A case in point is the Avis Dam near Windhoek in Namibia, which was designed by Rehbock in the 1920s with a spillway capacity of 700 m³/s (Rehbock, 1926:4). This discharge had been estimated in 1896, during an observed flood in the Kleinwindhoek River, Windhoek, near the proposed site for the Avis Dam (Rehbock, 1898:143). In Rehbock's report to the Town Council of Windhoek, he claimed that the selected design flood was 'excessively high', implying that the design included a significant margin of safety. The Avis Dam was constructed in 1931, presumably with a spillway capacity of 700 m³/s, since no design or as-built plans could be found.

In January 1934 a significant flood caused erosion damage to the newly constructed spillway (Kerby, 1934:1). The flood size was estimated at 24,000 cusec (Stengel, 1974:83), which converts to approximately 680 m³/s. Therefore, in hindsight, the flood of 1896 may not have an annual exceedance probability as low as anticipated. Refer to Appendix L for a picture of the damage to the spillway in 1934 as well as a picture taken during the construction phase of the Avis Dam in 1931, using river rubble as construction material.

On 10 February 1934 the Director of Works, Mr D Holtzhausen, wrote to the Secretary of South West Africa (Holtzhausen, 1934:1), and mentioned that the severely eroded part of the spillway was repaired with gabions, also that the spillway was being 'lengthened by excavation on the left flank, where better rock occurs.' The author, however, checked the spillway capacity in 2013 and found it to be approximately 720 m³/s, with provision for wind and wave freeboard (Refer to section 5.3.2. for an explanation of 'Freeboard'). The capacity was therefore not much increased by the left flank excavation into the rock.

The SANCOLD report no. 4, 'Safety in Relation to Floods', indicates that the Avis Dam is a high hazard dam (SANCOLD, 1991:7). Therefore the dam should safely be able to pass the 1 in 200 year flood with sufficient freeboard available. The 1 in 200 year flood, from Kovacs (1988:19), is 0.65 x RMF. The RMF is 1009 m³/s, hence the design discharge capacity of the Avis Dam should be 656 m³/s. Therefore the current spillway capacity is sufficient at 720 m³/s. However, according to the SANCOLD guidelines (SANCOLD, 1991:30), the SEF must also be able to pass over the dam without causing failure of the dam. The author determined that the flood which reaches the NOC level of the dam will be approximately

900 m³/s, which underestimates the Safety Evaluation Flood (SEF), of 1 335 m³/s, by approximately 33%. Hence the current spillway capacity, or freeboard, needs to be upgraded according to the SBA, or at least reconsideration.

Similarly, upgrades to flood models in other countries have the same outcome such as the Early flood models for the Guadalentin River in Spain discussed previously. A recent dam safety evaluation required revisiting the flood model for the river. The updated model indicated a recommended design discharge of 2 350 m³/s and, for the safety check flood, 3 450 m³/s, which is a significant increase from the original design of 550 m³/s. (Benito *et al.*, 2006:2114).

5.3.2 *Design floods and safety check floods*

For the design of new dams, or for safety evaluation purposes, regulators have set standards which prescribe the annual recurrence interval of the flood that must be able to pass over the spillway of a dam. For instance, Spanish dam safety regulations recommend the 1 000 year flood as the design flood (Benito *et al.*, 2006:2117). In South Africa dam regulation prescribes a 200 year flood as the recommended design flood for high risk dams (SANCOLD, 1990:14).

The design philosophy is that the design flood shall pass over the spillway with appropriate freeboard allowances without causing any damage to the dam or spillway structure: freeboard for a dam is the vertical distance between the design flood water level and the Non-Overspill Crest (NOC) of a dam (USB, 1981:1). Refer to Figure 5.1; the components which make up the freeboard are (a) which represents the elevation required for wind setup, (b) represents the components of wave action plus the wave run-up, and (c) represents the height required to pass the routed design flood (e.g. the 1 000 year flood) over an ungated spillway. In the case of a gated dam, component (c) will likely be zero. FSL indicates the reservoir full supply level, NOC indicates the non-overspill crest.

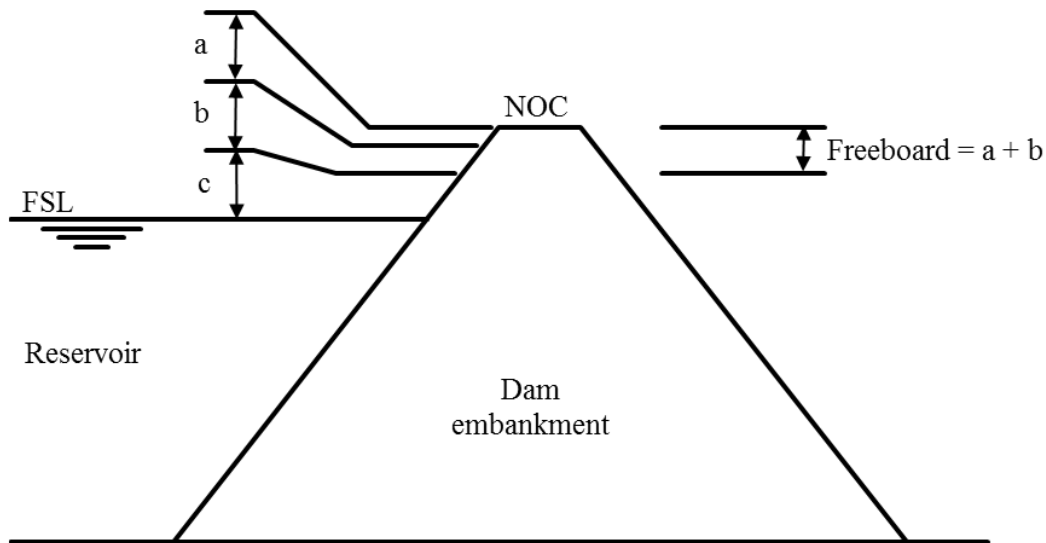


Figure 5.1: The cross-section of a typical embankment dam, depicting the basic freeboard components: (a) wind setup, (b) wave action, (c) flood surge.

The safety check flood, on the other hand, shall also pass over the spillway, but leave no allowance for freeboard, hence the entire freeboard is utilised for flood water storage. In this case, some damage is expected to occur at the dam and the spillway, but without catastrophic failure of the dam.

5.3.3 Flood frequency analysis for extreme events

Regarding extreme flood events, the systematic data records are relatively short compared to the annual recurrence intervals required to qualify an event as extreme. As stated by Klemeš (1993:175), in practice it is necessary to extrapolate beyond the bounds of all data and experience. There is no way of knowing if the properties of the known data are the same as the properties of the extrapolated data that includes extreme values. The problem faced here, in the case of extreme floods, is that the data must be extrapolated ‘from the earthly relative frequencies of 10^{-1} , across the void of several orders of magnitude, to the heavenly probabilities of 10^{-4} and beyond’. Klemeš (1993:169) suggests that if more light is to be shed on the probabilities of hydrological extremes, then it will have to come from more information on the physics of the phenomenon, not from more mathematics.

To improve or validate the extrapolated flood data curve, palaeoflood studies can be

performed which use indirect discharge measurements to determine ancient flood discharges (Baker, 2008:1). The palaeoflood data can be combined with the systematic data range, providing a record of several discrete flood peaks, the age of which could range from several hundred to several thousand years ago (Benito *et al.*, 2006:2114).

As discussed during the 2013 annual ICOLD meeting in Seattle, USA, the general consensus is that the safety check flood should have an annual recurrence interval of 10 000 years which can be determined from the flood model.

5.4. Methodology

The Rational Quantitative Optimal approach (RQO) establishes the characteristics of the marginal cost of life saving due to increase in spillway capacity of a dam against the probability of flood discharge for each of a portfolio of dams as basis for decisions on dam safety investment based on maximising the expected life savings.

This process does not encourage full rehabilitation for each dam within a portfolio, but only partial rehabilitation in order to optimize the available budget.

5.4.1 *The structure of the Rational Quantitative Optimal approach*

The components which form the structure of the RQO approach are discussed below in its order of application, culminating in the risk due to failure, as presented by the following points:

- Flood hydrology: probability of extreme flood events as a function of the flood discharge,
- Probability of dam failure when the flood discharge exceeds the spillway capacity.
- Investment in life-saving activities: raising the embankment to increase freeboard.
- Spillway capacity increase: freeboard height vs. flood discharge.
- Likely loss of life in case of dam failure in case of dam failure due to overtopping.
- Risk to life due to dam failure as function of the likely loss of life and probability of dam failure.

For the purpose of calculating risk comparatively, several assumptions were adopted and employed in this research. These assumptions are explained below before discussing the

components which make up the RQO process.

5.4.1.1 Assumptions

The following three assumptions deal with the general approach to the RQO process. Although they may be considered obvious, they need to be specifically applied to ensure credible results.

- The owner of a portfolio of dams consistently applies the same flood generating methodology to all the dams within the portfolio, to determine the size and recurrence period of extreme flood events.
- Within the portfolio of dams, the same techniques are used to estimate the Population at Risk (PAR) in case of dam failure, and the subsequent Loss of Life (LOL).
- Overtopping of the Non-Overspill Crest (NOC) of an embankment dam leads to failure of the dam, with the risk of failure presented by the following equation from SPANCOLD (2013:8):

$$R_f = p(l_f) \cdot p(f | l_f) \cdot C(l_f, f) \quad (5.1)$$

where: R_f is the risk of failure with resultant loss of life,

$p(l_f)$ is the annual exceedance probability of the flood which overtops the NOC,

$p(f | l_f)$ is the conditional probability of failure given the flood event, and

$C(l_f, f)$ is the consequences (LOL) in case of failure due to the flood event.

The conditional probability $p(f | l_f)$ represents the probability that the dam will fail if it is overtopped. This value is assumed to be equal to unity, since incipient motion conditions of sediment transport, i.e. the minimum moment required for the commencement of non-cohesive sediment motion (Papanicolaou, 2012:1), are reached almost immediately once the water starts flowing over the NOC. It could be argued that if the dam storage capacity is very small and the duration of the flood peak is short, this probability $p(f | l_f)$ could be less than one, since the flood water level in this particular dam will most likely subside before external

erosion has an opportunity to incise from the downstream face through the dam embankment to the upstream side. However, for the purpose of this dissertation, the assumption remains that the dam will fail, hence $p(f | l_f) = 1$.

5.4.1.2 Flood hydrology: Constructing a flood frequency model

A flood frequency model is essential for estimating the probable return period of various sized floods, which is required in the RQO process. A continuous flood record would be ideal for a probabilistic approach for a unique flood frequency model for each dam. However, in most cases continuous data spans only 50 to 100 years, whereas the relevant flood recurrence intervals range from several hundred to several thousand years.

In the absence of long, continuous flood peak records, regional flood models can be used to construct extreme flood frequency models. Such models are the empirical Regional Maximum Flood (RMF) model or the deterministic Probable Maximum Flood (PMF) model. These models provide expected maximum flood peaks (Kovács, 1988:3). Cloete et al. (2014:542) found the recurrence interval of these extreme floods to be in the region of 10 000 years, and Brown & Gosden (2004:30) proposes that the PMF has a recurrence interval of 10^6 years.

For the RMF method, Kovács (1980:13) analysed K values of entirely independent flood peaks and their representative periods and determined a fraction of the RMF which represents the 200 year flood; the fraction is 0.65. Kovács (1988), based on the first value (1980) and on experience, made provisional approximations for fractions which represent the 100, the 50 and the 20 year flood. These are 0.575, 0.5 and 0.2 respectively.

In 1988 Kovács (1988:19) presented a different approach in determining the RMF fractions by taking into consideration the catchment area size and also the K-region. This method, however, produces high frequency recurrence intervals for the RMF flood, in the range of 200 to 500 years, which does not correspond with the probabilistic flood analysis findings of this dissertation:

The Kovács 1988 fractions for the 200, 100 and 50 year floods at the Seeheim site on the Fish River are 0.91, 0.82 and 0.70 respectively (Kovács, 1988:52). These differ significantly from the 1980 fractions which are 0.65, 0.575 and 0.5 for the same return periods. As a first approximation, by drawing a line through the 1980 fractions, the line intersects the RMF line at approximately the 10 000 year recurrence interval, similar to the systematic data extrapolated through the palaeo flood point. As previously discussed, the Kovács-1988 flood

fraction points intersect the RMF line approximately at a 500 year, or less, recurrence interval. Thereby, given that the upperbound paleoflood data and also the probabilistic data both support a recurrence interval for the RMF at 10 000 years, the model structure of the TR 137 fractions, for the 200 to 50 year floods, requires review.

Refer to Figure 5.2 and 5.3 for a graphical presentation of the 1988 as well as the 1980 Kovács-fractions for the RMF flood at Seeheim and Ais-Ais in the Fish River. These fractions represent the 200, 100 and 50 year flood events. These are plotted together with the probabilistic distribution of the systematic data at these sites, as well as the upper bound palaeo flood data which was translated by means of the square root method to this point, translated from the Echo Camp to Seeheim and Ais-Ais.

In Figures 5.2 and 5.3 the RMF lines and the Kovács 1980 and 1988 flood fractions for the 200, 100 and 50 year recurrence floods are shown, as well as the Echo Camp upperbound palaeo flood peak translated respectively to Seeheim and Ais-Ais gauging sites.

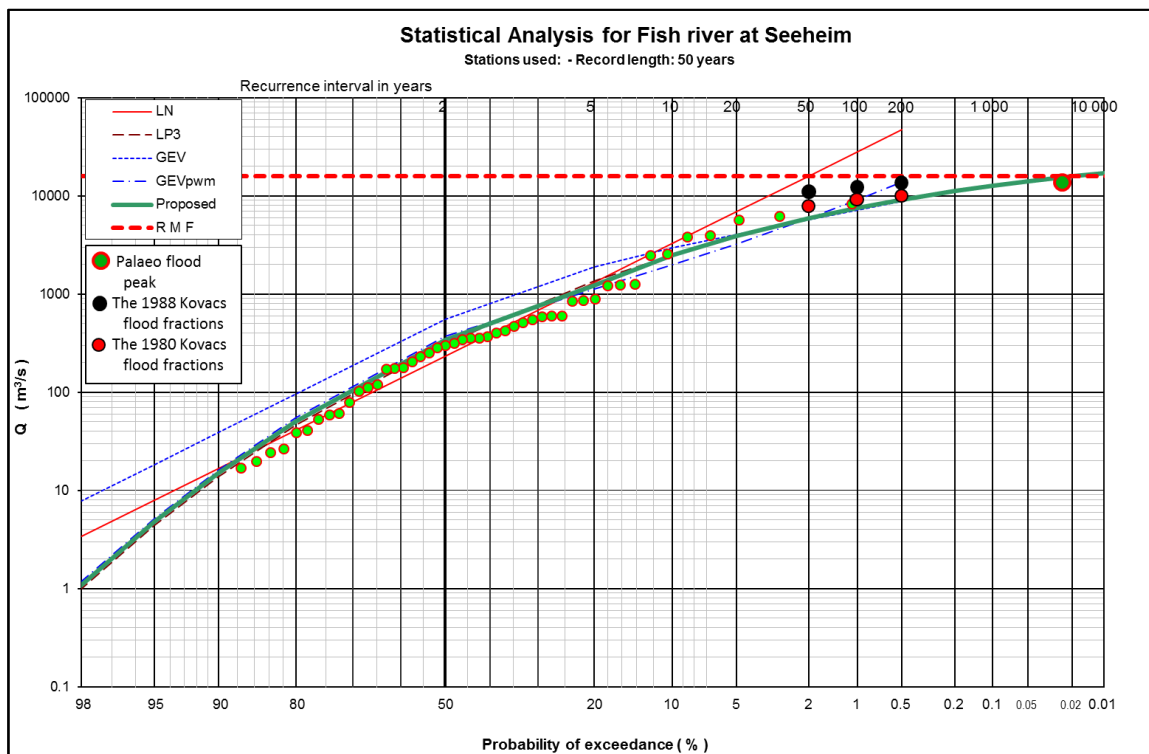


Figure 5.2: Various probabilistic models represent the annual flood peaks of the Fish River at Seeheim (46 400 km² catchment area). The Kovács flood fractions as well as the palaeoflood data points are included.

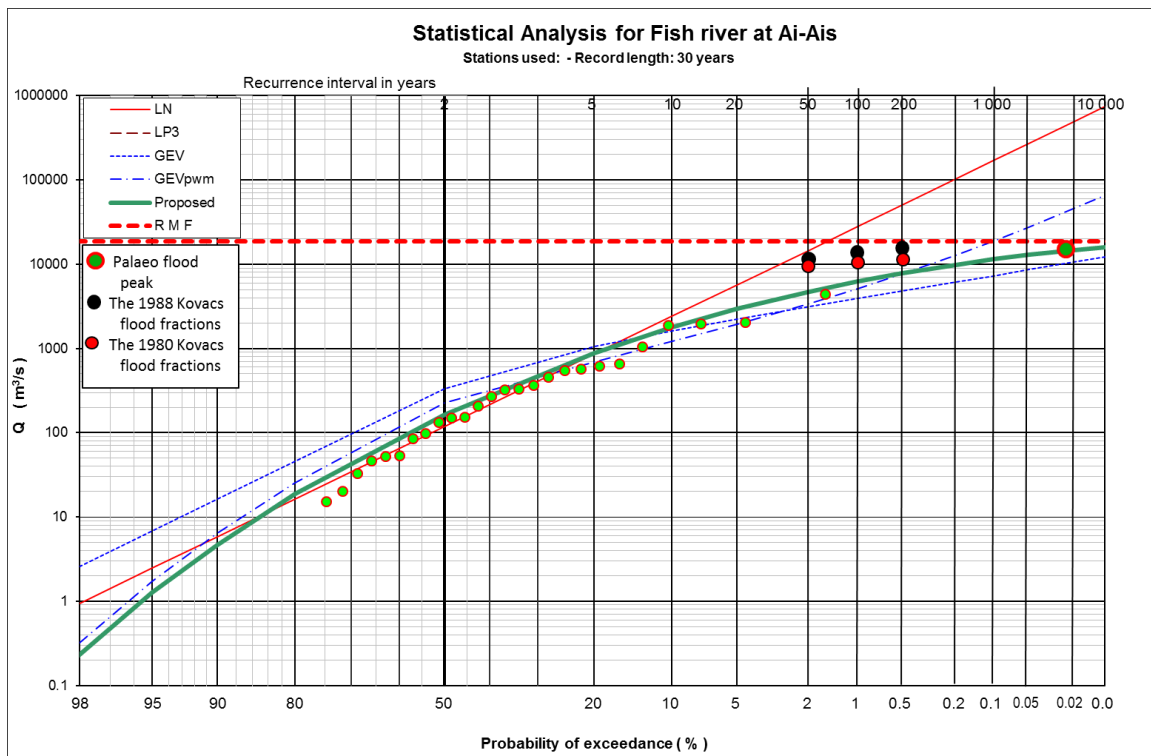


Figure 5.3: Various probabilistic models represent annual flood peaks of the Fish River at Ais-Ais (63 300 km² catchment area). The Kovács flood fractions as well as the palaeoflood data points are included.

Considering the information above, it is clear that the Kovács flood fractions of 1988 do not fit the data well. The introduction of the palaeo flood data made a significant contribution in this regard; fixing a flood peak at a recurrence interval of approximately 4 000 years (the average of the 3 000 to 5 000 years proposed by Dorn & Oberlander (1982:324)). Therefore, for further calculations, Kovács's simplistic 1980 approach (TR 105, 1980) was used to determine a function in terms of the fractions and the recurrence interval for the 200, 100 and 50 year floods. Refer to Figure 5.4 below. To update the more rigorous TR 137 recurrence interval for the higher frequency floods requires an in depth investigation which falls outside the scope of this dissertation.

With reference to the probabilistic distribution at Seeheim and Ais-Ais, see Figures 5.2 and 5.3, the TR 105 fractions for the 200, 100 and 50 year flood provide a better representation of the higher frequency floods than does the TR 137 fractions.

However as more extreme flood peak data becomes available, one can revisit the Kovács-1980 approach and derive an updated set of fractions applicable for the whole country as an upperbound from an envelope of curves. Alternatively region specific fractions could be derived as proposed by Kovács in 1988, however significantly more data would be required to make it practical.

Representative functions for the flood fractions:

Considering dam engineers outside Namibia who may be interested in applying the risk approach presented in this work, and who do not have a RMF model developed in their respective countries, the PMF flood model could also be used since it is well known and applied widely. Therefore both the RMF and the PMF flood fractions for higher frequency floods are presented in Figure 5.4 below, but the author continues to use the RMF and associated fractions for the further development of the risk model.

Regarding the PMF, which is a preferred alternative method in some countries, research by the Institute for Civil Engineers (ICE) in the UK provides design flood inflow as fractions of the PMF, being 0.5, 0.3, 0.2 and 0.17 for the 10 000, 1 000, 150 and 100 year flood respectively (Brown & Gosden, 2004:26).

Utilizing the fractions for the RMF or the PMF, one can determine functions in terms of these fractions and the recurrence interval. Refer to Figure 5.4.

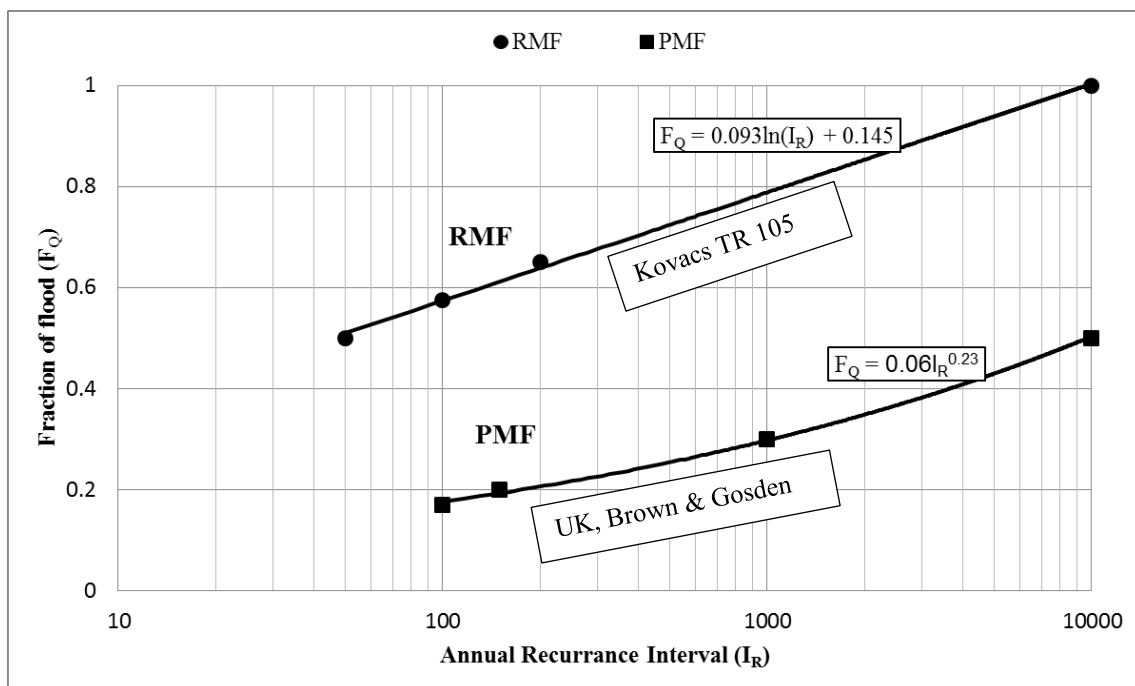


Figure 5.4: The fitted functions representing the fractions of the RMF and PMF against annual recurrence interval. Functions representing the RMF and PMF fraction-curves are indicated.

The functions are as follows:

For the RMF:

$$F_Q = 0.093 \ln(I_R) + 0.145 \quad (5.2)$$

For the PMF:

$$F_Q = 0.06 I_R^{0.23} \quad (5.3)$$

where: F_Q is the flood fraction of a selected flood over the RMF or PMF, whichever model is used, and

I_R is the Annual Recurrence Interval of the flood that exceeds the spillway capacity

Either of these functions, depending on which flood model you choose to work with, is required to determine the annual recurrence interval of the flood that exceeds the spillway discharge capacity for the dam under consideration. This is discussed in detail in the Probability of Dam Failure in section 5.4.1.3. below.

5.4.1.3 Probability of dam failure

The probability of dam failure is directly related to the probability of the occurrence of the flood which exceeds the NOC of the dam embankment, as discussed in the assumptions above. Therefore the discharge capacity of the spillway (Q_s) for the safety check flood is calculated utilising the full freeboard height for water storage: $Q_s = f(A, V)$ where area (A) and velocity (V) are both functions of spillway height (H_s), where height H_s refers to the entire energy head from the spillway sill up to the NOC. With reference to Figure 5.1, the height H_s is equal to the sum of components a , b and c .

Using the RMF flood model, calculate the RMF flood as well as the discharge capacity of the spillway (Q_s). The flood fraction (F_Q) = Q_s /RMF can then be determined. (At this stage, dam engineers from foreign countries who propose to use this Risk Model may prefer to work with the PMF flood model for instance if an RMF model has not yet been developed in their respective countries. It is imperative, however, that one model be consistently used for all dams within a portfolio of dams.)

Rewrite Equation (5.2) with annual recurrence (I_R) being the subject of the equation:

$$I_R = e^{((F_Q - 0.145)/0.093)} \quad (5.4)$$

By substituting the flood fraction (F_Q) in Equation (5.4), the annual recurrence interval of the flood that reaches the NOC is calculated. The inverse of this recurrence interval then produces the annual exceedance probability of a flood that reaches the NOC. From assumption number three, this probability is then also attributed to the probability of failure of the dam.

5.4.1.4 Increasing the flood discharge capacity of the dam

Increasing the NOC level of a dam increases the available energy height H_s of the water at the spillway, on condition that the spillway sill level remains the same. Refer to Figure 5.5; H_{s_0} refers to the current height above the spillway that is available to discharge extreme floods. By increasing the NOC level of the dam to level x or y or z , the energy height at the spillway is increased to H_{s_x} , H_{s_y} or H_{s_z} . Discharge is a non-linear function of H_s , hence the discharge capacity of the spillway (Q_s) increases exponentially:

$$Q_s = C_d B H^{1.5} \quad (5.5)$$

where: B is the width of the spillway,

H is energy height above the spillway sill,

C_d is the relevant discharge coefficient for various spillway structures; ogee, broad crest, labyrinth, etc. The value of C_d has to be derived empirically.

From Equation (5.5), if Q_s increases then the Annual Exceedance Probability (AEP) is reduced. This implies that for each increment by which the NOC is raised, the AEP of the flood required to overtop the dam is reduced.

As a guideline, the exercise of raising the embankment should continue up to a level which exceeds the height required to pass the safety evaluation flood, which has an AEP of 0.0001.

5.4.1.5 The cost of life safety investments

The investment in saving lives requires expenditure on the structure of the dam and/or the spillway to accommodate larger floods without overtopping the NOC level. With reference to Figure 5.5, the investment is associated with the cost of raising the NOC level of a dam,

effectively increasing the discharge capacity of the spillway and hence reducing the probability of failure of the dam. ‘Raising’ in this context means constructing additional earthworks on top of the existing embankment to increase the NOC level, as illustrated in Figure 5.5.

The cost of life safety is better described as follows: Raising the embankment in small steps, theoretically for the application of the RQO process, can only be done in a sequential order. This permits the calculation of the construction cost of every increment by which the dam NOC is raised. For every increment the dam is raised, the recurrence interval of the flood required to exceed the NOC (and cause failure of the dam) is increased, hence probability is reduced (see 6.1.4). Therefore the risk to life is reduced for every increment by which the embankment is raised, which can be directly translated to the cost required for the construction works to raise the embankment NOC.

The process of raising the embankment is depicted in Figure 5.5. The first increment is raised to level (x) for which the cost will be $C(x)$. The second increment to which it is raised is level (y), for which the cost will be $C(x+y)$, and the next level is (z) with the cost being $C(x+y+z)$, and so on for any additional increments raised.

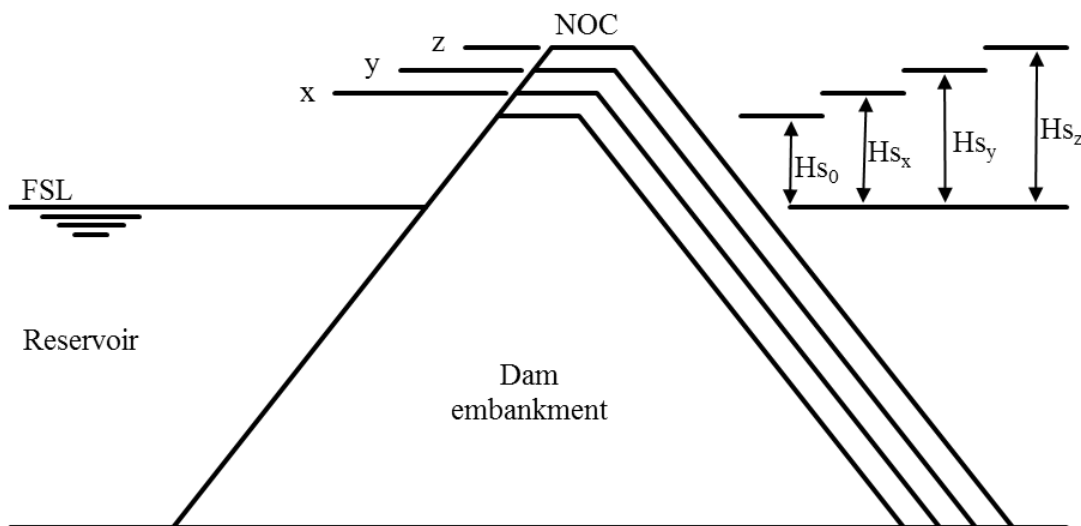


Figure 5.5. The cross-section of a typical embankment dam illustrating incremental raising of the embankment NOC, first to level (x), then to level (y), and then to level (z). The various heights (H_{s_0} to H_{s_z}) indicate the increasing spillway discharge head for the different NOC levels.

The cost of raising the embankment will produce a non-linear function since valleys in which embankment dams are constructed usually have convex upper bounds; for every increment by which the embankment is raised, the top length of the dam embankment increases exponentially and so also the surface area of the (downstream) face of the embankment. Hence a unique function can be developed for the incremental cost increase of each dam.

5.4.1.6 *The Loss of Life*

Loss of life (LOL) is a function of the Population at Risk (PAR) downstream of a dam. The fraction of LOL/PAR lies between zero and one, and the warning time and shape of the valley downstream of the dam influence the outcome. DeKay and Mecklelland (1993:200) determined that where valleys are narrow and the water flows deep and swiftly, the chances of survival are less than is the case where the water flows over wide plains on which the depth and velocity of flood water is expected to be less. They differentiated between these two scenarios by compiling formulae for high lethality and for low lethality. The formulae are presented in Hartford and Baecher (2004:101) and are as follows:

$$\text{LOL} = \text{PAR} (1.5207 \text{ PAR}^{0.513} e^{(3.83\text{WT}-4.012)})^{-1} \quad \text{for high lethality} \quad (5.6)$$

$$\text{LOL} = \text{PAR} (1 + 0.5207 \text{ PAR}^{0.513} e^{(0.822\text{WT})})^{-1} \quad \text{for low lethality} \quad (5.7)$$

where: *LOL* is the likely Loss Of Life,

PAR is the Population At Risk,

WT is the Warning Time the people have before the flood water reaches them.

The application of these formulae is left very much to the analyst's judgement since conditions defining lethality are not defined quantitatively.

Apart from the lethality of a flood event caused by a dam-break, there are two other variables which must also be considered; one must differentiate between the PAR resulting from the initiating flood event calculated as if the dam were indestructible, and then the PAR resulting from a dam-break flood caused by overtopping. ICOLD (1998:43) refers to it as a dam failure flood superimposed over certain natural base flood conditions. Serrano-Lombillo (2011:1001), however, proposes that one calculates the consequences of the flood, or LOL,

for the same flood event but for two different scenarios; first for a dam failure scenario, and secondly for a non-failure scenario (or indestructible dam). The difference in LOL between these two scenarios provides the incremental increase in LOL due to the dam failure. Refer to the following equation by Serrano-Lombillo (2011:1001):

$$R_A(r) = p(r) \cdot [c(r) - c(s)], \quad (5.8)$$

where: $R_A(r)$ represents the incremental risk associated to the failure of the dam,

$p(r)$ is the probability of the failure of the dam,

$c(r)$ is the consequences in case of failure and

$c(s)$ is the consequences in the case of non-failure.

Note: the ‘incremental’ risk discussed by Serrano in Equation 5.8 should not be confused with the increments of dam raising discussed in this dissertation; Serrano uses the term ‘incremental’ to specify the marginal increase of LOL between the non-failure and failure events of a dam during an extreme flood.

5.4.1.7 The risk

Risk, as discussed in this dissertation, is the product of the LOL, in the event of a dam failure, and the AEP of the flood which causes the dam to fail:

$$Risk = AEP * LOL \quad (5.9)$$

where: Risk is the societal risk to life associated with the failure of the dam due to external erosion which results from overtopping the NOC,

AEP is the annual exceedance probability that the NOC, for each increment raised, will be overtopped, and

LOL is the likely loss of life for each incident of overtopping associated with the increments by which the NOC is raised.

The objective of the RQO process is to optimally reduce risk over a portfolio of dams by investing in the flood discharge capacity of the dams. The decision maker has control over the independent variable, investment. The dependant variable, risk, then provides guidance to the decision maker regarding continued investment.

5.4.2 The Technology Curve

The term ‘Technology Curve’ is used widely by economists and industry, and generally is seen as something that one must ‘stay ahead of’. Most executives ‘see it as an important lever for a competitive advantage’ (The Economist, 2005:6). However, in the context of risk and civil engineering structures such as dams, the technology curve represents a ‘curve showing the available technology or best praxis for risk reduction’ (Schubert 2009:112).

The technology curve indicates the extent that risk to life can be reduced by investing an amount of money on life saving measures. Societal resources for life saving activities are limited and need to be invested in the most efficient risk reduction measures (Kraemer, Kohler & Faber, 2010:1). A typical technology curve according to Fischer (2012a:22) is shown in Figure 5.6.

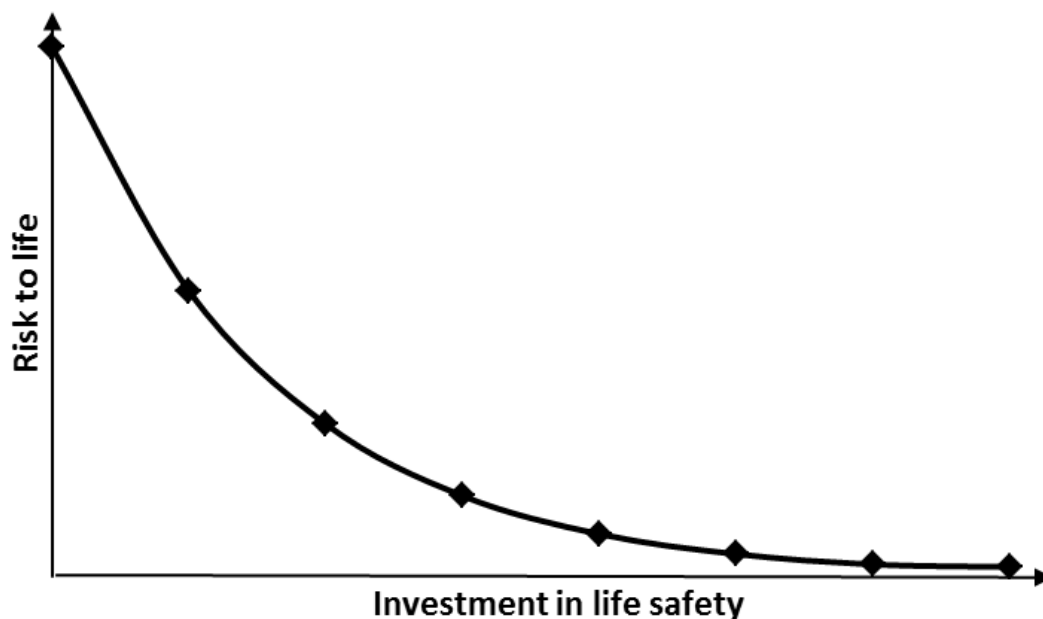


Figure 5.6: The typical technology curve; investment in life saving activities brings about a reduction in risk to life.

5.4.2.1 Constructing the Technology Curve

The technology curve illustrates the relation of the risk and the risk reducing activities, or investment cost. All the components required to develop the technology curve which is the next step of the RQO process, have been discussed in sub-section 5.4.

The results are presented in Table 5.1. There are (n) increments (H_1 to H_n) by which the dam NOC is raised (Column 1). For each of these increments the total cost for raising the NOC (C_1 to C_n) is calculated (Column 2). Also, each of the increments raised in Column 1 produces a reduced AEP (Column 3) of the flood which is expected to cause dam failure. The PAR and resultant LOL is then determined for each increment by which the dam NOC is raised (Columns 4 and 5). The product of the AEP and the LOL (Column 3 and 5, respectively) produces the Risk associated with the dam failure (Column 6).

R_0 in Table 5.1 represents the risk associated with the ‘do nothing’ option, i.e. the risk status remains unchanged, since no investment is made in rehabilitation work that needs to be done at the dam ($H_0 = 0$ m).

Table 5.1: The components of incremental rehabilitation, associated cost and risk are presented.

1	2	3	4	5	6
Incremental rehabilitation (NOC height raised)	Cost of rehabilitation (Investment)	Annual exceedence probability (AEP)	Population at risk	Loss of life f (PAR)	Risk ($P \times LOL$)
H_0	C_0	P_0	PAR_0	LOL_0	R_0
H_1	C_1	P_1	PAR_1	LOL_1	R_1
H_2	C_2	P_2	PAR_2	LOL_2	R_2
.
.
H_n	C_n	P_n	PAR_n	LOL_n	R_n

Utilising discrete data pairs found in Table 5.1, i.e. Cost of Rehabilitation (C_i) in Column 2 and Risk (R_i) in Column 6, the technology curve as indicated in Figure 5.6 is generated. The Cost of Rehabilitation is presented as ‘Investment in life safety’ in Figure 5.6.

5.4.2.2 The Inverted Technology Curve

The technology curve displayed in Figure 5.6 starts at some random risk value, representing the current status of the dam: if zero money is spent on rehabilitation work (the ‘do nothing’ option), then the risk associated with external erosion will be at its highest. However, as funds are invested in raising the dam, the risk reduces.

By considering the change in risk as a result of increasing the spillway capacity by raising the

dam, an Inverted Technology Curve (ITC) is obtained, expressed as the ‘Marginal Lives Saved’, as a function of the ‘Investment in Life Safety’. Refer to Figure 5.7.

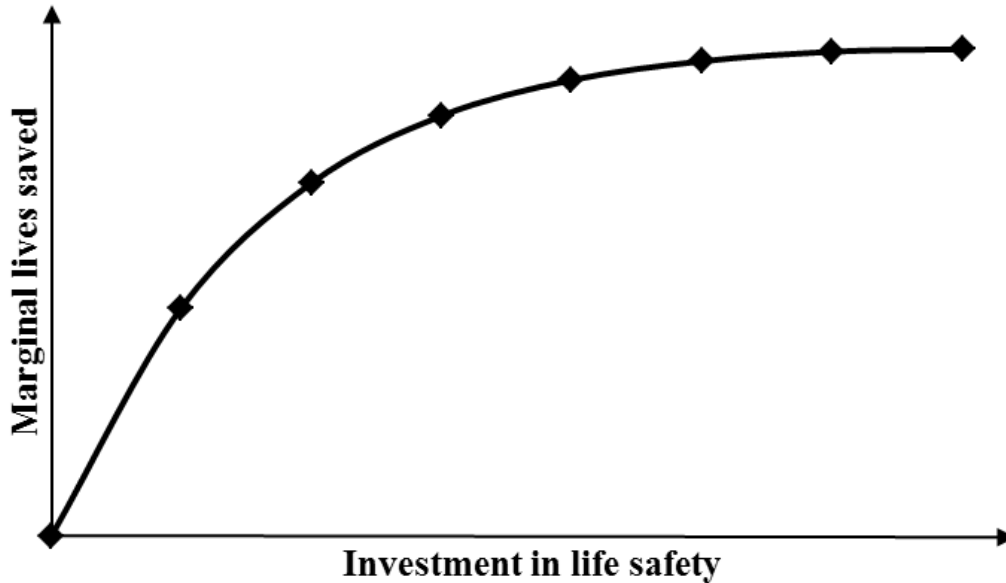


Figure 5.7: The Inverted Technology Curve (ITC) for a dam

The inversion process involves the discrete data points for the incremental raising of the embankment, and can be performed as follows:

$$MLS(i) = R(0) - R(i) \quad \text{for} \quad (i) = (0) \text{ to } (n) \quad (5.10)$$

where: $MLS(i)$ represents Marginal Lives Saved (or risk) for each incremental raising of the dam NOC (n increments, from 0 to n).

$R(0)$ defines the highest risk which is associated with the current condition of the dam before any rehabilitation work is done.

$R(i)$ is the risk associated with each of the (n) incremental steps by which the dam NOC had been raised; there are (n) steps from $R(0)$ to $R(n)$.

A polynomial function is fitted to the data points for the graph, for convenient analytical treatment of the ITC. The slope of the graph represents the gain in marginal lives saved per incremental investment. Since the graph starts at the origin without any offset, the function is $a_1x + a_2x^2 + \text{etc.}$

5.4.3 Reducing risk over a portfolio of dams

One of the objectives of risk reduction over a portfolio of dams is to identify and rehabilitate the highest risk dams first, and thereafter direct rehabilitation activities to the next highest risk dams, as far as resources permit.

A portfolio of dams can be ranked in terms of the initial slope of their respective ITC graphs to indicate the order in which dams are to be selected for rehabilitation, as the first matter for decision. The next class of decision is when to move over to the next dam for rehabilitation. This process is first treated by considering only two dams, from which generalisation to a portfolio of dams follow. Refer to Figure 5.8.

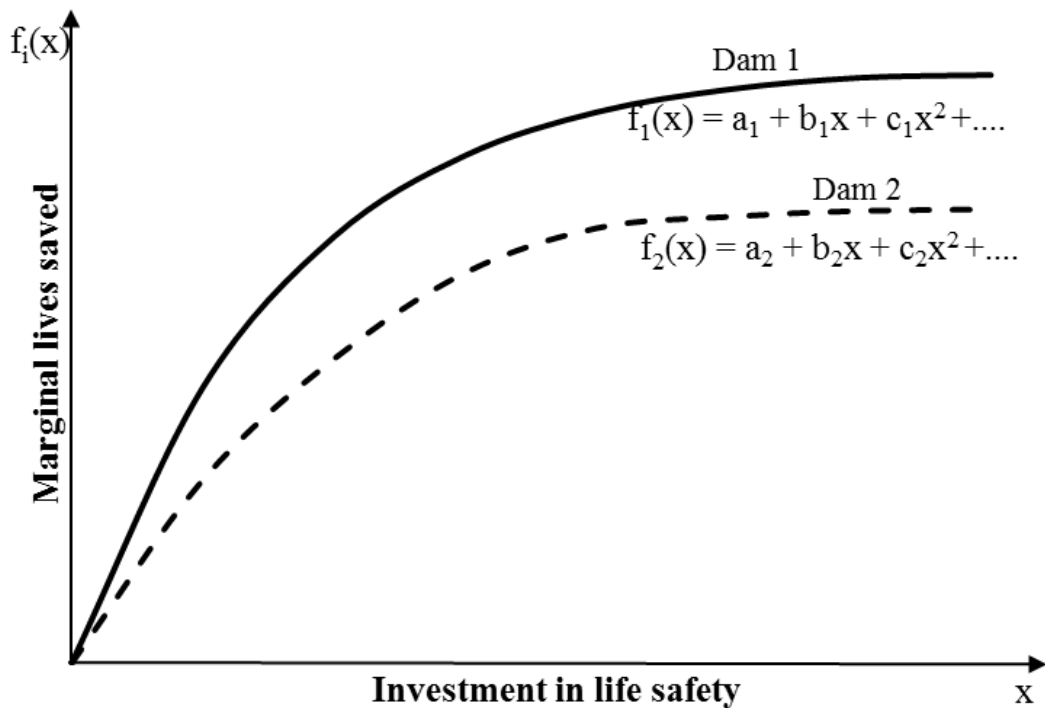


Figure 5.8: Inverted Technology Curves representing polynomial functions for two hypothetical dams in a portfolio of dams.

5.4.3.1 The starting point and sequence of rehabilitation

With reference to the functions of each ITC curve as displayed in Figure 5.8, the first derivative ($f'(x)$) produces the slope of the curve. Therefore the first constant of the first derivative of the polynomial expression, b_i , represents the initial slope of the ITC graph, allowing for the ranking of the dams according to $b_1 > b_2 > b_3$ etc.

In a large portfolio of dams, the dams with the second, third, fourth, etc. steepest starting slopes will, in the same order, form the sequence by which investment in rehabilitation will take place.

5.4.3.2 Optimising the investment

Optimising the investment according to the RQO approach implies that the decision maker uses resources to save the most lives for the given budget. This approach is not driven by the SBA, which requires rehabilitation to meet a prescribed standard; rather, it evaluates the reduction in risk gained through investment over several dams within a portfolio: investing in the highest risk dams first as in the rehabilitation list discussed above, then transferring the investment to a lower risk dam at a point where more lives would be saved through continuing investment in a following dam rather than continued investment on the current dam, thereby optimally utilising the available budget to save the most lives.

5.4.3.3 The transition point of expenditure

To optimise the investment over the portfolio, a transition from one rehabilitation project to the next is required. Refer to the transition from the higher risk dam to the lower risk dam shown in Figure 5.9.

The transition point is explained by the following expression:

With reference to Figure 5.8, when $f_2'(0) \geq f_1'(x)$, investment in the rehabilitation of Dam 2 commences and expenditure on Dam 1 is terminated. As discussed, it becomes more beneficial to invest in Dam 2 than to continue investing in Dam 1.

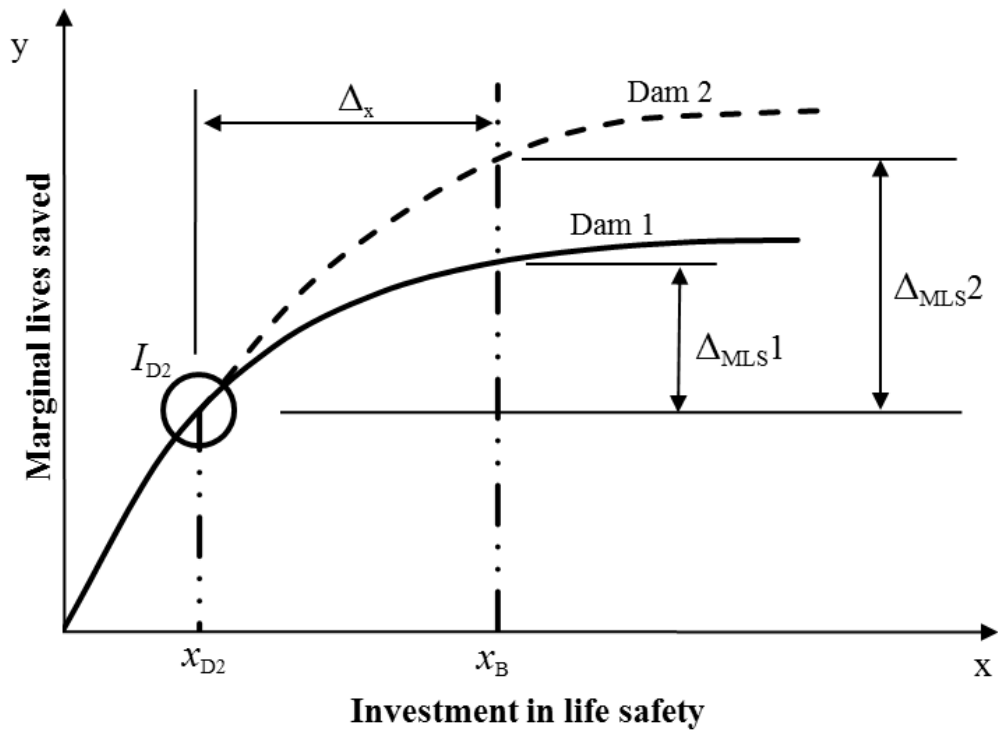


Figure 5.9: The combined ITC for two dams (ITC_{1+2}); starting with the dam with the steepest initial slope (ITC_1); at an investment x_{D2} the slope of ITC_1 is exceeded by the initial slope of ITC_2 ; by shifting ITC_2 to the transition point at $x = x_{D2}$, ITC_{1+2} is obtained.

Refer to Figure 5.9 for results of the RQO process. Explanation of the information depicted in Figure 5.9 follows below.

- Dam 1 displays the most lives gained for the initial investment (see Figure 5.8); $f_1'(0) > f_2'(0)$; or from the polynomial function $b_1 > b_2$. Therefore the rehabilitation starts with Dam 1.
- At point x_{D2} the starting slope of the Dam 2 curve, $f_2'(0) = b_2$, is equal to the slope of the Dam 1 curve, $f_1'(x)$, written as $b_2 = b_1 + 2c_1(x_{D2}) + 3d_1(x_{D2})^2 \dots$. From this expression x_{D2} can be determined. From this point onwards it is more beneficial to invest in life saving on Dam 2 than to continue investing in Dam 1. Therefore x_{D2} is the transition point from Dam 1 to Dam 2.
- At x_B the budget limit for investing in rehabilitation measures over the portfolio of dams is reached. At this point all available funds for investment have been exhausted.

- Note from the graph that $\Delta_{MLS2} > \Delta_{MLS1}$. Therefore the gain in expected lives saved for the budgeted investment (x_B) by transferring the investment from Dam 1 to Dam 2 at x_{D2} , is $\Delta_{MLS2} - \Delta_{MLS1}$.
- Following the RQO approach, the maximum number of lives have been saved using the available budget.

5.5 Decision making in RQO process: a hypothetical case

Where the sizes of the dams differ considerably, the results of the RQO process may not be practical in their application; in theory the RQO process ranks a portfolio of dams in a sequential order for rehabilitation, starting with the worst first and maintaining the highest rate of marginal lives saved for the available budget. In practice, however, the rate of change of slope for the next dam in the sequence may not be smaller than that of the previous one, therefore continuing the investment in the larger dam may be more advantageous. Refer to Figure 5.10. The transition from one dam to the next may also follow very closely on a previous transition, implying that one starts renovation on one dam and then finds that expenditure should be transferred to the next before any significant upgrading has been done.

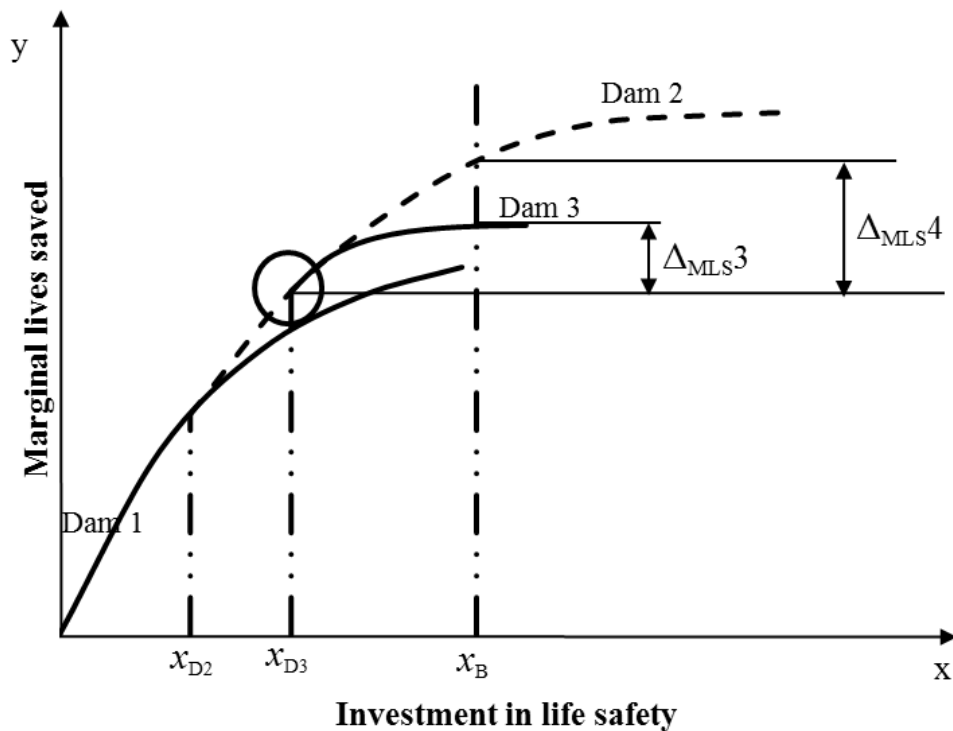


Figure 5.10: A third, smaller dam is added to the two existing dams used in Figure 5.9. The RQO process proposes the transition of expenditure at point x_{D3} . However,

consideration of total lives saved within the available budget suggests that the investment should remain with Dam 2.

From Figure 5.10 the following:

- At point x_{D3} , $f_3'(0) = f_2'(x_{D3})$. According to the QRO process this would imply that expenditure should be transferred from Dam 2 to Dam 3.
- From the graph $\Delta_{MLS4} > \Delta_{MLS3}$; therefore, the gain in expected lives saved for the budgeted investment (x_B) by maintaining expenditure on Dam 2 is more beneficial than transferring expenditure to Dam 3.
- When the transfer of investment from one dam to the next is very close to a previous transfer of investment, for example when x_{D2} is very close to x_{D3} , then, due to the high site establishment costs associated with dam rehabilitation, which could be between 30% and 50% of the cost of the rehabilitation, it will be more beneficial to continue investing in Dam 2 than to transfer to Dam 3.
- From the previous bullet point; if the budget permits, one could continue to invest in Dam 2 and in parallel invest in Dam 3, until the Dam 3 investment has reached a plateau, where further investment would not contribute to more marginal lives saved, and at this point terminate investment at Dam 3 and continue investing in Dam 2 until the budget has been exhausted, or until investment in another dam becomes more profitable.

5.6 Observations regarding the RQO method

Flood frequency models are used to assign a probability to a flood which exceeds an embankment NOC. The palaeoflood evidence indicates that the RMF flood fraction determined in the TR 105 produces better results than does the fractions indicated in the TR 137. It is therefore recommended that the TR 105 fraction for the 200 year flood, and subsequent fractions for the 100 year and 50 year floods be used for Namibia.

Considering the previous section, it is clear that the RQO process is an effective tool in ranking and prioritising activities within an available budget for a portfolio of dams. However, it remains a tool which requires an experienced decision maker to evaluate the

results.

The results of the RQO process, as indicated in Figure 5.10, are not practically applicable to every dam within a portfolio: the combined technology curve is dominated by dams with a high risk and high-rehabilitation cost, therefore a relatively small dam may have a high initial gain in marginal lives saved for a relatively small investment, but then, with continued investment, the additional marginal lives saved become negligible compared to a higher ranked dam, which may have a more steady continued rate of marginal lives saved for continued investment.

The cost of upgrading a dam embankment to accommodate a larger flood with a smaller frequency is not limited to raising the embankment. One could increase the spillway capacity without altering the elevation of the NOC or, for further improvement, raise the NOC after adjustments to the spillway. However, for the RQO process to work, the steps and costing for improving the flood discharge capacity of a dam needs to be done in a sequential order.

6. Applying the RQO process to real dams in Namibia

Having developed a quantitative risk approach which could be used to assist the decision maker in optimising resources to reduce risk over the portfolio of dams, the process is applied to three real dams in Namibia. For the first dam the RQO process is explained fully within the body of the text. Since the process is similar for the other two dams, only their results are included in the body of the text, with the full description appearing in Appendix L.

The typical risk bearing embankment dam in Namibia is constructed of rock fill embankment material and a concrete seal layer of the upstream face. This is due to the coarse nature of embankment material found in this mostly arid country where clayey material is scarce, as described in Section 5.1.2.

6.1. The selection of dams for the trial-run

The three dams used in the RQO portfolio assessment are the Avis Dam on the outskirts of Windhoek, the capital city in central Namibia, the Hardap dam near the town Mariental in the south, and the Von Bach Dam near the town Okahandja, also in central Namibia. The construction work on the dams was completed in 1932, 1962 and 1970 respectively.

All three dams are embankment dams which are classified as Concrete Faced Rock fill Dams (CFRD), typically the type of dam structure selected for arid regions where clay material is scarce. Although they are called rock fill, the bulk of the embankment consists of river rubble scraped from the river channels and surrounding hillsides, and not from crushed rock. Refer to Figure 6.1 for a photograph of the Avis Dam during construction. Appendix L includes additional pictures of the dam during construction.

The Avis Dam has a concrete face or seal layer on the upstream side of the embankment, whereas the Von Bach and Hardap Dams both have asphaltic seal layers.

CFRD dams have been found to have an inherent failure-resistance against internal erosion. A case in point is the Hardap Dam in the 1970's; a depression formed several metres below the water surface within the asphaltic seal layer. Cracks formed around the circumference of the depression which opened flow paths for water. A significant leakage stream was detected downstream with a discharge rate of approximately one cubic metre per second. This leak continued for several weeks before it was located and sealed. Although the leakage water was flowing right through the core of the embankment, no settlement or any other damage was detected. Several similar leaks have occurred since then and could be repaired by only filling

the depression and fixing the seal layer at the point of leakage; no structural repair work to the embankment was required.



Figure 6.1. Construction work underway at the Avis Dam in central Namibia during 1931. The embankment material consists of river rubble scraped together.

Although CFRD dams are generally safe against internal erosion, they are still prone to external erosion and failure due to water spilling over the non-overspill crest. Therefore, these dams are suitable candidates for the RQO process.

The RQO approach, however, can also be applied to traditional embankment dams with clay core and filter layers. The risk associated with overtopping of the NOC is dealt with in the same way as the CFRD dams, as discussed in this dissertation.

6.2. Constructing the inverted technology curves

The three dams selected for the case study all have spillways which cannot accommodate the safety evaluation flood, also, each of the three dams has a significant number of people living downstream of it; who are thus people at risk (PAR). Of the three dams, the Hardap dam has the largest storage capacity at 295 million cubic metres (Mm^3), with the Von Bach Dam second largest at $48.5 Mm^3$ and the Avis Dam with a capacity of $2.4 Mm^3$. Regarding people at risk, the Avis Dam has the largest number, then the Hardap and lastly the Von Bach Dam.

The RQO process is not guided by set standards indicating that the spillway capacity is or is not sufficient, it is guided rather by the risk of failure associated with the probability of overtopping. For example if the spillway could only handle a 200 year flood, but the risk to life were near zero if it failed (e.g. a dam in a very remote, unpopulated area), then the process would not require any expenditure on the dam even though it did not comply with the set standard of say the 10 000 year flood. The opposite is also true.

The PAR at the Hardap Dam was estimated at 3 075 according to Hattingh (2007:13). Most of the town of Mariental, 20 km downstream of the dam, would be inundated if the dam should break. According to Serrano-Lombillo (2011:1001), only the fraction of people at risk due to the dam-break event should be included in the risk estimation. Hence this does not include the PAR at risk from the flood event alone (if the dam were not to break). The PAR due to a dam-break caused by a flood event at Hardap Dam, overtopping the NOC, is 575 people, and the LOL is 33 (Refer to Appendix M, step 8 for Hardap Dam).

The Von Bach dam-break analysis for the Swakop River was not performed; however, the author estimated a population at risk of approximately 300, with the associated LOL at 25 people: there are informal settlements next to the river, which are likely to be at risk.

The first step would be to construct an inverted technology curve (ITC) for each dam where after it can be combined to form the ITC for a portfolio of dams. In Sections 6.2.1, 6.2.2 and 6.2.3, the ITC for the Avis Dam, the Hardap Dam and the Von Bach Dam are determined in a step-wise manner to allow the reader to follow the procedure.

The calculation of the dam break flood peak as well as the determination of the floodline, which is required to determine the population at risk, are not included in this dissertation; these are standard hydraulic calculations and modelling techniques as applied by dam safety practitioners.

The full procedure to determine the Technology Curve, consisting of 13 steps, is applied to the Avis Dam only. For the Von Bach and Hardap Dams, only the relevant graphs and final function are shown to avoid repetition of the process. Refer to Appendix M for the full Technology Curve development of the Hardap and Von Bach Dams.

6.2.1. The Avis Dam inverted technology curve

The Avis Dam is located on the outskirts of the City of Windhoek, upstream of the suburbs, Avis and Klein Windhoek. A photograph of the dam, shortly after construction, is shown in Figure 6.2. The PAR of the Avis Dam-break was determined by the author in 2013 as 744

people, with an estimated LOL of 620 people. The LOL figure is relatively high due to zero warning time for inhabitants living directly downstream of the dam. Therefore, although the dam is considered relatively small, it poses a high risk if it were to break, hence any small improvement to the dam wall will result in a significant reduction in risk, or rather a significant increase in marginal lives saved.



Figure 6.2. The Avis Dam several years after construction in the 1930's.

Below follows a breakdown of the process to determine the ITC for the Avis Dam. There are 13 steps in the process, with the last step indicating the polynomial equation required to plot the curve.

Step 1: Determine the 1:10 000 year flood (Q_{RMF}) from the new RMF model for Namibia:

Apply the Francou-Rodier Equation (4.1) to determine the peak discharge.

Regional K-value = 5 (from Figure 4.11)

Catchment area = 105 km²

$$Q_{RMF} = 1\,025 \text{ m}^3/\text{s}$$

Step 2: Determine the spillway capacity at NOC level

Elevation of NOC = 1723.1 mAMSL

Applying hydraulic calculations, determine the spillway discharge capacity at the NOC level (1723.1 m) = 943 m³/s

Therefore the 10 000 flood > the spillway maximum discharge rate.

Step 3: Determine the flood fraction (F_Q) of the spillway capacity flood from Equation (5.2):

$$F_Q = Q_{\text{spillway}}/\text{RMF} = 943/1025 = 0.92$$

Step 4: Determine the annual recurrence interval for the spillway flood from Equation (5.4):

$$I_R = e^{((F_Q - 0.145)/0.093)} = 4\ 163 \text{ years}$$

Step 5: Determine the AEP

From the annual recurrence interval, determine AEP:

$$\text{AEP} = 1/I_R = 0.00024$$

Step 6: Repeat steps 4 and 5 for several height increments above the NOC after determining the increase in spillway discharge capacity for each incremental new NOC level as displayed in Table 6.1.

Table 6.1: Avis Dam AEP for various height increments above the NOC.

mAMSL	Discharge	F_Q	I_R	AEP
(m)	(m ³ /s)		(years)	
1723.1	943	0.92	4 163	0.00024
1723.2	1001	0.98	7 675	0.00013
1723.3	1061	1.04	14 344	0.00007
1723.4	1122	1.09	27 164	0.000037
1723.5	1184	1.16	52 123	0.000019
1723.6	1247	1.22	101 317	0.00001

Step 7: Determine the volume and cost of additional embankment material required for each of the height increments above. Construction cost is based on the cost per cubic meter in section 3.4.2. (N\$ 1,057.70/m³ earthfil material). Table 6.2 indicates the cumulative cost for each increment raised.

Table 6.2: The Avis Dam cumulative cost table for each increment height with which the NOC is raised.

mAMSL	Spillway discharge	Incremental Height increase	Cumulative Volume of material	Cumulative Cost of earthworks
(m)	(m ³ /s)	(m)	(m ³)	(Million N\$)
1723.1	943	0	0	0
1723.2	1001	0.1	3 194	3.38
1723.3	1061	0.1	6 387	6.76
1723.4	1122	0.1	9 581	10.13
1723.5	1184	0.1	12 774	13.51
1723.6	1247	0.1	15 968	16.89

Step 8: Find the population at risk by determining the inundated areas by performing a floodline analysis. First determine the floodline and PAR resulting from the Safety Evaluation flood (SEF) as if the dam were indestructible (hence the water may flow over the NOC).

$$\text{PAR due to SEF only} = 3748 \text{ people (PAR}_{\text{SEF}})$$

Then determine the floodline and the PAR resulting from a dam-break, caused during the SEF event: the worst-case scenario flood whereby the dam wall breaks during the SEF.

$$\text{Total PAR due to dam-break} = 4492 \text{ people (T-PAR}_{\text{dmbrk}})$$

Then determine the incremental PAR due to the dam-break event over and above the PAR due to the SEF flood event, as in Equation (5.8) (Serrano-Lombillo, 2011:1001).

$$\text{Incremental PAR}_{\text{dmbrk}} = 744 \text{ people (PAR}_{\text{dmbrk}})$$

Step 9: Estimate the likely Loss Of Life (LOL) using either Equation (5.6) or (5.7) from (Dekay & Mclelland, 1993:200; Hartford & Baecher, 2004:101).

For the Avis Dam, the populated area is approximately 500 m downstream and lies on the floodplains of a relatively narrow valley alongside the river; high lethality (use PAR_{dmbrk} as in Step 8).

Flood warning time WT = 0.1 hours

Lethality = high

LOL = 620 persons

Step 10: From the above, determine the risk associated with the dam failure when the water level exceeds the NOC. Risk is calculated as in Equation (5.9). Refer to Table 6.3.

Assumption: the LOL associated with failure for each incremental increase in the dam's NOC level remains the same.

Table 6.3: Avis Dam risk associated with the probability of failure for each increment with which the dam is raised.

mAMSL	Cumulative Cost of earthworks	AEP	Loss of Life (LOL)	Risk
(m)	(Million N\$)			
1723.10	0	0.000240	620	0.148928
1723.20	3.38	0.000130	620	0.080778
1723.30	6.76	0.000070	620	0.043225
1723.40	10.13	0.000037	620	0.022824
1723.50	13.51	0.000019	620	0.011895
1723.60	16.89	0.000010	620	0.006119

Step 11: Plot the Technology curve for Avis Dam as per the example given in Figure 5.6. The data is provided in Table 6.3. The 'Risk' to life appears on the vertical axis and the investment (cost of earthworks) to reduce the risk appears on the horizontal axis. Refer to Figure 6.3.

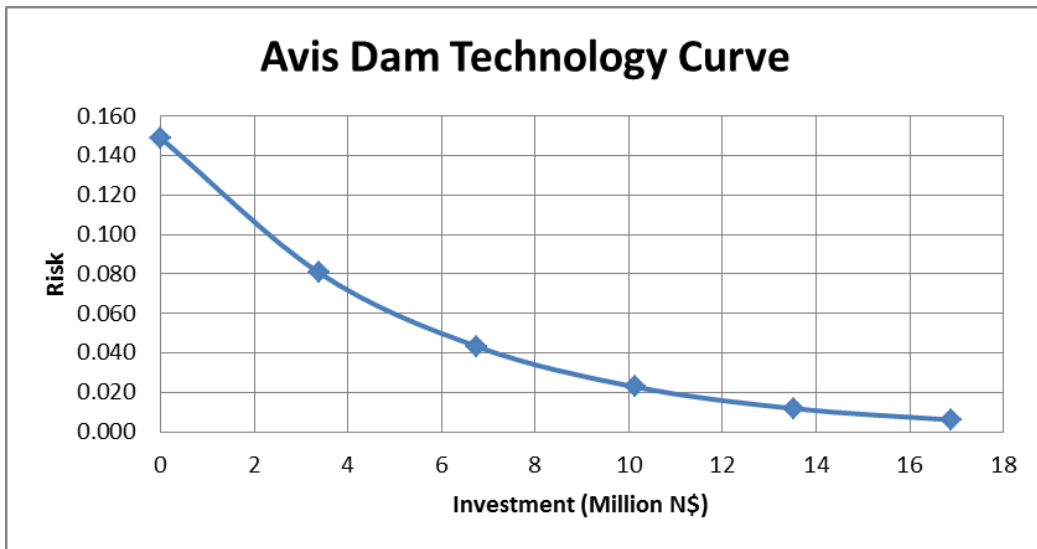


Figure 6.3: The technology curve for the Avis Dam.

Step 12: Plot the Inverted Technology Curve (ITC) as per Figure 5.7. ‘Marginal Lives Saved’ replaces ‘Risk’ on the vertical axis, the investment remains the same. Refer to Table 6.4. The values for ‘Marginal Lives Saved’ is determined from the risk by applying Equation (5.10).

The results are displayed in Figure 6.4

Table 6.4: Marginal Lives Saved which is the inverse of Risk

mAMSL	Cumulative Cost of earthworks	AEP	Loss of Life (LOL)	Risk	Marginal lives saved
(m)	(Million N\$)				
1723.10	0	0.000240	620	0.148928	0
1723.20	3.38	0.000130	620	0.080778	0.06815
1723.30	6.76	0.000070	620	0.043225	0.10570
1723.40	10.13	0.000037	620	0.022824	0.12610
1723.50	13.51	0.000019	620	0.011895	0.13703
1723.60	16.89	0.000010	620	0.006119	0.14281

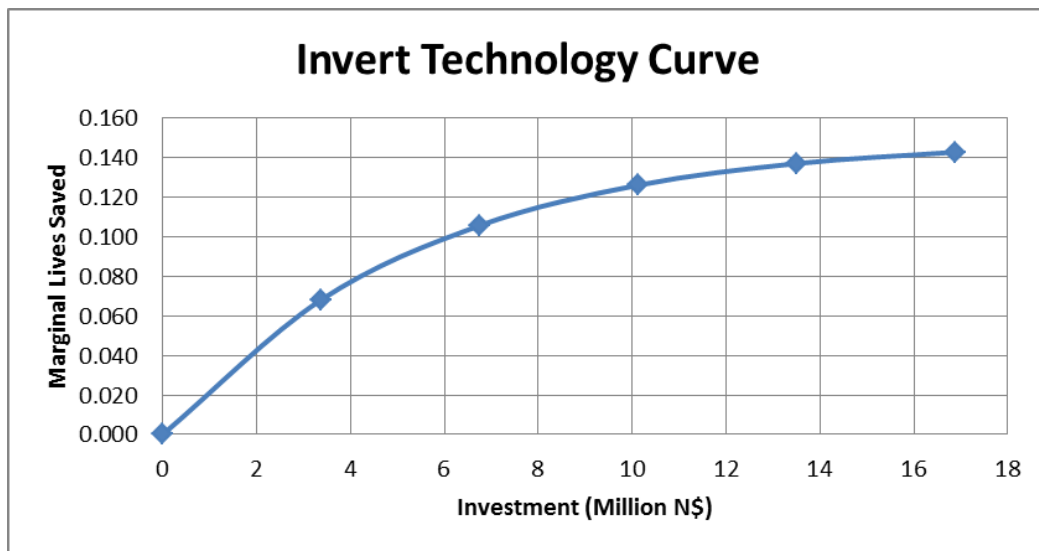


Figure 6.4: The inverted Technology Curve for the Avis Dam.

Step 13: Determine a polynomial function to represent the Avis Dam ITC.

From CurveExpert software version 1.3

4th Degree Polynomial Fit: $y = a + bx + cx^2 + dx^3 + ex^4$

Where y = marginal lives saved

x = Investment

The coefficient data are:

$a = 0$

$b = 0.026271$

$c = -0.002081$

$d = 8.55E-05$

$e = -1.46E-06$

6.2.2. *The Hardap Dam inverted technology curve*

The Hardap Dam is located approximately 15 km north of the town Mariental. It was constructed in the Fish River to supply water to the Hardap Irrigation Scheme as well as to the town of Mariental.

The PAR of the Hardap Dam-break was determined by Hattingh (2007:13) at 3 075 people, with an estimated LOL of 33 people due to a dam-break. The Hardap Dam is the largest storage dam in Namibia with a full supply capacity of 295 million cubic metres. Raising of the embankment would require a significant investment compared to the Avis Dam.

Refer to the Hardap Dam technology curve development steps in Appendix M.



Figure 6.5. The Hardap Dam spillway structure during the 2006 flood release which caused the inundation of approximately 200 homes in the town of Mariental, 20 km downstream of the dam.

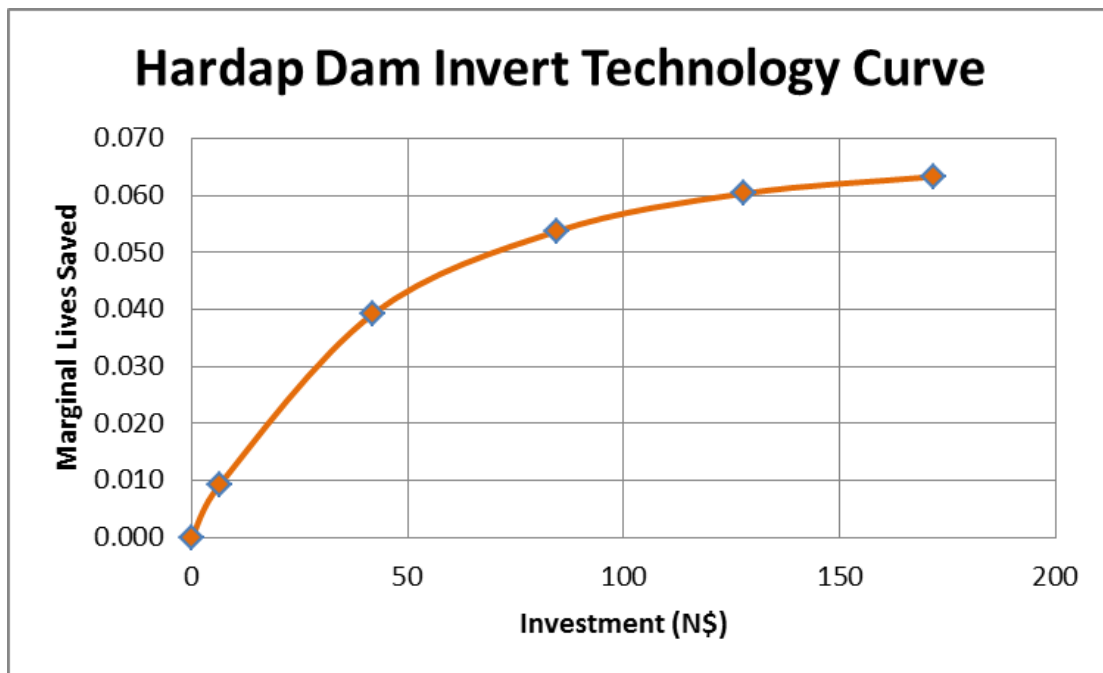


Figure 6.6: The inverted Technology Curve for the Hardap Dam.

Determine a polynomial function to represent the Hardap Dam ITC.

From CurveExpert software version 1.3

4th Degree Polynomial Fit: $y = a + bx + cx^2 + dx^3 + ex^4$

where y = marginal lives saved

x = Investment

The coefficient data are:

$a = 0$

$b = 0.00146317$

$c = -1.58E-05$

$d = 8.70E-08$

$e = -1.86E-10$

Detail of the development of the Hardap Dam ITC are included in Appendix M.

6.2.3. *The Von Bach Dam inverted technology curve*

The Von Bach Dam is located in the Swakop River, near the town Okahandja in Central Namibia. It was constructed in to supply water to the City of Windhoek as part of a three-dam system.

A detailed dam break analysis on the Von Bach Dam was not performed. For the purpose of this exercise, it was estimated that 500 people are at risk due to a dam-break event, with a subsequent LOL of 25 people.

Refer to the technology curve development steps in Appendix M.



Figure 6.7: The Von Bach Dam main embankment upstream face.

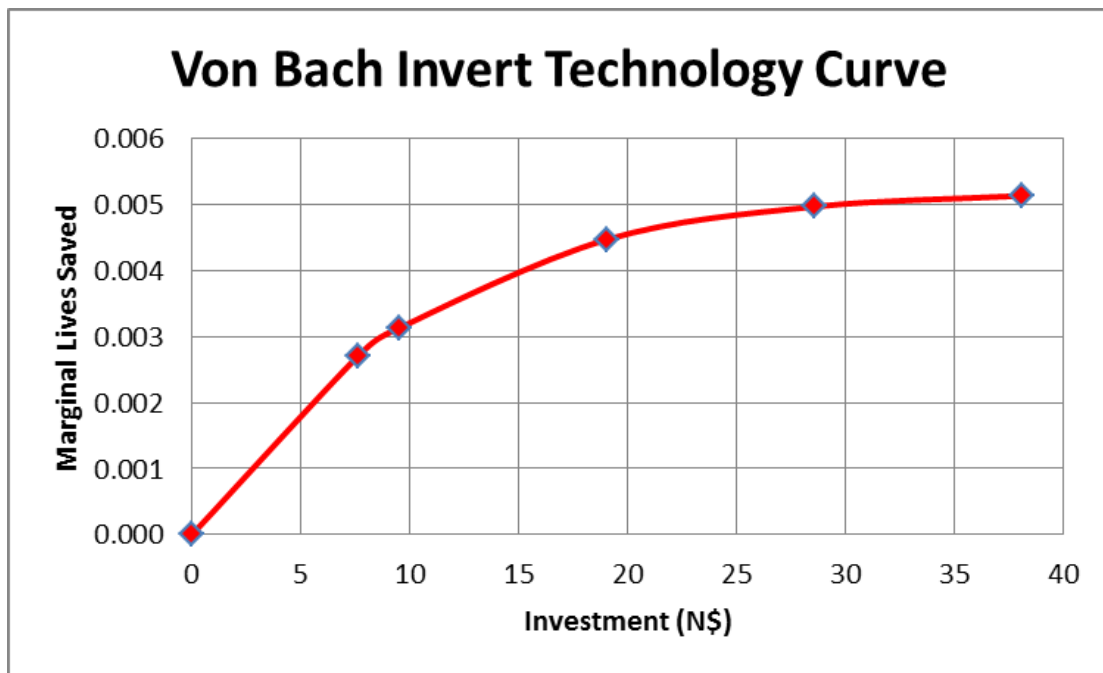


Figure 6.8: The inverted Technology Curve for the Von Bach Dam.

Determine a polynomial function for the Von Bach Dam to represent the ITC

From CurveExpert software version 1.3

4th Degree Polynomial Fit: $y = a + bx + cx^2 + dx^3 + ex^4$

Where y = marginal lives saved

x = Investment

The coefficient data are:

$a = 0$

$b = 0.000470991$

$c = -1.77E-05$

$d = 3.26E-07$

$e = -2.42E-09$

Detail of the development of the Von Bach Dam ITC are included in Appendix M.

6.2.4. *The inverted technology curves*

The Technology curves of the three dams are displayed together in Figure 6.11. In this case the higher risk dam is clearly identifiable. The size of the dam embankment also has a significant impact on the cost when compared to a relatively smaller dam.

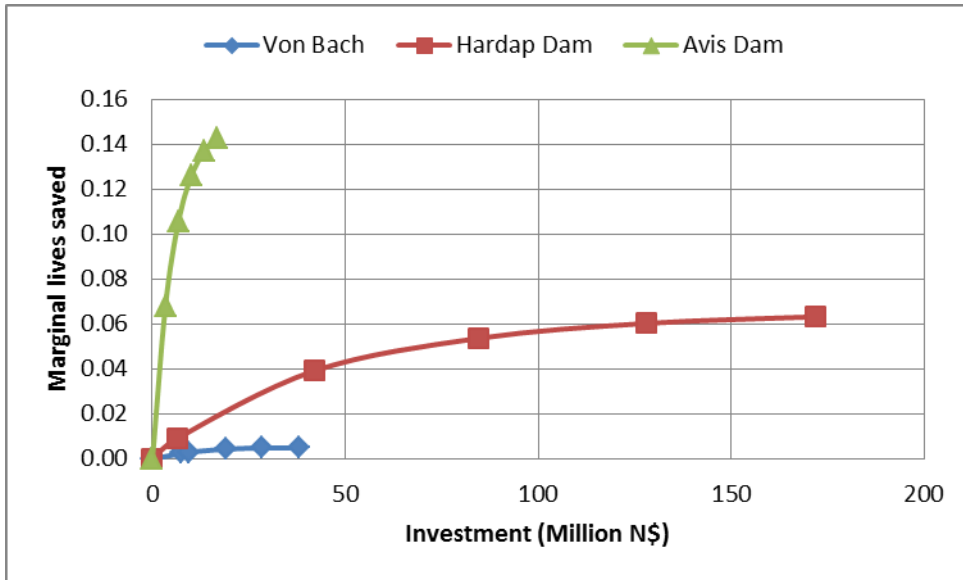


Figure 6.9. The inverted technology curves for the Von Bach, Hardap, and Avis Dams.

6.3. Constructing the combined inverted technology curves

Now that the technology curves have been constructed, the following steps are to rank the dams from highest initial risk to the lowest, and then to determine the point of transition to optimise investment; saving the greatest number of marginal lives within the available budget.

The first step would be to determine polynomial equations fitting the technology curves, as discussed in Section 6.2. Then determine the first derivative of each polynomial equation; refer to a discussion of this process in Section 5.4.3.1. The initial slope would then be the first constant of the first derivative.

The general expression for the polynomial equation is:

$$f(x) = a + bx + cx^2 + dx^3 + ex^4 + \dots$$

where $f(x)$ represents marginal lives saved

x represents investment value

The first derivative is:

$$f'(x) = b + 2cx + 3dx^2 + 4ex^3$$

Therefore the initial slope, where $x = 0$, then $f'(x) = b$

For the polynomial expressions described in Section 6.2, the initial slopes for each of the dams is as follows, starting with the steepest:

Avis Dam: $f'(x) = 0.0263$

Hardap Dam: $f'(x) = 0.0014$

Von Bach Dam $f'(x) = 0.0004$

From the above it can be seen that the Avis Dam takes first priority regarding investment, since the most lives will be saved for the initial investment. Thereafter follows the Hardap Dam and last the Von Bach Dam.

To determine the transfer of investment from the Avis- to the Hardap Dam, determine at which point the slope of the Avis Dam curve is equal to the initial slope of the Hardap Dam. At this point the Hardap Dam will begin to show a greater gain in marginal lives saved than the Avis Dam. At this point, further investment in the Avis Dam should cease and investment in the rehabilitation of the Hardap Dam should start.

The first change over from Avis to Hardap Dam takes place where the Avis Dam $f'(x) = 0.0014$. At this point the 'Investment Value' stands at N\$ 15.76 million. The second change over, from the Hardap to the Von Bach Dam, takes place where the slope of the Hardap Dam, $f'(x) = 0.0004$, is also the initial slope of the Von Bach Dam.

At this point the investment value of the Hardap Dam will stand at = N\$ 47.20 million. However, this N\$ 47.20 million accumulates on top of the N\$ 15.76 million invested in the Avis Dam; since one dam follows on the next, the cost of investment will be accumulative.

The starting point for investment on each of the dams is as follows:

Avis Dam N\$ 0.00 (the initial expenditure due to steepest initial slope)

Hardap Dam N\$ 15.76 million

Von Bach Dam N\$ 15.76 + N\$ 47.20 = N\$ 62.96 million

Refer to Figure 6.10 for the sequence of dam rehabilitation.

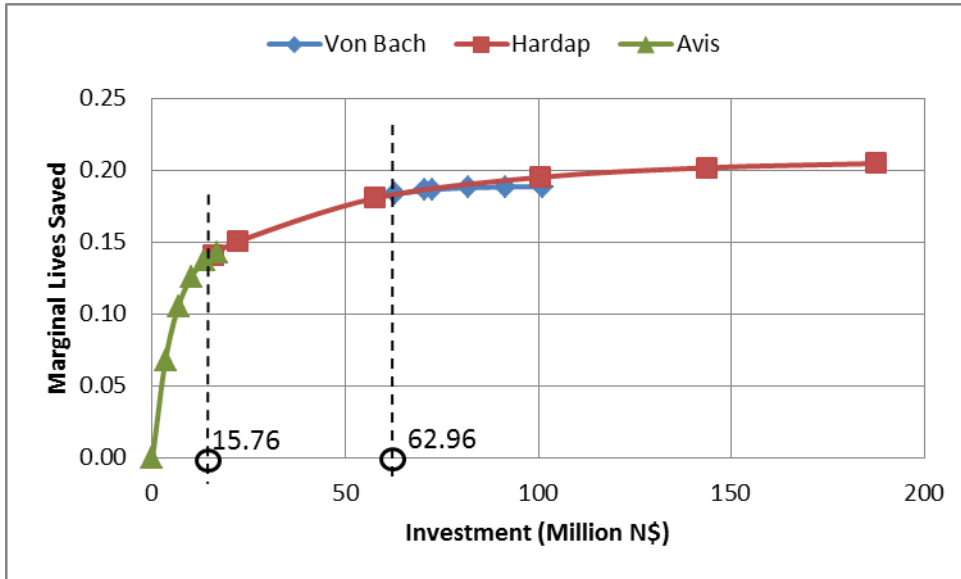


Figure 6.10. The combined inverted technology curves for the Hardap, Von Bach and Avis Dams. Indicated are the points proposed by the RQO process, at which investment is transferred from one dam to the next to optimise expenditure.

6.4. The decision making process

Until this stage, no decision making has been required from the analyst. However, now that the portfolio of dams has been ranked in order of the highest to lowest risk, and the changeover from one dam to the next has been established, so as to optimise the investment, the analyst will be required to evaluate the decisions and the practicality of the applied structure.

The initial rate of marginal lives saved for the Von Bach Dam does not exceed that of the Hardap Dam. As a matter of fact, it flattens off much more quickly than the Hardap Dam. Therefore it remains more beneficial regarding marginal lives saved rather to continue investing in the Hardap Dam than to change over to the Von Bach Dam.

Consider Figure 5.10; for the Von Bach Dam, the transition point, X_{D3} , can be shifted along to a point where $\Delta MLS3 > \Delta MLS4$, achieving gain toward the tail end of the combined technology curve.

6.5. Reviewing the RQO model

The RQO process provides a quantitative approach to risk based dam safety in Namibia which can be used by dam portfolio managers to compare risks, prioritise rehabilitation activities and propose the extent of rehabilitation required at each dam to optimize the resources.

The RQO relates the probability of occurrence of the flood magnitude equal to the spillway capacity and the associated lives lost expressed in risk terms as the expected lives lost, to the cost of raising the non-overspill crest to the flood magnitude. By applying this relationship to a range of raised levels the risk characteristics of a dam can be obtained as a technology curve. Rehabilitation of a portfolio of dams can be prioritised in terms of their respective technology curves.

Risks in the RQO model are dominated by flood events with recurrence intervals spanning thousands of years; flood intervals which traditionally had low confidence levels. The palaeoflood data however provides evidence which increases the confidence in the magnitude and recurrence interval of these extreme events.

7. Findings and Analysis

7.1 Flood hydrology of Namibia

Reviewing dam safety in Namibia after the Mariental flood event in 2006, it was noted that the extreme flood model most used in Namibia, the Regional Maximum Flood model (RMF), had not been updated since 1988. Now, with almost 30 years of additional systematic data, as well as new techniques being applied in palaeoflood hydrology, a great deal more flood peak data provided sufficient grounds to update the existing extreme flood model of Namibia.

The updated extreme flood model for Namibia generally has the same shape for the K-value regions, a regional coefficient which expresses the relative flood peak magnitude, as does the Kovacs flood model which was prepared in 1988. The updated model however has better definition along the Kalahari and Namib deserts. It also provided a new flood region in the northwest of Namibia.

The palaeoflood data, collected in the Fish, Kuiseb and Kahn Rivers, provided valuable input in the updating of the Namibian Regional Maximum Flood model: it provided flood peaks where no measurements had previously been done. These peaks, of which some occurred

several hundred to several thousand years ago, extended the short term data to allow more accurate prediction of low probability floods.

Palaeoflood data, collected in the Fish and Kuiseb Rivers contributed significantly to the new RMF K-value delimitation around the Kuiseb River as well as the Fish River: the K-values were increased for both the lower Kuiseb and Fish Rivers.

The method to determine K-values uses an envelope of flood magnitude versus area, which can only be extended by new data, not reduced; unless the region under investigation is modified.

There are remote areas within Namibia where no flood peak data is available. In these instances the RMF boundary lines of the hydrological homogeneous regions are not fixed, but indicated as tentative. Some of these areas are in the arid regions of the country; southwest and far south, typically places where suitable sedimentary evidence for palaeoflood studies is likely to be found. Others are north and north eastern parts of Namibia where dunefields and low gradients will make it challenging finding palaeoflood evidence.

RMF fractions presented by Kovacs in 1988, to determine higher frequency floods, have been found to overestimate the magnitude of the 200, 100 and 50 year flood.

From the flood data, the changeover in the RMF peak curves from the Transition Zone to the Flood Zone was fixed at a catchment area size of 100 km² for each of the five flood regions (2.8, 3.4, 4.0, 4.6 and 5.0), as opposed to the findings of Kovacs (1988) which proposed areas of 500 km² for regions 2.8 and 3.4, and 300 km² for region 4.0.

7.2 Risk based dam safety

The Rational Quantitative Optimal (RQO) approach presented in this dissertation does not cover the entire spectrum of risks associated with dam safety, but it addresses a failure mechanism which has the highest probability of occurrence: overtopping of the embankment due to insufficient spillway capacity, with subsequent failure of the embankment and a potential loss of life.

Generally risk based dam safety is seen by many as the future analysis method for determining the safety of dams and allocating resources. An acceptable approach to risk based dam safety which meets the approval of all stakeholders had not been developed until now.

Available risk models are based on judgmental inputs from the decision maker which, for some practitioners, are not acceptable for decision making where lives are concerned. Therefore current risk assessment approaches are applied qualitatively to rank dams in order of priority for rehabilitation. The extent of rehabilitation for each dam is however still determined by the SBA.

The RQO approach presents a transparent framework which evaluates risk quantitatively over a portfolio of dams, prioritising rehabilitation activities from the highest to the lowest risk dam. The process also guides the decision maker regarding the extent of risk reduction required at each dam, thereby optimally investing limited resources.

The RQO process estimates the probability of risk in terms of the flood which will overtop the Non-Overspill Crest of a dam, and the consequence in terms of lives lost due to failure.

In the RQO process, risk is not calculated as an absolute value, to be compared with independent absolute values. It compares the risks of different dams within a portfolio. As long as the variables in the model are dealt with consistently, the distribution of risk within a portfolio of dams will be comparable. The process will appeal to the technically minded person looking for a straightforward and purely quantitative approach.

This RQO process proposes to take risk-based dam safety a step beyond its current state of 'infancy', as mentioned by ICOLD in 2005(6).

The RQO approach was not developed to satisfy SBA principles, which require full rehabilitation in order to meet all prescribed standards. It was developed to optimise life-saving investment over a portfolio of dams, thereby encouraging partial rehabilitation in terms of the SBA, to produce the highest return in life safety for the available budget.

The spillway capacity of a dam could be increased without altering the elevation of the NOC, by increasing the effective width of the spillway. However, expert engineering judgment is required to investigate upgrading options since, for the application of the RQO process the modelling must be done in steps and in a sequential order, incrementally improving the flood handling capacity of a dam, accumulating the cost in order to obtain a function representing the technology curve. If the upgrade work is done by selecting between two separate options, as in an either-or scenario, then the RQO process would view these two options as separate dams, each with its own technology curve.

8 Conclusions

From the findings of this dissertation, the following conclusions are drawn:

8.1 Flood hydrology in Namibia

- The extreme flood hydrology model of Namibia, the Regional Maximum Flood (RMF) model of 1988, requires updating since palaeoflood evidence as well as probabilistic analyses of systematic flood peak data indicates that the current model underestimates the recurrence interval of extreme flood events.
- The latest flow gauging data, gathered over the last thirty years, as well as the palaeoflood data significantly increased available flood peak data for Namibia; by adding approximately 1900 years of recorded data as well as discrete extreme flood peaks, some dating back several thousand years.
- The newer systematic and palaeoflood data generated new K-regions in the west and north west of Namibia, and increased K-values along the lower Fish River as well as the lower Kuiseb, Tsondab and Tsauchab Rivers which flow into the Namib desert.
- Palaeoflood studies in the Kuiseb and Fish River systems provided valuable upper bound flood data: geomorphologic evidence which indicates that there is a ceiling to maximum flood peaks at specific sites in these rivers, thousands of years old.
- Similarly to the palaeoflood studies in the Fish, Kuiseb and Kahn Rivers, palaeoflood studies can also be applied to determine extreme floods in other remote arid areas, providing flood peak data which otherwise would take very long to be estimated using conventional methods.
- Palaeoflood hydrology provides valuable ancient as well as upper bound flood information which will assist in refining the boundaries of the flood regions in Namibia, and elsewhere. In so doing providing more reliable information on low probability floods, which become an input to the RQO model.
- Based on probabilistic analyses of the systematic flood peak data of the 55 flow gauging stations provided by the Namibia Department of Water Affairs, the RMF has an annual recurrence interval of approximately 10 000 years, similar to the findings mentioned by Van der Spuy (2008).
- The palaeoflood results at two sites in the lower Fish River indicate that the annual recurrence interval of the RMF, at these two sites, is approximately 10 000 years.

- The 200 year RMF fraction of 0.65, as determined by Kovács in 1980 (TR 105), with its associated 100 and 50-year fractions of 0.575 and 0.5 respectively, corresponds well with the results of the palaeoflood study, which proposes that an RMF flood has an annual recurrence interval of approximately 10 000 years.
- The size of the catchment area for the changeover from the Transition Zone to the Flood Zone, in the RMF model, is 100 km² for each of the five flood regions.
- The newly delineated RMF flood regions for Namibia have been updated with the latest systematic flood data as well as palaeoflood data and may be used in the interim until more data is available to delimitate flood regions in the remote parts of Namibia.

8.2 The RQO portfolio risk assessment process

- The aim of risk based dam safety is to find a mechanism of identifying and addressing the risk of failure of a dam, based on the risk imposed, and not on a non-compliance with the Standards Based Approach (SBA).
- Risk based dam safety internationally is used as a tool to prioritise rehabilitation activities over a portfolio of dams, in which case the SBA would still be used to determine the extent of rehabilitation.
- The Rational Quantitative Optimal (RQO) process presented in this dissertation is applied mechanistically, deriving the probability of dam failure from the updated Namibia flood model, estimating the consequences of failure deterministically, and thereby dealing with risk in a transparent, quantitative way.
- The process guides the decision maker on the extent of risk reduction required at each dam, thereby, optimally investing limited resources; since the outcome is presented in terms of the reduction in expected life loss due to dam failure as outcome, as a function of the amount spent on increasing the spillway capacity as decision variable.
- Internationally, the highest rate of dam failure is attributed to overtopping of embankment dams.
- The RQO method does not cover all aspects of risks. It addresses the probability of failure in terms of the recurrence interval of the flood which causes the dam to overtop, a typical failure scenario for Namibia.
- All types of embankment dams are prone to failure due to overtopping of the NOC. Therefore the RQO method can be applied to other type of embankment dams as well, not only CFRD. The risk estimation process remains the same.

- The RQO process provides a quantitative approach to risk based dam safety in Namibia which can be used by dam portfolio managers to compare risks, prioritise rehabilitation activities and propose the extent of rehabilitation required at each dam, in so doing, optimising resources
- Confidence in the RQO risk model depends on the reliability of the regional flood model, which in turn can be improved by applying palaeoflood hydrology.
- The RQO process can also be used with the higher frequency flood fractions of the PMF flood model, and not only the RMF flood model. This will permit dams engineers from other countries to also use this risk approach.
- The likely loss of life for each dam should be determined by applying the same model to the populations at risk and by adopting the same assumptions, regarding loss of life, at each dam. As long as the variables in the model are dealt with consistently, the distribution of risk within a portfolio of dams will be comparable. Hence the process will appeal to the technically minded person looking for a straightforward and purely quantitative approach.
- This RQO process presents a risk model which addresses the concerns raised by some dam owners and decision makers in dam safety: a quantitative result; however, not one expressed in term of an absolute risk value, but as a tool to compare risk for different dams within a portfolio.
- The RQO approach is not a replacement for the standards based approach (SBA), and also cannot be used in conjunction with the SBA. The RQO optimises resources over a portfolio, reducing risk based on the best gain in marginal lives saved, and not based on a fixed standard.
- One could increase the spillway capacity without altering the elevation of the NOC, or for further improvement raise the NOC after adjustments to the spillway, whilst still using the general RQO methodology. Expert engineering judgement is required to investigate upgrading options since, for the application of the RQO process, the upgrading must be done in steps and in a sequential order, incrementally improving the flood handling capacity of a dam, accumulating the costs, in order to graph the technology curve.
- The RQO is an effective tool to rank embankment dams in Namibia, and elsewhere, according to risk associated with failure due to external erosion, which also indicates the extent of rehabilitation at each dam, optimizing the resources.

9 Recommendations

From the conclusions drawn, the following recommendations are made:

- More palaeoflood studies should be done to increase the footprint of flood peaks in Namibia and in so doing to assist in further updating of the RMF flood model for Namibia; better defining the regional flood zone lines along these areas. Specific focus should be given to catchment areas smaller than 100 km² (the Transition Zone) in the K regions 2.8 and 3.4
- More palaeoflood investigations will also improve the reliability of recurrence intervals associated with extreme flood events which becomes an input to the RQO risk model.
- The boundary lines dividing the K = 3.4 and 2.8 zones needs revisiting as more data becomes available in the deserted areas.
- The Kovacs RMF flood fractions of 1988, for the 200, 100 and 50 year floods, in the TR 137 produce misleading overestimated results in the lower Fish River.
- Upper bound flood studies are required at existing flow gauging stations in Namibia. This will permit extrapolating the systematic data to join the palaeo data points. In so doing all these gauging stations will contribute to determine new fractions for the higher frequency floods, like the 200, the 100 and the 50 year flood.
- The Rational Quantitative Optimal (RQO) process can be used to evaluate the risk related to external erosion for a portfolio of dams and in so doing rank the dams from highest to lowest risk to establish the order in which rehabilitation should take place, and also to indicate the extent of rehabilitation required at each dam, in order to optimise the available resources.
- The cost of the rehabilitation, or of the raising of the dam embankment, is based on an empirical approach and little data. Research regarding the cost of rehabilitation is needed to confirm or improve the approach followed in this dissertation.
- The cost of site establishment is included in the unit cost of a cubic metre of earth fill material required for the raising of the embankment. Differentiating between the site establishment cost and the construction cost could assist in the decision making process regarding the transition of expenditure from one dam to the next in the sequence.
- After applying the RQO process, decision making is required to evaluate the gain in marginal lives saved compared to the investment made from one transition to the next.

References

1. Australian National Committee on Large Dams (2003a). Guidelines on dam safety management. ANCOLD. August 2003. Australia.
2. Australian National Committee on Large Dams (2003b). Guidelines on risk assessment. ANCOLD. October 2003. Australia.
3. Baker, V.R. (2008). Palaeoflood hydrology: Origin, progress, prospects. Elsevier, *Journal of Geomorphology*, 101: 1 - 3.
4. Baker, V.R. and Kochel, R.C. (1988). Flood sedimentation in bed-rock fluvial systems. In: Baker, V.R., Kochel, R.C. and Patton, P.C. (eds.) *Flood Geomorphology*. John Wiley & Sons Ltd., New York. 123 - 137.
5. Baker, V.R., Webb, R.H. and House, P.K. (2002). The scientific and societal value of palaeoflood hydrology. In: House PK, Webb RH, Baker VR, Levish DR (eds.) *Ancient Floods, Modern Hazards: Principles and Applications of Paleoflood Hydrology*. Water Science and Application Series Vol. 5. Washington DC: American Geophysical Union. 127 - 146.
6. Beck, J.S. and Basson, G.R. (2003). The hydraulics of the impacts of dam development on the river morphology. WRC Report No. 1102/1/03. Pretoria. Water Research Commission.
7. Bedford, T. and Cooke, R.M. (2001). *Probabilistic Risk Analysis: Foundations and Methods*, Cambridge University Press, Cambridge and New York.
8. Benito, G. and O'Connor, J. E. (2013). Quantitative palaeoflood hydrology. In *Treatise on Geomorphology*, J. Shroder, (Editor in Chief), Vol. 9, *Fluvial Geomorphology*, Wohl, E.E. (ed), 459 - 474, San Diego: Academic Press.
9. Benito, G., Rico, M., Thorndycraft, V.R., Sánchez-Moya, Y., Sopena, A., Díez Herrero, A., Jiménez, A. (2006). *Palaeoflood records applied to assess dam safety in SE Spain*. In: Ferreira, R., Alves, E., Leal, J., Cardoso, A. (Eds.), *International Conference on Fluvial Hydraulics*, September 6-8, Lisbon, Portugal, 2113 - 2120.
10. Benito, G., Sanchez-Moya, Y. and Sopena, A. (2003a) Sedimentology of high-stage flood deposits of the Tagus River, central Spain. *Sedimentary Geology* 157: 107-132.
11. Benito, G., Sopena, A., Sanchez-Moya, Y., Machado, M.J. and Perez-Gonzalez, A. (2003b). Palaeoflood record of the Tagus River (Central Spain) during the Late Pleistocene and Holocene. *Quaternary Science Reviews* 22: 1737 - 1756.

12. Benito, G. and Thorndycraft, V.R. (2004) *Systematic, Palaeoflood and Historical Data for the Improvement of Flood Risk Estimation: Methodological Guidelines* (1st ed.). MADRID: CSIC. 116.
13. Benito, G., Thorndycraft, V.R., Enzel, Y., Sheffer, N.A., Rico, M., Sope, A., Sánchez-Moya, Y. (2004). Palaeoflood data collection and analysis. In: Benito, G., Thorndycraft, V.R. (Eds.), *Systematic, Palaeoflood and Historical data for the improvement of flood risk estimation: Methodological guidelines*. Serrano, Madrid, Spain: CSIC. 15 - 27.
14. Boshoff, P., Kovács, Z., Van Bladeren, D. and Zawada, P.K. (1993). Potential benefits from palaeoflood investigations in South Africa: technical note. *SAICE Journal, South African Institute of Civil Engineers*. **35**(1): 25 - 26.
15. Bowles, D.S. (2013). *Overview of portfolio dam safety risk management*. Proceedings of the 81st annual meeting of the International Commission on Large Dams. 12-16 August, Seattle, USA. Risk Informed Dam Safety Management.
16. Brown, A.J. & Gosden, J.D. (2004). DEFRA Interim guide to quantitative risk assessment for UK reservoirs. Thomas Telford. London.
17. Charlwood, R., Bowles, D., Muller, B., Regan, P., Halpin, E. (2007). *Recent trends in dam safety management in the USA*. Presentation delivered at the ICOLD Symposium, 2 April 2007, Stockholm, Sweden.
18. Cloete, G.C., Basson, G.R., Sinske, S.A. (2014). Revision of Regional Maximum Flood (RMF) Estimation in Namibia. *Water SA*, **40**(3). 535 - 548.
19. Cullis, J. 2006. *Guide to best practice in management and operation of dams for NamWater*. Burmeister and Partners Report no. W1035/R1475. October 2006. Windhoek, Namibia.
20. DEFRA. 2002. Research contract 'Reservoir safety - Floods and reservoir safety integration'. Final Report, Volume 1 of 3. Ref. XU0168 Rev A05, August 2002. Garston, Surrey, UK: Building Research Establishment.
21. DeKay, M.L. and McClelland, G.H. (1993). Predicting Loss of Life in cases of dam failure and flash flood. *Journal of Risk Analysis*, **13**(2). 193 - 205.
22. Dorn, R.I. (1989). Cation-ratio dating of rock varnish: a geographic assessment. *Progress in Physical Geography*, 1989 (13): 559 - 596, doi: 10.1177/030913338901300404

23. Dorn, R.I., Oberlander, T.M. (1982). Rock varnish. *Progress in Physical Geography*, 1982 (6): 317 - 367, doi:10.1177/030913338200600301
24. Enzel, Y., Ely, L.L., House, P.K. and Baker, V.R. (1993) Paleoflood evidence for a natural upper bound to flood magnitudes in the Colorado River basin. *Water Resources Research*, **29**(7). 2287 - 2297.
25. Enzel, Y., Ely, L.L., Martinez-Goytre, J., Vivian, R.G. (1994) Paleofloods and a dam-failure flood on the Virgin River, Utah and Arizona. *Journal of Hydrology*, **153**(3). 291 - 315.
26. Enzel, Y. (2009). Personal communication, October 2009. Prof Yehouda Enzel, The Freddy and Nadine Herrmann Institute of Earth Sciences, The Hebrew University of Jerusalem, Givat Ram, Jerusalem 91904, Israel.
27. Fischer, K. (2012a). Introduction to the Life Quality Index. Marginal Life Saving Costs Principle Derivation & Calibration of the LQI: Simple Application Examples. Presentation delivered at Stellenbosch University, Department of Civil Engineering. Stellenbosch. South Africa. 12 April 2012.
28. Fischer, K. (2012b). Personal communication, April 2009. Dr Katharina Fischer, Scientific Assistant at the Institute of Structural Engineering, Department of Civil Engineering, ETH Zürich.
29. Fischer, K., Virguez, E., Sanchez-Silva, M., Faber, M. (2013). On the assessment of marginal life saving costs for risk acceptance criteria. *Structural Safety* **44** (2013). 37 - 46.
30. Goudie, A. S. (2007). Desert landforms in Namibia - a Landsat interpretation. In: Goudie, A.S., Kalvoda, J. (eds.). *Geomorphological Variations*. Prague: P3K, 19 - 36.
31. Görgens, A.M.H. (2000). *Chapter 5, Probabilistic Methods. Hidrologie 414 (Vloedhidrologie)* lecture notes, Department of Civil Engineering, Stellenbosch University.
32. Greenbaum, N., Schwartz, U., Benito, G., Porat, N., Cloete, G.C., Enzel, Y. (2014) Paleohydrology of extraordinary floods along the Swakop River at the margin of the Namib Desert and their paleoclimate. DOI: 10.1016/j.quascirev.2014.08.021
33. Grodek, T. and Enzel, Y. (2007) Paleoflood study in the Kuiseb River, Namibia; a short summary and slide show. The Hebrew University of Jerusalem, Israel.
34. Grodek, T., Benito, G., Botero, B.A., Jacoby, Y., Porat, N., Haviv, I., Cloete, G. and Enzel, Y. (2013) The last millenium largest floods in the hyperarid Kuiseb River basin, Namib Desert. *Journal of Quaternary Science*. **28**(3): 258 - 270.

35. Hattingh, L. C. (2007). *Task 2d: Re-evaluation of the safety of the Hardap Dam Flood risk reduction: Mariental Town and Hardap Irrigation Scheme*. Dam safety report, no. 11/11/3/1/2/H05. December 2007. Windhoek, Namibia: Ministry of Agriculture, Water and Forestry.
36. Hartford, D.N.D. and Baecher, G.B. (2004). *Risk and uncertainty in dam safety*. London: Thomas Telford.
37. Holtzhausen, D. (1934). *Letter from Mr Holtzhausen to the Secretary for South West Africa regarding Damage to Spillway of Avis Dam*, dated 10 February 1934. Municipality of Windhoek, File no. 10/25/43. Windhoek: National Archives of Namibia.
38. Hydrologic Engineering Centre (2001) *HEC-RAS, River Analysis System, Hydraulics Reference Manual*. Washington: US Army Corps of Engineers.
39. International Commission on Large Dams (1995). *Bulletin 99: Dam Failures, Statistical Analyses*. Paris: ICOLD.
40. International Commission on Large Dams (1998). *Bulletin 111: Dam-break flood analyses*. Paris: ICOLD.
41. International Commission on Large Dams (2005). *Bulletin 130: Risk assessment in dam safety management. A reconnaissance of benefits, methods and current application*. Paris: ICOLD.
42. International Commission on Large Dams (2010). *Bulletin 144: Cost savings in dams*. Paris; ICOLD.
43. Klemeš V (1987) Hydrological and engineering relevance of flood frequency analysis. In: Singh VP (ed.) *Hydrologic Frequency Modelling*. Norwell, Mass: D Redel. 1 - 18.
44. Klemeš, V. (1993). *Probability of extreme hydrometeorological events – a different approach*. Proceedings of the Yokohama Symposium, July 1993. IAHS Publ. no. 213, 167 - 176.
45. Kochel, R.C., Baker, V. (1982) Palaeoflood hydrology. *Science, New Series* **215**(4531), 353 - 361.
46. Kovács, Z. (1980). *Maximum flood peak discharges in South Africa: an empirical approach*. Technical Report TR 105. Division of Hydrology. Pretoria: Department of Environmental affairs.
47. Kovács, Z. (1988). *Regional maximum flood peaks in Southern Africa*. Technical Report TR 137. Directorate of Hydrology. Pretoria: Department of Water Affairs.

48. Kraemer, K., Kohler, J., Faber, M. H. (2010). *The derivation of acceptance criteria for risk to life based on optimal resource allocation*. Proceedings of the 8th International Conference on Performance-Based Codes and Fire Safety Design Methods, June 16-18, 2010. Lund, Sweden.
49. Kerby, G. (1934). *Letter from Mr Kerby to the Secretary for South West Africa regarding Damage to Spillway of Avis Dam*, dated 31 January 1934. Municipality of Windhoek, File no. 10/25/43. Windhoek: National Archives of Namibia.
50. Kreuzer, H. (2000). *The use of risk analysis to support dam safety decisions and management*. Proceedings: ICOLD 20th Congress, Beijing, China. Question 76, 769 - 834.
51. Lang, M., Fernandez Bono, J.F., Recking, A., Naulet, R., Grau Gimeno, P. (2004). Methodological guide for palaeoflood and historical peak discharge estimation Palaeoflood data collection and analysis. In: Benito, G., Thorndycraft, V.R. (Eds.), *Systematic, palaeoflood and historical data for the improvement of flood risk estimation: Methodological guidelines*. Serrano, Madrid, Spain: CSIC. 43 - 53.
52. Lui, T., Broecker, W.S. (2013). Millennial-scale varnish microlamination dating of late Pleistocene geomorphic features in the drylands of western USA. *Geomorphology* **187**: 38 - 60
53. Mason, P. (2008). *A letter written by Dr. Peter Mason on 9 October 2008, addressed to Prof. Andy Hughes of ATKINS WATER regarding the QRA questionnaire*. October 2008, United Kingdom.
54. Mendelsohn, J., Jarvis, A., Roberts, C., Robertson, T. (2002) *Atlas of Namibia: A Portrait of the Land and its People*. Namibian Ministry of Environment and Tourism. Cape Town: David Phillip.
55. Mostert, A. (2007). Personal communication, 2007. Mr Andre Mostert, Manager: Hydrology, Department of Engineering and Scientific Services, Namibia Water Corporation, Windhoek.
56. National Research Council. (1985) *Safety of Dams, Flood and Earthquake Criteria*. National Academy Press, Washington. 321.
57. Hughes, A. 2009. The QRA Questionnaire, e-mail to G.C. Cloete, 19 August 2009. United Kingdom.
58. Papanicolaou, A. N. (2012). *Papanicolaou Research Group; Environmental Hydraulics and Sediment Transport. Application notes: Sediment Transport, P1*. The University of Iowa, College of Engineering. USA.

59. Rademeyer, P. (2013) Personal communication, 14 March 2013. Mr Pieter Rademeyer, Scientific Manager – Flood Studies, Directorate: Hydrological Services, Department of Water Affairs, Pretoria.
60. Rehbok, T.H. (1898). Seine wirtschaftliche erschliessung unter besonderer berücksichtigung der nutzbarmachung des wassers (A scientific opening up under specific consideration of the utilization of water), Report. Dietrich Reimer (Ernst Vohsen). Berlin 1898.
61. Rehbok, T.H. (1926). *Municipality of Windhoek: Report on a dam scheme for the water supply of Windhoek and irrigation of the Klein Windhoek Valley*. 27 July 1926. File number: 110/12B/43, National Archives of Namibia
62. Schalk, K. (1961) The water balance of the Ulenhorst cloudburst in South West Africa. *CCTA Publication 66*. Nairobi 1961. 442 - 449.
63. Schubert, M. (2009). *Konzepte zur informierten Entscheidungsfindungim Bauwesen*. Unpublished Doctoral Dissertation. Institut für Baustatik und Konstruktion ETH Zürich. Zürich. (In part, translated from German to English by K. Fischer, Zürich).
64. Serrano-Lombillo, A., Escuder-Bueno, I., de Membrillera-Ortuno, M. G., Altarejos-Garcia, L. (2011). Methodology for the calculation of annualized incremental risks in systems of dams. *Wiley Journal of Risk Analysis*, **31**(6): 1000 - 1015.
65. Sims, G.P. 2009. The rehabilitation of dams and reservoirs. In Takahasi, Y. (ed.). *Water Storage, Transport and distribution – Volume 1. Encyclopaedia of Life Support Systems*. UNESCO. ISBN: 978-1-84826-626-1
66. Snorteland, N. (2013). *Overview of U.S. Army Corps of Engineers portfolio risk management*. Risk Informed Dam Safety Management: Proceedings of the 81st Annual Meeting of the International Commission on Large Dams, 12-16 August, Seattle, USA.
67. South African National Committee on Large Dams (1990). *Safety evaluation of dams: Guidelines on freeboard for dams*. Report no. 3. Pretoria: SANCOLD.
68. South African National Committee on Large Dams (1991). *Safety in Relation to Floods*. Report no. 4. Pretoria: SANCOLD.
69. Spanish National Committee on Large Dams (2013). *Technical guides on Dam Safety: Technical guide on operation of dams and reservoirs, Volume 1: Risk analysis applied to management of dam safety*. Spain: SPANCOLD.
70. Stengel, H.W. (approximately 1974) A Floods Various Report: *Flood capacities observed in rivers at various sites 1902-1972*. Notes on historical flood events and

related fields, in loose leaves 31cm. Department of Water Affairs. A. Floods Various. MFN 311. 89/1416.

71. Stellenbosch University (SU), Department of Civil Engineering (2009). *Design of hydraulic structures*. Application notes: Short course 9-12 March 2009. Stellenbosch, South Africa.
72. Stellenbosch University (SU), Department of Civil Engineering (2002). *Design and rehabilitation of dams*. Application notes: Short course 10-12 June 2002. Stellenbosch, South Africa.
73. Tasker, G.D. and Stedinger, J.R. (1987) Regional Regression of Flood Characteristics Employing Historical Information. *Hydrology*. **96**: 255 – 264.
74. Technician's Manual (1988). *Technician's training manual on hydrological methods, techniques and application*. Hydrology Division, Namibia Department of Water Affairs. Windhoek. 1988, 1 – 63.
75. The Economist (2005). *Economist Intelligence Unit executive summary – Staying ahead of the Technology curve*, September 2005. London. 1 - 14.
76. United States Bureau of Reclamation (1981). *Freeboard criteria and guidelines for computing freeboard allowances for storage dams*. ACER Technical memorandum no.2. Denver, Colorado, USA.
77. United States Bureau of Reclamation (2011). *Rationale Used to Develop Reclamation's Dam Safety Public Protection Guidelines*. Technical report. USBR dam safety office. Denver, Colorado.
78. Van der Spuy, D. (2008 to 2013). Personal communication, April 2008. Mr Danie van der Spuy, Specialist Engineer – Flood Studies, Directorate: Hydrological Services. Pretoria: Department of Water Affairs.
79. Van Langenhove, G. (2006 to 2008). Personal communication, 14 February 2008. Chief of Hydrology, Namibia Ministry of Agriculture, Water and Forestry, Department of Water Affairs. Windhoek.
80. Wessels, P. (2014). Personal communication, 6 November 2014. Specialist Engineer, Directorate Hydrological Services, Pretoria. Department of Water Affairs.
81. Yevjevich, V. and Harmancoiglu, N. B. (1987). Application of Frequency and Risk in Water Resources. In *Research needs on flood characteristics*. V.P. Singh (ed.) Print ISBN978-94-010-8254-9. Dordrecht, Holland: D. Reidel. 1 - 21.

Appendices

Appendix A: List of Rain Gauge Stations

Namibia 3 day maximum rainfall data							
no.	StationID	Station-Name	Latitude (South)	Longitude (East)	Year-Month	3day Max rainfall (mm)	Record length (> 30 years) (years)
1	12694482	Katima Mulilo	17.47	24.25	Jan-1945	438.5	58
2	12526590	Engela	17.48	16.33	May-1952	234.0	30
3	12084758	Rundu	17.92	19.77	Jan-1940	198.0	69
4	12076214	Bunja	17.85	19.35	Jan-1953	159.0	48
5	12071418	Rupara	17.85	19.08	Jun-1958	360.0	37
6	12064961	Tondoro	17.77	18.78	Oct-1931	154.0	50
7	12061871	Kuring Kuru	17.62	18.62	Jan-1924	174.4	73
8	12011375	Oshigambo	17.82	16.07	Jan-1922	221.5	71
9	1200866A	Ondangwa	17.93	15.98	Jul-1913	212.9	71
10	1199872X	Ombalantu	17.52	15.02	Jan-1930	269.0	69
11	11998208	Oshikuku	17.67	15.47	Oct-1930	160.8	66
12	11986750	Tshandi	17.75	14.88	Dec-1913	173.7	55
13	11607833	Andara	18.07	21.47	Jun-1914	167.0	80
14	1145573C	Opuwo	18.05	13.83	Dec-1939	189.7	30
15	11045356	Koukuas	18.92	18.3	Jan-1967	163.0	38
16	11042024	Choantsas	18.87	18.12	Jan-1951	162.5	57
17	11024028	Grenzland 312	18.7	17.23	Oct-1951	211.0	32
18	11022740	Oshivelo	17.17	18.62	Aug-1960	178.5	33
19	11021615	Onguma 314	18.68	17.1	Jan-1940	158.0	42
20	10577232	Sonop	19.05	18.92	Jan-1968	212.0	33
21	10572047	Klein Huis	19.4	18.62	Jan-1918	158.5	54
22	10567174	Gaikos	19.45	18.4	May-1979	155.2	31
23	10566974	SUS 276	19.12	18.4	Jan-1914	131.0	43
24	10558092	Toggenburg	19.48	17.95	Feb-1952	151.5	47
25	10554475	Gaub	19.45	17.75	Jan-1914	155.5	83
26	10553743	Tsumeb	19.23	17.72	Sep-1913	250.4	92
27	10526411	Halali	19.18	16.37	Nov-1965	114.5	41
28	10518000	Ombika	19.33	15.95	Jan-1966	242.4	40
29	10517316	Okaukuejo	19.18	15.92	Jan-1934	162.7	74
30	10488538	Otjovazandu	19.22	14.35	Jan-1966	167.5	41
31	10453800	MOWE BAY	19.33	12.72	Dec-1968	36.3	34
32	10150355	Tsumkwe	19.58	20.53	Nov-1963	173.5	38
33	10120948	Simondeum	19.57	19.07	Mar-1959	240.0	44
34	10111309	Otjituuu	19.67	18.58	Jun-1913	227.0	68
35	10102167	Grootfontein Met	19.57	18.13	Jan-1917	150.4	77
36	10101182	Gabasis	19.97	18.07	Jan-1931	221.0	67
37	10098526	Otjirukaku	19.7	17.98	Jan-1927	191.0	80
38	10098502	Uitkomst	19.67	17.98	Mar-1961	166.9	38
39	10096398	Awagobibtal	19.65	17.87	Jan-1927	176.9	75
40	1009467X	Rietfontein-Grootfontein	19.78	17.77	Jul-1913	165.4	87
41	10086607	Una	20	17.37	Apr-1954	152.5	49
42	10085780	Otavi	19.63	17.33	Sep-1913	165.5	75
43	10083022	Goabforte	19.53	17.18	Jan-2000	188.4	58
44	10077259	Arbeidsgenot	19.58	16.92	Oct-1956	136.5	50
45	10066254	Nettleton	19.92	16.35	Apr-1962	152.0	42
46	10041552	Sendeling	19.58	15.1	Jun-1959	152.5	44
47	10036086	Kamanjab Police	19.63	14.85	Apr-1930	334.0	66
48	1003139x	Kakatswa Onguati	19.82	14.58	Jul-1930	184.1	30
49	9647830	Omambonde Tal 166	20.05	17.95	Sep-1949	150.0	59
50	9646011	Annenhof	20.02	17.85	Jul-1922	164.0	62

Appendix A: List of Rain Gauge Stations

Namibia 3 day maximum rainfall data							
no.	StationID	Station-Name	Latitude (South)	Longitude (East)	Year-Month	3day Max rainfall (mm)	Record length (> 30 years) (years)
51	9622378	Otjiwarongo	20.45	16.63	Sep-1913	200.2	72
52	9618647	Omatjenne	20.4	16.48	Jan-1940	195.3	60
53	9612479	Outjo	20.12	16.15	Jul-1913	159.0	82
54	9588339	Khorixas	20.38	14.97	Aug-1955	111.5	52
55	0919505X	La Paloma	20.92	17.78	Apr-1952	157.0	44
56	9181284	Okosongomingo	20.63	17.08	Jan-2004	257.3	42
57	9175826	Hohenfels	20.7	16.83	Aug-1913	207.3	93
58	9174420	Omusema Uarei	20.87	16.75	Jan-1913	176.0	50
59	9166980	Erundu	20.63	16.4	Jan-1940	162.0	69
60	9163231	Kalkfeld	20.88	16.18	Jan-1940	185.5	63
61	9158370	Otjeriwanga	20.95	15.97	Jul-1962	121.7	34
62	0915781X	OTJITOROA WES	20.05	15.95	Mar-1952	139.0	45
63	0915623X	Eremutua (NE) Farm I	20.88	15.85	Jun-1930	124.8	33
64	9154463	Eremutua	20.93	15.75	Jan-1940	144.0	70
65	0876037X	Otjosondjou	21.12	18.53	Apr-1958	201.0	42
66	8754490	Amatola	21.42	18.25	Jan-1962	142.0	38
67	8751070	Kalidona	21.28	18.07	Jan-1930	146.5	77
68	0874649X	Hochfeld	21.5	17.85	Sep-1919	148.0	92
69	0873397X	Otjikururume	21.12	17.23	Jul-1917	146.4	87
70	8731175	Okandjose	21.45	17.07	Jul-1917	203.5	46
71	8714116	Omburo Suid	21.35	16.23	Apr-1920	171.0	75
72	8712786	Eheratengua	21.13	16.17	Feb-1923	170.0	85
73	8708064	Omaruru	21.42	15.93	Jan-1916	186.6	66
74	8314399	Steinhausen	21.82	18.25	May-1913	240.5	72
75	8302384	Otjisauna Suid	21.97	17.63	Sep-1947	168.0	32
76	8298550	Vooruitgaan	21.75	17.48	Oct-1952	154.9	41
77	8296482	Otjiruze	21.8	17.37	Apr-1929	122.9	48
78	8293057	Agagia	21.55	17.33	Nov-1926	142.0	42
79	0828748A	Okahandja	21.97	16.92	Jan-1975	129.0	35
80	8278486	Otjombuindja	21.63	16.48	Sep-1950	149.0	56
81	8275650	Wilhelmstal	21.92	16.32	Jul-1913	137.0	78
82	8261494	Usakos	21.98	15.58	Feb-1961	91.9	34
83	7897986	Buitepos	22.3	19.95	Oct-1948	176.5	49
84	0788182X	Sandveld	22.02	19.15	Jul-1969	250.7	33
85	7878388	Gobabis	22.47	18.97	Jan-1914	179.0	88
86	7868658	Witvlei	22.42	18.48	Jul-1913	190.0	92
87	0786283X	Omateva	22.22	18.17	Jul-1918	261.0	91
88	7860978	Kanonschoot	22.12	18.07	Mar-1951	125.0	57
89	7854901	Okahua	22.17	17.78	Mar-1917	209.5	89
90	7851835	Otjikundua	22.05	17.62	Oct-1931	142.0	63
91	7851775	Seeis	22.45	17.58	Jul-1913	171.0	33
92	0784839B	Hosea Kutako I. Airpo	22.48	17.47	Feb-1966	136.6	45
93	7848260	Otjituezo	22.27	17.47	Jan-1914	148.5	44
94	7847209	Sonleitten	22.5	17.4	Oct-1926	150.5	81
95	7837686	Otjiseva	22.3	16.93	Jul-1913	146.5	61
96	7835775	Okaundua	22.12	16.83	Sep-1935	104.3	55
97	7828736	Erora Ost	22.05	16.5	Jan-1914	186.0	92
98	7827049	Westefallenhof	22.23	16.4	Jan-1927	170.0	82
99	0781815X	Okongava Ost	22.08	15.97	Sep-1913	175.0	70
100	7813099	Abbabist Ost	22.15	15.68	Jan-1951	141.6	49

Appendix A: List of Rain Gauge Stations

Namibia 3 day maximum rainfall data							
no.	StationID	Station-Name	Latitude (South)	Longitude (East)	Year-Month	3day Max rainfall (mm)	Record length (> 30 years) (years)
101	7811080	Dorstrivier	22.3	15.57	Jun-1952	122.0	44
102	7444197	Rosendal	22.98	19.23	Nov-1956	243.9	52
103	7437388	Spatzenfeld 70	22.8	18.92	Sep-1931	129.0	37
104	7431172	Styria	22.95	18.57	Dec-1915	167.5	67
105	7415873	Wolfsgrund 122	22.65	17.63	Nov-1931	214.9	45
106	7413261	Dordabis	22.43	17.68	Nov-1920	173.5	78
107	7407921	Hohenau	22.7	17.45	Jan-1914	169.9	91
108	7407111	Rietfontein-Khomas	22.85	17.4	May-1913	192.7	91
109	7406778	Binsenheim	22.78	17.38	Jan-1936	147.0	73
110	0740154X	Windhoek Met. Hq.	22.57	17.1	Jan-1913	157.7	98
111	0740097A	Eros Airport	22.62	17.07	Jan-1932	134.2	39
112	7386478	Terra Rossa	22.78	16.37	Oct-1970	186.8	36
113	7385191	Abochaibis	22.65	16.3	Nov-1956	109.0	50
114	7350117	Swakopmund	22.68	14.52	Jan-1914	58.9	70
115	7347735	Walvis Bay Pelican P	22.95	14.5	Feb-1958	67.5	46
116	6971390	Rehoboth	23.32	17.08	May-13	144.5	83
117	6965041	Marienhof	23.4	16.78	Jan-25	111.1	33
118	6964925	Naos	23.2	16.78	Jan-35	145.0	70
122	6960269	Isabis	23.43	16.52	Oct-77	109.0	31
123	6953968	Tantus	23.1	16.23	Sep-19	110.0	39
124	6565419	Leonardville	23.5	18.78	Jan-29	132.1	76
125	6564579	Reitz	23.62	18.77	Jul-63	133.0	41
126	6555037	Gomchanas Ost	23.88	18.28	Feb-40	162.0	68
127	6546463	Mbela	23.77	17.92	Jan-55	143.3	40
128	6490648	Gobabeb	23.57	15.05	Oct-62	40.7	42
129	6144061	Omrah	24.27	19.23	Mar-52	149.0	45
130	6141889	Aranos	24.13	19.12	Sep-48	131.0	59
131	6128182	Rohrbeck	24.13	18.47	Feb-59	127.0	40
132	5705316	Gochas	24.85	18.8	Oct-48	106.0	59
133	5688179	Mariental	24.62	17.97	Mar-18	136.7	67
134	0566860X	Maltahohe	24.83	16.98	May-13	119.4	83
135	5663091	Karab	24.65	16.68	Dec-51	123.0	41
136	5656668	Friedland	24.6	16.38	Mar-34	123.5	62
137	5321732	Eindpaal	25.38	19.1	Dec-31	126.5	70
138	5316182	Persip	25.3	18.85	Aug-29	136.7	35
139	5294526	Gibeon Reservaat	25.03	17.77	Apr-13	170.0	72
140	4955346	Grabstein	25.9	19.3	May-37	152.0	61
141	4934828	Koes	25.95	19.15	Jul-13	125.0	53
142	4932337	Tses	25.88	18.13	Oct-27	149.5	73
143	4925094	Berseba	25.98	17.78	Jul-27	118.5	63
144	4906233	Helmeringhausen	25.88	16.85	Jan-24	140.0	69
145	4901328	Aruab	25.7	16.58	Jul-13	147.0	90
146	0489336X	Haremub	25.6	16.35	Aug-67	97.8	40
147	4586396	Morgenzon Suid	26.15	19.37	Jun-52	300.0	51
148	4560273	Gellap Ost	26.45	18.02	Jun-14	110.1	88
149	4542700	Bethanien	26.5	17.15	Oct-13	95.3	90
150	4528176	Excelsior 59	26.12	16.47	Jan-51	102.2	53

Appendix A: List of Rain Gauge Stations

Namibia 3 day maximum rainfall data							
no.	StationID	Station-Name	Latitude (South)	Longitude (East)	Year-Month	3day Max rainfall (mm)	Record length (> 30 years) (years)
151	0422538X	Louwsvley	26.97	19.8	Sep-27	134.0	80
152	4222579	Aroab	26.78	19.65	Sep-08	138.5	73
153	4216962	Salztal	26.6	19.4	Oct-27	127.3	53
154	4196650	Stampriet	24.33	18.4	Feb-50	42.5	38
155	4191829	Keetmanshoop Airpo	26.53	18.12	Jan-49	119.5	61
156	4166118	Kuibis	26.68	16.85	Jan-14	107.2	68
157	4150451	Aus	26.68	16.32	Jul-13	135.0	83
158	0413158X	Luderitz (Diaz Point)	26.63	15.1	Jan-13	55.8	72
159	3860686	Tranental Oos	27.13	19.55	Sep-32	120.5	36
160	3855160	Warmfontein	27.1	19.3	Mar-52	118.0	51
161	3852335	Hangas	27.38	19.05	Aug-53	131.0	52
162	3848520	Naos	27.2	18.98	Mar-29	137.5	62
163	3844082	Rishon	27.3	18.73	Jun-56	101.5	47
164	3840235	Noachabeb	27.38	18.52	Sep-13	186.9	66
165	3826122	Oase 195	27.2	17.85	Aug-53	92.5	34
166	3805197	Rooiberg	27.15	16.8	Apr-52	81.0	30
167	3505426	Davignab Suid	27.53	19.82	Jul-13	143.0	52
168	3501519	Nimmerrust	27.52	19.6	Dec-50	130.7	56
169	3501133	Nabas	27.88	19.57	Apr-52	121.0	51
170	0349158X	Blinkoog	27.63	19.1	Jan-22	96.2	59
171	3490822	Noibis	27.87	19.05	Mar-52	102.0	53
172	3488193	Duurdrift Noord 26	27.65	18.97	Jan-39	83.5	35
173	3443704	Lorelei(Witputs Suid)	27.67	16.72	Mar-31	70.0	32
174	3145776	Ariamsvlei	28.12	19.83	Feb-27	112.0	79
175	3144826	Ukamas	28.03	19.78	Jul-13	180.5	57
176	3140327	Heirachabis	28.03	19.53	Jul-13	81.3	91
177	0313457X	Hamrivier	28.12	19.27	Oct-29	76.0	39
178	0312422X	Karasburg	28.03	18.75	Jul-13	166.5	81
179	3124171	Warmbad	28.45	18.73	Jul-13	149.6	79
180	3123970	Naruchas	28.12	18.73	Oct-37	115.1	49
181	2737545	Oranjemund	28.58	16.45	Oct-30	49.0	56

Appendix B:

List of Recorded Flood Peaks: New data from DWA Hydrology 2010

Namibia Flood Station Data List														
Data Source	River Name	Gauging Station Name	Catchment Area (km ²)	Flood Peak Discharge (m ³ /s)	Date of Flood Peak	Representative period N (yr)	Y (Lat S)		X (Long E)		Francou Rodier K	Old TR137 K values	New 2013 K value	RMF annual recurrence interval in years
							deg	min	deg	min				
Namibia Department of Water Affairs (2010)	AbaHuab	Rooiberg	1570	289.6	Feb 2009	36	20	29	14	35	2.64		4.0	>10,000
	Auob	Stampriet	19200	47.6	Jan 2000	30	24	19	18	27	-1.63		2.8	>10,000
	Auob	Gochas	19600	95.0	Mar 2000	33	25	1	18	54	-0.85		2.8	>10,000
	Bismark	Stanco	276	120.9	Feb 1997	33	22	44	16	36	2.95		4.6	>10,000
	Black Nossob	Henopsrus	4530	87.5	Mar 1978	37	22	9	18	50	0.66		3.4	>10,000
	Black Nossob	Mentz	8160	33.9	Jan 1988	34	23	7	18	42	-0.93		2.8	>10,000
	Djab	KosTower	231	67.5	Feb 1978	29	23	12	16	9	2.60		4.0	>10,000
	Fish	Fish Tses	37600	2919.4	Mar 1988	30	25	54	17	59	2.60		4.6	>10,000
	Gab	Holoog	2510	377.8	Feb 1989	27	27	27	17	59	2.56		4.0	>10,000
	Hoanib	Sesfontein	11000	747.7	Feb 1995	32	19	10	13	35	2.10		3.4	>10,000
	Huab	Vrede	10600	198.4	Mar 2002	29	20	22	14	11	0.68		3.4	>10,000
	Hutup	Breckhorn	4780	196.2	Apr 2001	27	24	50	17	10	1.42		4.6	>10,000
	Hutup	Rietkuil	5850	538.2	Feb 1974	33	25	7	17	31	2.28		4.6	9,000
	Khan	Spes bona	2310	184.1	Jan 1997	34	21	47	15	57	2.46		4.6	>10,000
	Khan	Ameib	4010	987.4	Feb 1985	41	21	50	15	38	3.16		4.6	5,000
	Khan	Usakos	6000	1087.3	Feb 1985	34	22	1	15	35	2.98		4.0	1,300
	Konkiep	Mooifontein	2080	251.3	Feb 2006	28	26	0	16	59	2.31		4.0	>10,000
	Konkiep	Bethanien	4140	293.7	Oct 1997	33	26	27	17	8	1.94		3.4	10,000
	Kuiseb	Us	1900	333.0	Feb 1986	33	22	58	16	24	2.63		4.6	>10,000
	Kuiseb	Schlesian Tower	6530	841.4	Jan 1963	47	23	17	15	48	2.65		3.4	10,000
	Kuiseb	Gobabeb	11700	594.2	Mar 2000	31	23	30	14	58	1.79		3.4	10,000
	Kunene	Ruacana	89600	1524.2	Mar 1963	18	17	24	14	13	0.76		2.8	>10,000
	Kwando	Kongola	170000	120.6	May 1969	35	17	47	23	21	-4.15		2.8	>10,000
	Loewen	Loewen Geduld	3200	284.8	Mar 1997	30	26	46	18	29	2.11		4.0	>10,000
	Loewen	Altdorn	7000	1260.3	Feb 1989	34	26	48	18	14	3.02		4.0	>10,000
	Nausgomab	Changns	690	139.9	Feb 1985	31	23	5	15	55	2.53		4.0	10,000
	Okavango	Mukwe	26000	1473.4	Feb 1968	59	18	2	21	26	2.10		2.8	>10,000
	Okavango	Rundu	97300	962.3	Apr 1969	64	17	54	19	46	-0.02		2.8	>10,000
	Omaruru	Omburo	1320	764.3	Feb 1984	35	21	18	16	12	3.61		4.6	10,000
	Omaruru	Etemba	3810	760.2	Jan 1974	39	21	26	15	41	2.94		4.6	>10,000
	Omatako	Ousema	4970	434.8	Jan 1963	43	21	13	17	6	2.19		4.6	>10,000
	Omuhonga	Ombuku	1620	457.4	Feb 1994	25	17	16	13	19	3.03		4.0	3,000
	Ondova	Minimahoro	117	246.0	Mar 1984	28	17	15	13	13	3.92		4.0	
	Otjiseva	Deusternbrook	1250	467.8	Jan 1988	40	22	16	16	54	3.21		4.6	10,000
	Seeis	Ondekermba	326	195.6	Feb 1996	31	22	29	17	25	3.24		5.0	>10,000
	Simminau	Wasservallei	266	97.5	Dec 1983	32	22	48	16	32	2.81		4.6	>10,000
	Swakop	Westfalenhof	8860	482.0	Jan 1963	44	22	17	16	25	1.82		4.6	>10,000
	Swakop	Dorstrivier	16300	48.5	Feb 2004	21	22	27	15	38	-1.39		4.0	>10,000
	Swart-modder	Swart-modder	240	176.3	Apr 2003	15	23	24	17	6	3.32		4.6	>10,000
	Tsauchab	Sesriem	1480	360.2	Jan 1997	29	24	31	15	47	2.87		3.4	1,500
Ugab	Vingerklip	14200	416.7	Feb 1985	42	20	25	15	28	1.22		4.0	>10,000	
Ugab	Ugab Slab	28900	257.7	Feb 1985	32	21	5	13	48	-0.14		3.4	>10,000	
Usib	Nauasprt	727	135.4	Mar 1972	40	23	4	17	12	2.47		4.6	>10,000	
White Nossob	Amasib	9250	100.9	Feb 1978	34	23	5	18	39	0.09		2.8	>10,000	
Zambezi	Katima Mulilo	334000	8151.9	Apr 1969	66	17	29	24	18	1.56		2.8	>10,000	

Appendix B:

List of Recorded Flood Peaks: Palaeoflood data 2010

Paleoflood data														
Data Source	River Name	Gauging Station Name	Catchment Area (km ²)	Flood Peak Discharge (m ³ /s)	Date of Flood Peak	Representative period N (yr)	Y (Lat S)		X (Long E)		Francou Rodier K	Old TR137 K values	New 2013 K value	RMF annual recurrence interval in years
							deg	min	deg	min				
Cloete (unpublished)	Fish	Vogelkrantz	11050	6400.0			24	18.5	17	38.3	4.46		4.60	
Cloete (unpublished)	Fish	Echo	57000	16140.0			27	20.5	17	42.1	4.48		4.60	
Grodek et al. (2012)	Gaub	G-10	2540	400.0			23	29.5	15	38.5	2.61		3.40	
Greenbaum et al. (2014)	Kahn	KahnMine	8200	1600.0			22	26.5	15	7.3	3.16		3.40	
Grodek et al. (2012)	Kuiseb	K-130	7660	1450.0			23	28.8	15	38.7	3.10		3.40	
Grodek et al. (2012)	Kuiseb	K-401	10440	810.0		20000	23	39.3	15	32.2	2.23		3.40	

Appendix B:

List of Recorded Flood Peaks: TR 137 flood peaks, 1988

TR 137 Data														
Data Source	River Name	Gauging Station Name	Catchment Area (km ²)	Flood Peak Discharge (m ³ /s)	Date of Flood Peak	Representative period N (yr)	Y (Lat S)		X (Long E)		Francou Rodier K	Old TR137 K values	New 2013 K value	RMF annual recurrence interval in years
							deg	min	deg	min				
	Aratagaras	Gammams III	430	595.0	Feb 1948	16	22	27	16	58	3.99	5.0	5.0	
	Aroab	Usakos	900	700.0	Feb 1985	(25)	21	47	15	30	3.75	4.6	4.0	
	Aub	road bridge	350	390.0	Feb 1977	54	24	32	17	58	3.75	4.6	4.0	
	Avis	Avis Dam	102	685.0	Apr 1934	54	22	34	17	8	4.72	5.0	5.0	
	Black Nossob	Hummelshain	220	243.0	1949	39	22	0	17	35	3.61	4.0	4.6	
	Cuito	Dirico	72000	596.0	Feb 1968	39	17	58	20	48	-0.26	<2.8	2.8	
	Dabib	Near Hardap	390	800.0	Mar 1968	(80)	24	30	17	57	4.27	4.6	4.6	
	Fish	Hardap Dam	13600	6100.0	Mar 1972	25	24	30	17	52	4.27	4.6	4.6	
	Fish	Seeheim	46400	8300.0	Mar 1972	27	26	49	17	48	3.76	4.6	4.6	2,000
	Fish	Ais-Ais	63300	5460.0	Mar 1972	27	27	55	17	29	2.93	3.4	4.6	>10,000
	Gab	Arbeit	385	320.0	Dec 1985	(60)	27	20	18	17	3.55	4.0	4.0	
	Gaub	Greylings	2490	306.0	Mar 1975	14	23	29	15	46	2.37	3.4	3.4	10,000
	Ham	Tsamab	2470	1010.0	Jan 1974	(50)	28	9	19	15	3.50	4.0	4.0	1,000
	Hoarusib	Oute	2540	450.0	Apr 1984	(35)	18	2	13	29	2.72	3.4	3.4	
	Hoarusib	Lower Purros	13600	1500.0	Apr 1984	(30)	18	47	12	56	2.70	3.4	3.4	
	Kam		1080	>351	Feb 1985	15	23	49	16	37	>3.04	4.6	4.6	
	Kam		3450	819.0	Mar 1978	12	24	12	17	2	3.08	4.6	4.6	
	Khan Tributary	Ameib	110	600.0	1949	(200)	21	45	15	35	4.59	4.6	4.6	
	Kuiseb		1900	1260.0	Jan 1963	54	23	1	16	22	3.86	4.6	4.6	
	Kuiseb	Rooibank	14700	406.0	Jan 1963	27	23	11	14	39	1.15	<3.4	3.4	>10,000
	Lewer	Gelukwater	11400	4750.0	Feb 1975	(45)	25	28	17	40	4.11	4.6	4.6	
	Loewen	Naute dam	8630	2200.0	Feb 1974	26	26	56	17	56	3.46	4.0	4.0	
	Loewen Tributary	Braus	270	270.0	Jan 1974	(60)	26	38	18	47	3.59	4.0	4.0	
	Oanob		2730	522.0	Feb 1986	18	23	20	17	3	2.81	4.6	4.6	
	Oanob tributary	Claratal Haus	100	900.0	Jan 1963	(200)	22	51	16	47	4.92	5.0	5.0	
	Okandja	Kompanene	357	550.0	Jan 1964	(35)	21	21	16	2	4.02	4.6	4.6	
	Okwayo	Spes Bona	141	350.0	Feb 1985	(45)	21	40	15	51	4.09	4.6	4.6	
	Omaruru		11500	1100.0	Feb 1985	(20)	21	55	14	29	2.49	3.4	3.4	
	Omatako		4970	435.0	Jan 1963	27	21	13	17	6	2.19	3.4	4.6	
	Omatjene	Omatjena dam	780	850.0	Feb 1942	54	22	25	16	28	3.99	4.6	4.6	
	Ombatjipuro	Tevrede	100	31.0	Nov 1983	5	20	43	17	13	2.49	3.4	4.0	
	Packriem		1520	499.0	Apr 1984	12	24	21	17	35	3.15	4.6	4.6	
	Riet	Haribes	150	600.0	Jan 1944	44	25	0	17	17	4.47	4.6	4.6	
	Satco	Bondelsdam	340	400.0	Jan 1974	(200)	28	2	18	40	3.79	4.0	4.0	
	Swakop	near Okahandja	3000	2000.0	1934	54	22	1	16	54	4.03	4.6	4.6	
	Swakop	Nudis	16000	4750.0	Jan 1934	75	22	27	15	39	3.88	4.6	4.0	
	Swakop	Swakopmund	29000	3800.0	Jan 1934	75	22	41	14	32	3.16	3.4	3.4	
	Tsuab	Voigtsgrund	380	810.0	1934	73	24	46	17	20	4.30	4.6	4.6	
	Unjab	mouth	4060	770.0	1934	(60)	20	12	13	12	2.91	3.4	3.4	
	White Nossob	Otjivero silt dam	2070	500.0	Feb 1987	19	22	17	17	57	2.95	4.0	4.6	
	Zambezi	Katima Mulilo	326000	8440.0	Mar 1958	81	17	25	24	12	1.66	2.8	2.8	
	Zamnarib		130	430.0	Jan 1944	44	24	23	17	35	4.28	4.6	4.6	

Appendix C: Palaeoflood study

This Appendix describes the stratigraphic profiles of sediment which were exposed and fully developed at each of the palaeoflood sites. Not all of the excavated profiles were described.

Table C1 shows the Legend for the various symbols used to describe the stratigraphic layers.

<u>LEGEND</u>					
	Parallel lamination		Slope washflow		Charcoal
	Climbing ripples		Gravel levels		OSL sample
	Climbing ripples In phase		Aeolian sand		Bioturbation
	Ripples lamination		Carbonates		Bedrock
	Wavy Cross bedding		Mud cracks		Small aeolian coppice dunes
	Planar (2d) Cross bedding		Roots		Rip-up clast
	Trough (3d) Cross bedding				

Table C2 shows the Legend for the various symbols related to the finer sediment the description of the sequence of layers.

<u>GRAIN SIZE</u>	
	Clayed silt
C+sl	= Clay-Silt
S	= NUMBER OF SEQUENCE (each represents one flood only)

Three palaeoflood sites were fully developed at Vogelkranz in the Upper Fish River, and three at Camp Echo in the Lower Fish River. These are VK1, VK2 and VK4 in the upper Fish, and EC1, EC4 and EC6 in the lower Fish River.

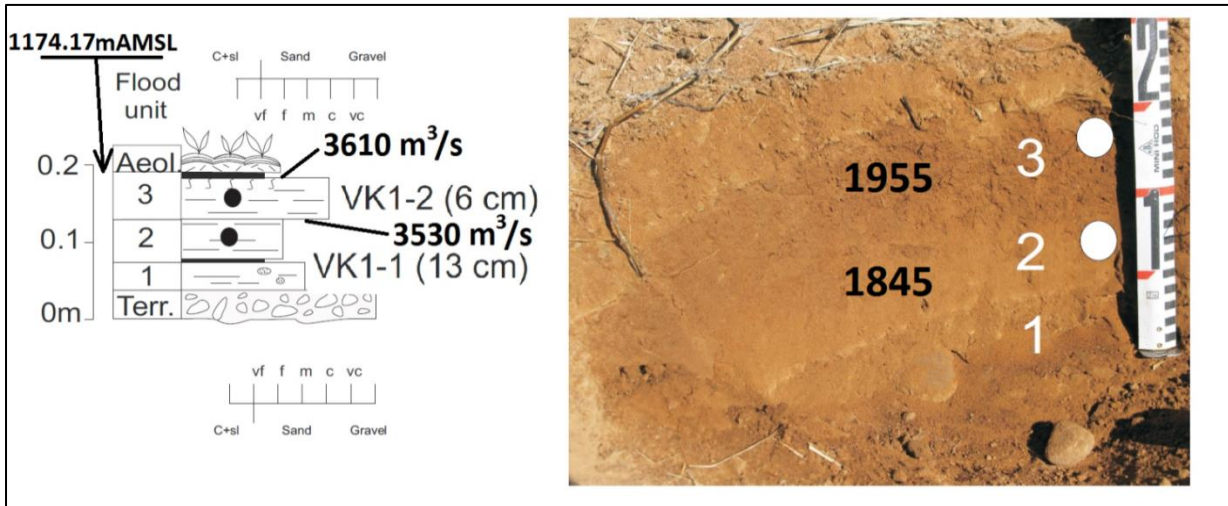


Figure C1: Vogelkranz site, profile VK1. This profile lies on top of a gravel bar. Refer to Figure 3.8. VK1-2 refers to the second flood unit (layer) from the bottom of the profile. The distance (6 cm) refers to the distance from the top of the profile to the top of the flood unit from which a sample is taken. The OSL-dated year in which the sample was deposited is indicated on the layer. The discharges associated with each sample layer are indicated at the top of the layer.

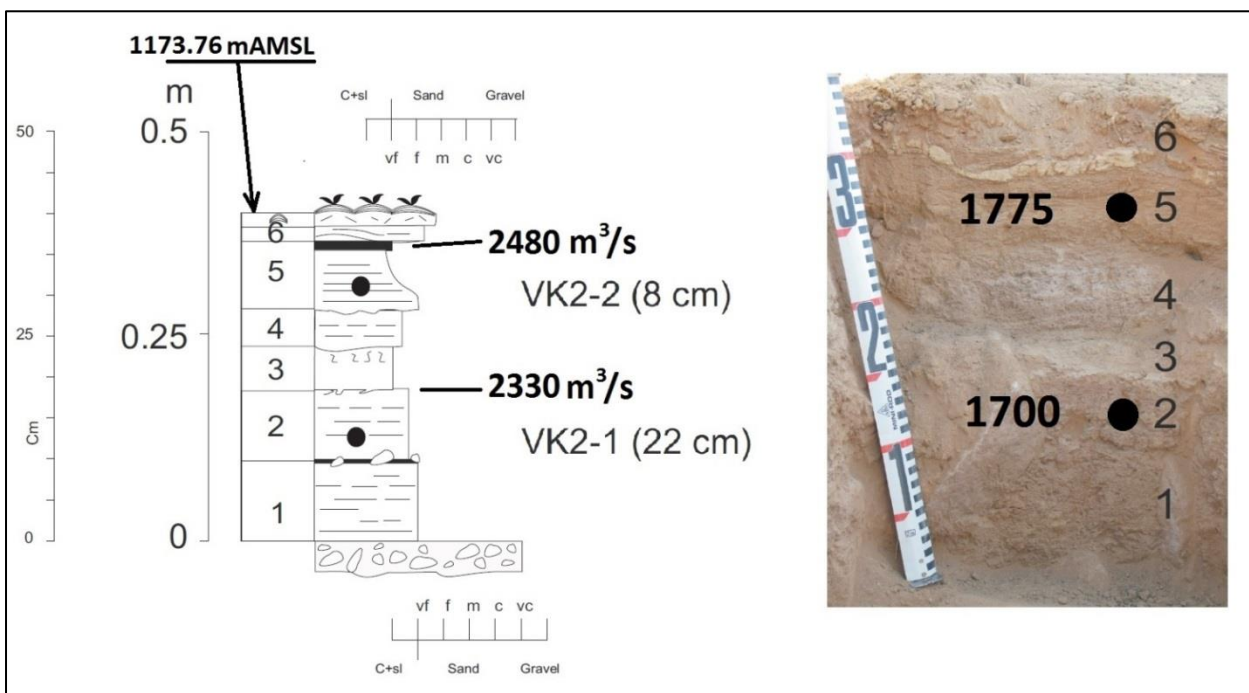


Figure C2: Vogelkranz site, profile VK2. This profile lies on top of a gravel bar. Refer to Figure 3.8. VK2-2 refers to the second sampled flood unit (layer) from the bottom of the profile; VK2-2 lies in flood unit 5. The distance (8 cm) refers to the distance from the top of the profile to the top of the flood unit from which a sample is taken. The OSL-dated year in which the sample was deposited is indicated on the layer.

Appendix C:

Palaeoflood study

Volgelkranz & Echo Site

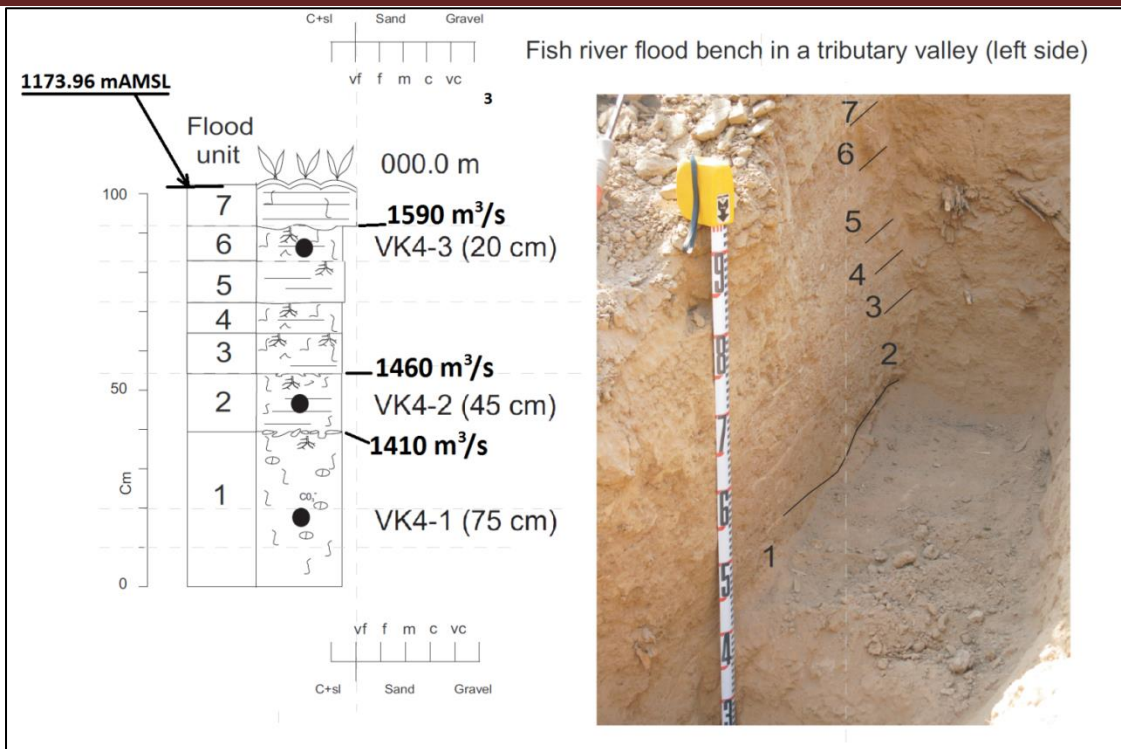


Figure C4: Vogelkranz site, profile VK4. This profile is in a left bank tributary. Refer to Figure 3.8. VK4-3 refers to the third sampled flood unit (layer) from the bottom of the profile, which lies within flood unit six in the stratigraphy. The distance (20 cm) refers to the distance from the top of the profile to the top of the flood unit from which a sample is taken. OSL samples were taken here but no dating was performed.

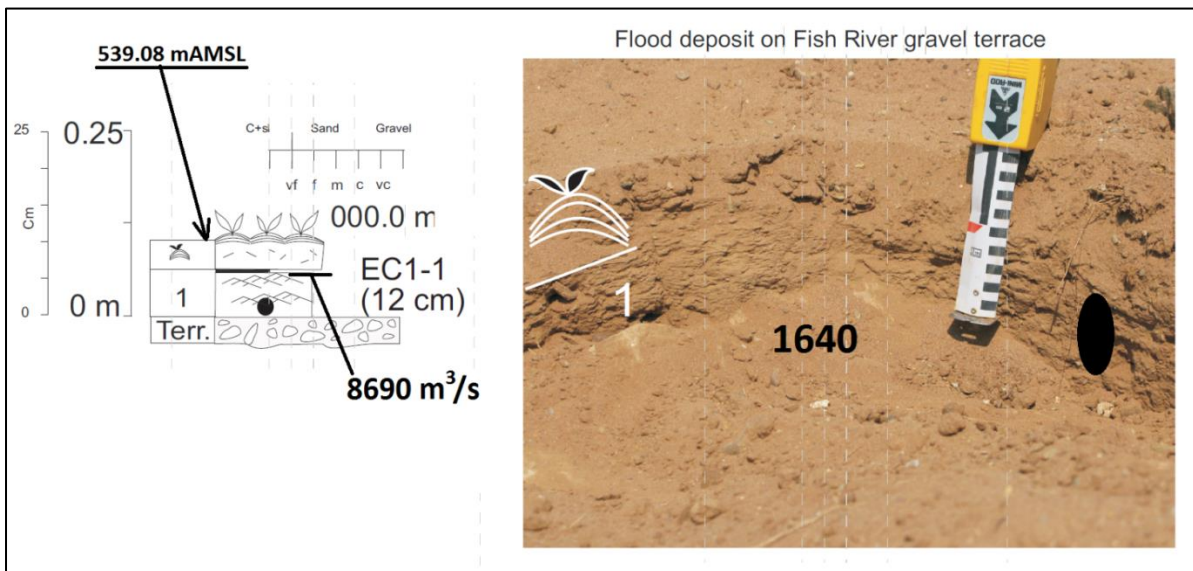


Figure C5: Camp Echo site, profile EC1. This profile is on a right bank gravel bar. Refer to Figure 3.10. EC1-1 refers to the only flood unit exposed in this profile. The distance (12 cm) refers to the distance from the top of the profile to the top of the flood unit from which a sample is taken. The OSL-dated year in which the sample was deposited is indicated on the layer. Note the high discharge rate.

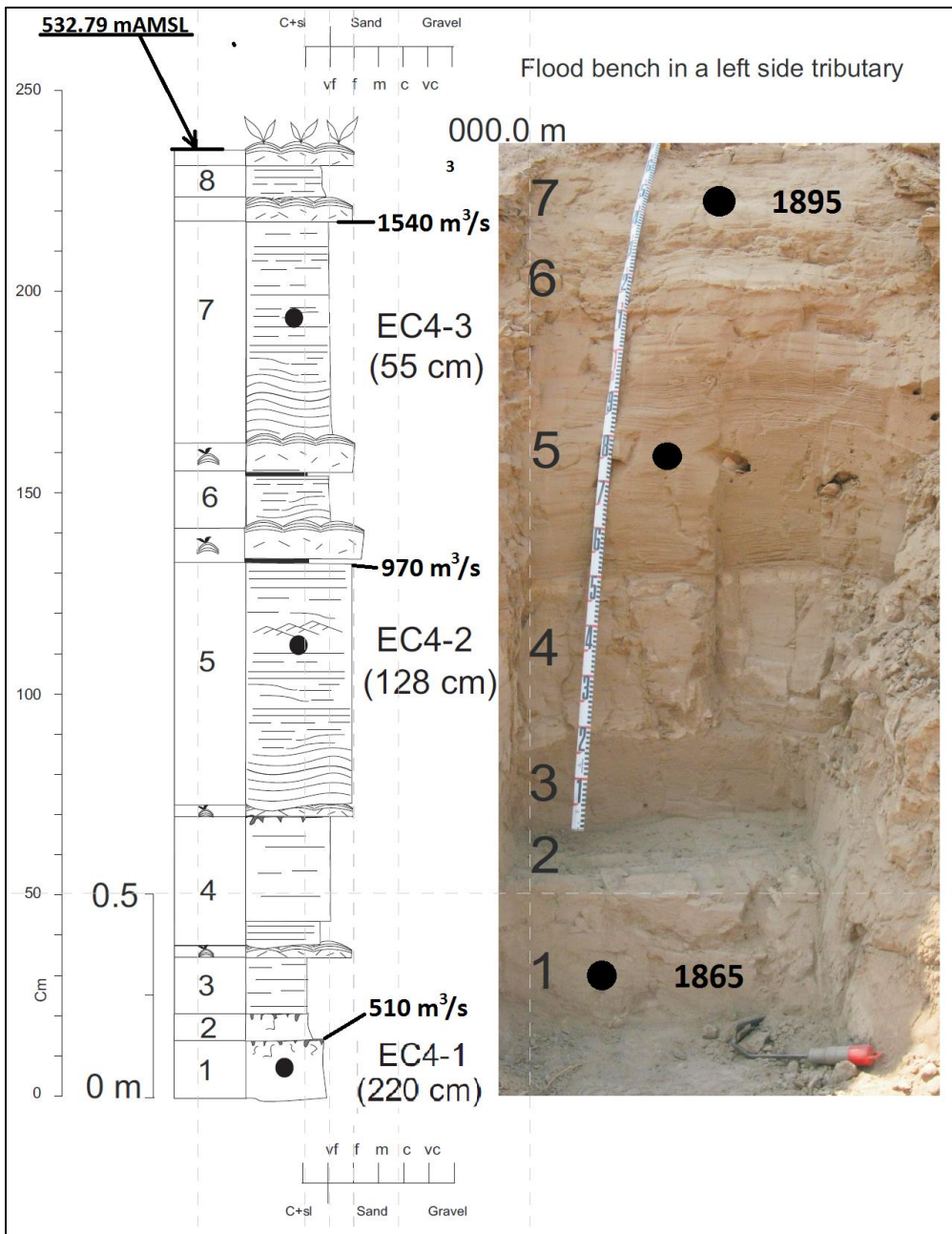


Figure C5: Camp Echo site, profile EC4. This profile is in a left bank tributary. Refer to Figure 3.10. EC4-2 refers to the fourth flood unit (layer) from the bottom of the profile. The distance (128 cm) refers to the distance from the top of the profile to the top of the flood unit from which a sample is taken. The OSL-dated year in which samples EC4-1 and EC4-3 were deposited is indicated on the layer. The discharges associated with each sample layer is indicated at the top of the sample layer.

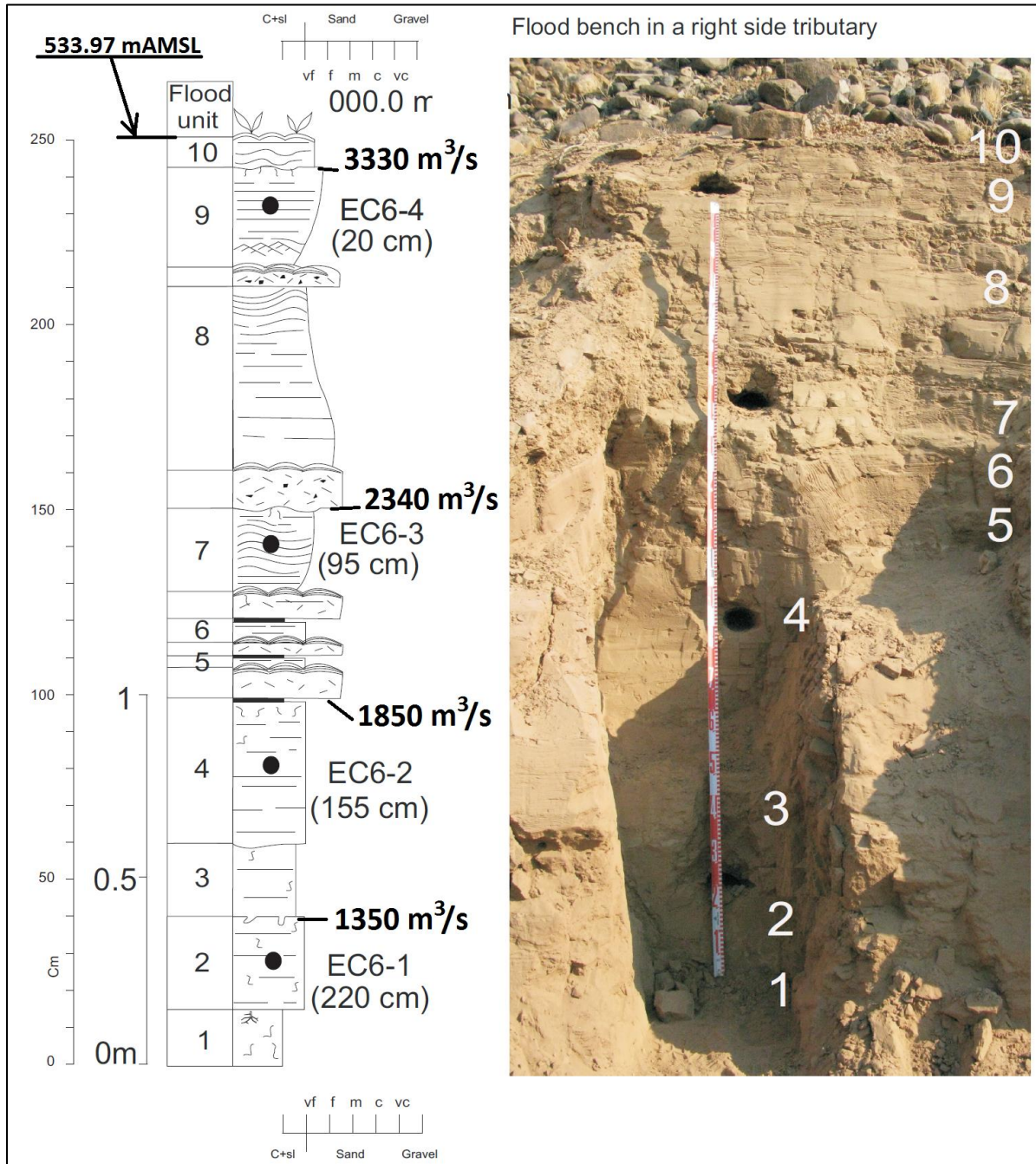


Figure C6: Camp Echo site, profile EC6. This profile is on a right bank sand bar. Refer to Figure 3.10. EC6-2 refers to the second sample, taken in the fourth flood unit (layer) from the bottom of the profile. The distance (155 cm) refers to the distance from the top of the profile to the top of the flood unit from which a sample is taken. The OSL-dated years for EC6 samples were not determined. The discharges associated with each sample layer are indicated at the top of the layer.

Appendix D:

Desert Varnish Stratigraphy

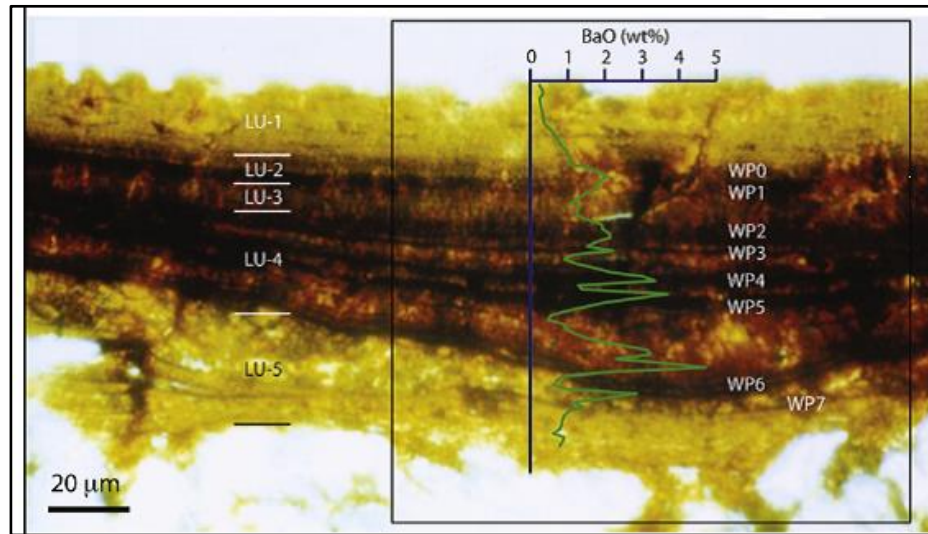
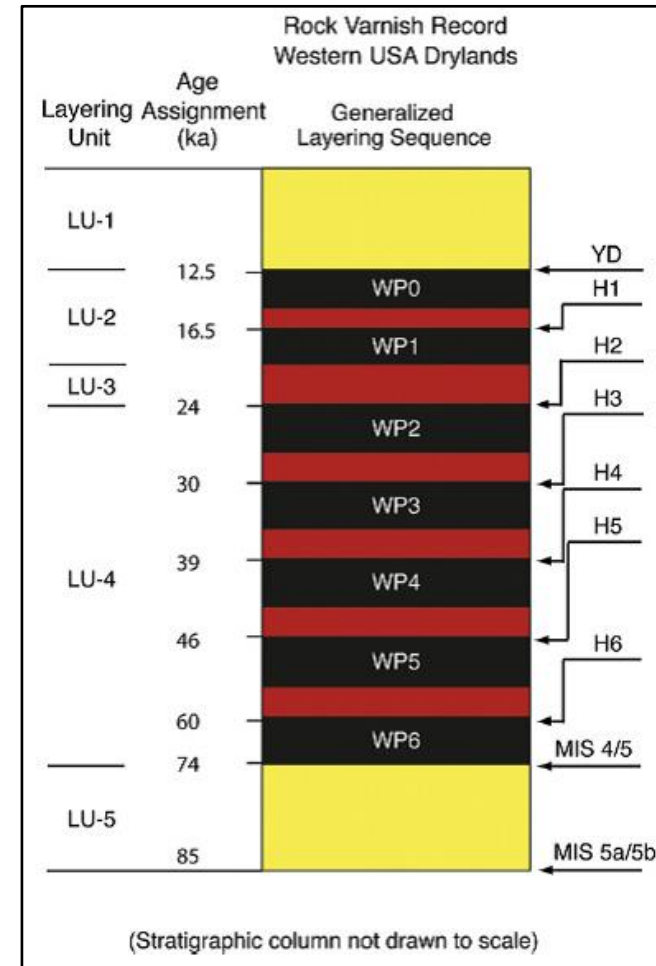


Figure D1 (above). An image of desert varnish micro stratigraphy seen in ultra-thin section under a light-microscope with transmitted polarized light (Lui, 2013)

Figure D2 (right). Late Pleistocene varnish record, from the image in Figure D1, sampled in the drylands of western USA. The color scheme represents relative concentrations of Mn and Ba in varnish microstratigraphy: black=Mn- and barium (Ba)-rich; orange=Mn- and Ba-intermediate; yellow=Mn- and Ba-poor. YD=Younger Dryas, LU=layering unit, WP=wet event in Pleistocene, MIS=Marine Isotope Stage. ka = thousand years. (Lui, 2013).



Appendix F: 1:50 000 map of lower Fish River palaeo site search

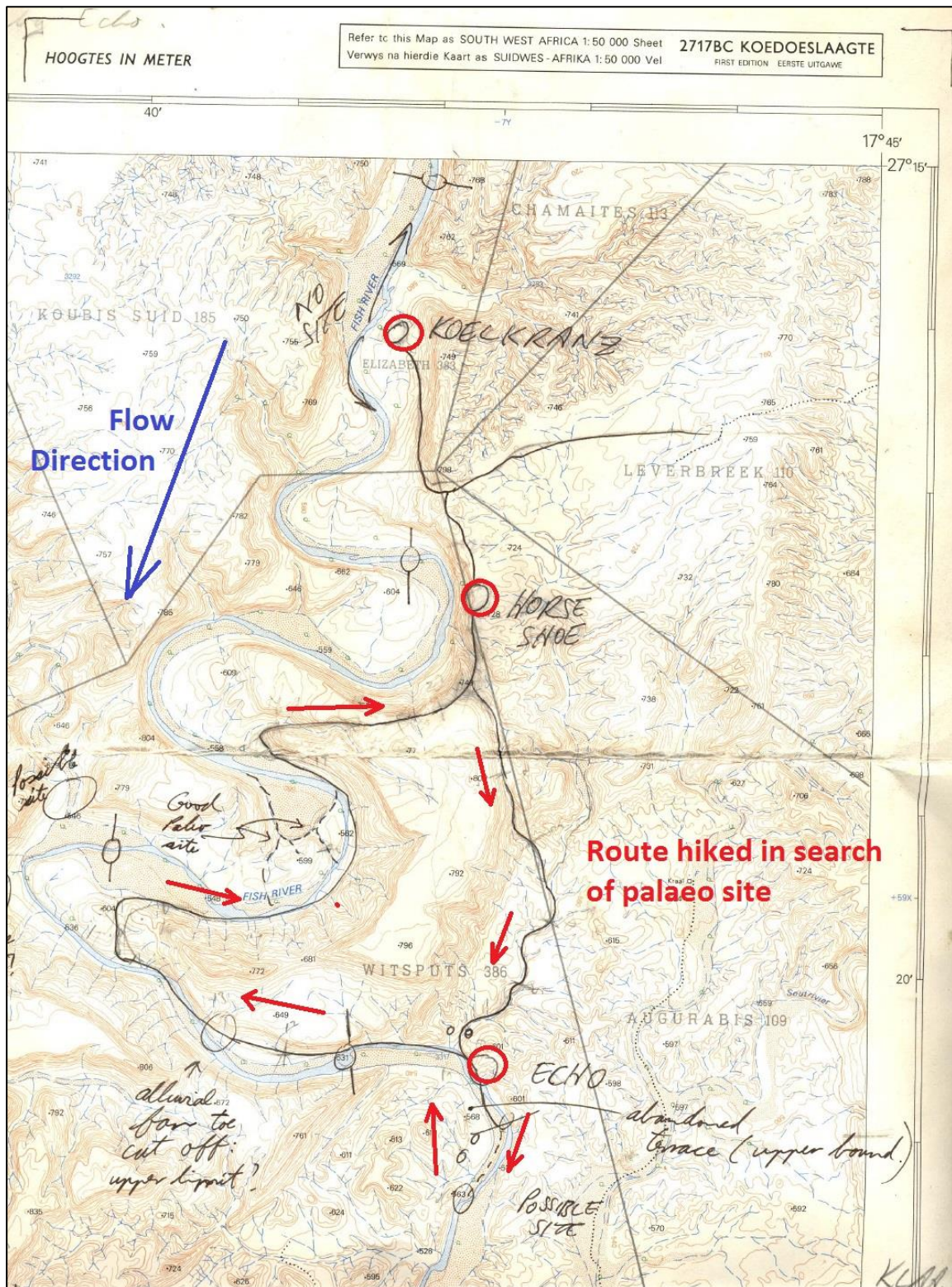


Figure F1. A scanned portion of a 1:50 000 map showing the Horseshoe camp as well as the Echo Campsite and the route trekked, approximately 27 km, in search of suitable palaeoflood deposits along the Fish River. Team split up into two; one party walking north along the Koelkranz reach of the river where no suitable site was identified, and the other took the longer trek to the south where several sites were identified. However the favoured option was Camp Echo due to accessibility and time restraints.

Appendix G: Carbon Dating Report



*Consistent Accuracy . . .
... Delivered On-time*

Beta Analytic Inc.
4985 SW 74 Court
Miami, Florida 33155 USA
Tel: 305 667 5167
Fax: 305 663 0964
Beta@radiocarbon.com
www.radiocarbon.com

Darden Hood
President

Ronald Hatfield
Christopher Patrick
Deputy Directors

November 23, 2010

Dr. Yehouda Enzel
The Hebrew University of Jerusalem
Institute of Earth Sciences
Jerusalem, 91904
Israel

RE: Radiocarbon Dating Result For Sample VK-3

Dear Dr. Enzel:

Enclosed is the radiocarbon dating result for one sample recently sent to us. It provided plenty of carbon for an accurate measurement and the analysis proceeded normally. The report sheet contains the method used, material type, and applied pretreatments and, where applicable, the two-sigma calendar calibration range.

This report has been both mailed and sent electronically. All results (excluding some inappropriate material types) which are less than about 20,000 years BP and more than about ~250 BP include a calendar calibration page (also digitally available in Windows metafile (.wmf) format upon request). Calibration is calculated using the newest (2004) calibration database with references quoted on the bottom of the page. Multiple probability ranges may appear in some cases, due to short-term variations in the atmospheric ¹⁴C contents at certain time periods. Examining the calibration graph will help you understand this phenomenon. Don't hesitate to contact us if you have questions about calibration.

We analyzed this sample on a sole priority basis. No students or intern researchers who would necessarily be distracted with other obligations and priorities were used in the analysis. We analyzed it with the combined attention of our entire professional staff.

Information pages are also enclosed with the mailed copy of this report. If you have any specific questions about the analysis, please do not hesitate to contact us. Someone is always available to answer your questions.

Thank you for prepaying the analyses. As always, if you have any questions or would like to discuss the results, don't hesitate to contact me.

Sincerely,


Digital signature on file

**BETA ANALYTIC INC.**

DR. M.A. TAMERS and MR. D.G. HOOD

 4985 S.W. 74 COURT
 MIAMI, FLORIDA, USA 33155
 PH: 305-667-5167 FAX:305-663-0964
beta@radiocarbon.com

REPORT OF RADIOCARBON DATING ANALYSES

Dr. Yehouda Enzel

Report Date: 11/23/2010

The Hebrew University of Jerusalem

Material Received: 11/8/2010

Sample Data	Measured Radiocarbon Age	¹³ C/ ¹² C Ratio	Conventional Radiocarbon Age(*)
Beta - 287852 SAMPLE : VK-3 ANALYSIS : AMS-Standard delivery MATERIAL/PRETREATMENT : (wood): acid/alkali/acid 2 SIGMA CALIBRATION : Cal AD 1890 to 1910 (Cal BP 60 to 40) AND Cal AD 1950 to beyond 1960 (Cal BP 0 to 0)	30 +/- 30 BP	-25.0 o/oo	30 +/- 30 BP

Dates are reported as RCYBP (radiocarbon years before present, "present" = AD 1950). By international convention, the modern reference standard was 95% the ¹⁴C activity of the National Institute of Standards and Technology (NIST) Oxalic Acid (SRM 4990C) and calculated using the Libby ¹⁴C half-life (5568 years). Quoted errors represent 1 relative standard deviation statistics (68% probability) counting errors based on the combined measurements of the sample, background, and modern reference standards. Measured ¹³C/¹²C ratios (delta ¹³C) were calculated relative to the PDB-1 standard.

The Conventional Radiocarbon Age represents the Measured Radiocarbon Age corrected for isotopic fractionation, calculated using the delta ¹³C. On rare occasion where the Conventional Radiocarbon Age was calculated using an assumed delta ¹³C, the ratio and the Conventional Radiocarbon Age will be followed by "**". The Conventional Radiocarbon Age is not calendar calibrated. When available, the Calendar Calibrated result is calculated from the Conventional Radiocarbon Age and is listed as the "Two Sigma Calibrated Result" for each sample.

Appendix G: Carbon Dating Report

CALIBRATION OF RADIOCARBON AGE TO CALENDAR YEARS

(Variables: C13/C12=-25;lab. mult=1)

Laboratory number: **Beta-287852**

Conventional radiocarbon age: **30±30 BP**

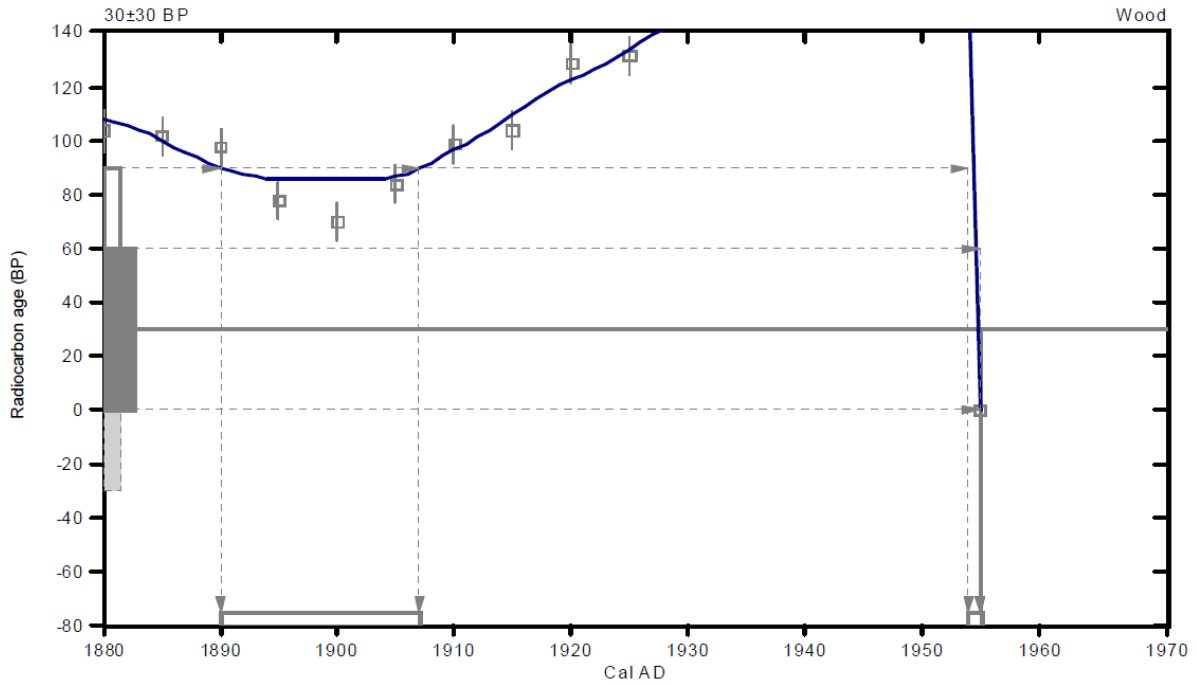
2 Sigma calibrated results²: Cal AD 1890 to 1910 (Cal BP 60 to 40) and
 (95% probability) Cal AD 1950 to beyond 1960 (Cal BP 0 to 0)

² 2 Sigma range being quoted is the maximum antiquity based on the minus 2 Sigma range

Intercept data

Intercept of radiocarbon age
 with calibration curve: Cal AD 1960 (Cal BP 0)

1 Sigma calibrated result: Cal AD 1960 to 1960 (Cal BP 0 to 0)
 (68% probability)



References:

- Database used*
 INTCAL04
- Calibration Database*
 INTCAL04 Radiocarbon Age Calibration
IntCal04: Calibration Issue of Radiocarbon (Volume 46, nr 3, 2004).
- Mathematics*
 A Simplified Approach to Calibrating C14 Dates
 Talma, A. S., Vogel, J. C., 1993, Radiocarbon 35(2), p317-322

Beta Analytic Radiocarbon Dating Laboratory

4985 S.W. 74th Court, Miami, Florida 33155 • Tel: (305)667-5167 • Fax: (305)663-0964 • E-Mail: beta@radiocarbon.com

Appendix H: Rehabilitation activities on real dams

The dams are discussed in the same order as the list of dams in Table 3.6. Only the Mankazana Dam and the Grassridge Dam had their embankments raised. The Glenbrock Dam had a significant volume of earthworks done while the Cata- and Mnyameni Dams had very little earthworks done.

H.1 MANKAZANA DAM – SCOPE OF WORK

The proposals put forward are provided taking cognisance of the following:

- The requirement to make the dam embankment safe
- The requirement to pass the required flow through the spillway.
- The need to provide safe pedestrian and vehicular traffic across the crest and over the spillway all in accordance with the stated requirements of the Department of Roads and Transport.

1.1 SPILLWAY

The spillway remains largely unchanged. **Increased capacity is to be achieved by raising the NOC**, levelling the control section of the spillway to RL 66.5 and widening it to 65m at the bridge centre line.

1.2 SPILLWAY CROSSING

A reinforced concrete bridge solution is the most cost effective and hydraulically efficient.

The advantages can be summarised as follows:-

- No additional widening of spillway channel required
- Fewer piers and larger discharge openings are required.

1.3 UPSTREAM SLOPE PROTECTION

Rip-rap from commercial sources is prohibitively expensive. Quartzite rip-rap from surrounding areas requires DME approval and is also relatively expensive.

Given the problems experienced by DWAF in the past with the use of Armorflex in this application, the use of Soil Cement or Mudstone Rip Rap is put forward.

Appendix H: Rehabilitation activities on real dams

Given the lower cost of mudstone over soil cement DWAF are in favour of the it's use in this application and is put forward as the preferred option

Because the materials are to be derived from modifications of the spillway channel, the requirement for obtaining DME permits is negated.

1.4 EMBANKMENT

It is proposed that the embankment be raised using the material excavated from the existing embankment where the new rip-rap is to be placed. Additional material may be obtained from the proposed spillway excavations.

1.5 ROAD OVER CREST

The embankment is to be raised to a new NOC of RL 70.0 by raising the downstream embankment at a nominal 1V:2,5H slope and steepening the upstream slope above RL 65,0m to 1V:2,96H. Because of slight deviance in the actual embankment cross section and in order to provide a straightened horizontal alignment these slopes may vary from those shown in the theoretical cross section but will not exceed 1V:2,0H on the downstream embankment and 1V:2,5H on the upstream embankment

The road is to have two opposing lanes with pedestrian accommodation and asphalt premix surfacing.

1.6 EMBANKMENT TOE DRAINS

It is proposed that the sub-surface drain will be a 100mm diameter geo-pipe laid in a sand filter surround about 1.5m deep and will lead out into the valley floor downstream of the dam wall.

It is proposed that the storm water drain is to be concrete lined and trapezoidal in section.

1.7 PROTECTION OF TRAINING EMBANKMENT

It is proposed that the protection of the training embankment comprise a concrete toe and soil cement embankment slope protection.

Appendix H: Rehabilitation activities on real dams

H.2 GLEN BROCK DAM – SCOPE OF WORK

2.1. Description

The Glen Brock Dam is a homogenous earthfill embankment dam some 27,0 metres high, originally constructed in 1982, and located in the Tarkastad region of the Eastern Cape. The current DWAF Dam Safety Classification is Category III, with a high hazard potential. Dam safety reports identified the dam as having an inadequate spillway and an embankment that was suffering excessive erosion on the downstream face.

2.2. Spillway

The existing excavated by-wash spillway on the right flank will be widened to 31m from an average of 10m to provide sufficient capacity to pass the SEF.

2.3. Embankment

Rockfill generated from the spillway excavations will be used to stabilize and protect the downstream face of the embankment from further erosion. Decomposed dolerite gravels obtained in these excavations will be used as a transition layer between the existing earthfill face and rockfill shell.

The upstream riprap protection layer needs to be improved.

New toe drains and concrete lined stormwater drains will be required along the abutments and the downstream toe of embankment. In addition, a stormwater drain is required on the hillside face of the left bank access road up to the dam crest.

A 1.5m high parapet wall is to be constructed by hand of stone masonry on the existing (re-graded) crest. This wall will be reinforced to withstand wave action and water pressure in the event of extreme floods.

A reinforced concrete surfaced boat ramp is required down the right abutment along the upstream toe of the embankment for access to the new floating intake..

2.4. Outlet Works

Under water removal of approximately 4 metres of sediment around the intake of the outlet pipe at the upstream toe of the embankment will be necessary to enable divers to safely

Appendix H: Rehabilitation activities on real dams

connect a flexible pipe to a new floating intake. Problems with silt collapsing over the intake may make this connection difficult, so this is to be undertaken by specialist divers.

The outlet pipe isolating valves at the dam toe and at the new river flow outlet tee will be replaced. The river flow outlet pipe will have a gate valve control and jet disperser at the end. New valve chambers will be required to house all the new valves and a concrete energy dissipation chamber is required at the jet disperser.

2.5. Access Road

The existing gravel access road is a district road that is in poor condition. This will be upgraded into a reliable access road as part of the rehabilitation contract. Upgrading will include the construction of a number of culverts. Gravel borrow pits will require rehabilitation to comply with current environmental legislation.

H.3 GRASSRIDGE DAM – SCOPE OF WORK

The rehabilitation will entail the following:

- The Contractors establishment on site, and maintenance thereof during the Contract period;
- Raising of the crest level of the dam to increase freeboard.
- Upstream slope of embankment – addition of rip rap
- Downstream slope of embankment – addition of rockfill and fill materials as indicated on the Drawings.
- Downstream toe – removal of alluvial material at the toe of the dam for founding additional rockfill.
- Construction of graded filter layers on the faces of the embankment where required.
- Provision of subsurface drainage along the embankment toe and downstream combined with the lowering of the water surface in the old river channel.
- Placing of a wearing course on the crest of the Earthfill Embankment.
- Additional concrete works and modifications to the crest profile on the spillways to improve stability, control toe erosion and improve discharge characteristics.
- Improvements to the measuring facilities of releases through the radial gates.

Appendix H: Rehabilitation activities on real dams

- Carrying out of necessary remedial works on the radial gates that are deemed necessary by the engineer on site.
- Construction of extensions to the stilling basin downstream of the left bank outlet radial gates and the construction of a crump measuring weir at the end of the extended stilling basin.
- Partial drawdown of dam and/or construction of a small coffer dam to gain access for laying of a 1.2m diameter, low flow outlet pipe and the construction of associated civil works.
- Concreting the floor of the unlined right bank outlet tunnel.
- The removal of all equipment, plant and surplus materials and clearing of the site after completion of the works.

3.1 Upstream Embankment

A 1000mm thick riprap shall be placed at a slope of 1V:2H from RL 1055 to RL 1060.44, from which the slope shall be steepened to 1V:1.5H, to NOC at RL 1061.95. A 300mm crusher run shall be provided between the earthfill and the new riprap layer. The contractor shall maintain consistent riprap thickness throughout. The dam has already been maintained at a low level, but the Contractor shall, by prior arrangement with the dam operators, draw down the reservoir to the minimum permitted level for construction (RL 1054.08) to facilitate riprap placement at that level as well as the construction of the intake section of the low flow outlet works.

3.2 Raising of the NOC:

The crest of the embankment is to be raised by 1.51m. This will be achieved by adding material to the downstream face and rip-rap to the upstream face. Thus the embankment will be made safe against overtopping by major floods as well as improving its stability to meet acceptable criteria. This will include additional drainage at the toe of the dam and downstream of it.

Raising the non-overspill crest (NOC) will be done by using rockfill material from the toe up to the current NOC. A transitional fine and coarse filter layer shall be placed before the rockfill can be placed on top of earthfill material on the embankment as deemed necessary by

Appendix H: Rehabilitation activities on real dams

the Engineer. The existing rockfill toe will be extended by about 5.8m with new rockfill material. The contractor shall remove alluvium to found the additional rockfill on bedrock or residual material in the original river bed.

The embankment's NOC will be raised by 1.51m using earthfill material. The crest shall be provided with a 1:100 cross fall, to allow water to run into the upstream side. The crest width shall be 6.4m at the new level, including the new riprap layer on the upstream side.

The contractor shall provide a 150mm thick gravel surface compacted to 98% Proctor density.

3.3 Downstream drainage:

Sub-surface toe drains will run along the abutment toes towards the old river bed. Additional sub-surface drains will be required to drain off saturated areas on the left abutment. The sub-surface drain will comprise a 160mm diameter geo-pipe laid in a stone filter surround about 1.2m deep.

Concrete lined surface storm water drains shall be required as directed by the Engineer.

3.4 Spillways:

The existing spillways shall remain the same length but the sharp edged crest will be demolished for the construction of an ogee crest. The buttress crests shall also be demolished to allow the ogee spill crest to continue over the buttresses. The buttresses shall also be lengthened, with dowels grouted into the existing concrete. The mass concrete left bank spillway shall be increased in section as shown on the Drawings. Apron slabs shall extend 5m from the toe of both the buttress spillway and mass concrete spillway. The Apron slabs shall also contain anchor dowels grouted into bedrock as shown on the Drawings.

3.5 Mechanical and Electrical Works

The Contractor (Main Contractor) must take note that the refurbishment of the outlet works (old and new) as well as the construction of a new low flow outlet structure adjacent to the radial gate outlet structure will be put out on tender to procure a Mechanical-Electrical Sub-contractor to perform the work. The management of the Sub-contractor shall be the responsibility of the Main Contractor. Support from the PSP Team will be provided on Mechanical and Electrical Technical matters and quality control.

Appendix H: Rehabilitation activities on real dams

Support is required from the Main Contractor to the appointed Mechanical-Electrical Contractor. Civil works related to the 1200mm diameter low flow conduit (excavations and concrete works) will be the responsibility of the Main Contractor. The Mechanical Contractor will lay the pipes on trestles supported on concrete bedding provided by the Main Contractor. The main Contractor shall place the concrete encasing when the pipes have been satisfactorily installed and tested. The Main Contractor's method statement should show satisfactory precautions taken to secure the pipe from any movement or floatation during concreting.

3.6 Borrowpits and Quarry

The contractor shall establish a new quarry on site, and will be the source of dolerite for rockfill, riprap, coarse filter and fine filter materials as well as concrete aggregates. The fine filter will, if necessary, be produced by mixing fine particles from the quarry with silt material excavated from the dam basin, to produce correctly graded fine filter material.

H.4 CATA DAM – SCOPE OF WORKS

4.1 General

Approximately 1 ha of small wattle will have to be felled, grubbed and cleared downstream of the embankment toe pond.

The dam can be accessed via the upper access road which turns off the DR 07377 in Cata Village or the lower access road which turns off the DR 07378 and runs to the dam crest where it meets the upper access road. The upper access road is a short steep concrete road which turns into a gravel road just before reaching the dam crest. The lower access road is a gravel road in a poor condition and has three river crossings, one of which is a causeway part of which has been washed away. A 4x4 is required to use the lower access road in its present condition. Part of this contract involves the refurbishment of the lower access road.

A mechanical sub-contractor will be appointed separately by the Employer to undertake refurbishment work on the mechanical equipment at the dam. Depending on when this sub-contractor is appointed the work may be undertaken before, during or after the civil contract.

Appendix H: Rehabilitation activities on real dams

The Contractor must therefore make allowance for facilitating the access of the mechanical sub-contractor on site as well as sharing his camp.

4.2 Spillway Structure

Concrete rehabilitation is required in the spillway chute structure where reinforcing steel is bare or exfoliation is taking place. These areas are to be cut back and made good with proprietary repair materials. The material to be used is yet to be selected and will require further market research and approval with the Client.

About 230m of standard 1,2m high 7-strand double barbed wire fence will be required for safety on the left had side of the side channel spillway and spillway outfall.

4.3 Embankment

The Non-Overspill Crest requires re-surfacing with a selected gravel to re-establish the desired level and surface.

Existing ladder drain outlets need to be refurbished by installing manholes at each of the 12 outfalls.

Existing ladder drain outlets need to be refurbished by installing manholes at each of the 12 outfalls. Further to these, subsurface toe drains running down the toe of the embankment are required. The toe drains will also pass through the manholes at the ends of the ladder drains. Disturbed areas will have to be re-grassed.

The existing embankment surface water drainage consists of three rows of grassed berms running across the face of the embankment and stone pitched trapezoidal stormwater channels running down the sides of the embankment. The berms are to be reshaped to their original profile and the stone pitching of the stormwater drainage channels replaced with reinforced concrete trapezoidal channel sections.

Embankment settlement beacons must be refurbished, without disturbance.

The open natural channel draining the downstream toe pond must be deepened by a 2m wide excavation in decomposed rock and / or boulder material to an estimated maximum depth of 2m, over a length of some 40m.

Appendix H: Rehabilitation activities on real dams

A derelict instrumentation house on the downstream toe must be demolished. An excavation / concrete tank on the right flank downstream must be opened up, demolished and backfilled, with disposal of the concrete and brickwork in the excavation.

4.4 Down Stream Valve Chamber

The pipe work and valves in the downstream valve chamber will be replaced by the mechanical sub-contractor and a new river outlet installed. To achieve this, the existing valve chamber will need to be demolished and reconstructed around the new pipe work and river outlet. A channel will also have to be excavated and lined with erosion protection from the new river outlet to the toe pond.

4.5 Access Roads

The existing lower access road from the DR 07378 to the dam crest will need to be refurbished. The refurbishment work will involve:

- The construction of 1582m of 5m wide gravel roadway over the existing road with associated earthworks;
- construction of 603m of 5m wide concrete roadway over the existing road where it runs up the right flank of the dam;
- the causeway river crossing will need to be upgraded with longer approach slabs and erosion protection comprising downstream cut-off walls into to bedrock or below scour depth and rip-rap revetment along the downstream left bank;
- the rehabilitation of two concrete culverts;
- the installation of 500m of concrete V-drains and;
- the installation of storm water drainage pipes crossing the road with associated headwalls and outlet structures.

Appendix H: Rehabilitation activities on real dams

H5 MNYAMENI DAM – SCOPE OF WORK

5.1 General

Approximately 0,8ha of small wattle will have to be felled, grubbed and cleared for:

- i) the additional rock fill berm at the dam toe;
- ii) the contractor's camp; and
- iii) the access and working area for the Intake Control Works.

The dam can be accessed by a gravel road leading from the DR 0738 which is in a poor condition accessible only with a 4x4. Part of this contract involves the refurbishment of this access road. A track leading to the toe of the dam, from the main access road, will need to be upgraded over 1km to allow temporary access for construction purposes only. A stream crossing is included in this work. After completion of the rehabilitation works, this access track must be made impassable and returned to natural ground

A mechanical sub-contractor will be appointed separately by the Employer to undertake refurbishment work on the mechanical equipment at the dam. Depending on when this sub-contractor is appointed the work may be undertaken before, during or after the civil contract. The Contractor must therefore make allowance for facilitating the access of the mechanical sub-contractor on site as well as sharing his camp.

5.2 Spillway Shaft, Tunnel and Outfall

No concrete rehabilitation is envisaged in the shaft and tunnel. (morning glory spillway) except where the Engineer deems necessary after more detailed inspections during construction of the rehabilitation works. The product to be used is yet to be selected and will require further market research and approval with the Client. Two or three "large ferrule holes" in the shaft, about 50mm diameter also need sealing. These can be closed by divers with elastomeric conical plugs from the outside. The contractor will have to pay particular attention to safety when working on the overspill section of the bell mouth intake.

The mechanical sub-contractor will replace the existing river flow outlet valve (presently located at the head of the spillway conduit) and locate a new valve in a chamber to be constructed downstream of the conduit exit portal. He will lay a new 300mm ND steel pipe connecting the existing tee to the new river flow outlet valve. The new pipe will be laid on the existing concrete encasement on the right side of the spillway conduit. The new concrete

Appendix H: Rehabilitation activities on real dams

chamber will be part of the civil works in this Contract and will need to be constructed around the new pipe work after it has been installed.

The mechanical sub-contractor will construct a steel walkway above the new river flow outlet pipeline in the spillway conduit.

A stairway from the embankment crest to the spillway outfall will be constructed using precast units installed on in-situ landings. The Contractor may prefer to construct this by placing concrete in-situ on the embankment slope should it be deemed more cost effective.

Hand railing is to be installed by the M&E sub-contractor on both sides of the stairway and on the spillway outfall head wall and wing walls. In all, about 250m of hand railing installation is required.

5.3 Access Path to Intake Control Structure

An existing footpath leading to the intake structure will require upgrading to a 2.5m wide concrete path. Due to the steep nature of the topography the existing hill side will need to be steepened with cut and fill to compensate for the wider path. The steeper slopes are to be stabilised with a Lofelstein block retaining wall or similar approved product.

A trapezoidal drain is to be provided on the hillside at the top of the retaining wall above the path. An Armco barrier is to be installed along the full length of the reservoir side of the path.

5.4 Intake Control Structure

The existing intake control structure is a rectangular concrete shaft, inclined at 33 degrees from the horizontal, on the right bank of the reservoir. Currently the shaft is accessed via a gravel footpath which is to be upgraded under this Contract.

The existing intake structure is accessed via an inspection cover. To improve access to the structure and make the operating equipment more secure a concrete operating room is to be constructed on the end of the existing shaft. This will require the concrete of the existing shaft to be cut back to allow access from the new control room.

The mechanical sub-contractor will refurbish the inlet control equipment and install the steel fixtures in the control room, such as the security door, crawl beam, ladder and louvers.

Appendix H: Rehabilitation activities on real dams

5.5 Embankment Materials and Drainage

Original drainage and soils characteristics of the embankment will have to be investigated, following which instructions will be given as to remedial works.

Investigations may consist initially of

- 4 no. trial pits along the crest to a depth of 3,5m. These will be logged and, if the Engineer decides, sampled for grading and indicator tests to determine the acceptability of this material to water from passing through during periods of high flood.
- Exploratory trenches at 20m centres (8 no.), 0.6m wide, 3m deep and 18m long, situated at the toe of the embankment and up the slope. Other trenches may then be required to open up existing toe collector drains.

Should the crest trial pits indicate the necessity of a cut-off trench along the embankment crest, this will have to be excavated to 3,5m depth and then backfilled with selected soil of low permeability or, if unavailable, a soil / bentonite mix, compacted to 95% Proctor density.

The downstream embankment toe drainage and storm water surface drainage will have to be rehabilitated. Depending on the findings of the exploratory trenches, chimney drains may have to be re-instated and a new subterranean toe drain constructed. Stormwater drainage must be provided by the installation of reinforced concrete trapezoidal drains.. Disturbed areas will have to be re-grassed.

5.6 Embankment Crest and Roadway

After completion of the drainage exploratory / remedial work described above, **the Non-Overspill Crest will require re-surfacing with a selected gravel to re-establish the design level, camber and surface.** Armco barriers are specified along both sides of the full 355m long crest.

A small section of precast block walling will be required at the right flank access to provide for local embankment widening to allow a 20m radius horizontal curve in the access road.

Access to the left flank of the dam must be provided across the inlet to the auxiliary spillway. This will require a ramp and a concreted roadway section 4m wide and about 155m long, with a slab thickness of 125mm.

Appendix H: Rehabilitation activities on real dams

Access control booms and no entry signs shall be installed at the right flank of the main embankment and at the start of the Auxiliary Spillway crossing.

5.7 Embankment Free Draining Toe Berm

A free draining toe berm shall be constructed from original ground level up to 32m below the embankment crest. This shall be 6m wide and will be constructed on existing rockfill or embankment, incorporating filters where necessary.

Disturbed areas shall be topsoiled for which an allowance of 1000m³ is billed. Spoil left downstream of the embankment toe along the left flank during previous construction activities is suitable and may be used at the discretion of the Engineer.

5.8 Auxiliary Spillway Rockfill

A rockfill weir shall be constructed across the auxiliary spillway, to a maximum height of 3,3m. If it is not possible to source the required grade of rock from the borrow area on site then it will need to be sourced from a commercial quarry.

5.9 Access Roads

The existing access road from the DR 0738 to the dam crest requires re-construction. The access road re-construction will need to be substantially complete before the civil and mechanical works can commence. The Contractor shall programme construction of the access road as a first priority.

This work comprises:

- Construction of 2112m of 5m wide gravel roadway over the existing road with associated earth works;
- erection of 1060m of Armco barriers;
- the installation of 460m of concrete V-drains and;
- the installation of 3 number storm water culverts beneath the new road;

The track branching off this road leading to the toe of the dam will require sufficient work to make it passable for transport to the downstream works. After completion of both civil works

Appendix H: Rehabilitation activities on real dams

and the mechanical and electrical works, this road shall be removed and the ground rehabilitated to satisfy environmental requirements.

Appendix I: Maps of Namibia depicting K-values, 3-day rainfall, topography, geology and other relevant information to demarcate the K-regions

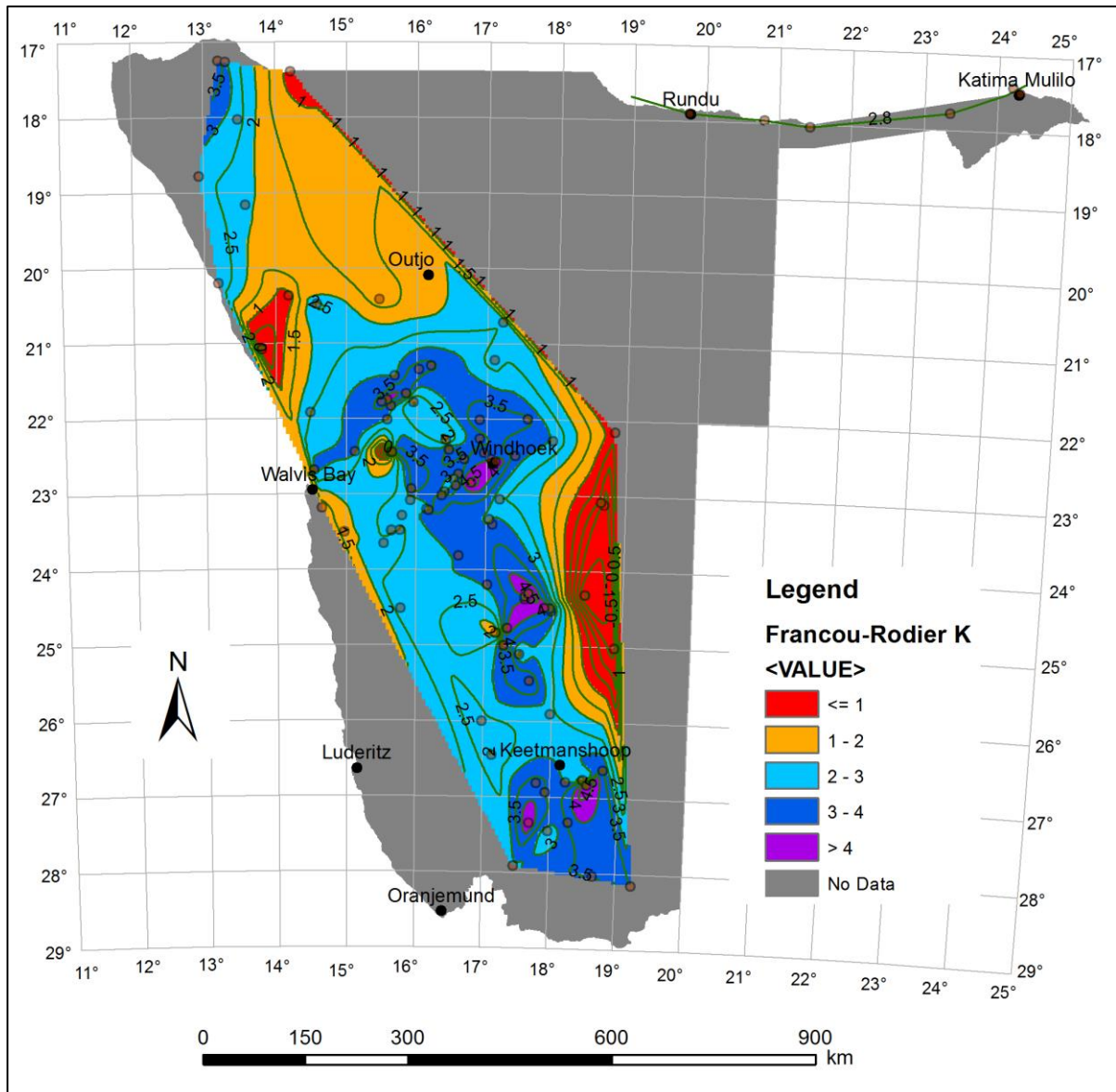


Figure I1. A plot of the new K-values for the available flood peak data. The grey areas on this plot indicates the areas where no flood peak data, or any streamflow data, exists. This highlights the need to extend data capturing and/or palaeoflood studies into these areas to have a better distribution of flood peak discharges covering the surface area of Namibia. It is recognized that the Namib Desert as well as parts of the Kalahari Desert have no river channels; therefore no K-value can be allocated to these regions.

Appendix I: Maps of Namibia depicting K-values, 3-day rainfall, topography, geology and other relevant information to demarcate the K-regions

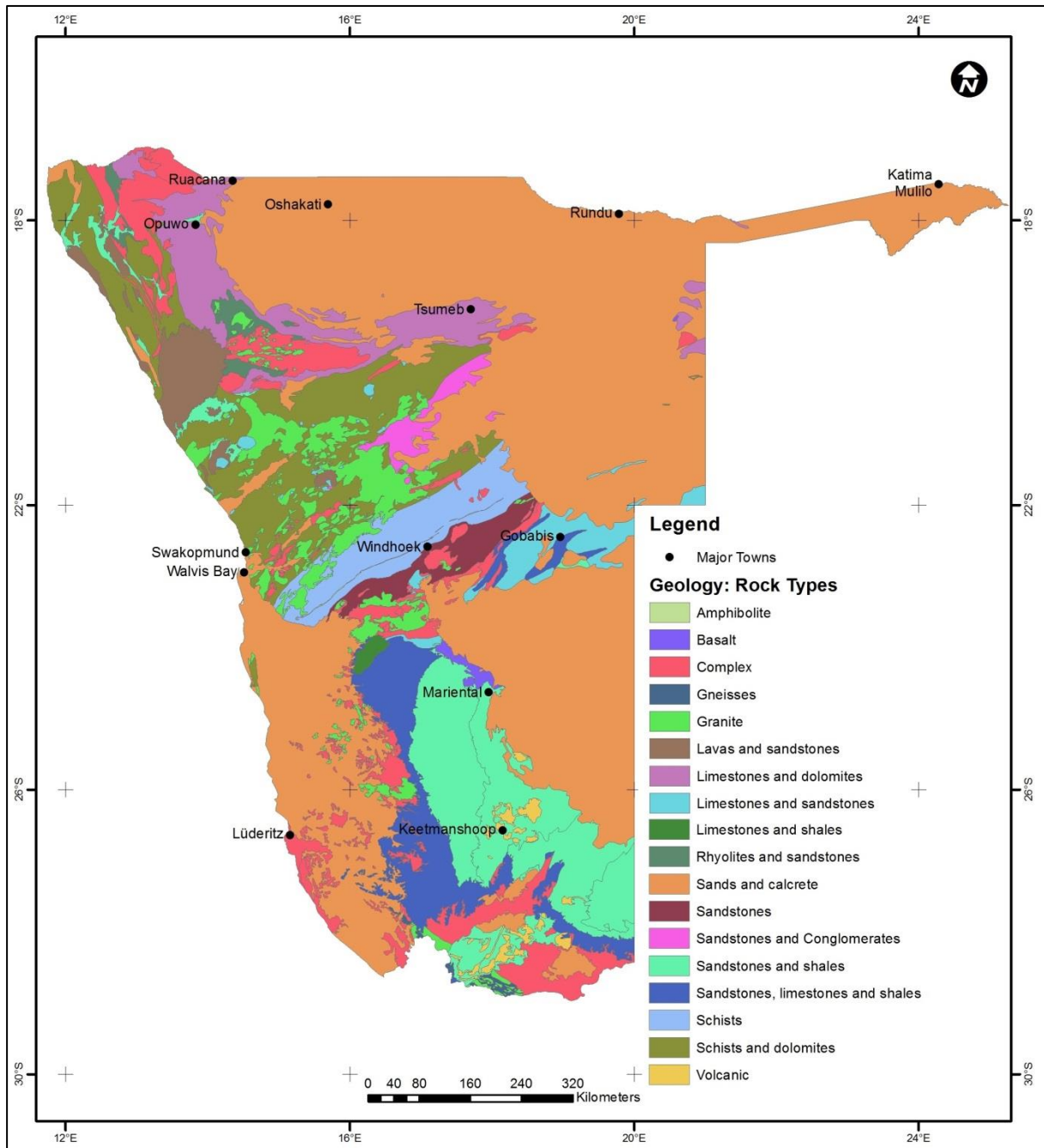


Figure I2. Geology of Namibia: Rock Types (From: Mendelsohn et al., 2002).

Appendix I: Maps of Namibia depicting K-values, 3-day rainfall, topography, geology and other relevant information to demarcate the K-regions

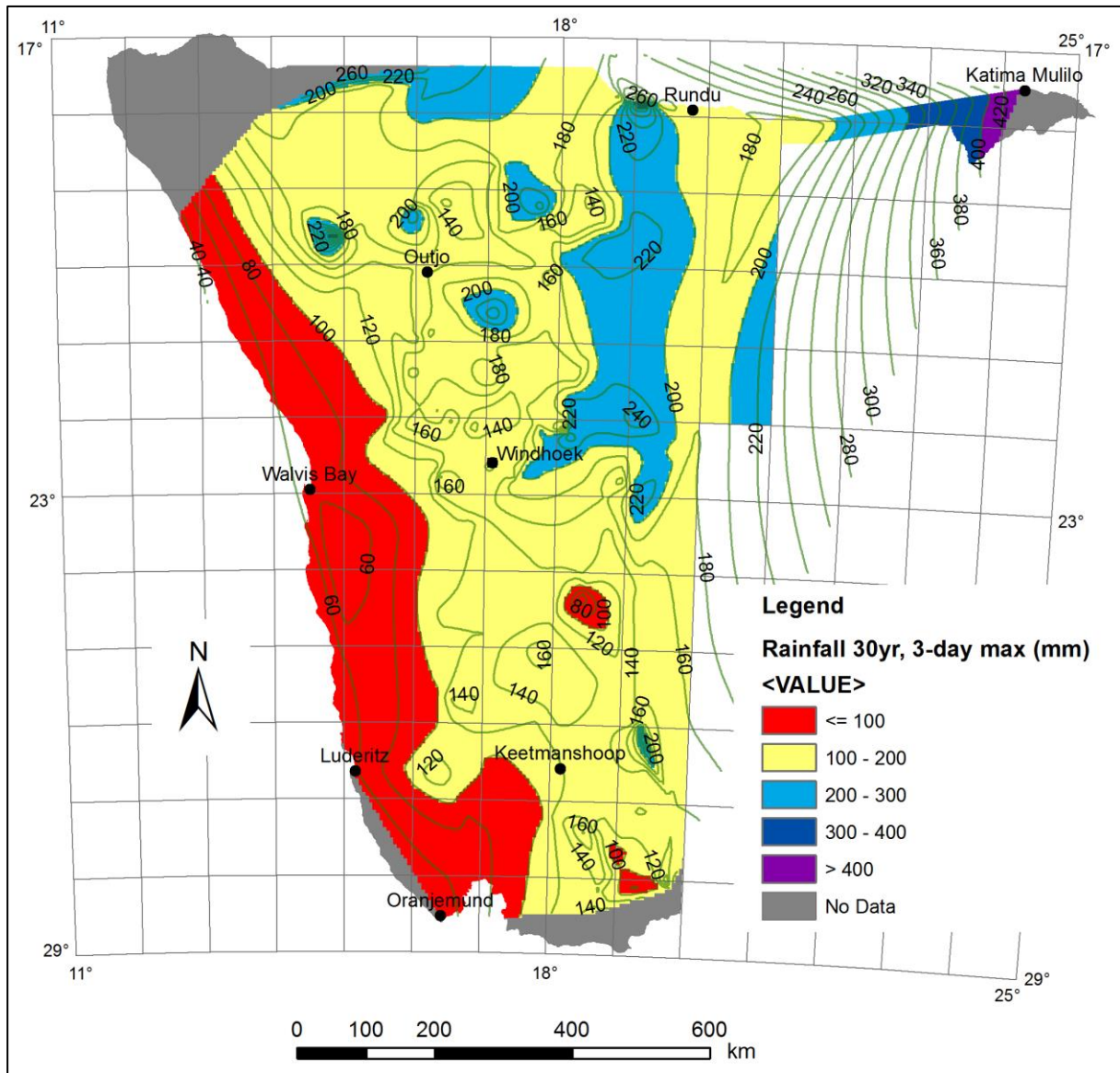


Figure I3. Isolines for the annual maximum 3-day rainfall measured at rain gauging stations with record lengths exceeding 30 years.

Appendix I: Maps of Namibia depicting K-values, 3-day rainfall, topography, geology and other relevant information to demarcate the K-regions

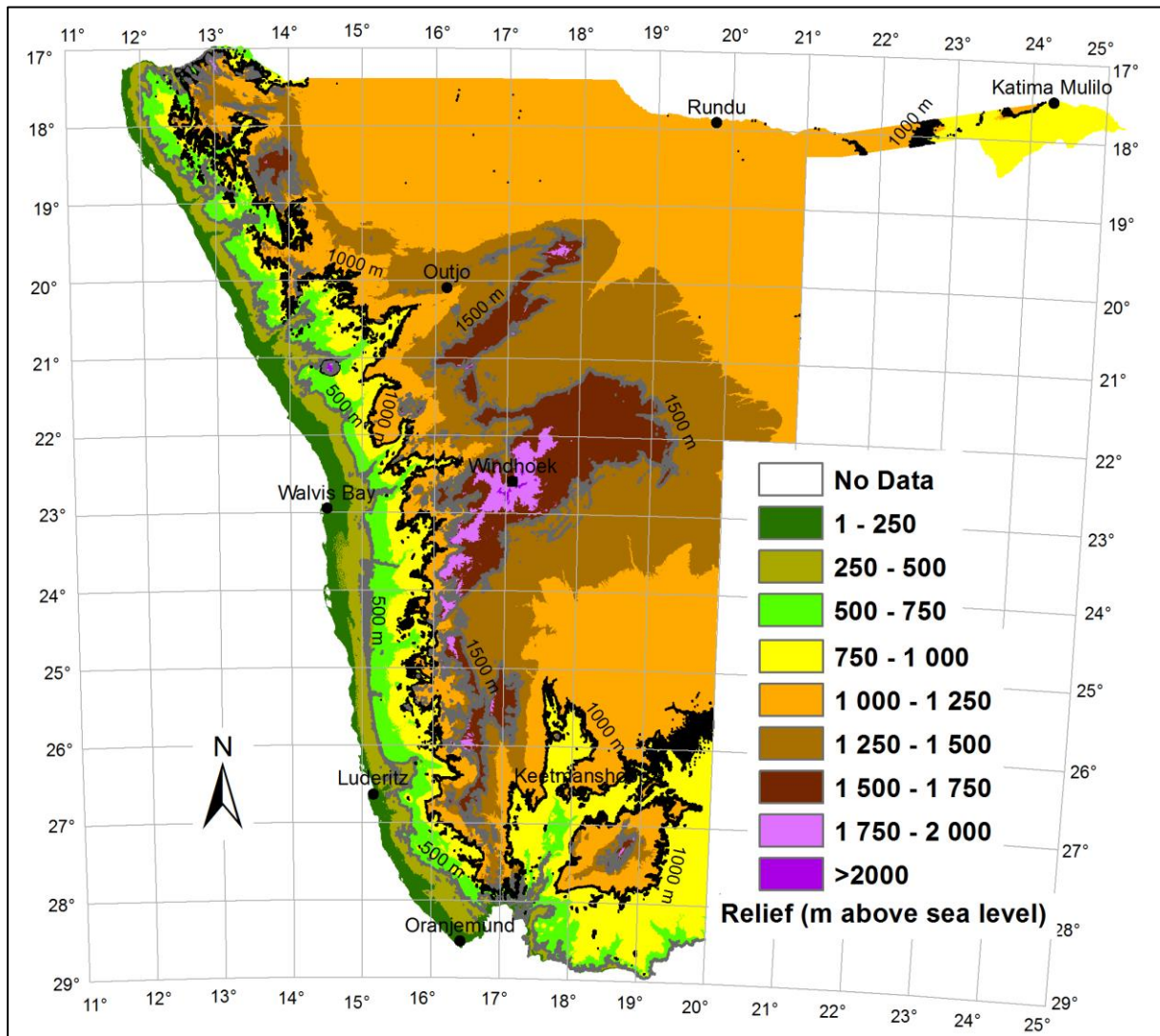


Figure I4. Relief; height in metres above mean sea level

Appendix I: Maps of Namibia depicting K-values, 3-day rainfall, topography, geology and other relevant information to demarcate the K-regions

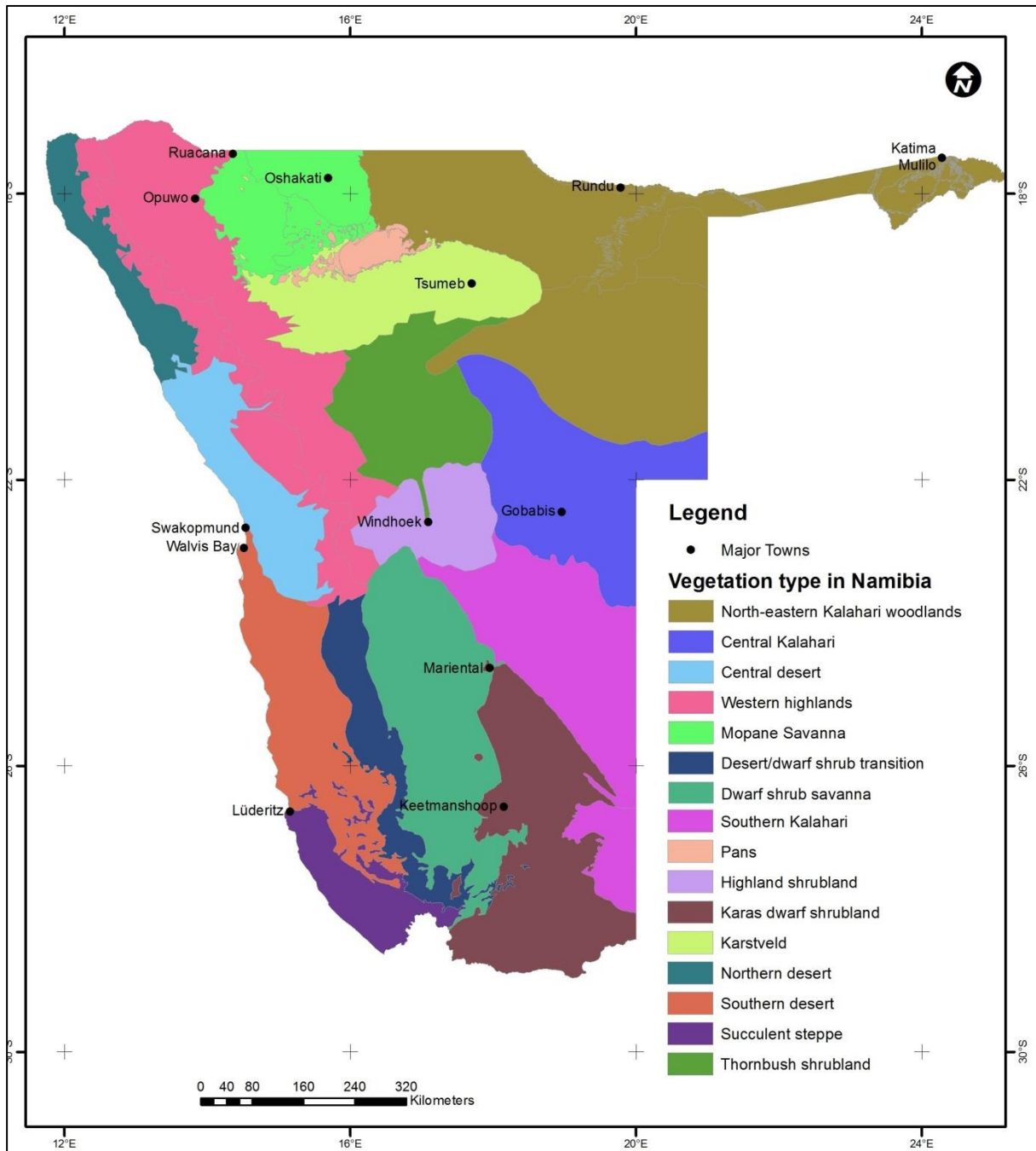


Figure I5. Vegetation types in Namibia (From: Mendelsohn et al., 2002).

Appendix J: Highest Recorded Flood Peaks in Regions

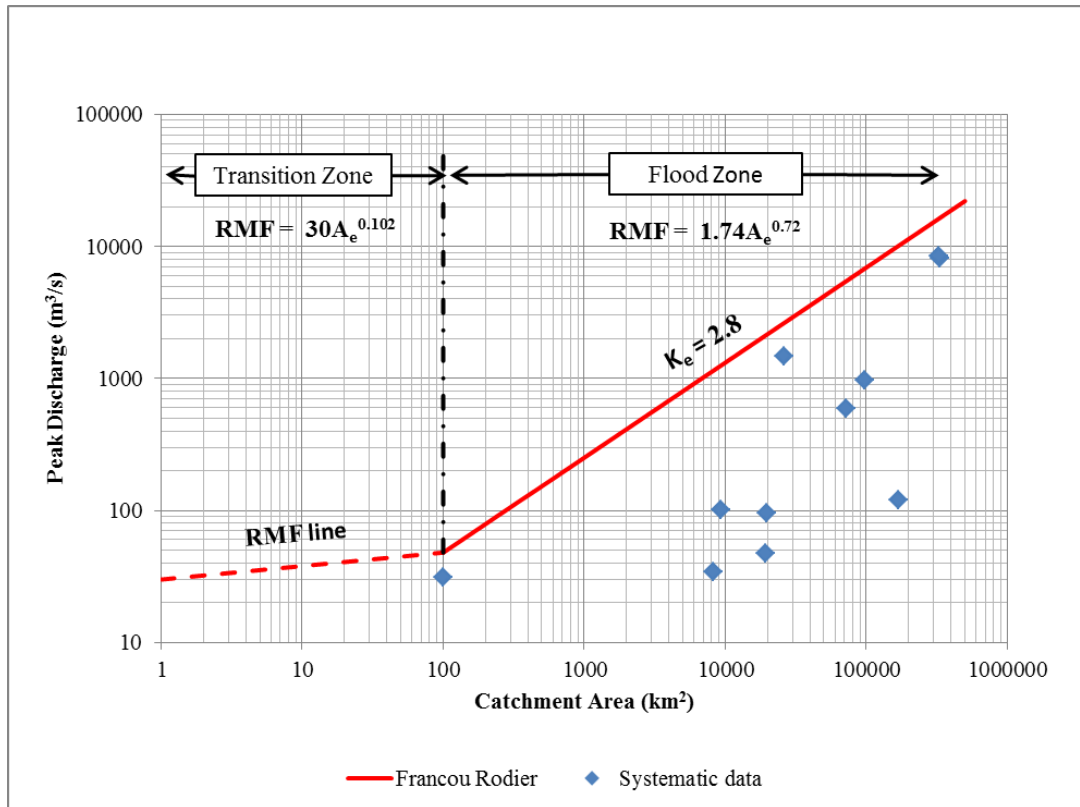


Figure J1. The highest recorded flood peaks and RMF in Region 2.8.

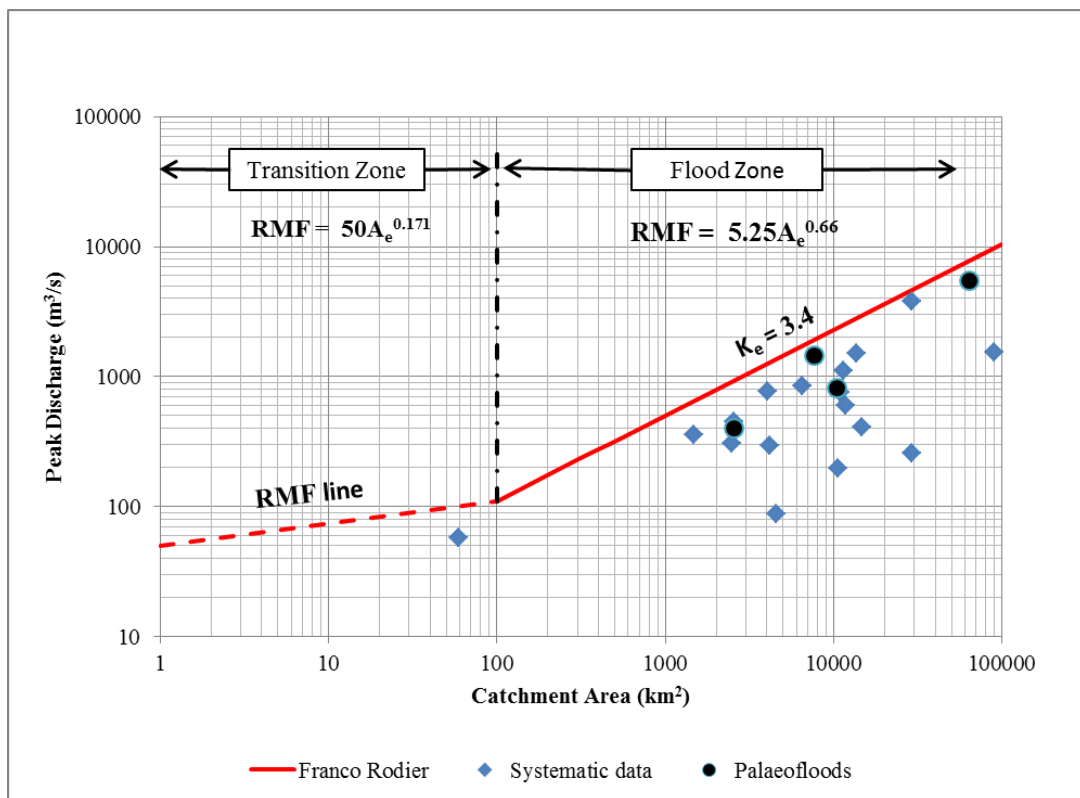


Figure J2. The highest recorded flood peaks and RMF in Region 3.4.

Appendix J: Highest Recorded Flood Peaks in Regions

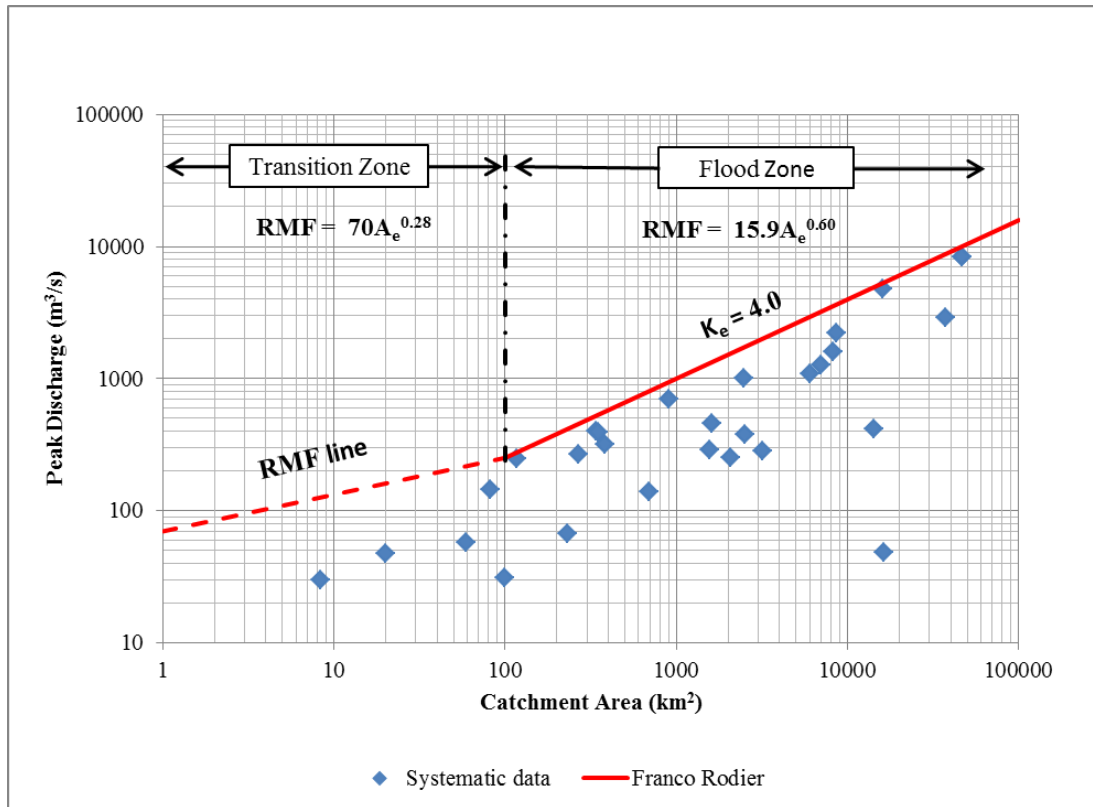


Figure J3. The highest recorded flood peaks and RMF in Region 4.0.

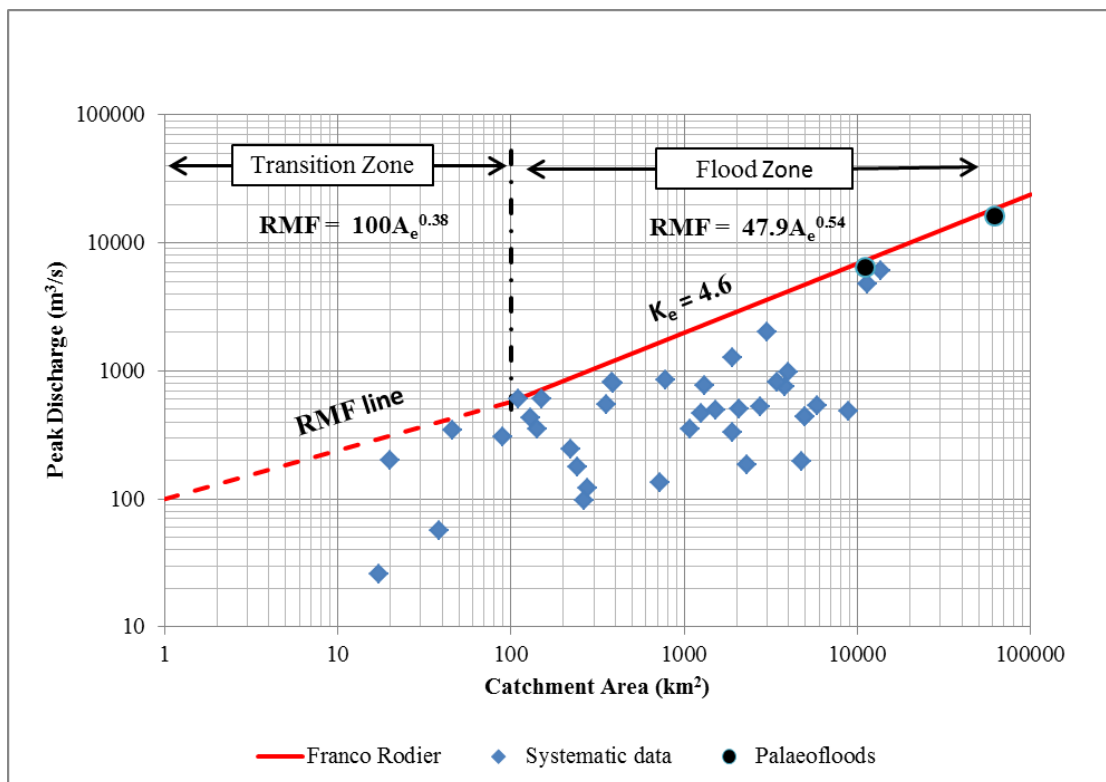


Figure J4. The highest recorded flood peaks and RMF in Region 4.6.

Appendix J: Highest Recorded Flood Peaks in Regions

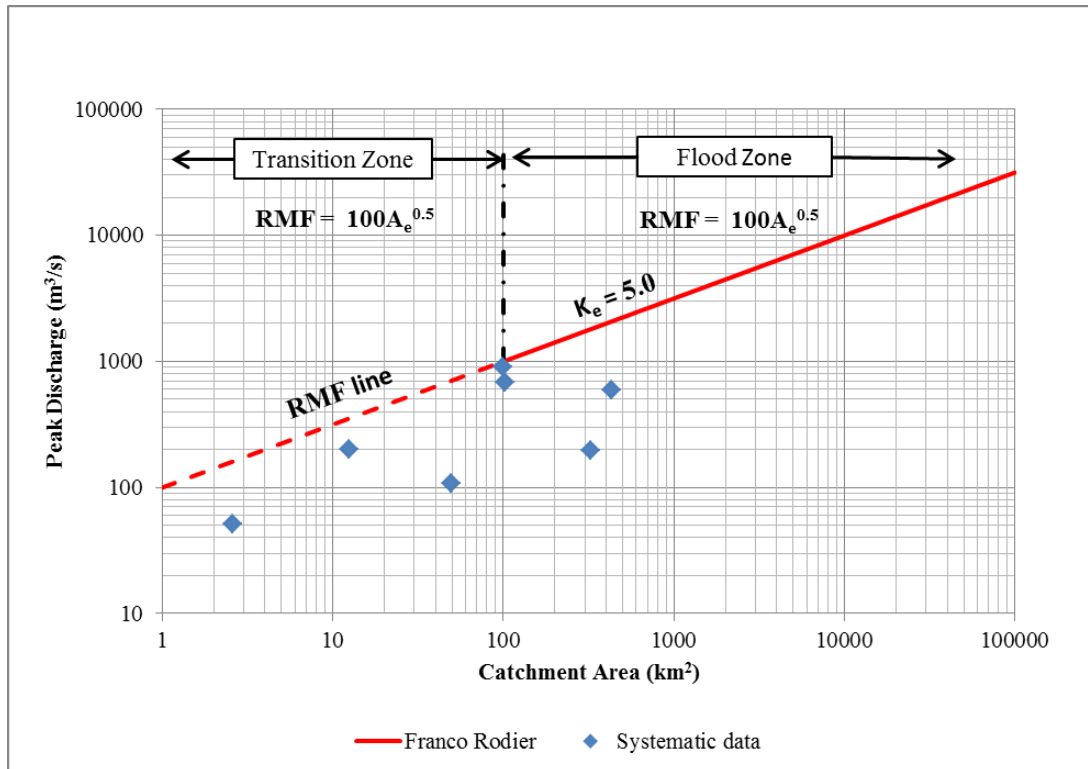


Figure J5. The highest recorded flood peaks and RMF in Region 5.0.

Appendix K: Regional Maximum Flood Peaks for Namibia

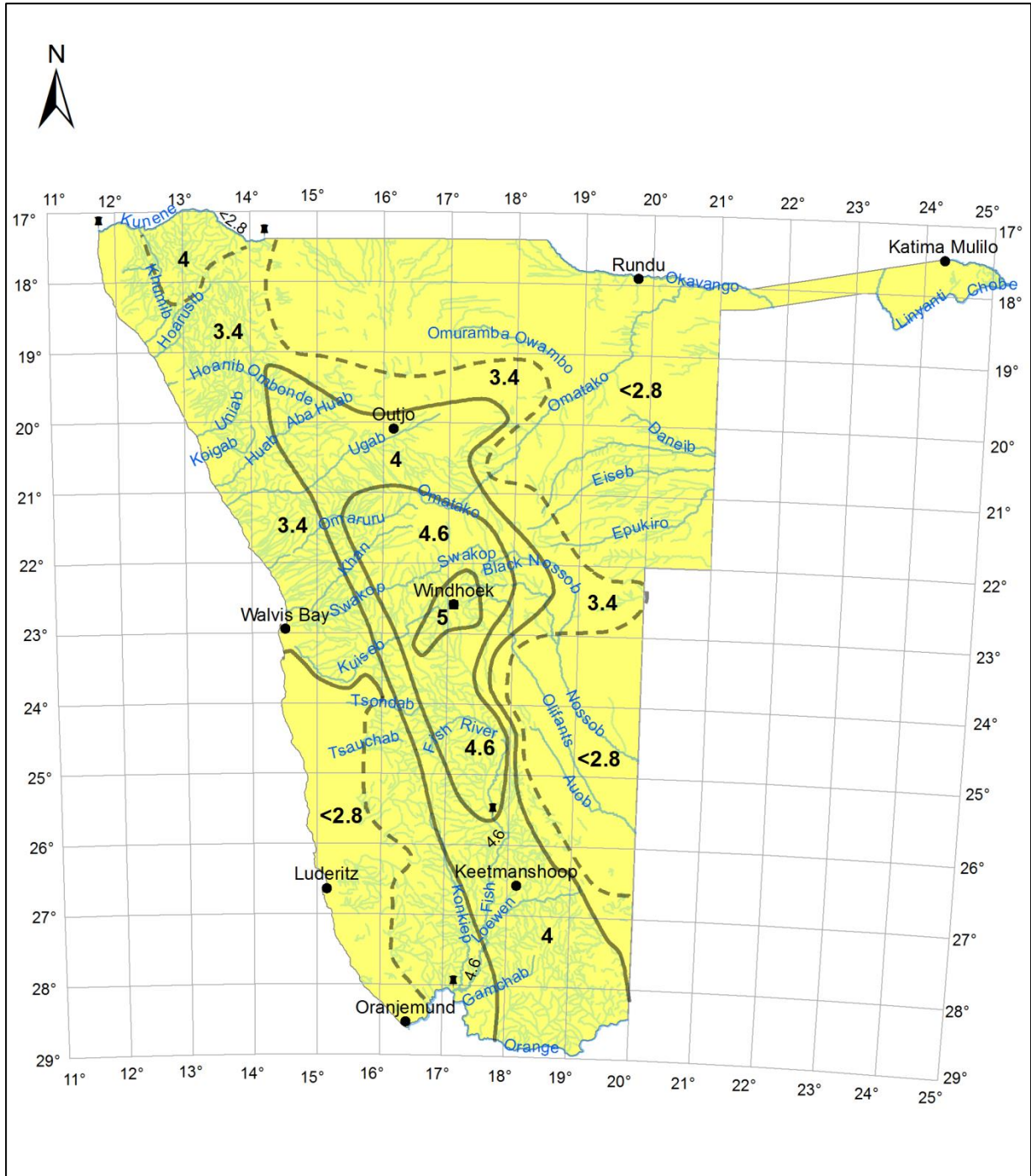


Figure K1. The new RMF flood zones based on new flood peak and palaeoflood data. The dotted line indicates that more information is needed to fix the position of the line

Appendix L: Photographs of the Avis Dam construction and flood damage. Windhoek, Namibia



Figure L1. A photograph of the construction of the Avis Dam during 1930 to 1931. The construction material is the coarse river rubble which was available in the area. Since no clayey material is available in the area, the dam was constructed as a Concrete Faced Rockfill Dam (CFRD).



Figure L2. Notice the 1934 erosion damage to the Avis Dam spillway. The spillway design capacity is $700 \text{ m}^3/\text{s}$, the 1934 flood was estimated at $680 \text{ m}^3/\text{s}$. The concrete structure is still there to this present day.

Appendix M: Constructing the Technology Curve for Hardap and Von Bach Dams

The Hardap Dam inverted technology curve

The PAR of the Hardap Dam-break was determined by Hattingh in 2007 at 3075 people, with an estimated LOL of 33 people. The Hardap Dam is the largest storage dam in Namibia with a full supply capacity of 295 million cubic metres.



Figure M1. The Hardap Dam during the 2006 flood release.

Step 1: Determine the 1:10 000 year flood (Q_{RMF}) from the new RMF model for Namibia:

Apply the Francou-Rodier Equation (4.1) to determine the peak discharge.

Regional K-value = 4.6 (from Figure 4.11)

Catchment area = 13 600 km²

$Q_{RMF} = 8\,174\text{ m}^3/\text{s}$

Appendix M: Constructing the Technology Curve for Hardap and Von Bach Dams

Step 2: Determine the spillway capacity at NOC level

Elevation of NOC = 1 141.9 mAMSL

Spillway capacity at NOC level (1 141.9 m) = 5 917 m³/s

the 10 000 flood > the spillway maximum discharge rate

Step 3: Determine the flood fraction (F_Q) of the spillway capacity flood

from equation (5.2), determine the flood fraction

$$F_Q = Q_{\text{spillway}}/RMF = 5917/8174 = 0.724$$

Step 4: Determine the annual recurrence interval for the spillway flood

from Equation (5.4), determine the flood fraction

$$I_R = e^{((F_Q - 0.145)/0.093)} = 505 \text{ years}$$

Step 5: Determine the AEP from the annual recurrence interval.

$$AEP = 1/I_R = 0.00198069$$

Step 6: Repeat steps 4 and 5 for several height increments above the NOC after determining the increase in spillway discharge capacity for each incremental new NOC level as displayed in **Table M1**.

Appendix M: Constructing the Technology Curve for Hardap and Von Bach Dams

Table M1. Hardap Dam AEP for various height increments above the NOC

mAMSL	Discharge	F_Q	I_R	AEP
(m)	(m ³ /s)		(years)	
1141.9	5917	0.72	505	0.001980
1142.0	6034	0.74	589	0.001697
1142.5	6617	0.81	1 269	0.000788
1143.0	7237	0.89	2 864	0.000349
1143.5	7882	0.96	6 695	0.000149
1144.0	8574	1.05	16 637	0.000060

Step 7: Determine the volume and cost of additional embankment material required for each of the height increments above. Construction cost is based on the cost per cubic meter as discussed in section 3.4.2 (N\$ 1,057.70/m³ earthfil material). **Table M2** indicates the cumulative cost for each increment raised.

Table M2: The Hardap Dam cumulative cost table for each increment height with which the NOC is raised.

mAMSL	Spillway discharge	Incremental Height increase	Cumulative Volume of material	Cumulative Cost of earthworks
(m)	(m ³ /s)	(m)	(m ³)	(Million N\$)
1141.9	5917	0	0	0
1142.0	6034	0.1	2 917	6.49
1142.5	6617	0.5	39 724	42.02
1143.0	7237	0.5	80 052	84.67
1143.5	7882	0.5	120 985	127.97
1144.0	8574	0.5	162 521	171.91

Appendix M: Constructing the Technology Curve for Hardap and Von Bach Dams

Step 8: Find the population at risk by determining the inundated areas by performing a floodline analysis. First determine the floodline and PAR resulting from the Safety Evaluation flood (SEF) as if the dam were indestructible (hence the water may flow over the NOC).

$$\text{PAR due to SEF only} = 2500 \text{ people (PAR}_{\text{SEF}})$$

Then determine the floodline and the PAR resulting from a dam-break, caused during the SEF event: the worst-case scenario flood whereby the dam wall breaks during the SEF.

$$\text{Total PAR due to dam-break} = 3075 \text{ people (T-PAR}_{\text{dmbrk}})$$

Then determine the incremental PAR due to the dam-break event over and above the PAR due to the SEF flood event, as in Equation (5.8) (Serrano-Lombillo, 2011).

$$\text{PAR due to dam break only} = 575 \text{ people (PAR}_{\text{dmbrk}})$$

Step 9: Estimate the likely Loss Of Life (LOL) using either Equation (5.6) or (5.7)

(Dekay & Mclelland, 1993; Hartford & Baecher, 2004) for Hardap Dam, the populated area is approximately 15 km downstream and lies on an open plain; low lethality (use $\text{PAR}_{\text{dmbrk}}$ as in Step 8).

$$\text{Flood warning time WT} = 0.25 \text{ hours}$$

$$\text{Lethality} = \text{Low}$$

$$\text{LOL} = 33 \text{ persons}$$

Step 10: From the above, determine the risk associated with the dam failure when the water level exceeds the NOC Risk is calculated as in Equation (5.9). Refer to **Table M3**.

Assumption: the LOL associated with failure for each incremental increase in the dam's NOC level remains the same. Alternatively a dam-break analysis can be performed for each increment raised.

Appendix M: Constructing the Technology Curve for Hardap and Von Bach Dams

Table M3: Hardap Dam risk associated with the probability of failure for each increment with which the dam is raised.

mAMSL	Cumulative Cost of earthworks	AEP	Loss of Life (LOL)	Risk
(m)	(Million N\$)			
1141.9	0	0.001980	33	0.065338
1142.0	6.49	0.001697	33	0.056009
1142.5	42.02	0.000788	33	0.026012
1143.0	84.67	0.000349	33	0.011521
1143.5	127.97	0.000149	33	0.004929
1144.0	171.91	0.000060	33	0.001984

Step 11: Plot the Technology curve as in Figure 5.6. The risk to life appears on the vertical axis and the investment (cost of earthworks) to reduce the Risk appears on the horizontal axis. Refer to **Figure M2**.

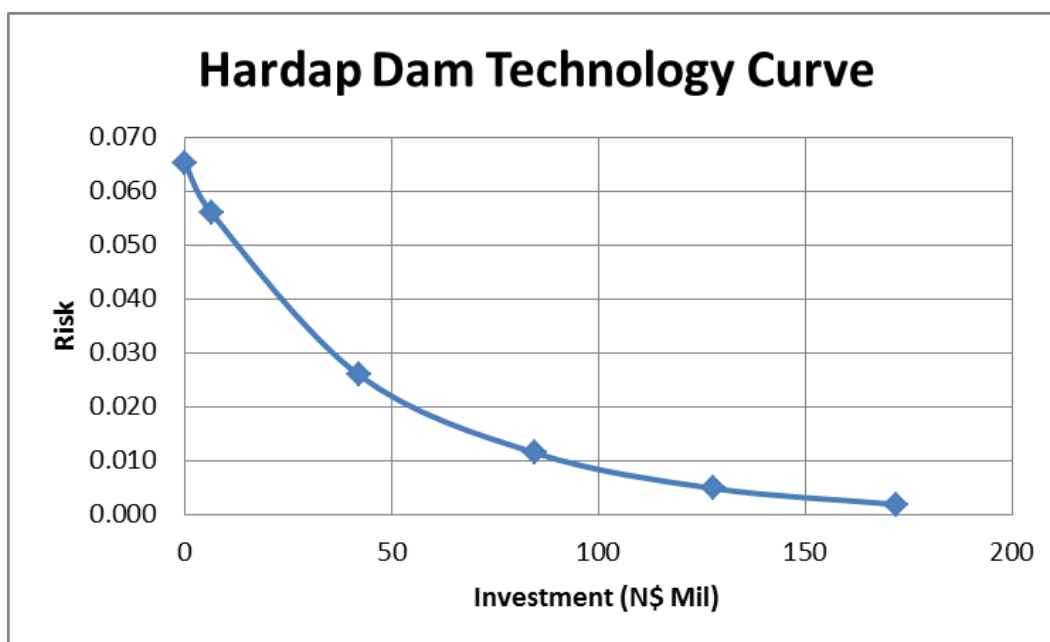


Figure M2: The technology curve for the Hardap Dam.

Appendix M: Constructing the Technology Curve for Hardap and Von Bach Dams

Step 12: Plot the Invert Technology Curve (ITC) as in **Figure 5.7**. ‘Marginal Lives Saved’ replaces ‘Risk’ on the vertical axis, the investment remains the same. Refer to **Table M4**. The values for ‘Marginal Lives Saved’ is determined from the risk by applying Equation (5.10).

The results are displayed in **Figure M3**.

Table M4: Marginal Lives Saved which is the inverse of Risk

mAMSL	Cumulative Cost of earthworks	AEP	Loss of Life (LOL)	Risk	Marginal lives saved
(m)	(N\$)				
1141.9	0	0.001980	33	0.065338	0
1142.0	6.49	0.001697	33	0.056009	0.00933
1142.5	42.02	0.000788	33	0.026012	0.03933
1143.0	84.67	0.000349	33	0.011521	0.05382
1143.5	127.97	0.000149	33	0.004929	0.06041
1144.0	171.91	0.000060	33	0.001984	0.06335

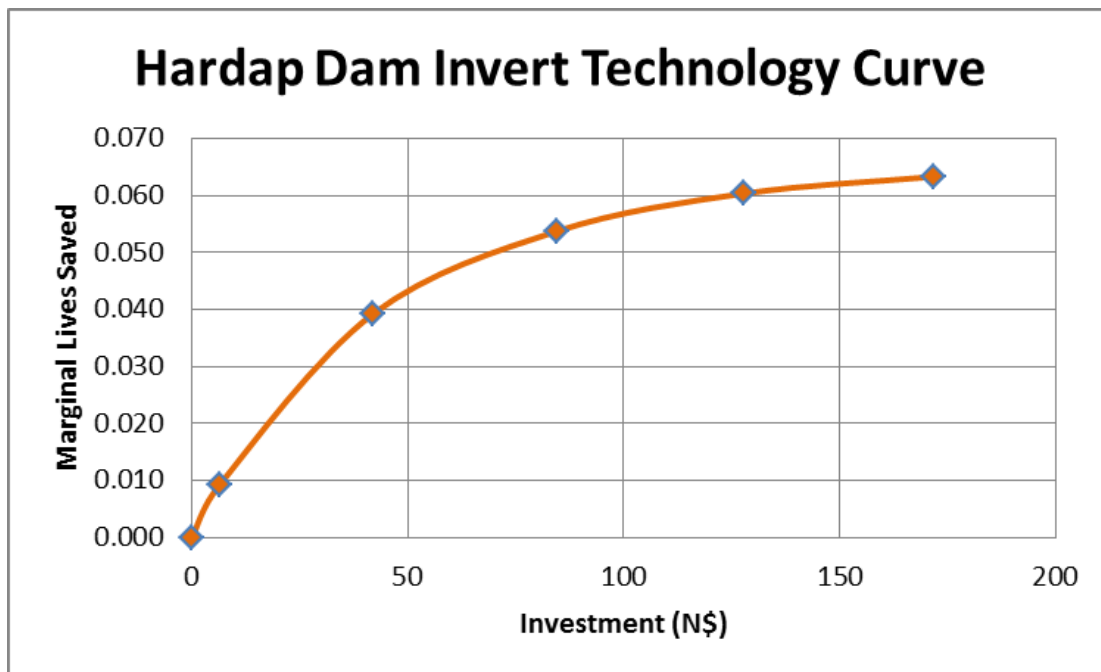


Figure M3: The inverted Technology Curve for the Hardap Dam.

Appendix M: Constructing the Technology Curve for Hardap and Von Bach Dams

Step 13: Determine a polynomial function to represent the Hardap Dam ITC.

From CurveExpert software version 1.3

4th Degree Polynomial Fit: $y = a + bx + cx^2 + dx^3 + ex^4$

Where y = marginal lives saved

x = Investment

The coefficient data are:

$a = 0.00012562$

$b = 0.00146317$

$c = -1.58E-05$

$d = 8.70E-08$

$e = -1.86E-10$

Appendix M: Constructing the Technology Curve for Hardap and Von Bach Dams

The Von Bach Dam inverted technology curve

The Von Bach Dam is located in the Swakop River, near the town Okahandja in Central Namibia. It was constructed as the main supply dam to provide water to the City of Windhoek.



Figure M4: Von Bach Dam asphalt seal layer.

A detailed dam break analysis on the Von Bach Dam was not performed. For the purpose of this exercise, it was estimated that 500 people are at risk due to a dam-break event, with a subsequent LOL of 25 people.

Below follows a breakdown of the process to determine the ITC for the Von Bach Dam. There are 13 steps in the process, with the last step indicating the polynomial equation required to plot the curve.

Appendix M: Constructing the Technology Curve for Hardap and Von Bach Dams

Step 1: Determine the 1:10 000 year flood (Q_{RMF}) from the new RMF model for Namibia:

Apply the Francou-Rodier Equation (4.1) to determine the peak discharge.

Regional K-value = 4.6 (from Figure 4.11)

Catchment area = 2 920 km²

$$Q_{\text{RMF}} = 3\,562 \text{ m}^3/\text{s}$$

Step 2: Determine the spillway capacity at NOC level

Elevation of NOC = 1 353.0 mAMSL

Spillway capacity at NOC level = 3 325 m³/s

the 10 000 flood > the spillway maximum discharge rate

Step 3: Determine the flood fraction (F_Q) of the spillway capacity flood

from Equation (5.2).

$$F_Q = Q_{\text{spillway}}/\text{RMF} = 3\,325/3\,562 = 0.933$$

Step 4: Determine the annual recurrence interval for the spillway flood

from Equation (5.4).

$$I_R = e^{((F_Q - 0.145)/0.093)} = 4\,808 \text{ years}$$

Step 5: Determine the AEP from the annual recurrence interval.

$$\text{AEP} = 1/I_R = 0.00020797$$

Step 6: Repeat steps 4 and 5 for several height increments above the NOC after determining the increase in spillway discharge capacity for each incremental new NOC level as displayed in **Table M5**.

Appendix M: Constructing the Technology Curve for Hardap and Von Bach Dams

Table M5: Von Bach Dam AEP for various height increments above the NOC

mAMSL	Discharge	F_Q	I_R	AEP
(m)	(m^3/s)		(years)	
1 353.0	3 325	0.93	4 808	0.000208
1 353.4	3 566	1.00	10 000	0.000100
1 353.5	3 630	1.02	12 093	0.000083
1 354.0	3 976	1.12	34 320	0.000029
1 354.5	4 356	1.22	108 374	0.000009
1 355.0	4 769	1.34	376 521	0.000003

Step 7: Determine the volume and cost of additional embankment material required for each of the height increments above. Construction cost is based on the cost per cubic meter as discussed in section 3.4.2. (N\$ 1 057.70/ m^3 earthfil material). **Table M6** indicates the cumulative cost for each increment raised.

Table M6: The Von Bach Dam cumulative cost table for each increment height with which the NOC is raised.

mAMSL	Spillway discharge	Incremental Height increase	Cumulative Volume of material	Cumulative Cost of earthworks
(m)	(m^3/s)	(m)	(m^3)	(Million N\$)
1 353.0	3 325	0	0	0
1 353.4	3 566	0.4	7 203	7.62
1 353.5	3 630	0.1	9 003	9.52
1 354.0	3 976	0.5	18 007	19.05
1 354.5	4 356	0.5	27 010	28.57
1 355.0	4 769	0.5	36 013	38.09

Appendix M: Constructing the Technology Curve for Hardap and Von Bach Dams

Step 8: Find the population at risk by determining the inundated areas by performing a floodline analysis. First determine the floodline and PAR resulting from the Safety Evaluation flood (SEF) as if the dam were indestructible (hence the water may flow over the NOC).

$$\text{PAR due to SEF only} = 500 \text{ people (PAR}_{\text{SEF}})$$

Then determine the floodline and the PAR resulting from a dam-break, caused during the SEF event: the worst-case scenario flood whereby the dam wall breaks during the SEF.

$$\text{Total PAR due to dam-break} = 800 \text{ people (T-PAR}_{\text{dmbrk}})$$

Then determine the incremental PAR due to the dam-break event over and above the PAR due to the SEF flood event, as in Equation (5.8) (Serrano-Lombillo, 2011).

$$\text{PAR due to SEF only} = 300 \text{ people (PAR}_{\text{dmbrk}})$$

Step 9: Estimate the likely Loss Of Life (LOL) using either Equation (5.6) or (5.7)

(Dekay & Mclelland, 1993; Hartford & Baecher, 2004)

For Von Bach Dam, the populated area is approximately 4 km downstream and lies on an open plain; low lethality (use $\text{PAR}_{\text{dmbrk}}$ as in Step 8).

$$\text{Flood warning time WT} = 0.15 \text{ hours}$$

$$\text{Lethality} = \text{Low}$$

$$\text{LOL} = 25 \text{ persons}$$

Step 10: From the above, determine the risk associated with the dam failure when the water level exceeds the NOC. The Risk is calculated as in Equation (5.9). Refer to Table M7.

Assumption: the LOL associated with failure for each incremental increase in the dam's NOC level remains the same. Alternatively a dam-break analysis can be performed for each increment raised, however increase in LOL will likely be negligible.

Appendix M: Constructing the Technology Curve for Hardap and Von Bach Dams

Table M7: Von Bach Dam risk associated with the probability of failure for each increment with which the dam is raised.

mAMSLL	Cumulative Cost of earthworks	AEP	Loss of Life (LOL)	Risk
(m)	(Million N\$)			
1 353.0	0	0.000208	25	0.005200
1 353.4	7.62	0.000100	25	0.002500
1 353.5	9.52	0.000083	25	0.002067
1 354.0	19.05	0.000029	25	0.000728
1 354.5	28.57	0.000009	25	0.000231
1 355.0	38.09	0.000003	25	0.000066

Step 11: Plot the Technology curve as in **Figure 5.6**. The risk to life appears on the vertical axis and the investment (cost of earthworks) to reduce the Risk appears on the horizontal axis. Refer to **Figure M5**.

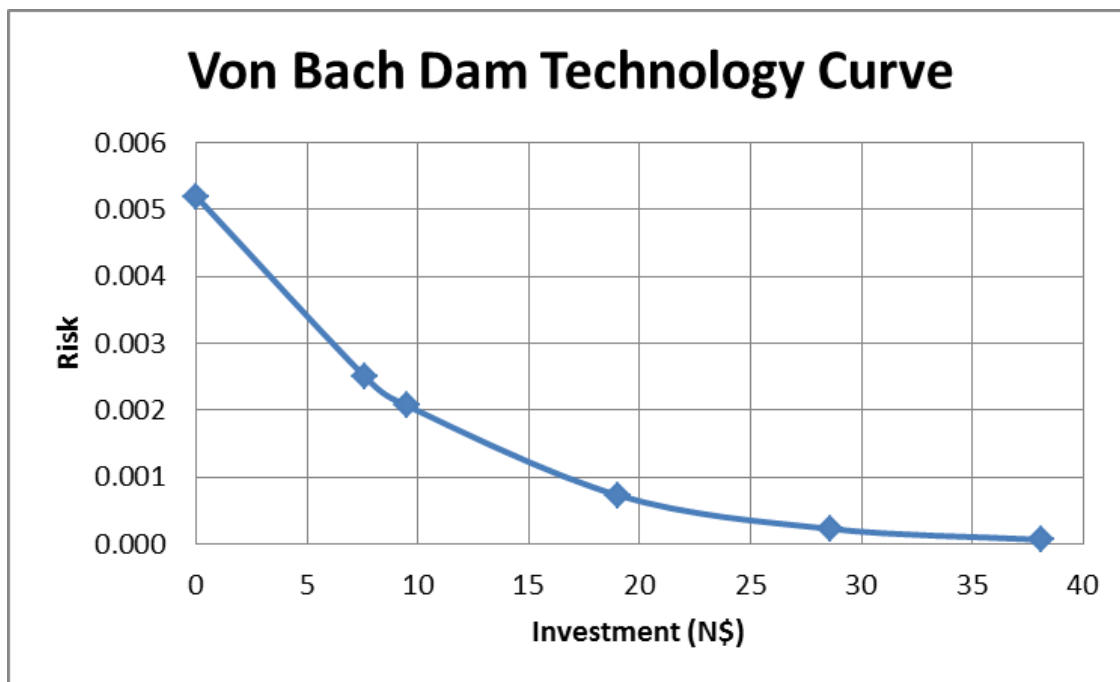


Figure M5. The technology curve for the Von Bach Dam.

Appendix M: Constructing the Technology Curve for Hardap and Von Bach Dams

Step 12: Plot the Invert Technology Curve (ITC) as in Figure 5.7 . ‘Marginal Lives Saved’ replaces ‘Risk’ on the vertical axis, the investment remains the same. Refer to **Table M8**. The values for ‘Marginal Lives Saved’ is determined from the risk by applying Equation (5.10).

The results are displayed in **Figure M6**

Table M8: Marginal Lives Saved which is the inverse of Risk.

mAMSL	Cumulative Cost of earthworks	AEP	Loss of Life (LOL)	Risk	Marginal lives saved
(m)	(N\$)				
1 353.000	0	0.000208	25	0.005200	0
1 353.400	7.62	0.000100	25	0.002500	0.00270
1 353.500	9.52	0.000083	25	0.002067	0.00313
1 354.000	19.05	0.000029	25	0.000728	0.00447
1 354.500	28.57	0.000009	25	0.000231	0.00497
1 355.000	38.09	0.000003	25	0.000066	0.00513

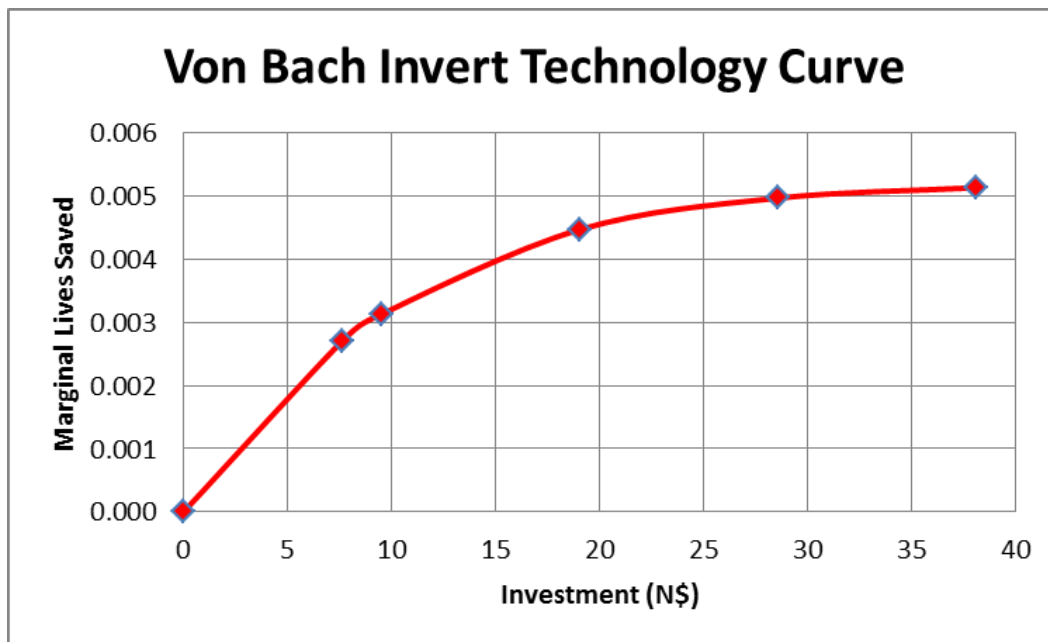


Figure M6 . The inverted Technology Curve for the Von Bach Dam.

Appendix M: Constructing the Technology Curve for Hardap and Von Bach Dams

Step 13: Determine a polynomial function for the Von Bach Dam to represent the ITC
From CurveExpert software version 1.3

$$\text{4th Degree Polynomial Fit: } y = a + bx + cx^2 + dx^3 + ex^4$$

Where y = marginal lives saved

x = Investment

The coefficient data are:

$$a = 1.80\text{E-}07$$

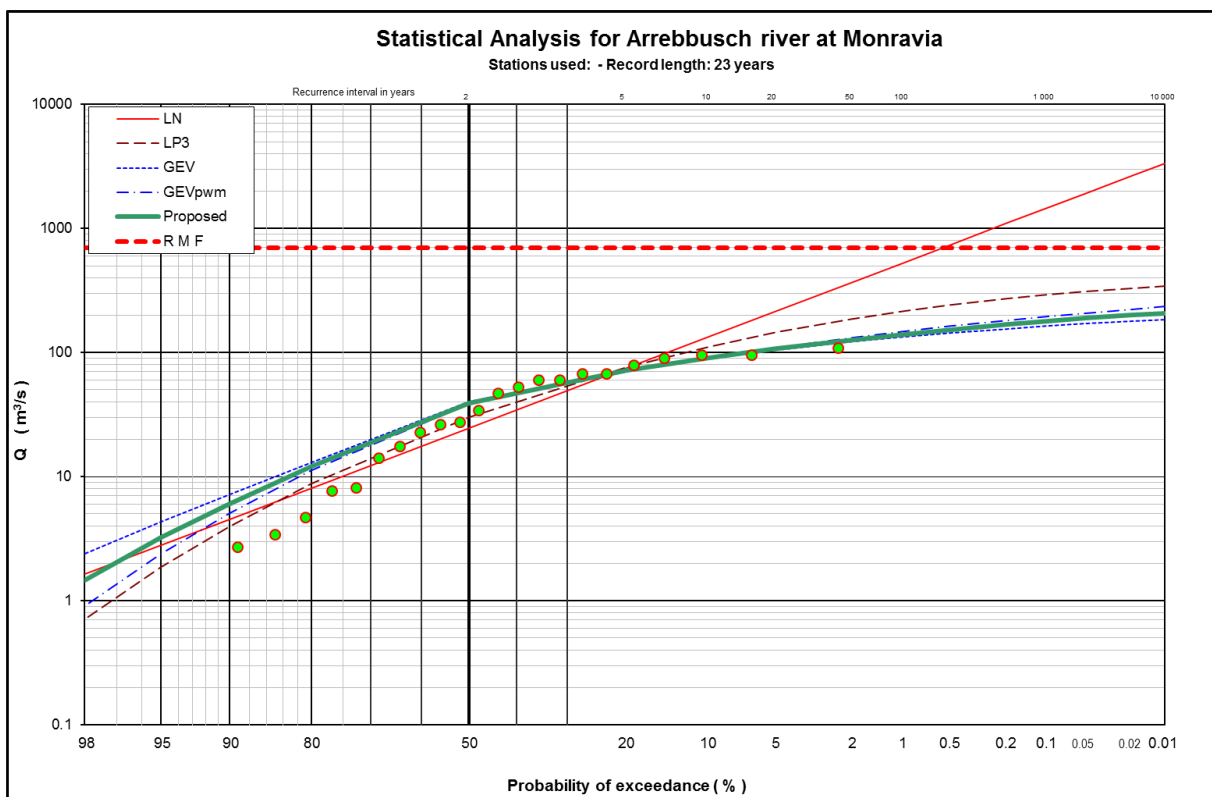
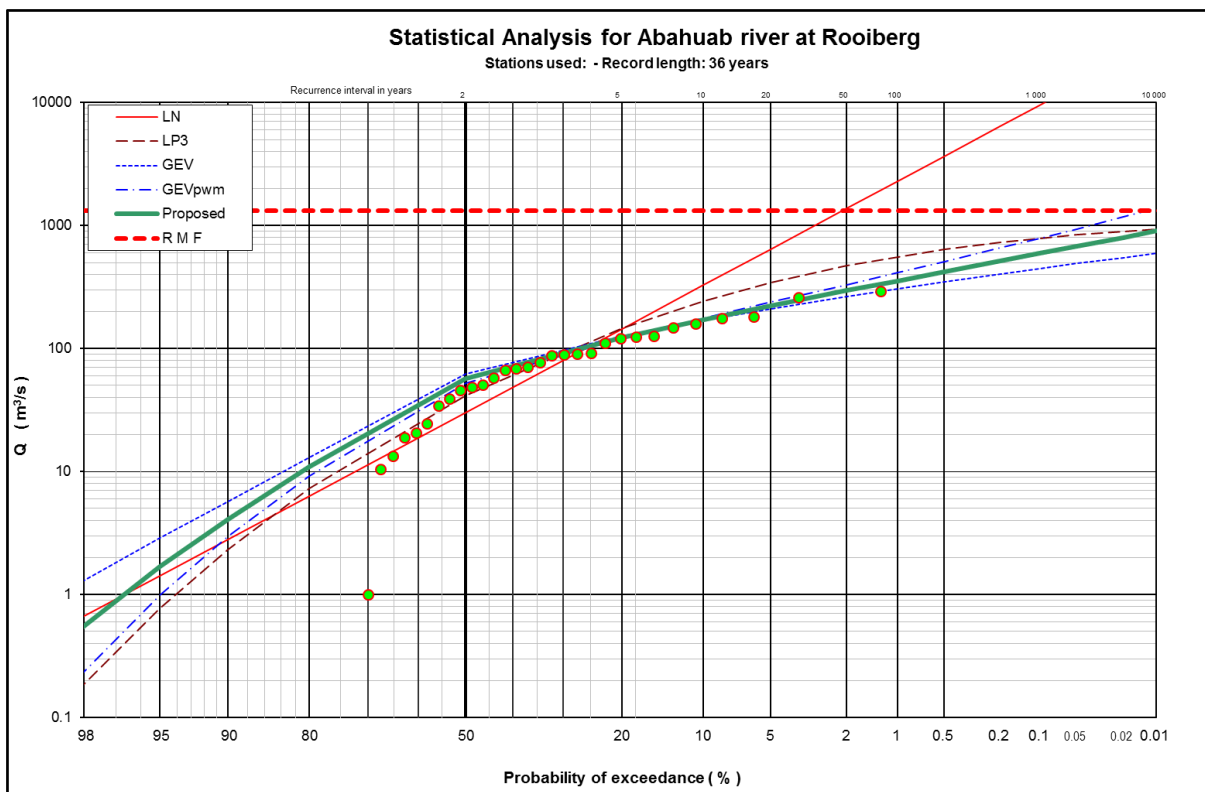
$$b = 0.000470991$$

$$c = -1.77\text{E-}05$$

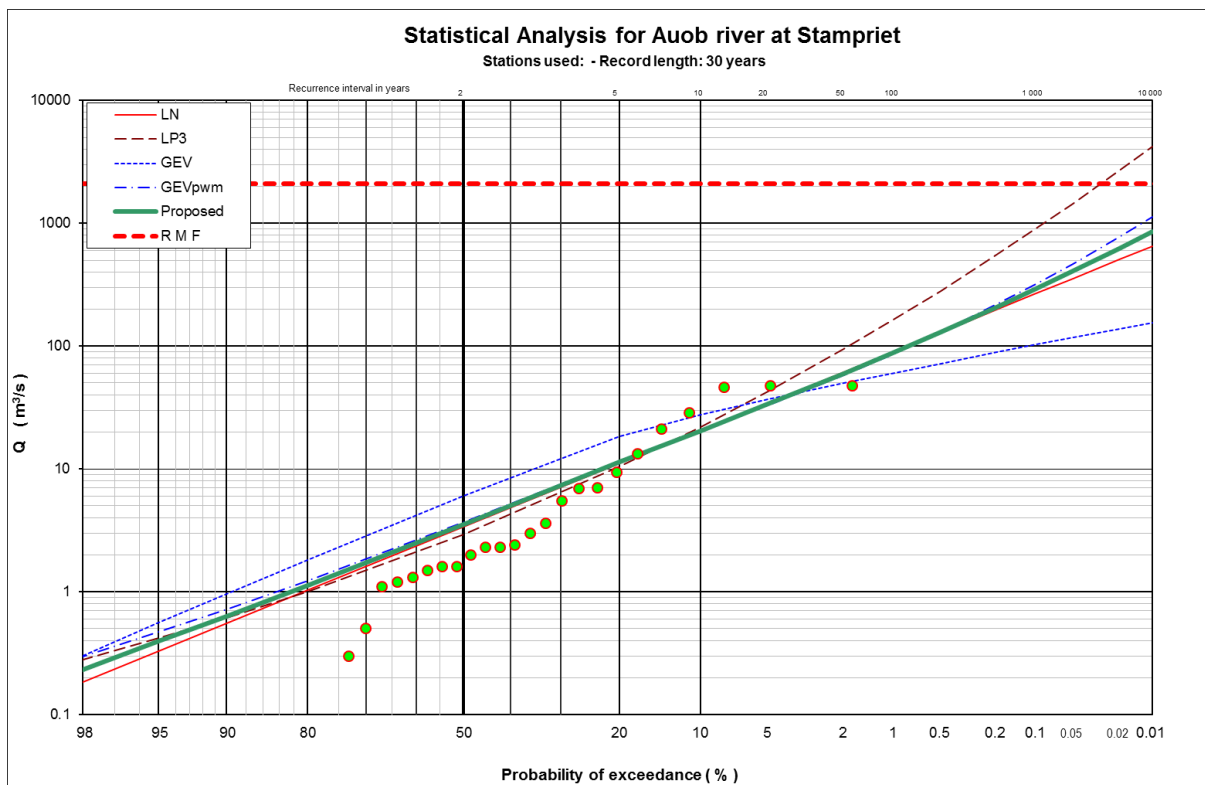
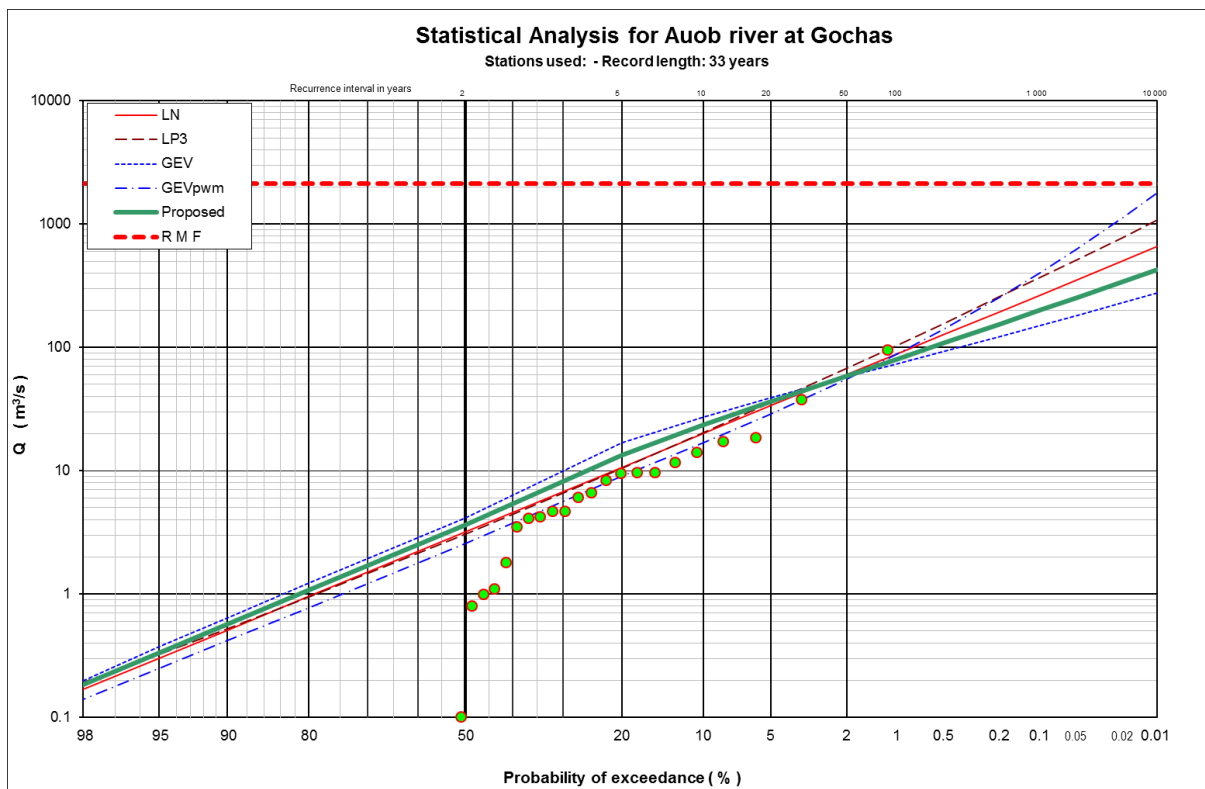
$$d = 3.26\text{E-}07$$

$$e = -2.42\text{E-}09$$

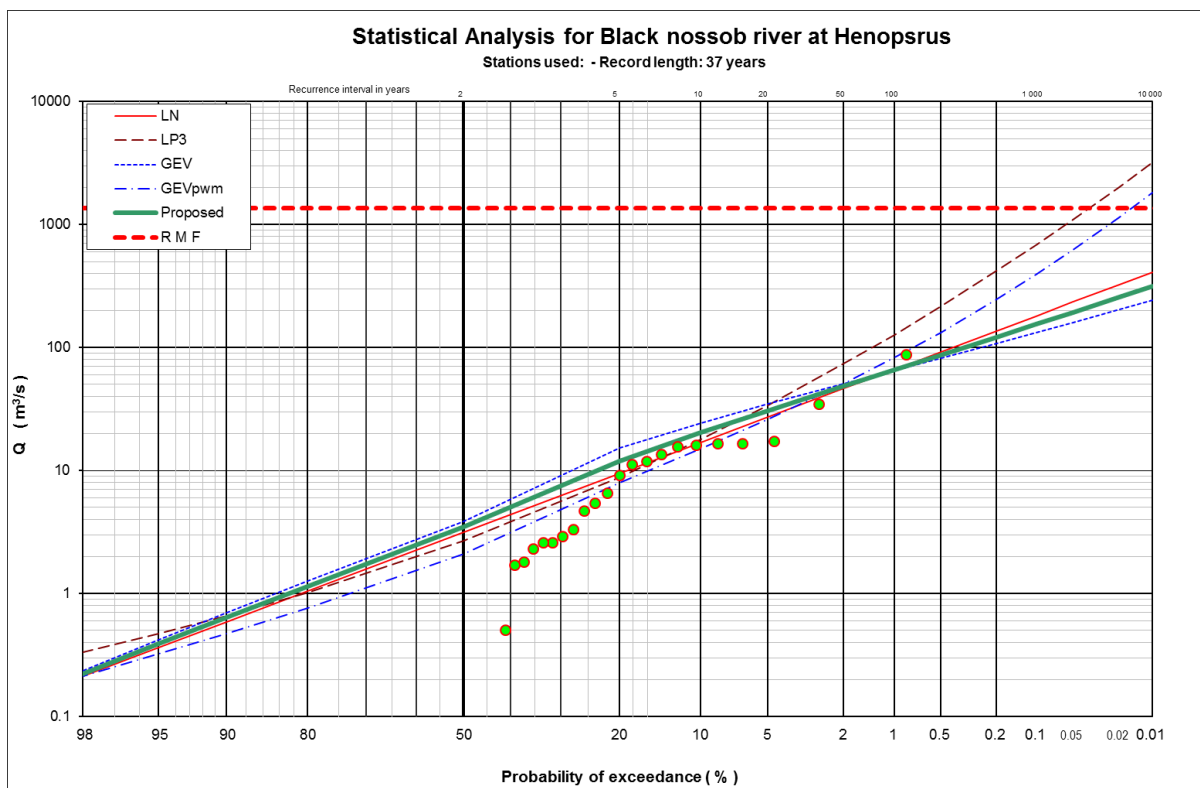
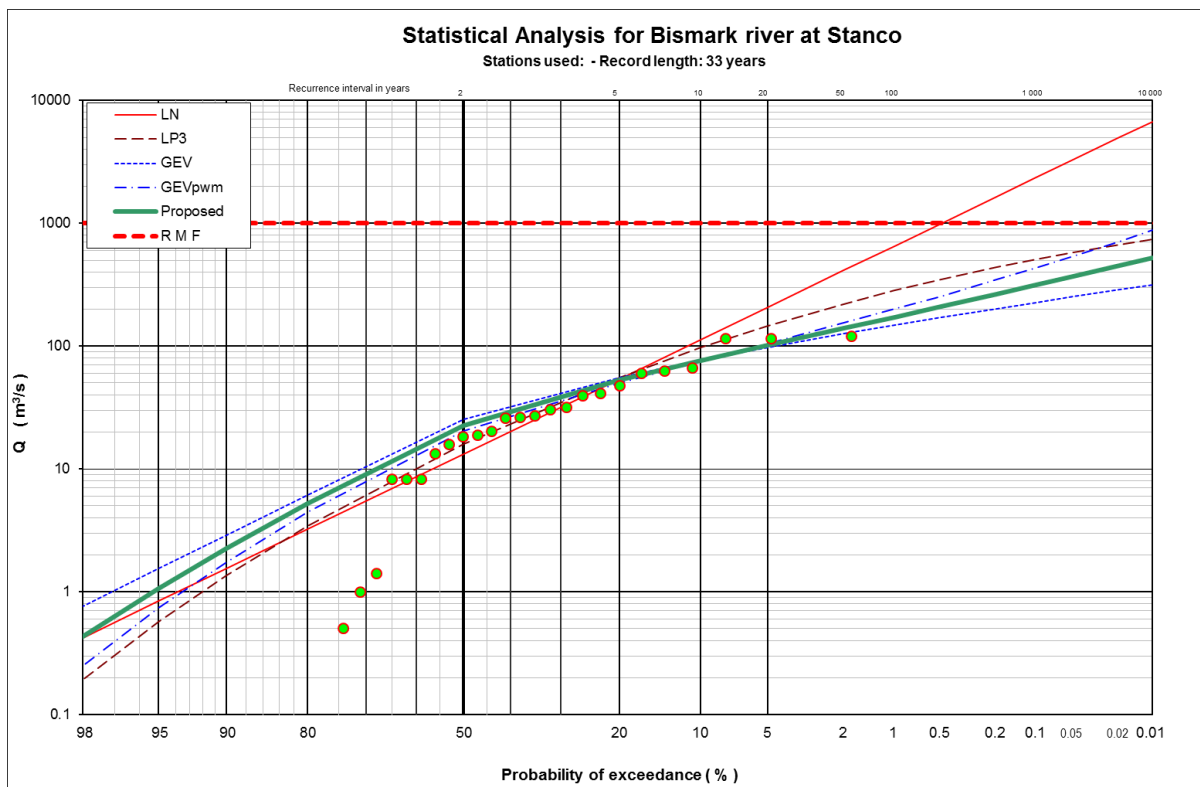
Appendix N: Flood peak distributions for the available flow gauging station data



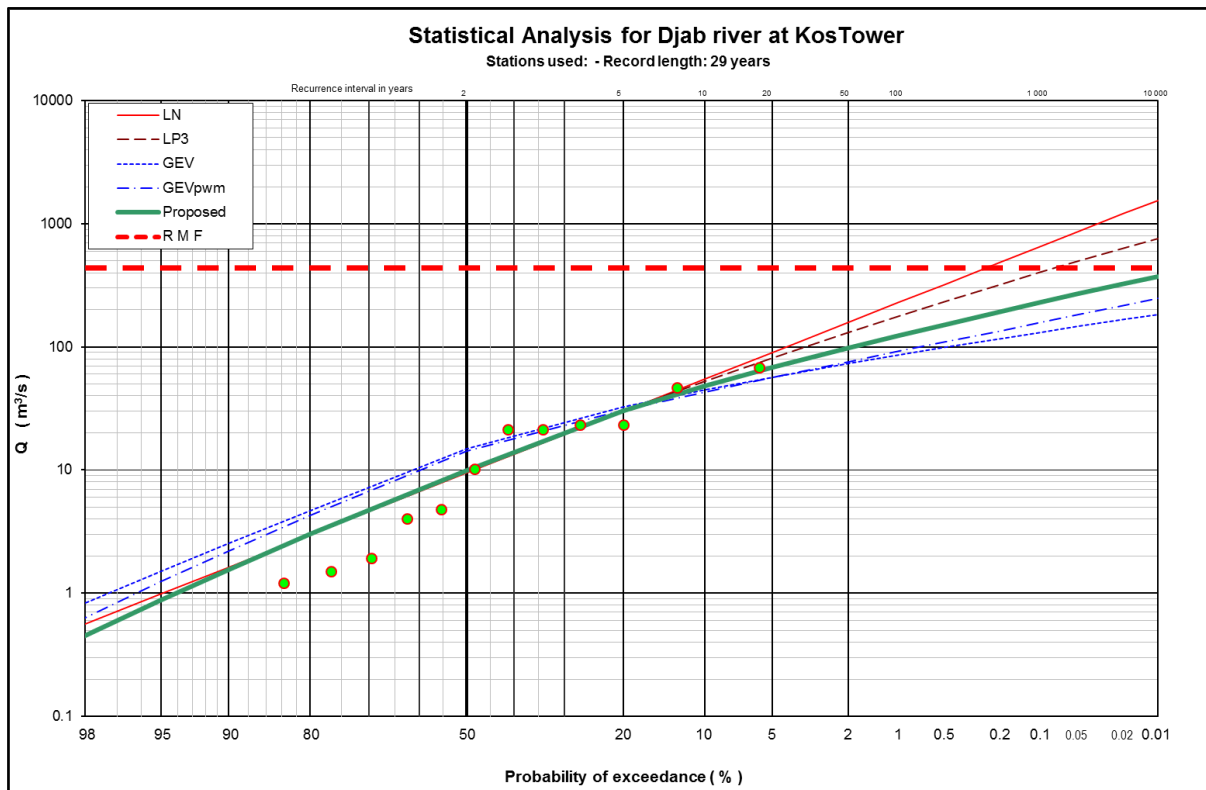
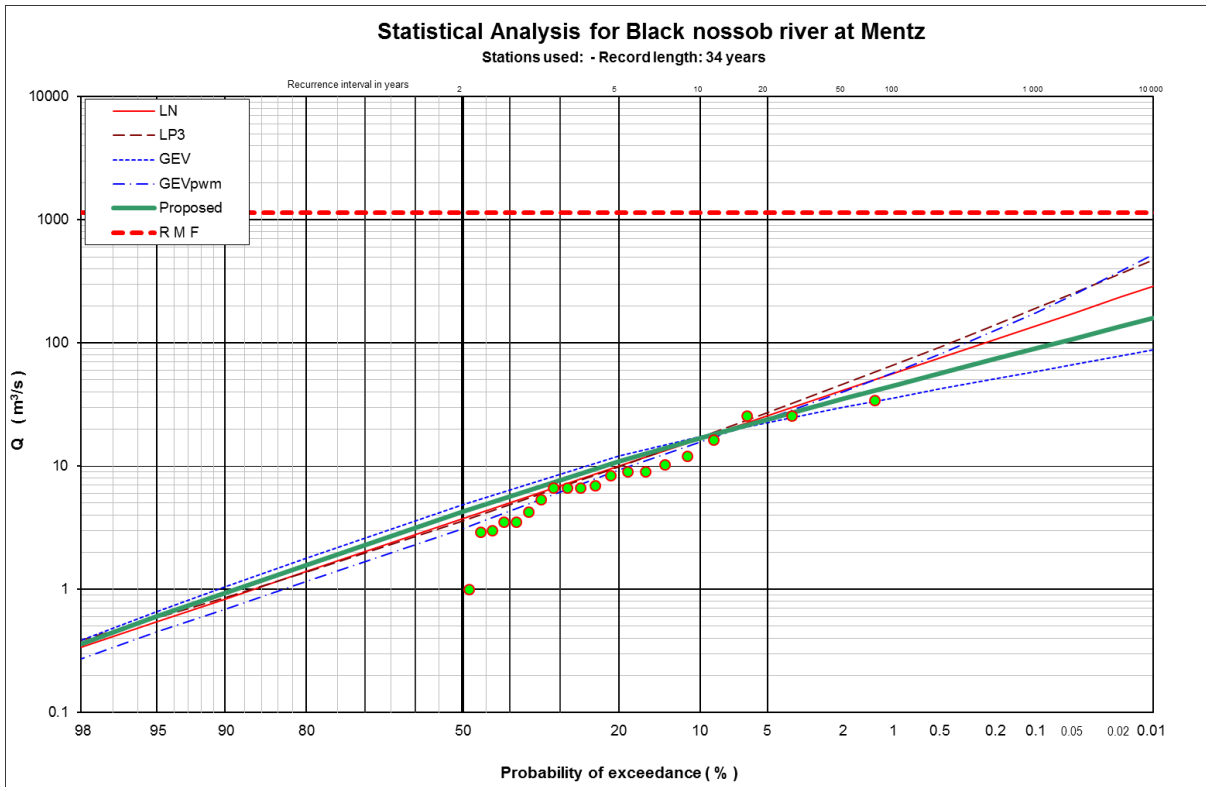
Appendix N: Flood peak distributions for the available flow gauging station data



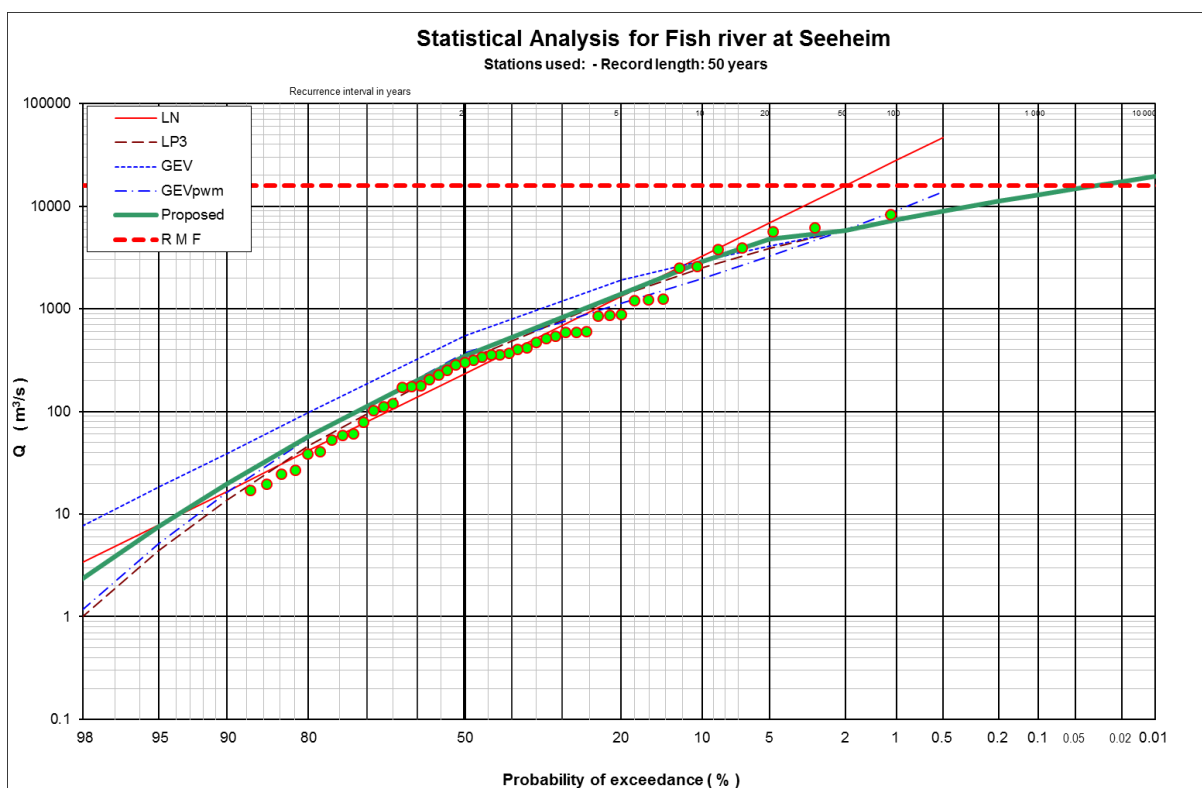
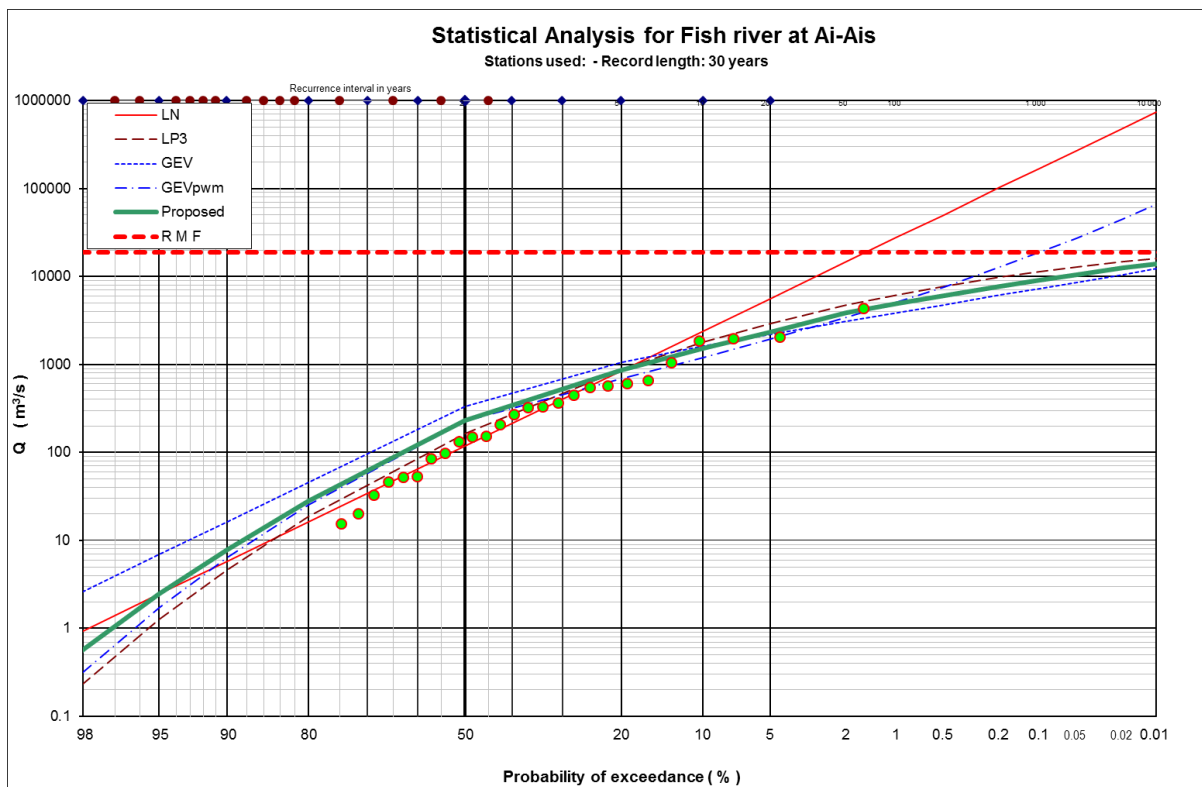
Appendix N: Flood peak distributions for the available flow gauging station data



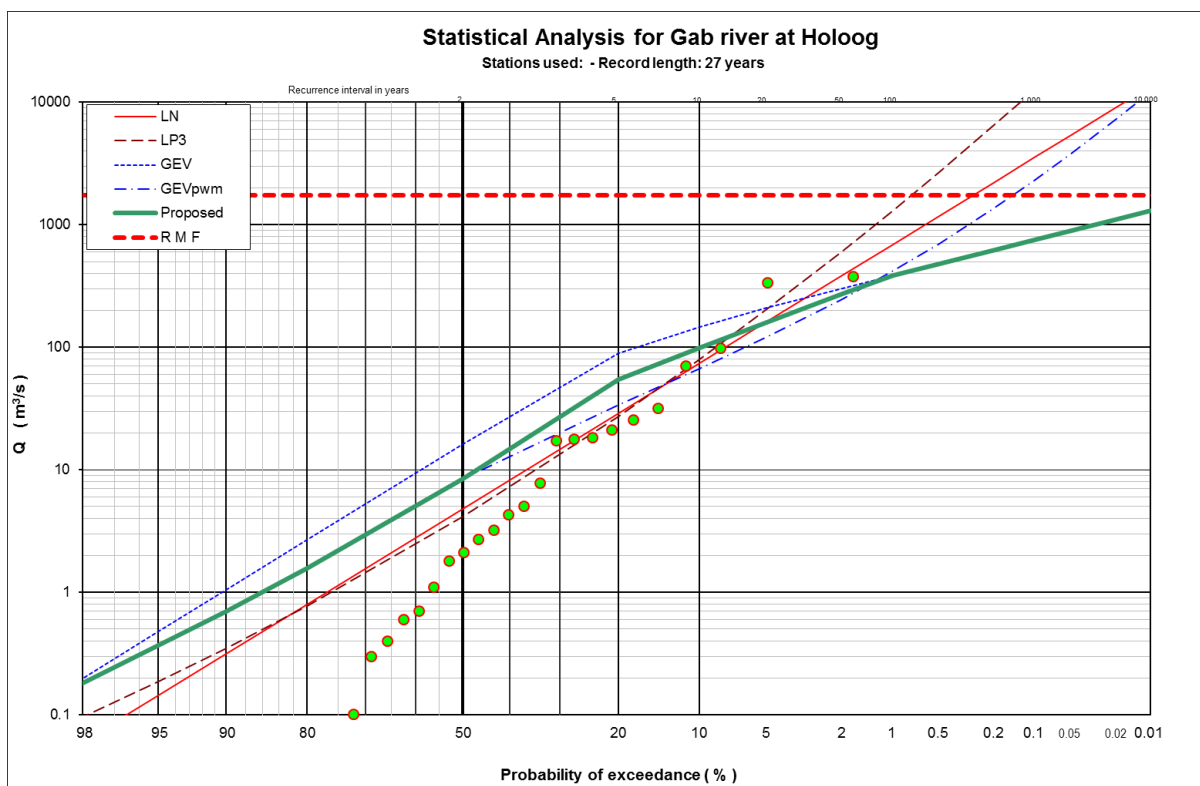
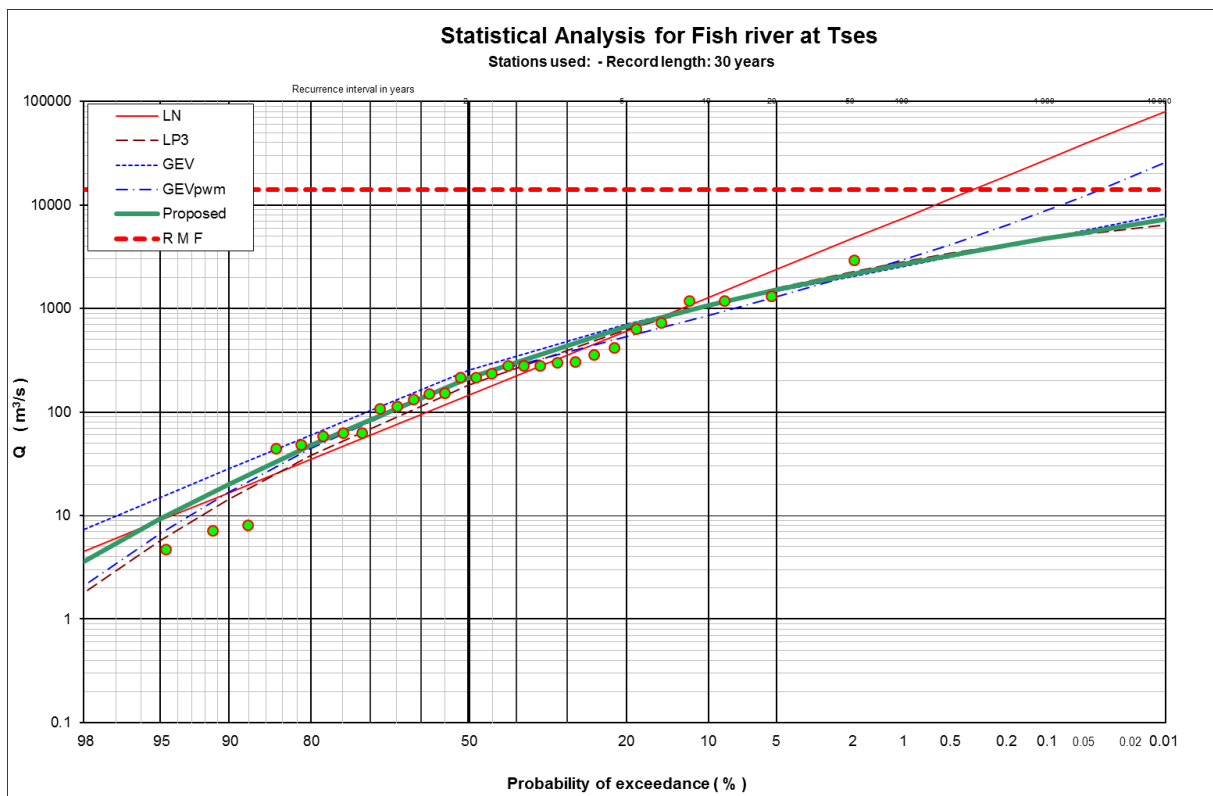
Appendix N: Flood peak distributions for the available flow gauging station data



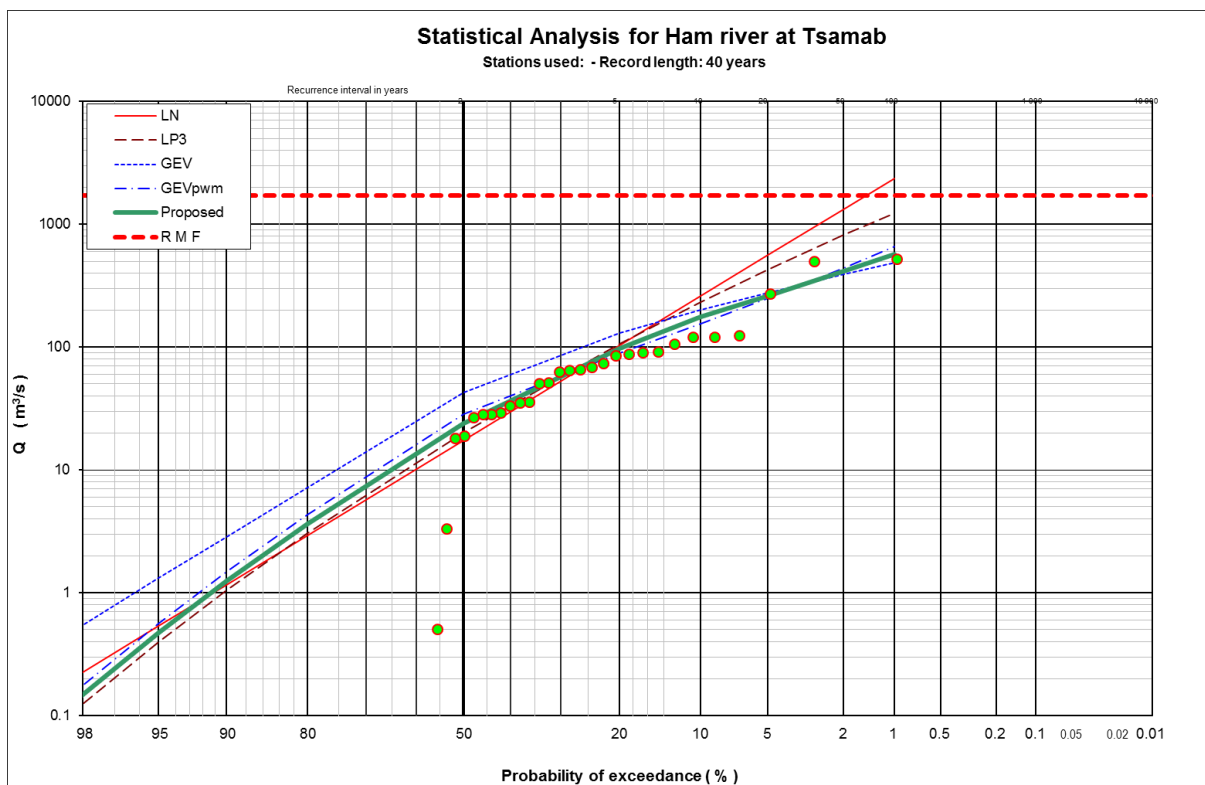
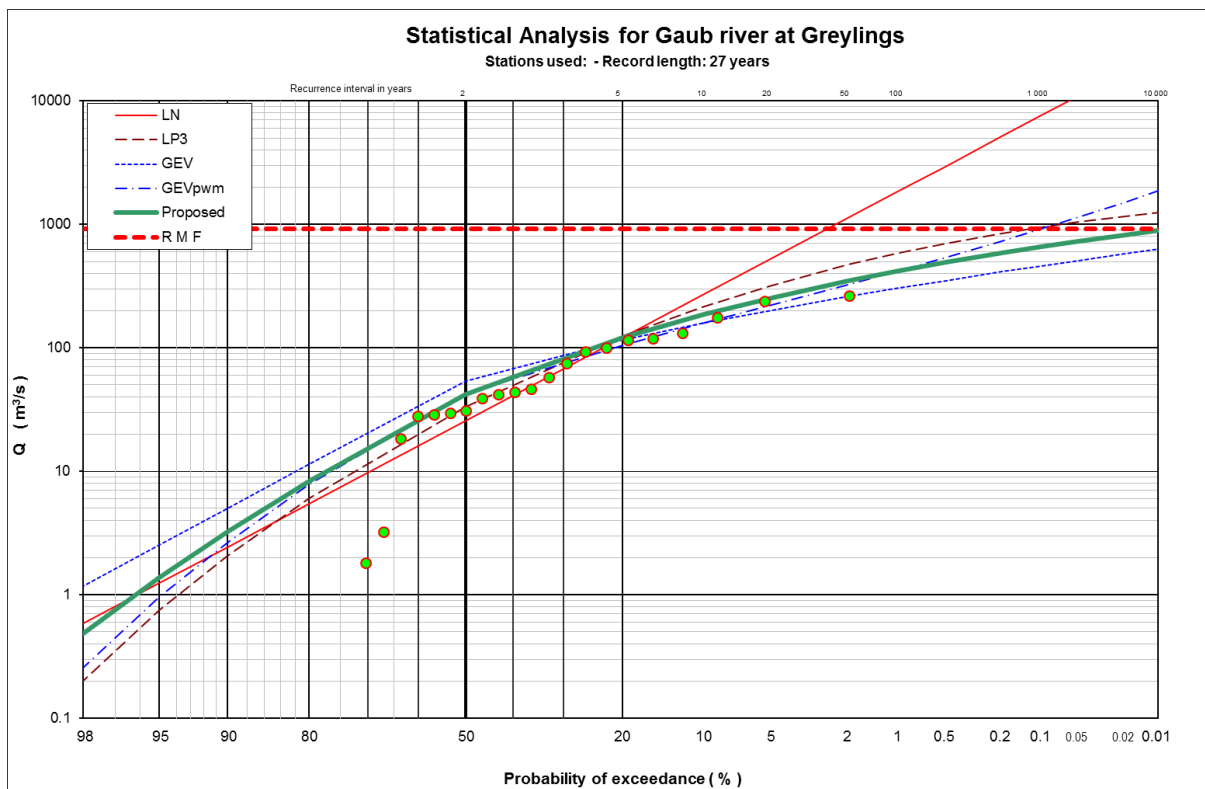
Appendix N: Flood peak distributions for the available flow gauging station data



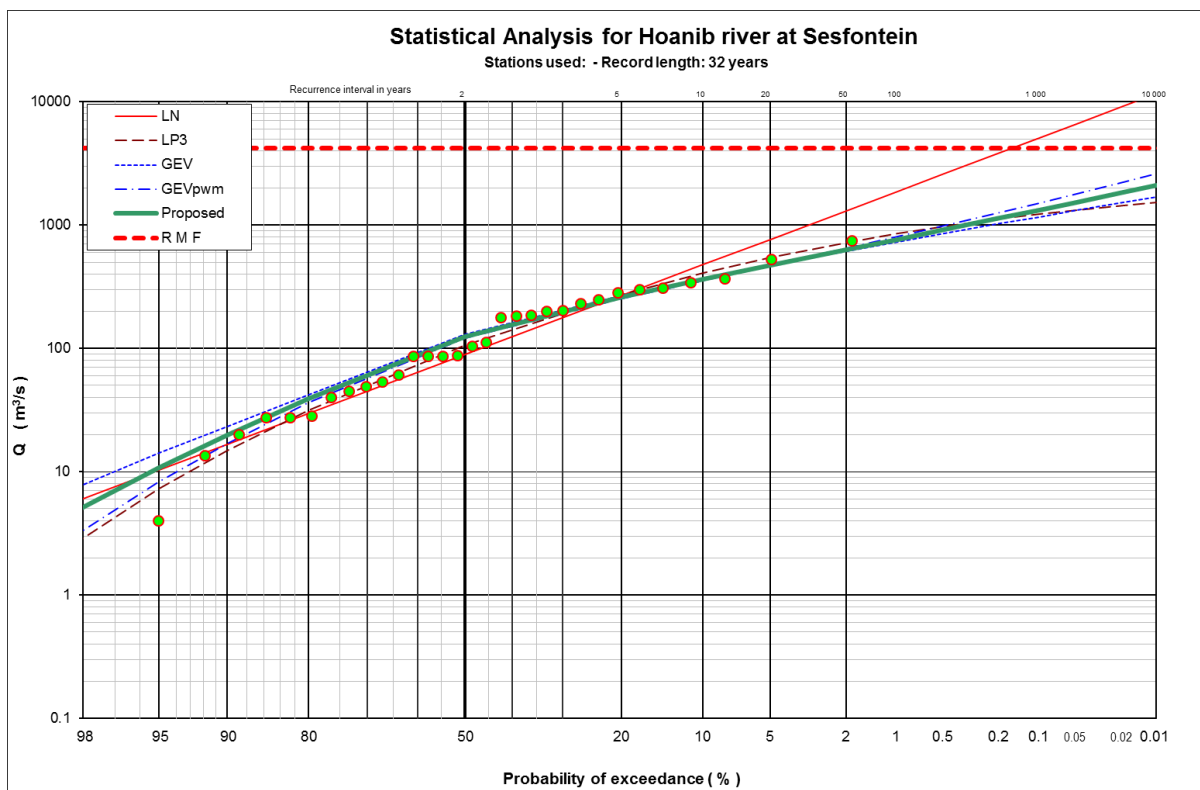
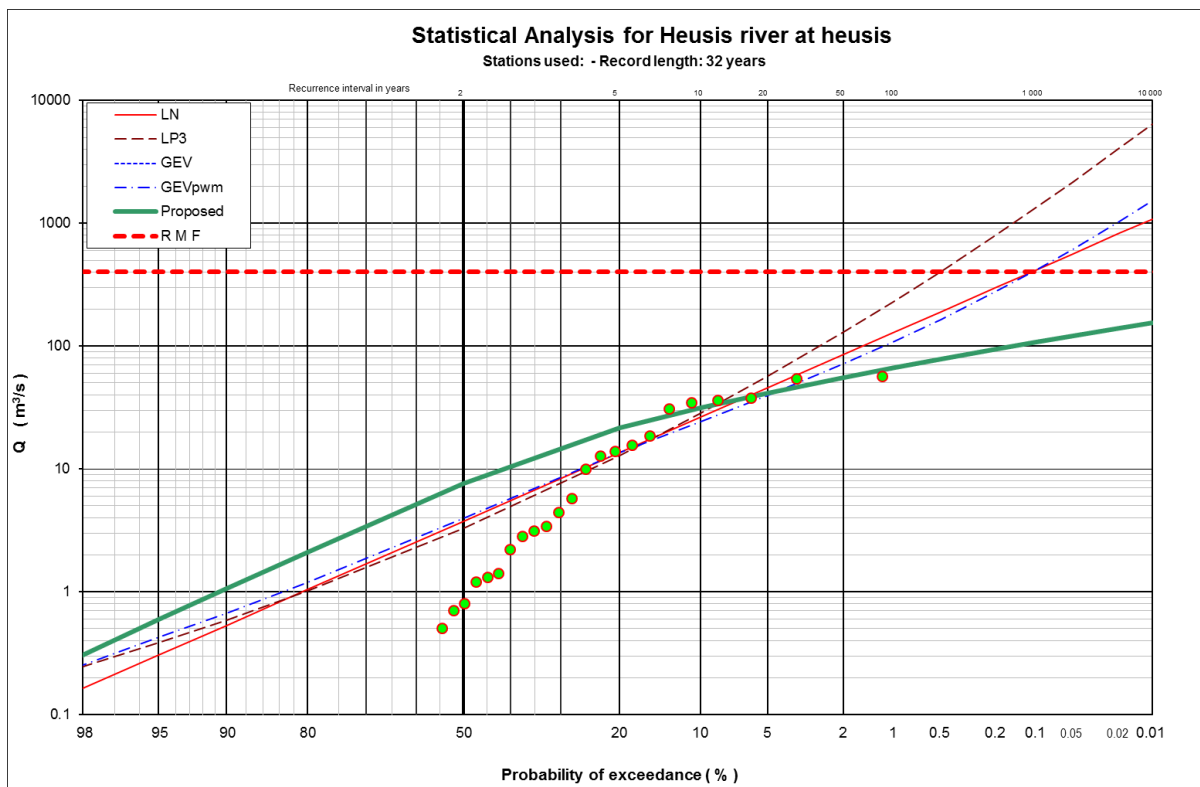
Appendix N: Flood peak distributions for the available flow gauging station data



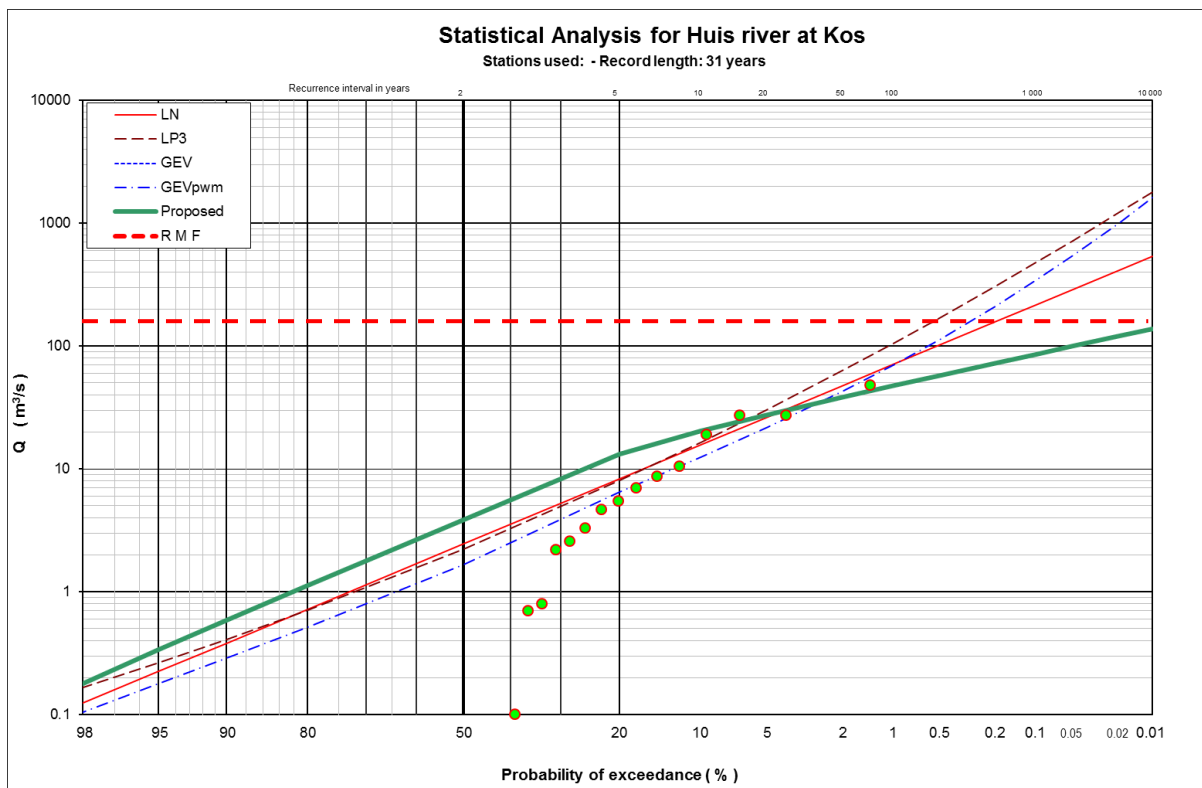
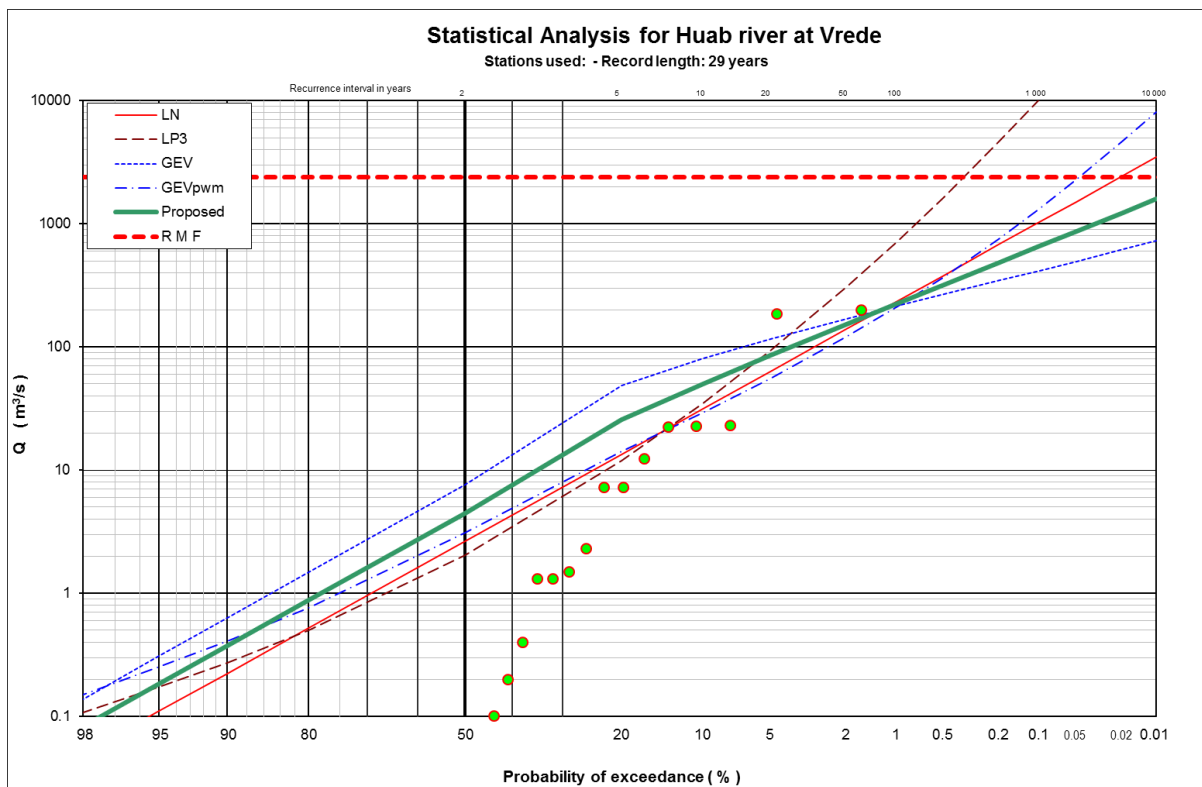
Appendix N: Flood peak distributions for the available flow gauging station data



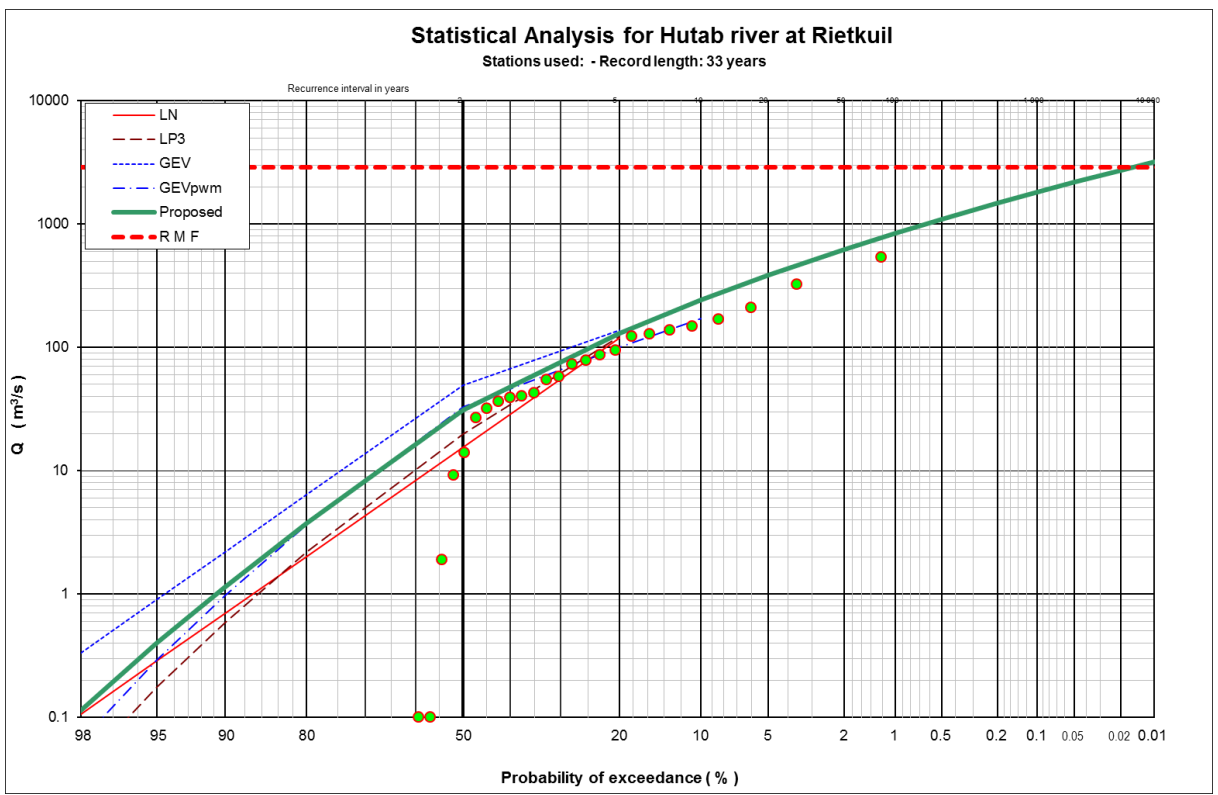
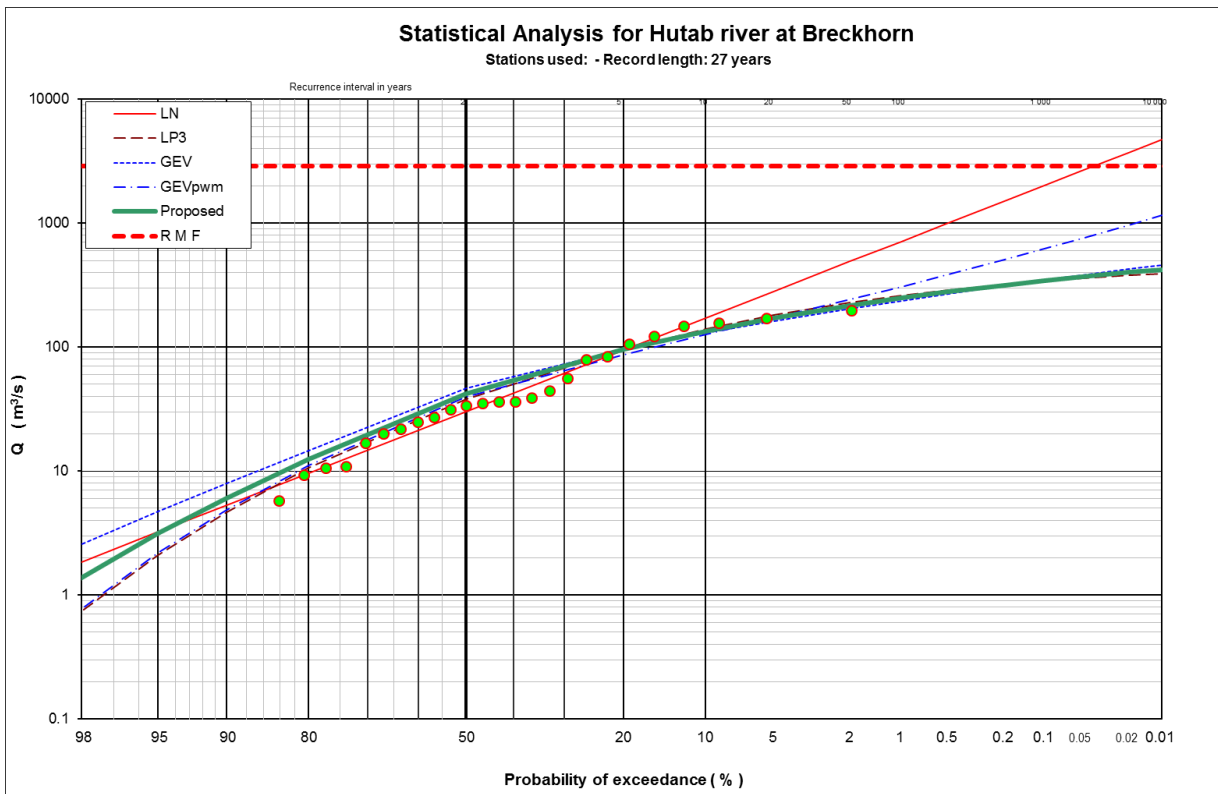
Appendix N: Flood peak distributions for the available flow gauging station data



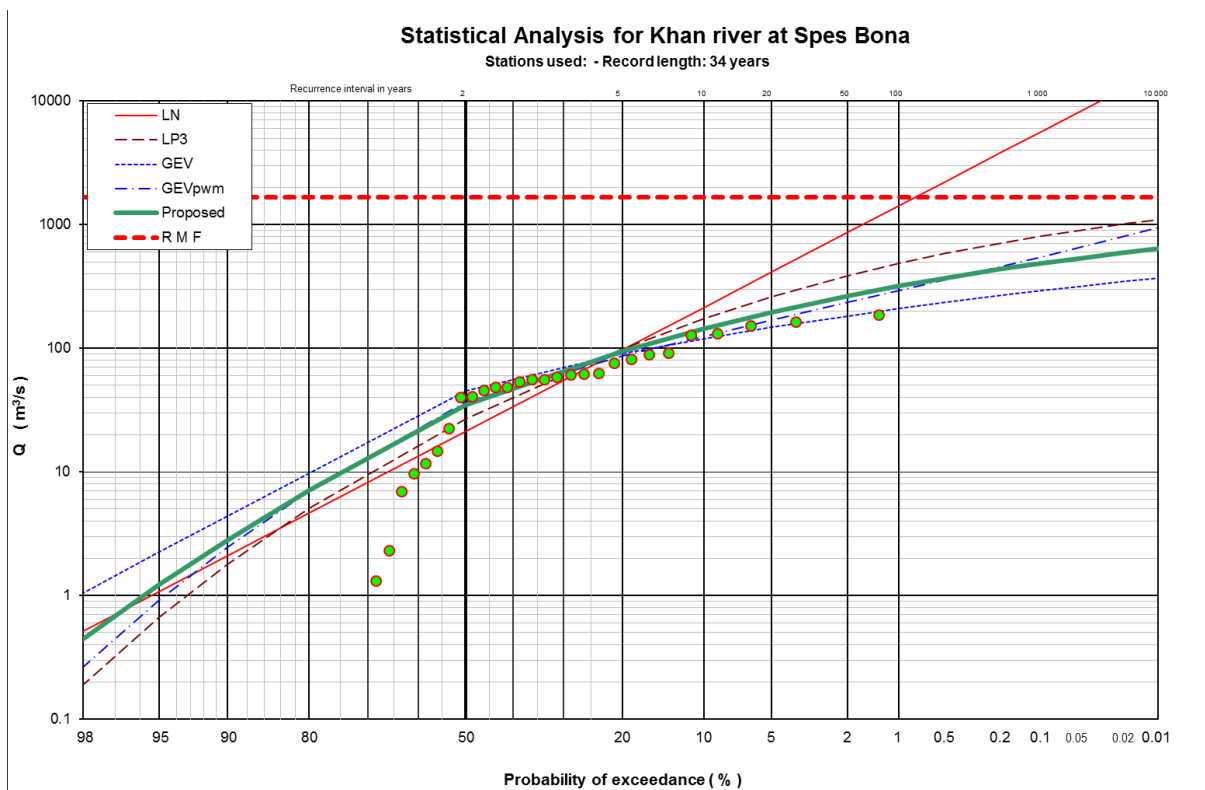
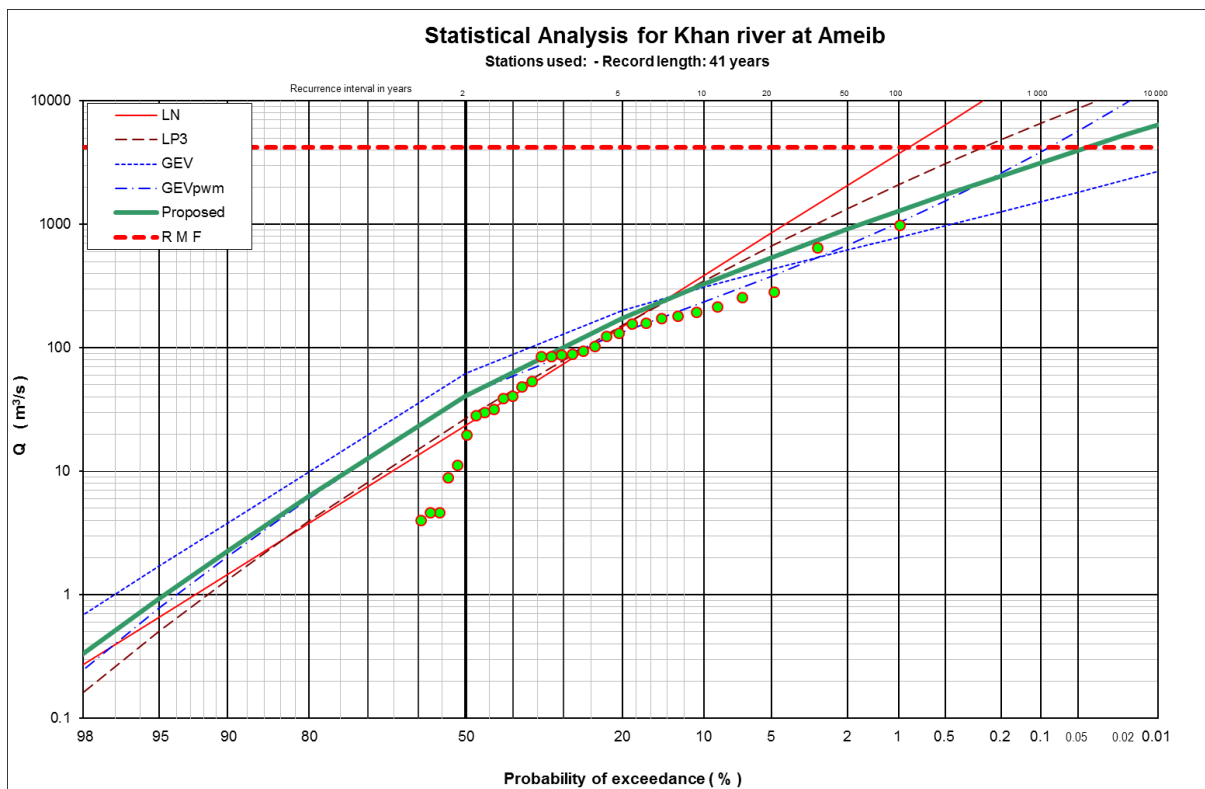
Appendix N: Flood peak distributions for the available flow gauging station data



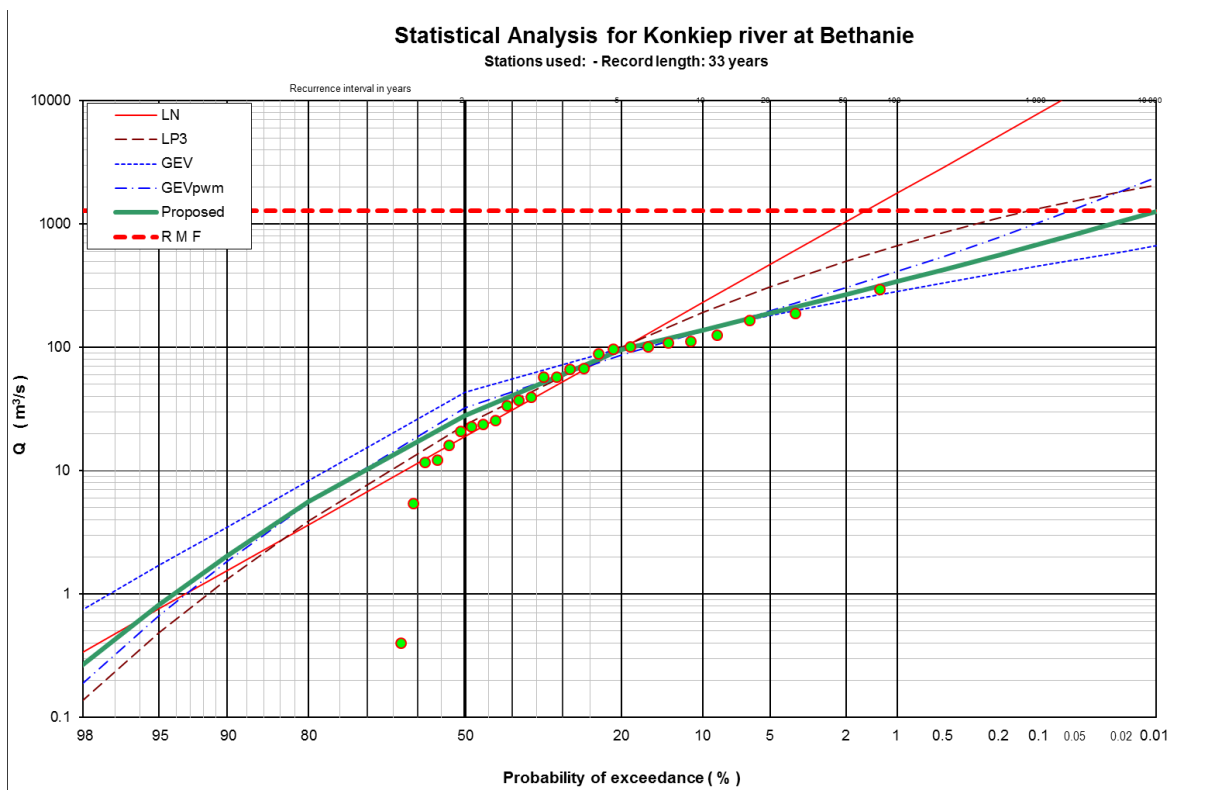
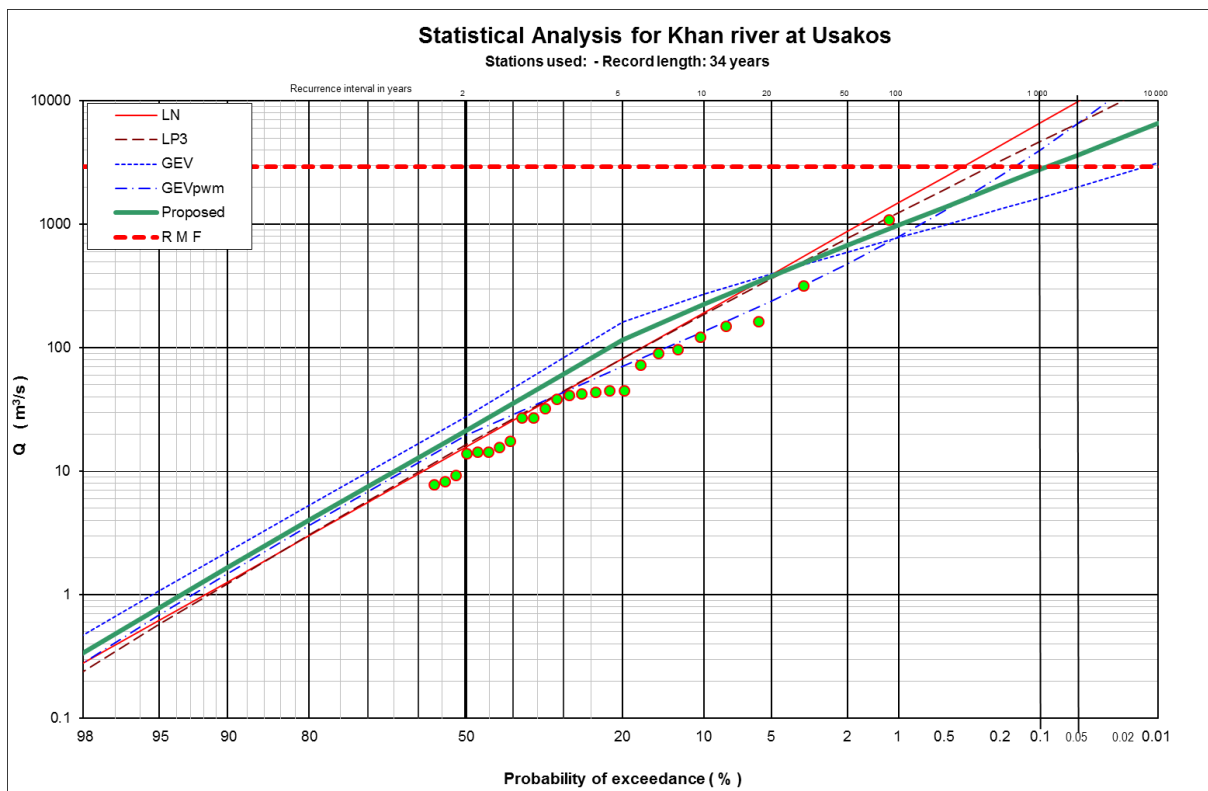
Appendix N: Flood peak distributions for the available flow gauging station data



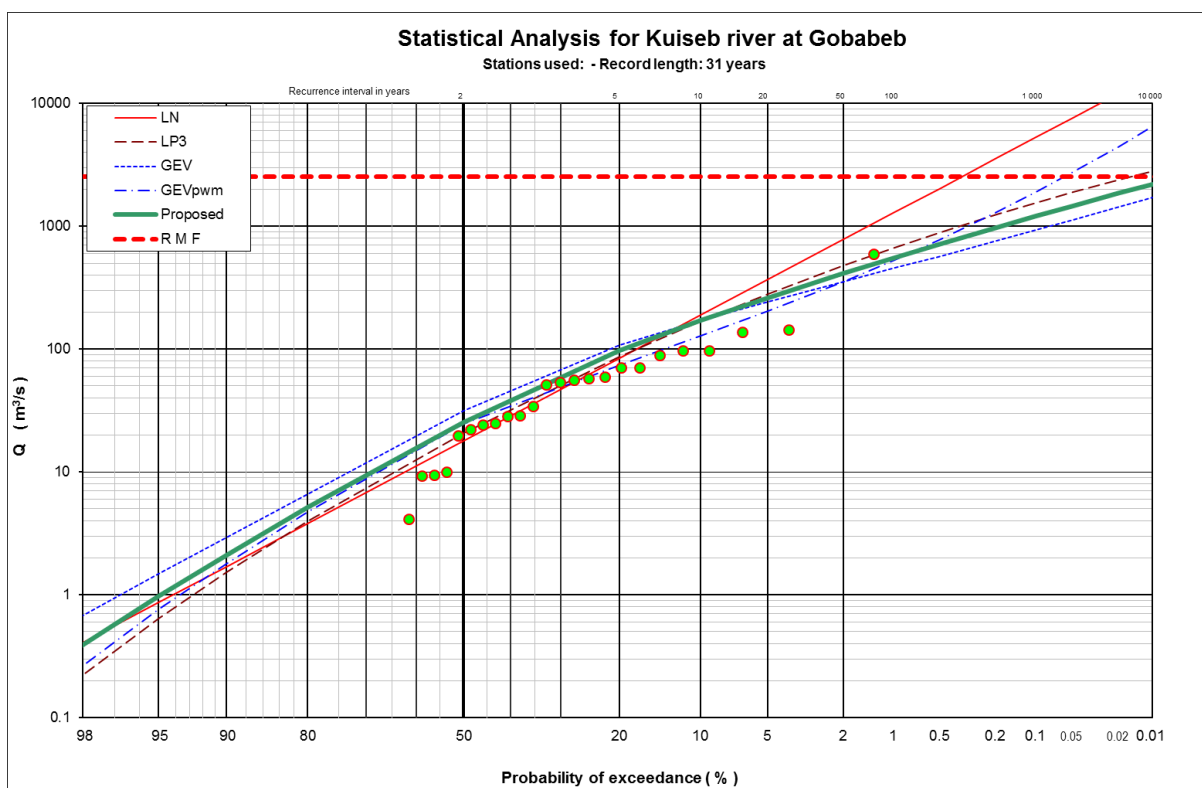
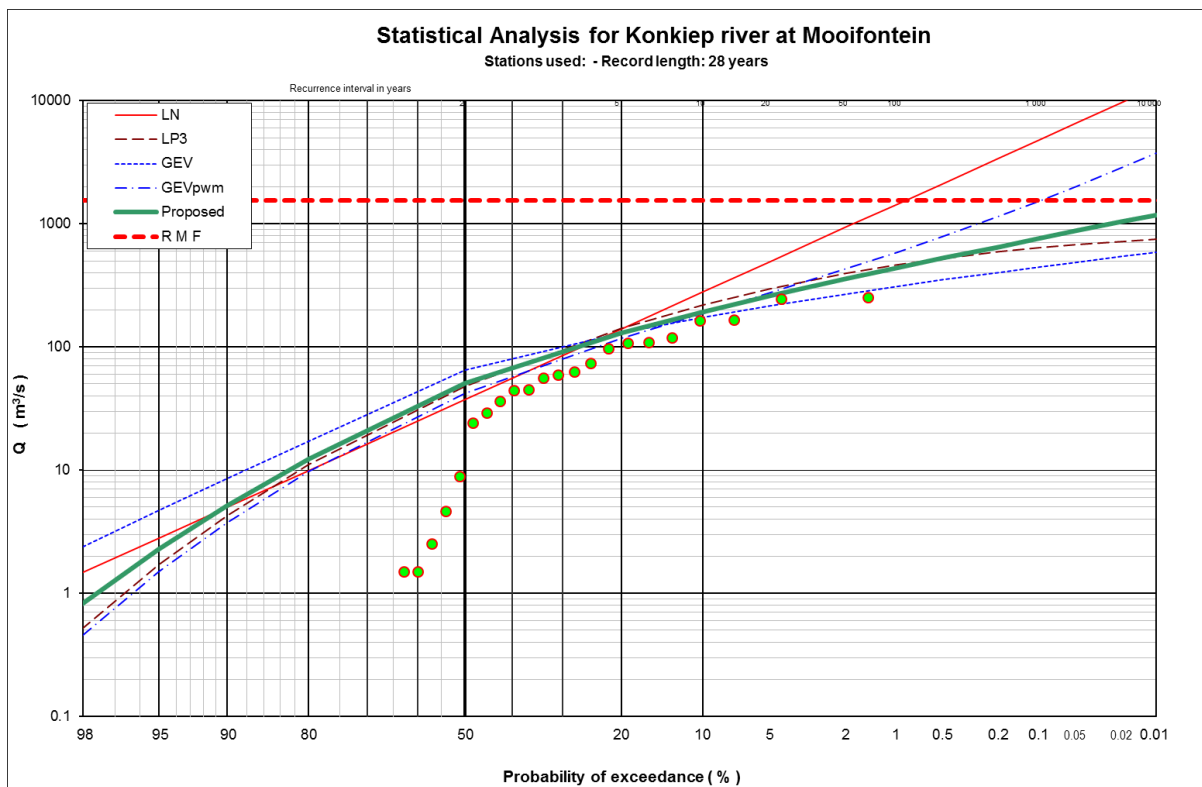
Appendix N: Flood peak distributions for the available flow gauging station data



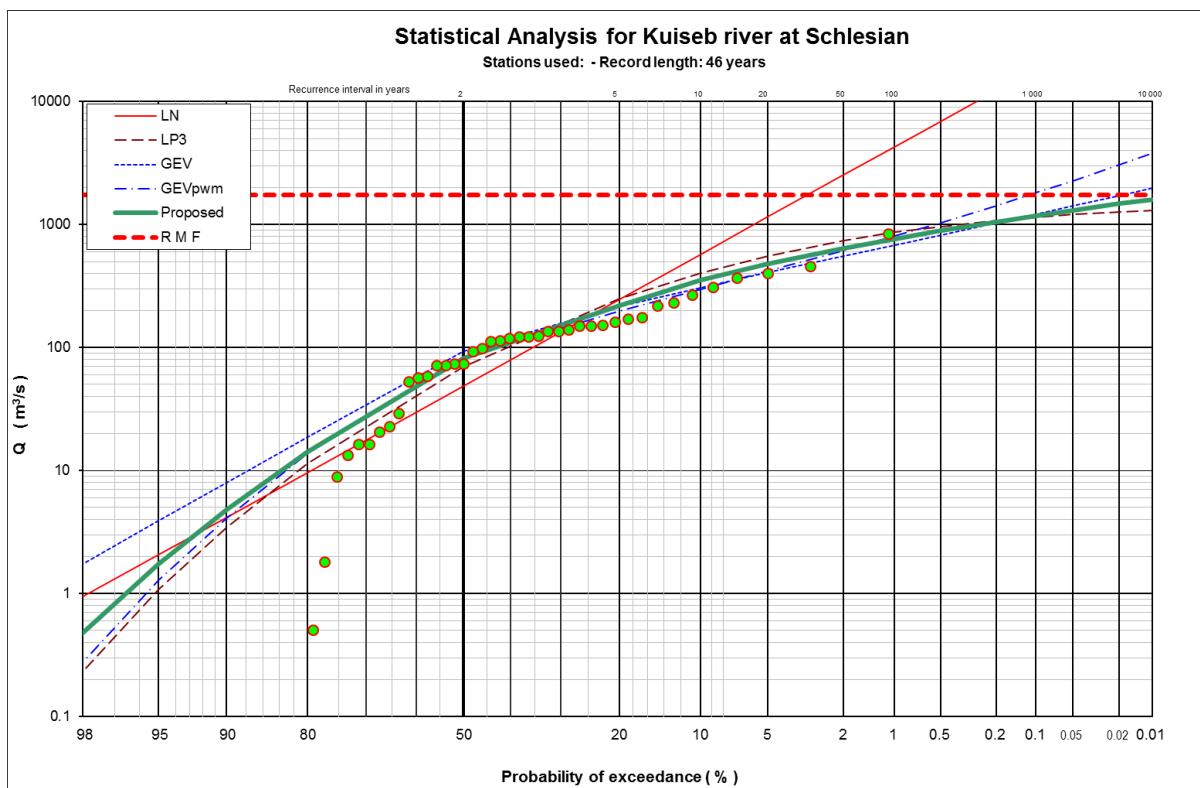
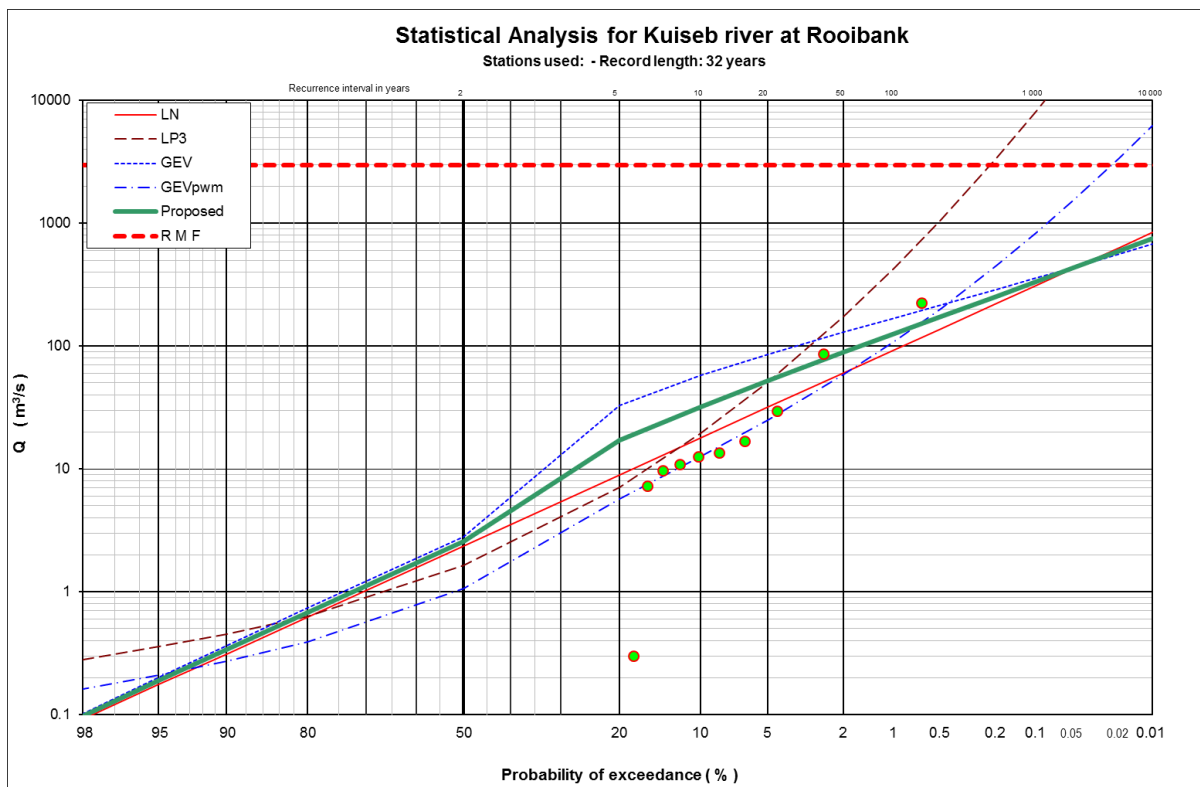
Appendix N: Flood peak distributions for the available flow gauging station data



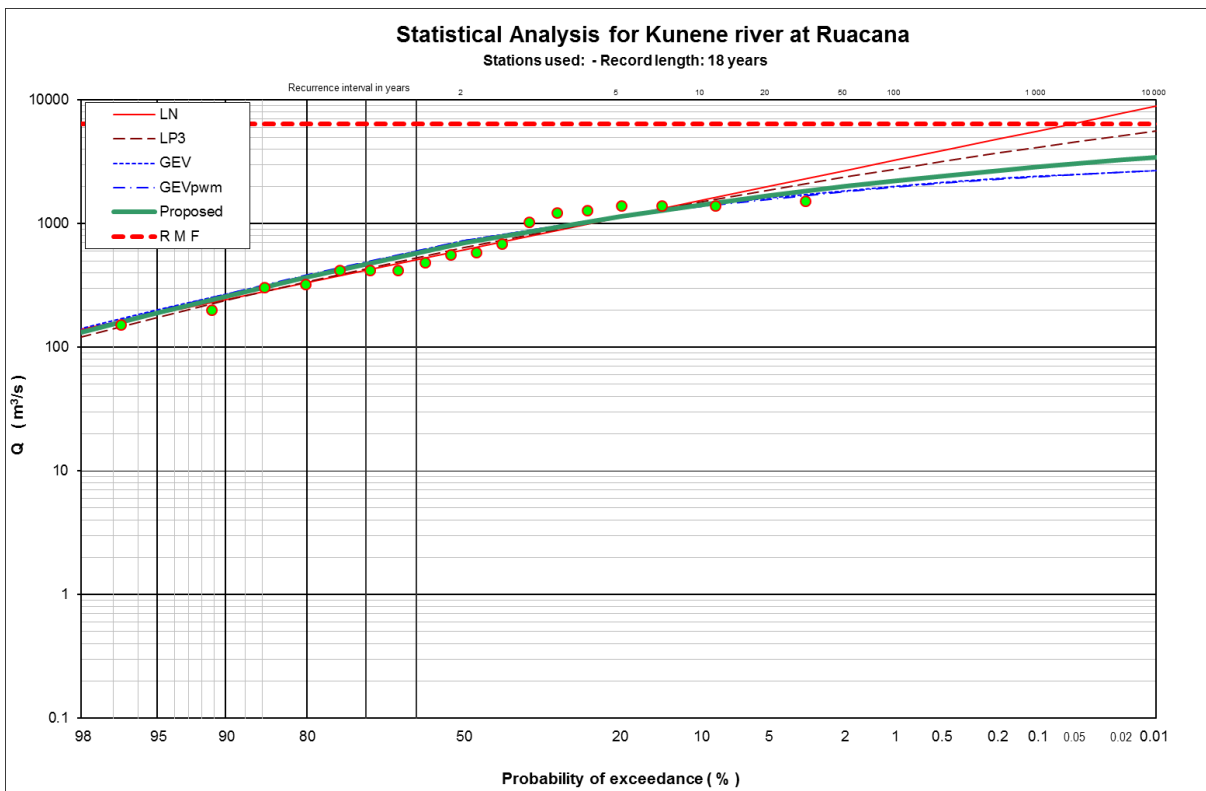
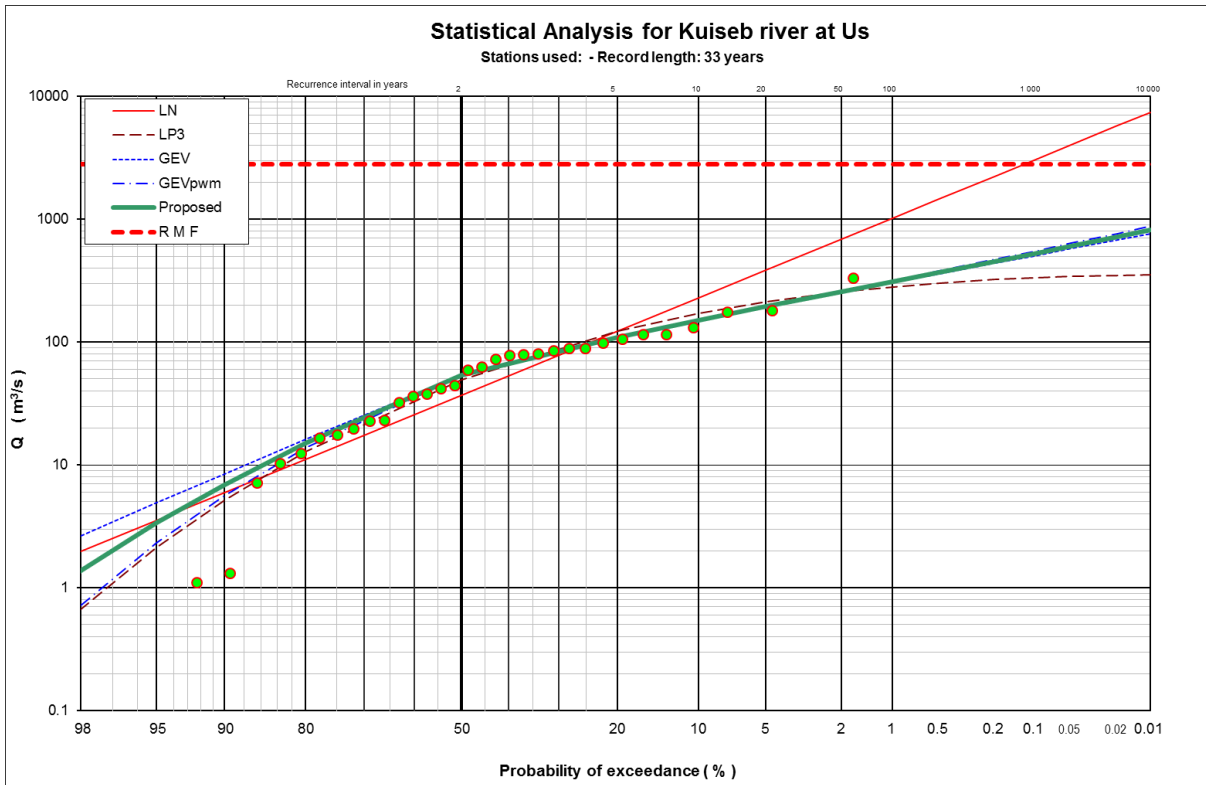
Appendix N: Flood peak distributions for the available flow gauging station data



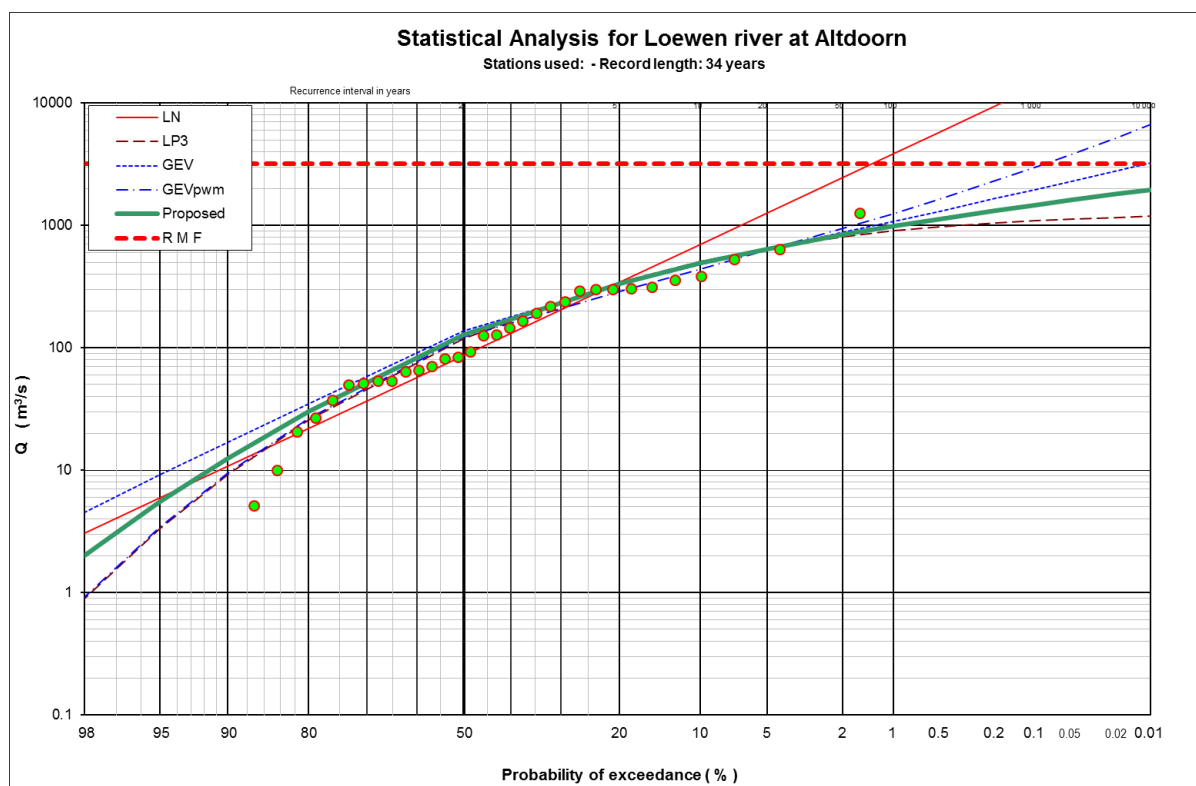
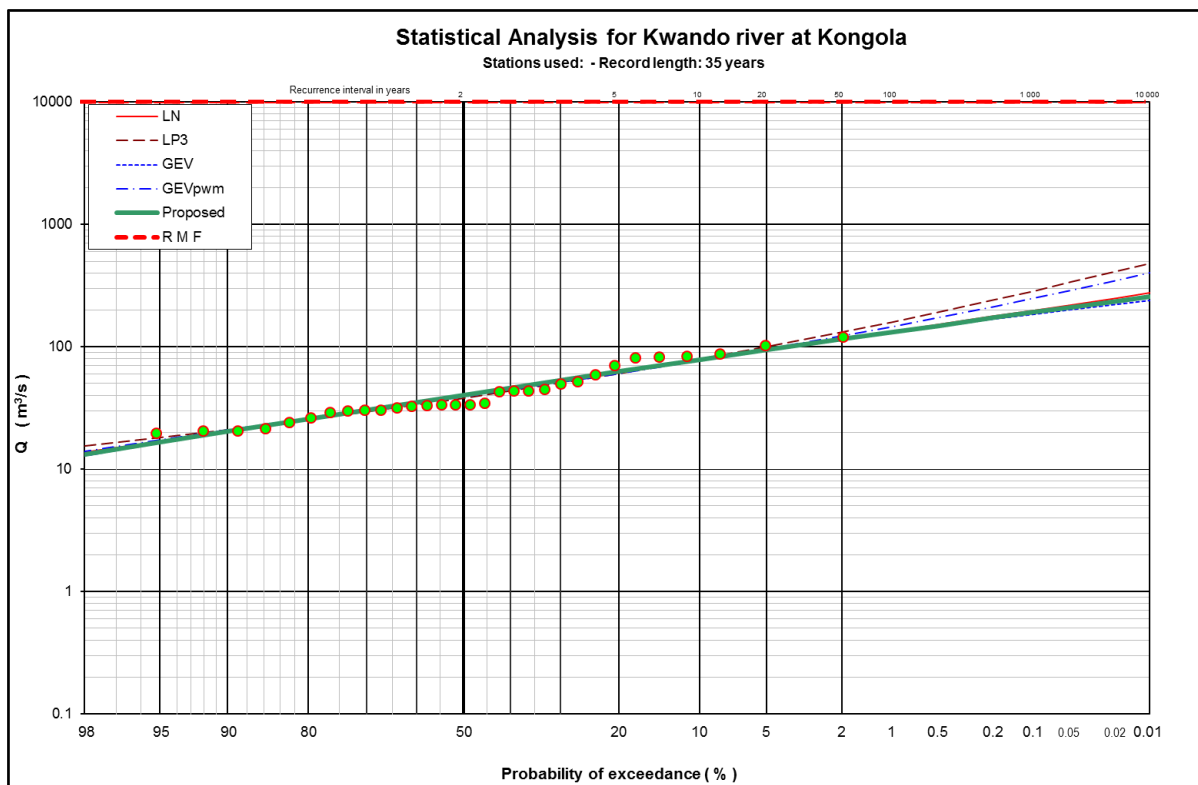
Appendix N: Flood peak distributions for the available flow gauging station data



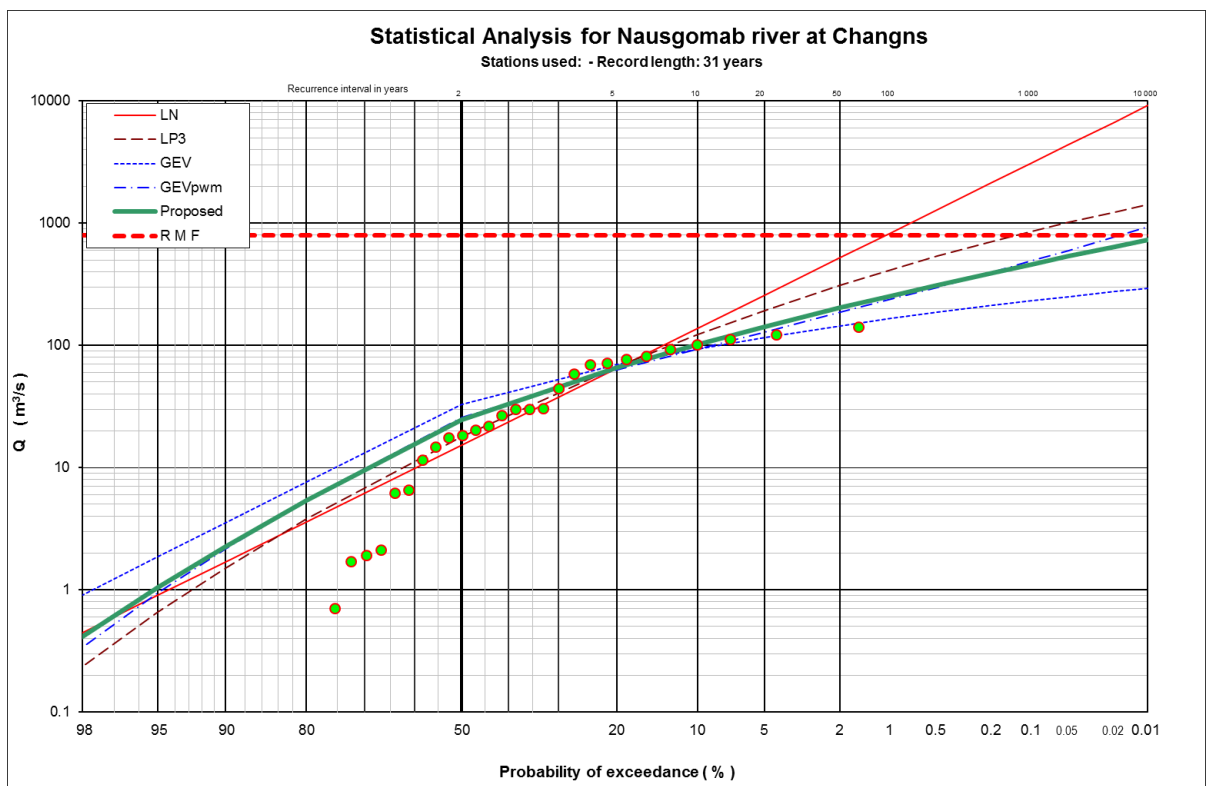
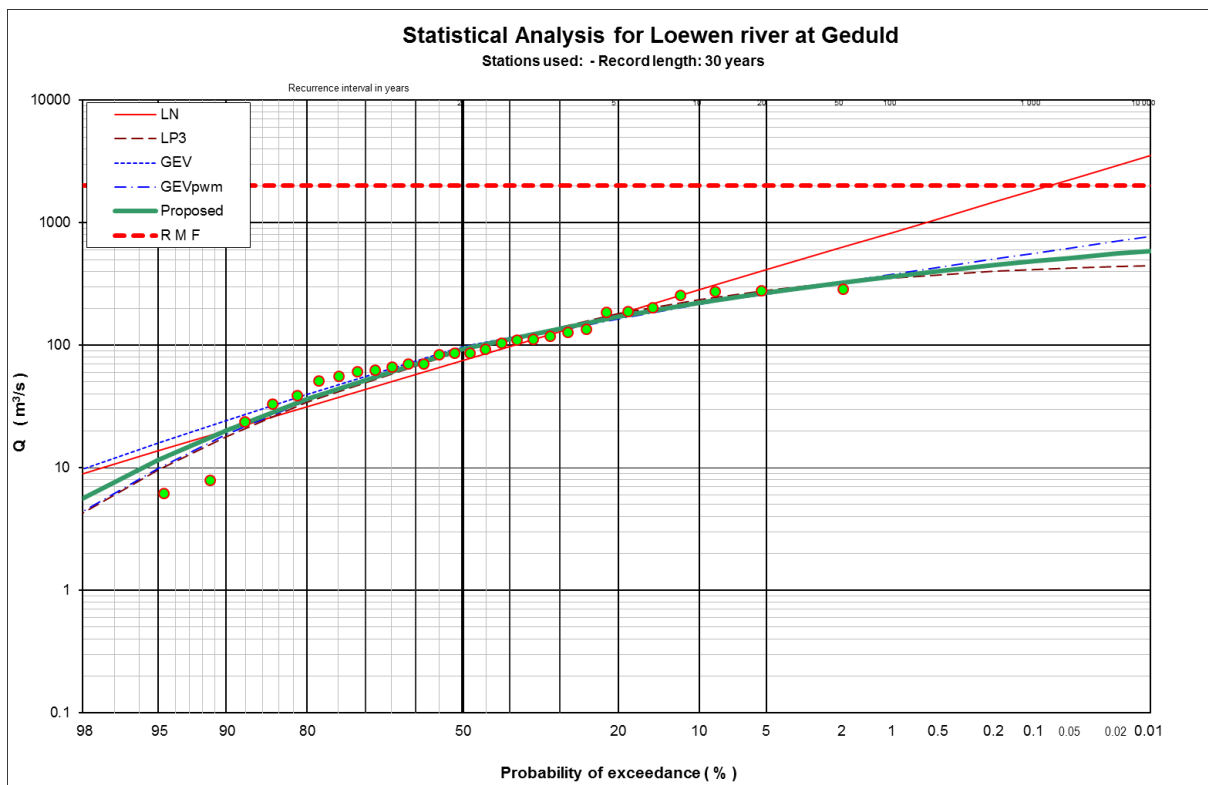
Appendix N: Flood peak distributions for the available flow gauging station data



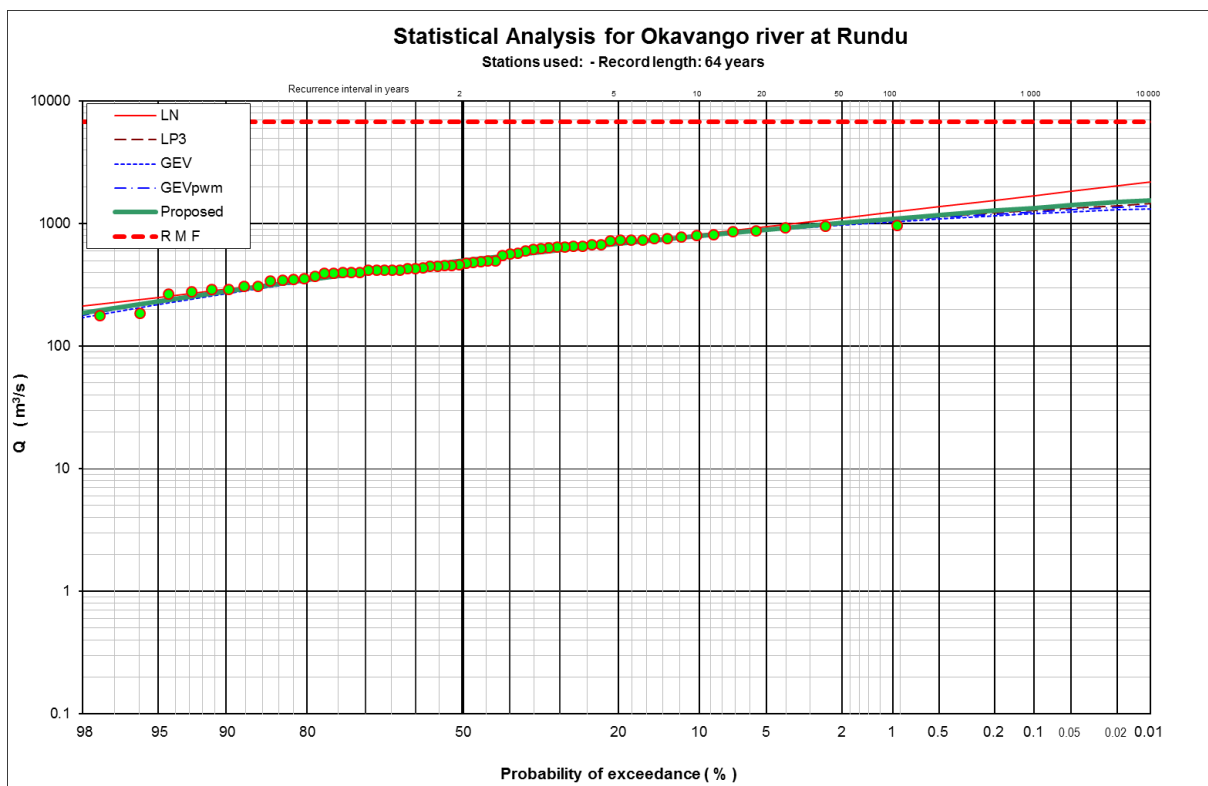
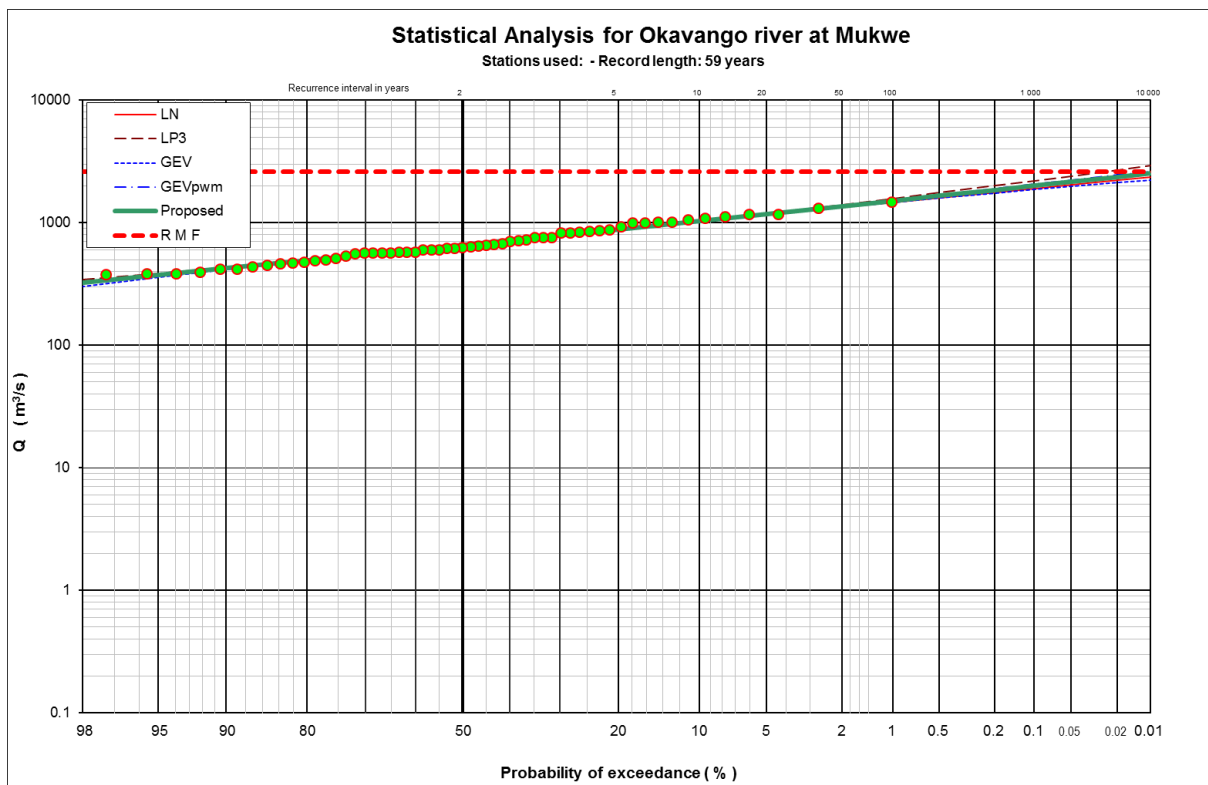
Appendix N: Flood peak distributions for the available flow gauging station data



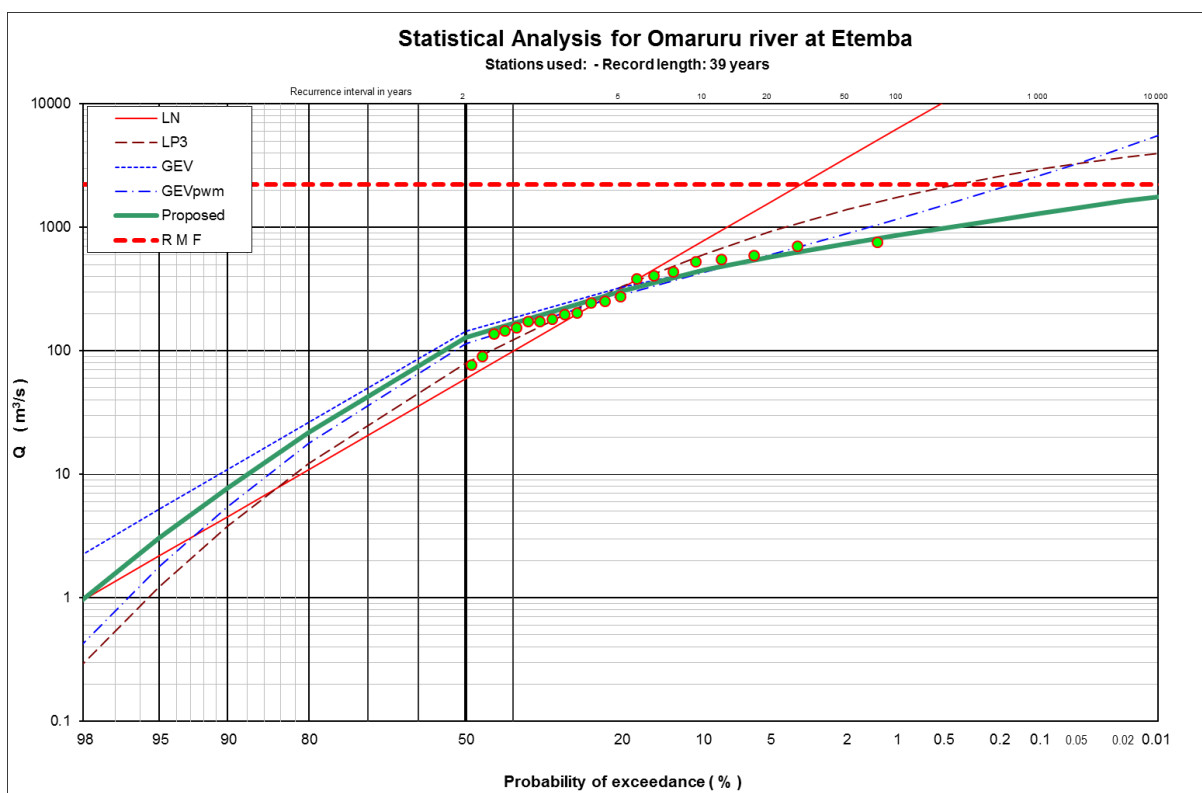
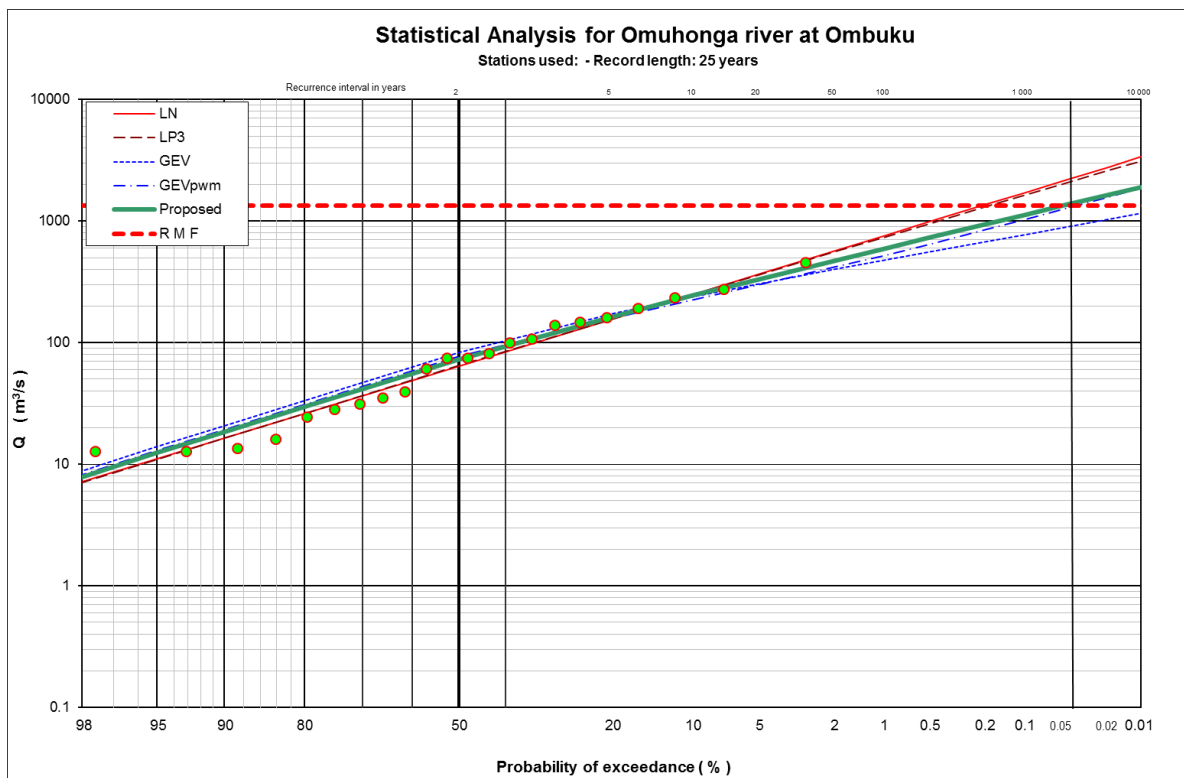
Appendix N: Flood peak distributions for the available flow gauging station data



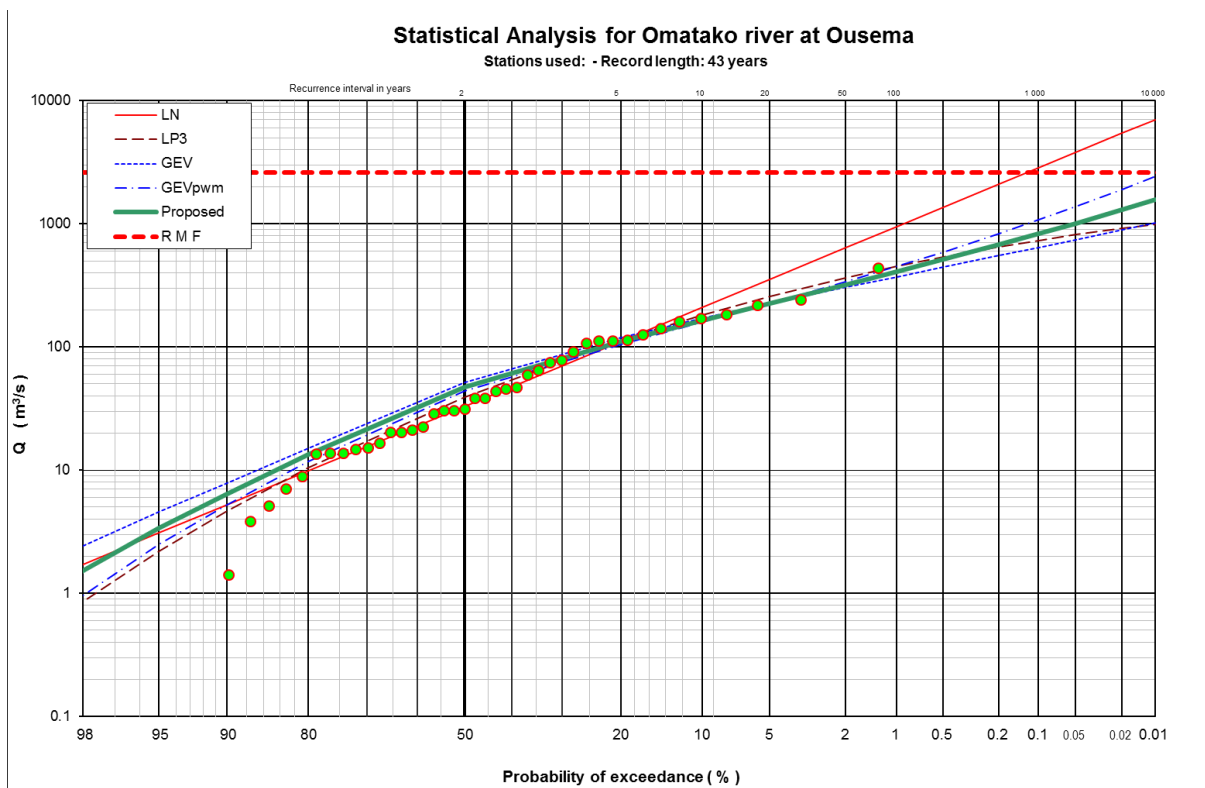
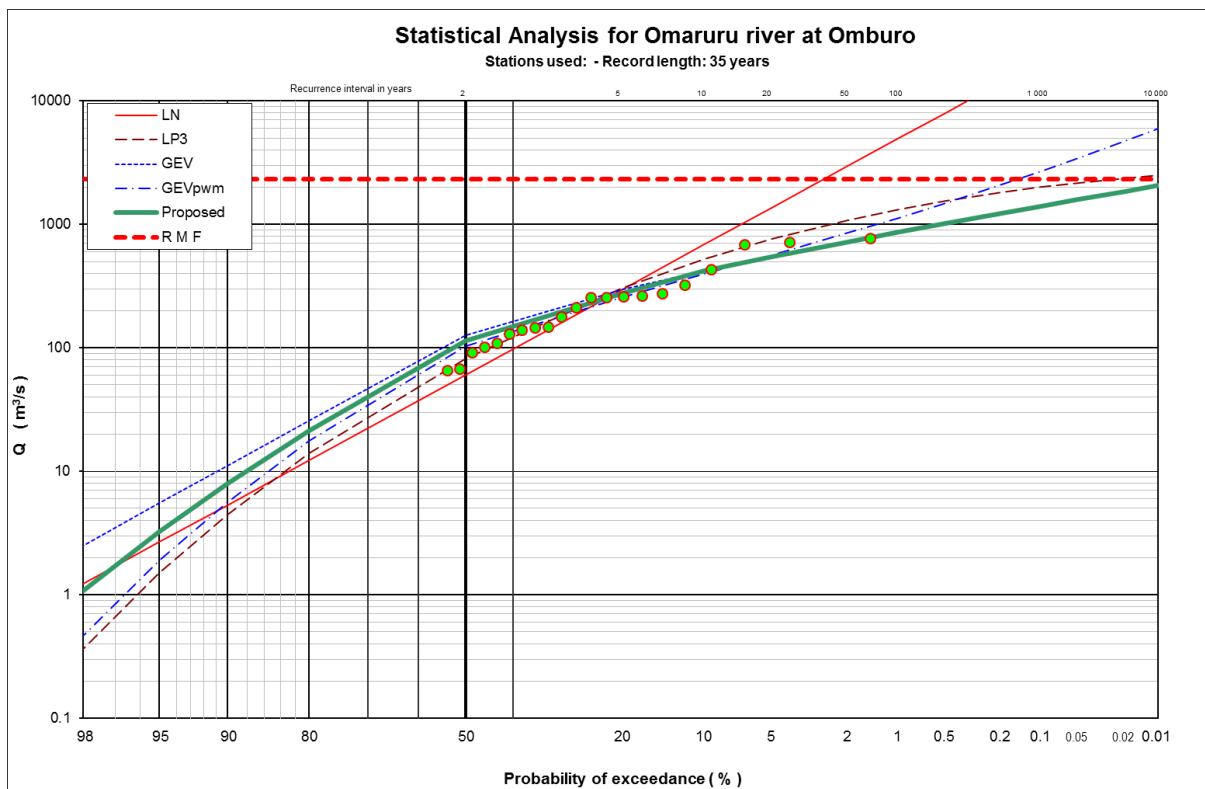
Appendix N: Flood peak distributions for the available flow gauging station data



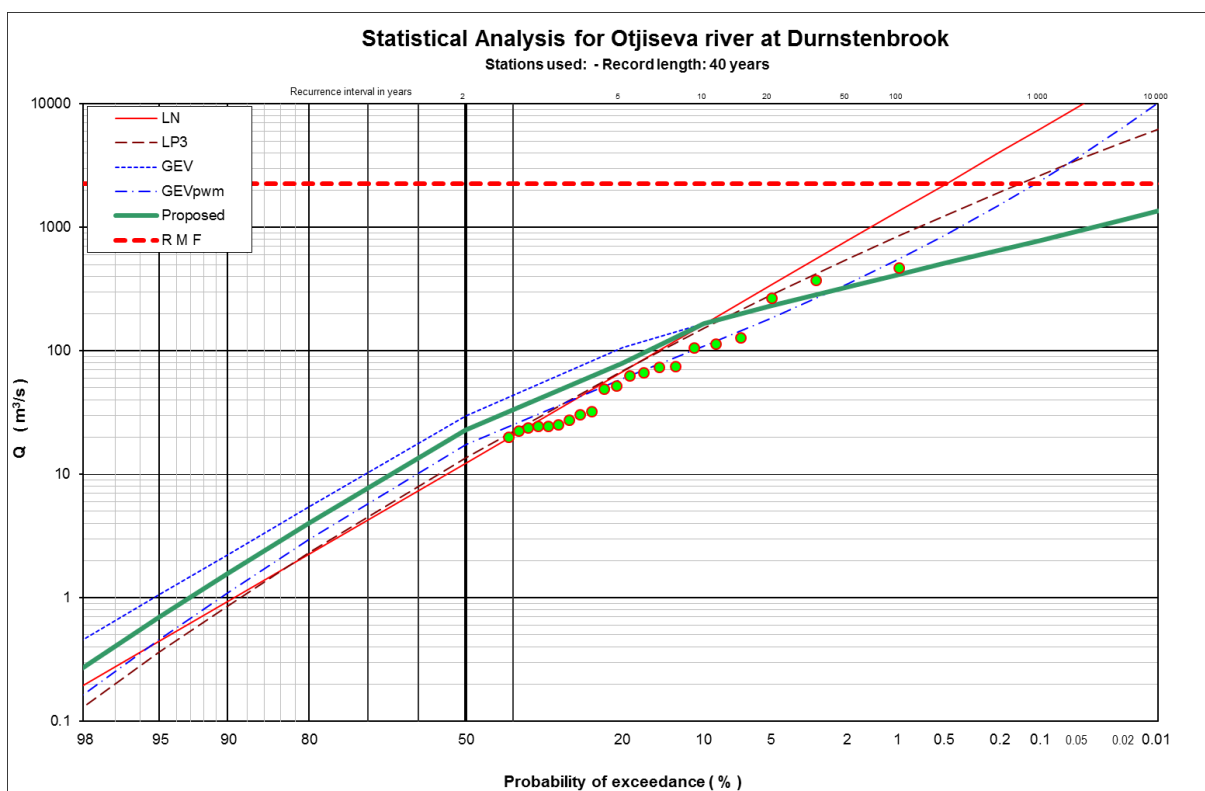
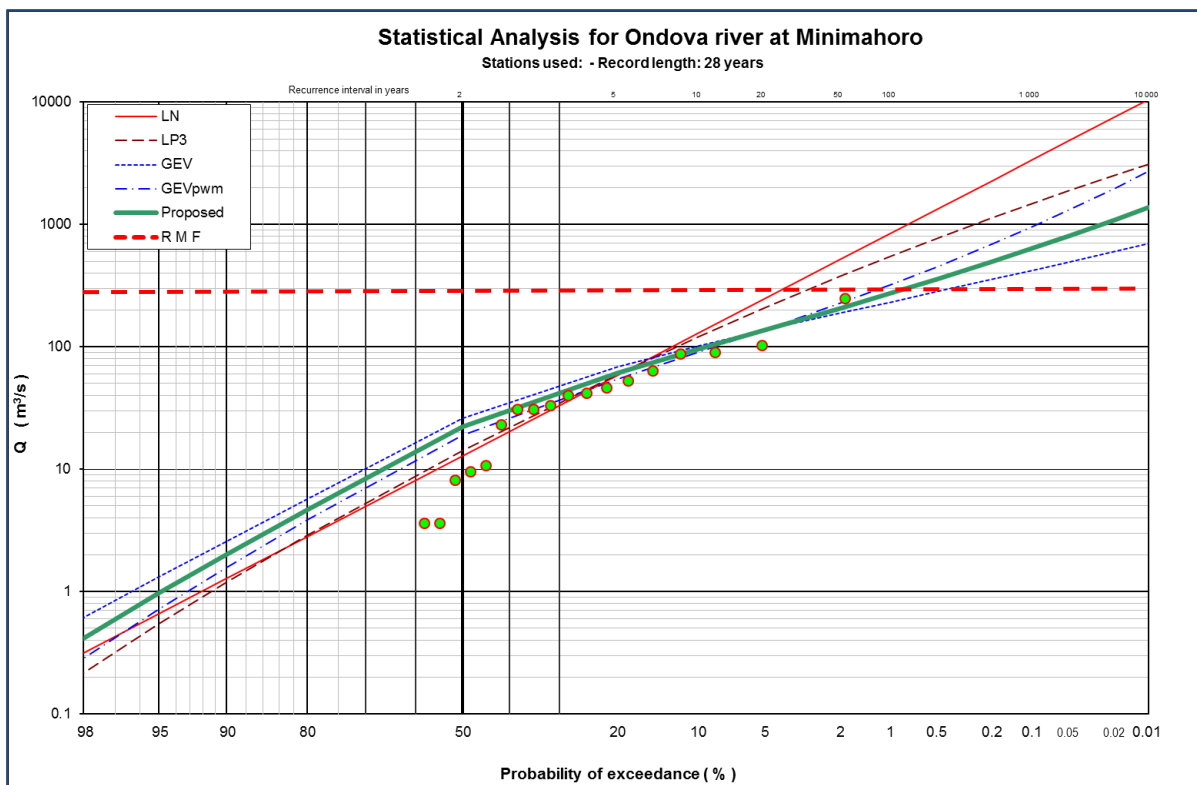
Appendix N: Flood peak distributions for the available flow gauging station data



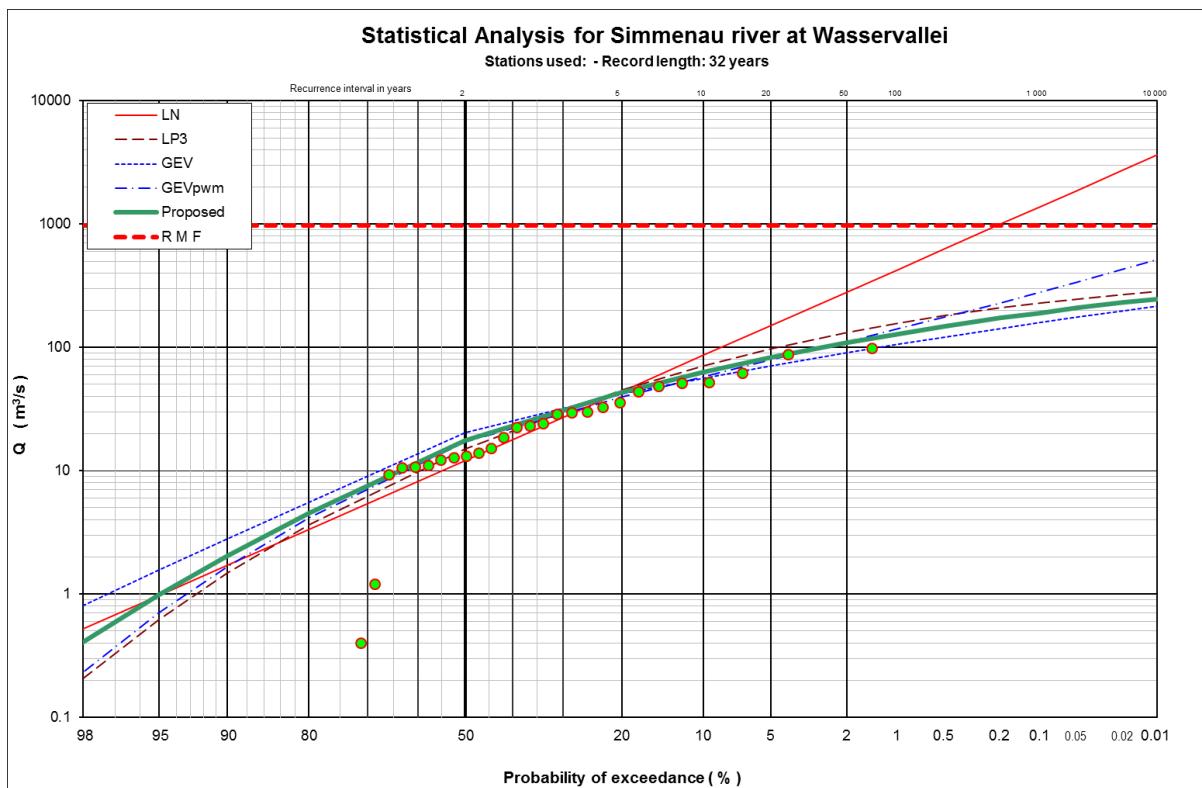
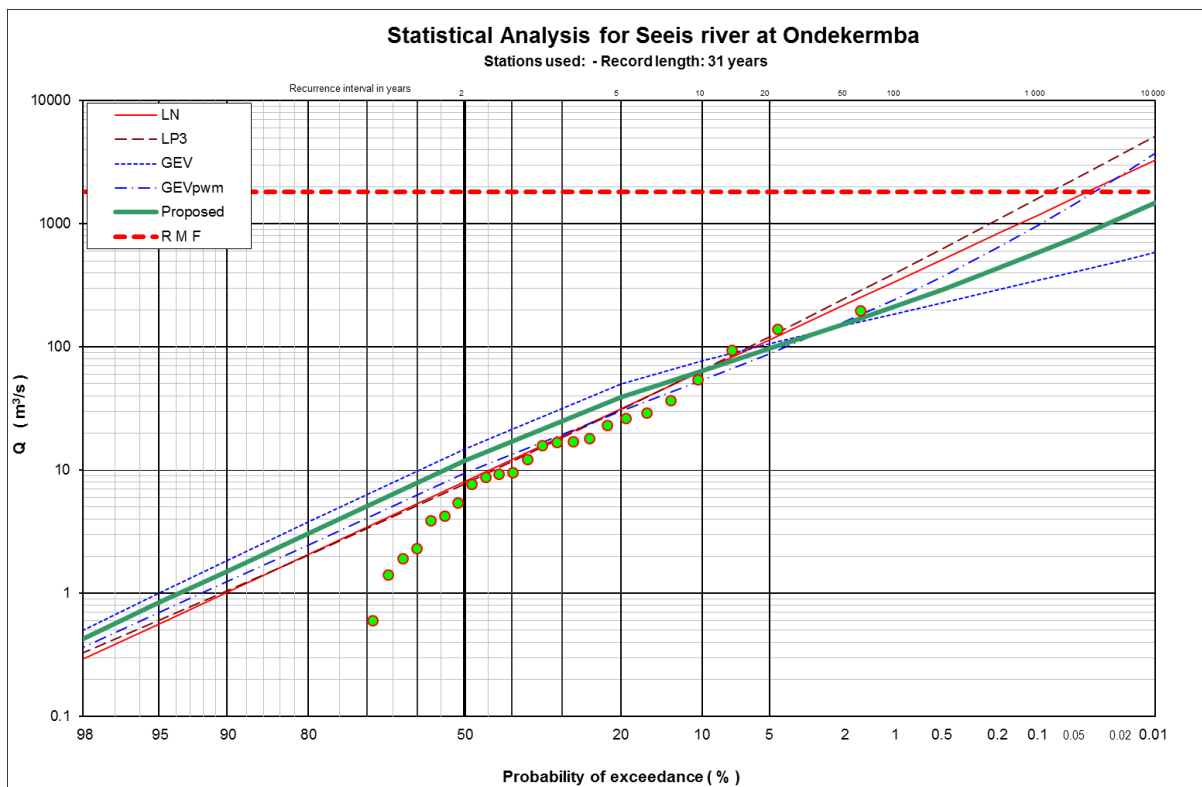
Appendix N: Flood peak distributions for the available flow gauging station data



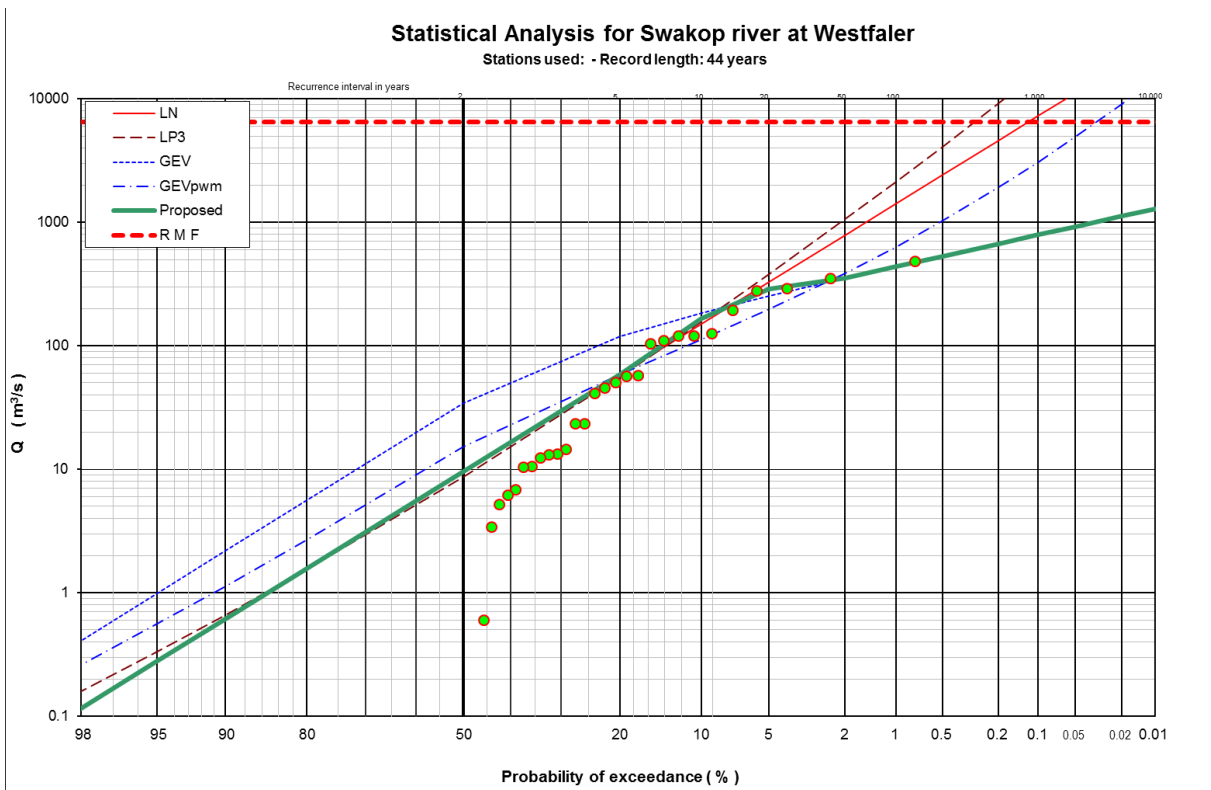
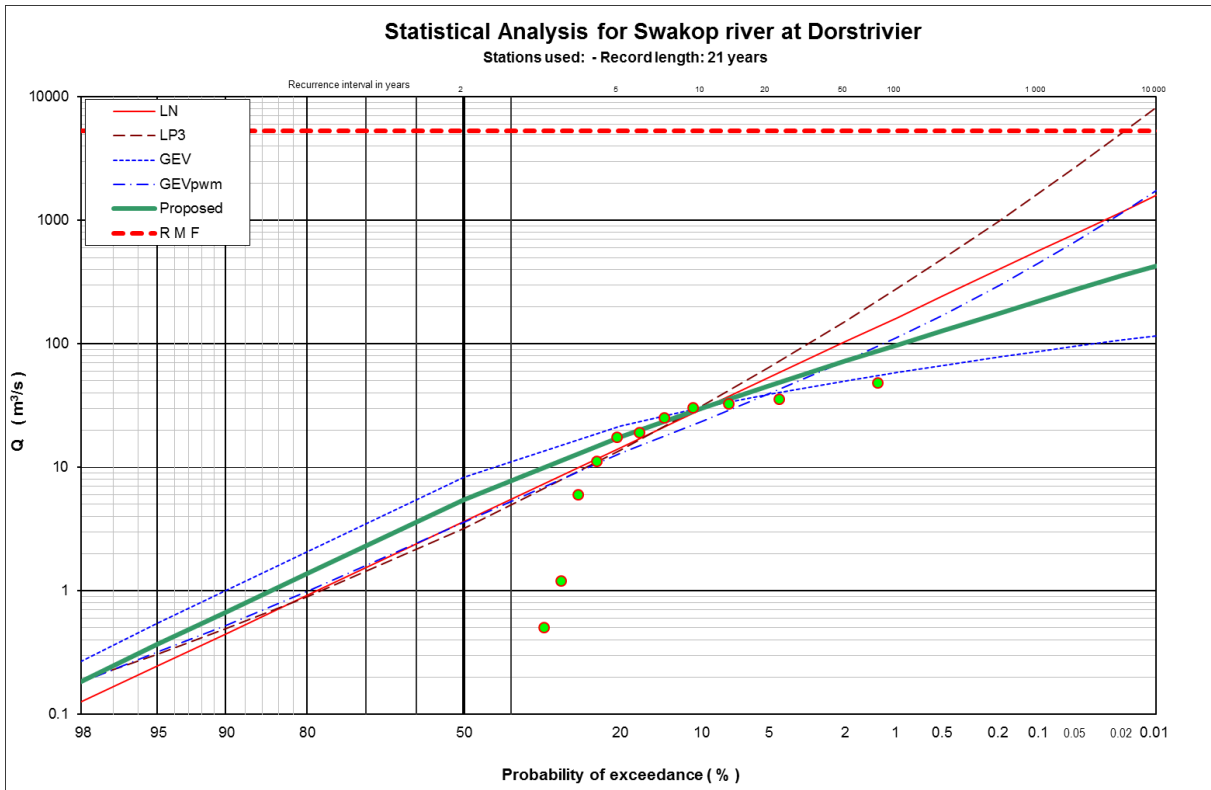
Appendix N: Flood peak distributions for the available flow gauging station data



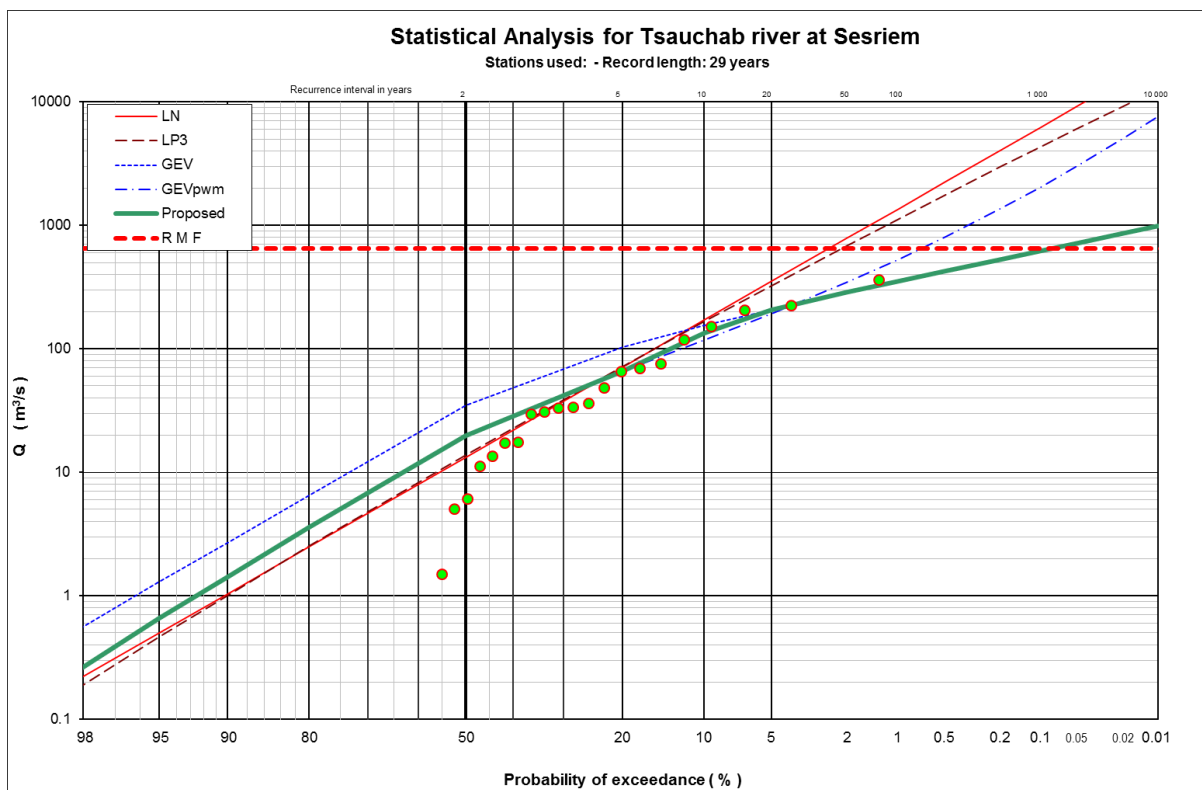
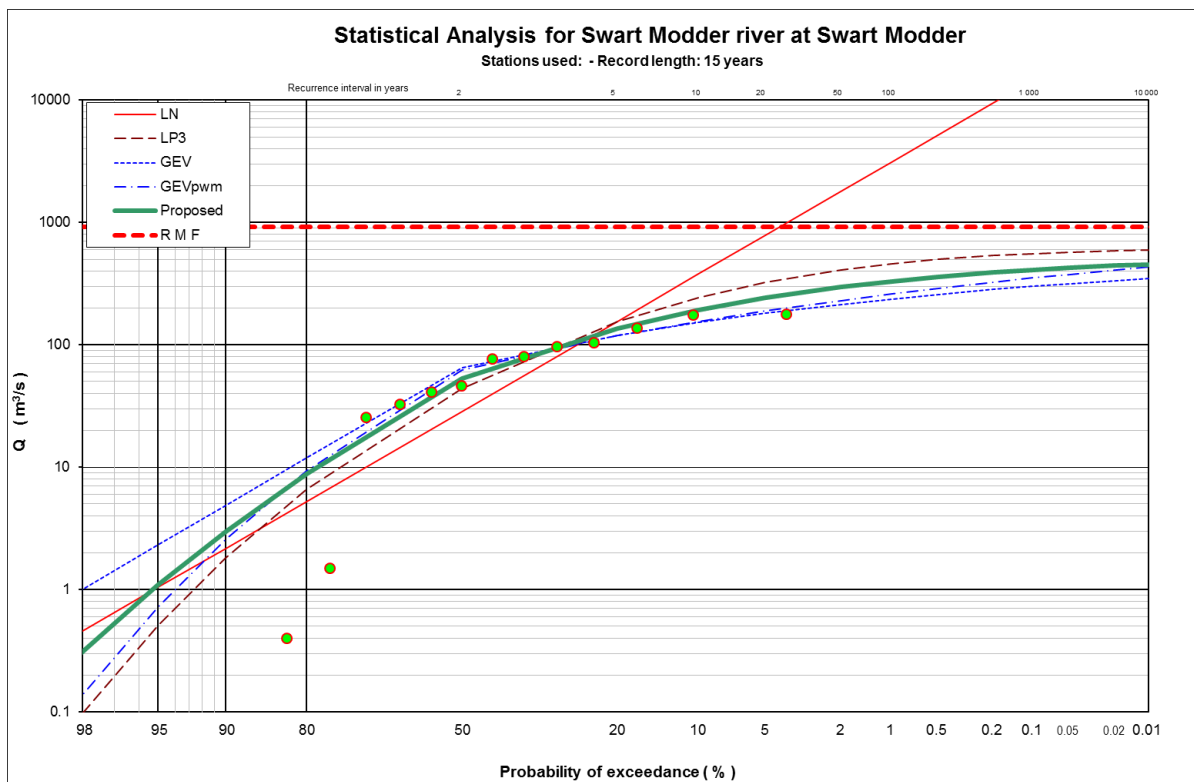
Appendix N: Flood peak distributions for the available flow gauging station data



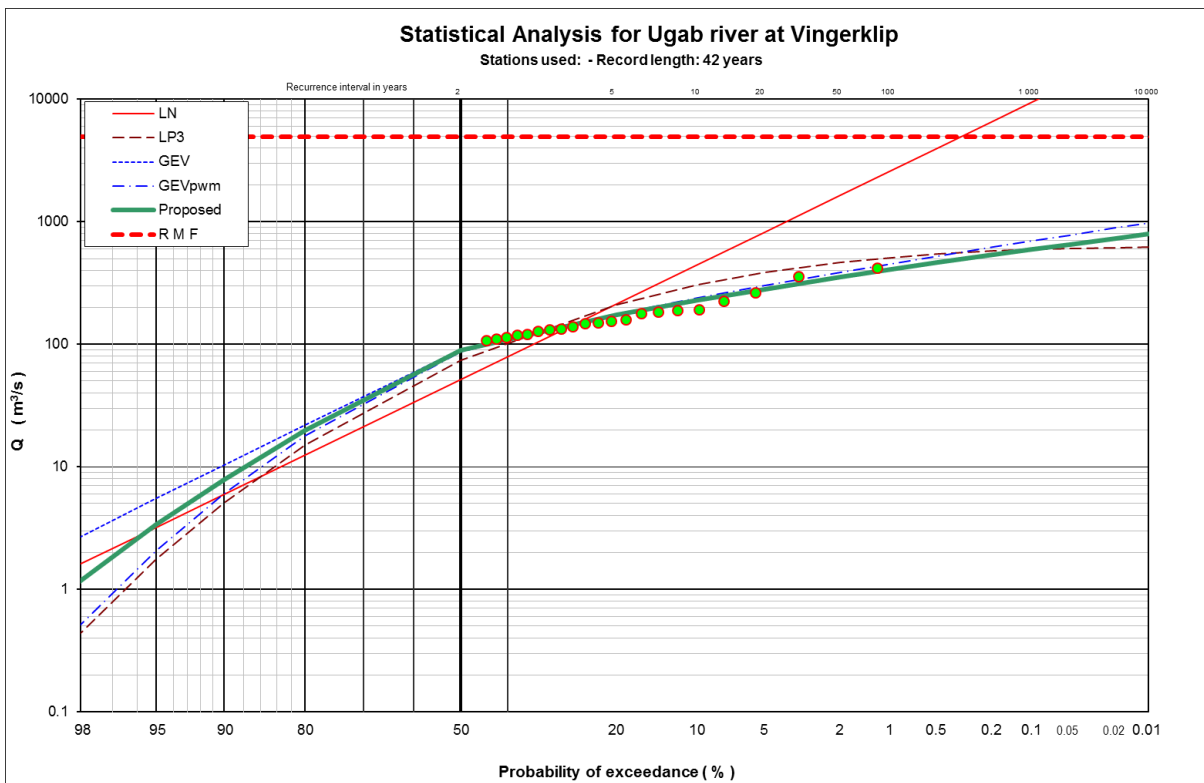
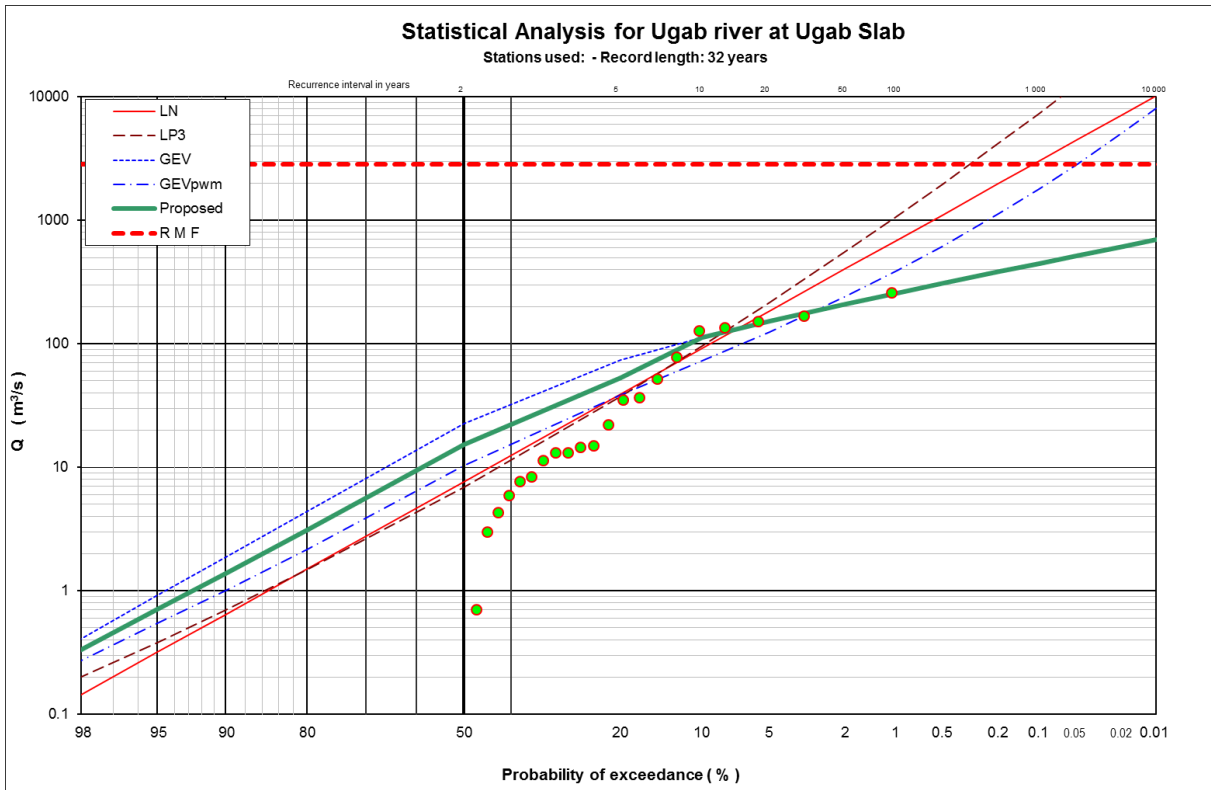
Appendix N: Flood peak distributions for the available flow gauging station data



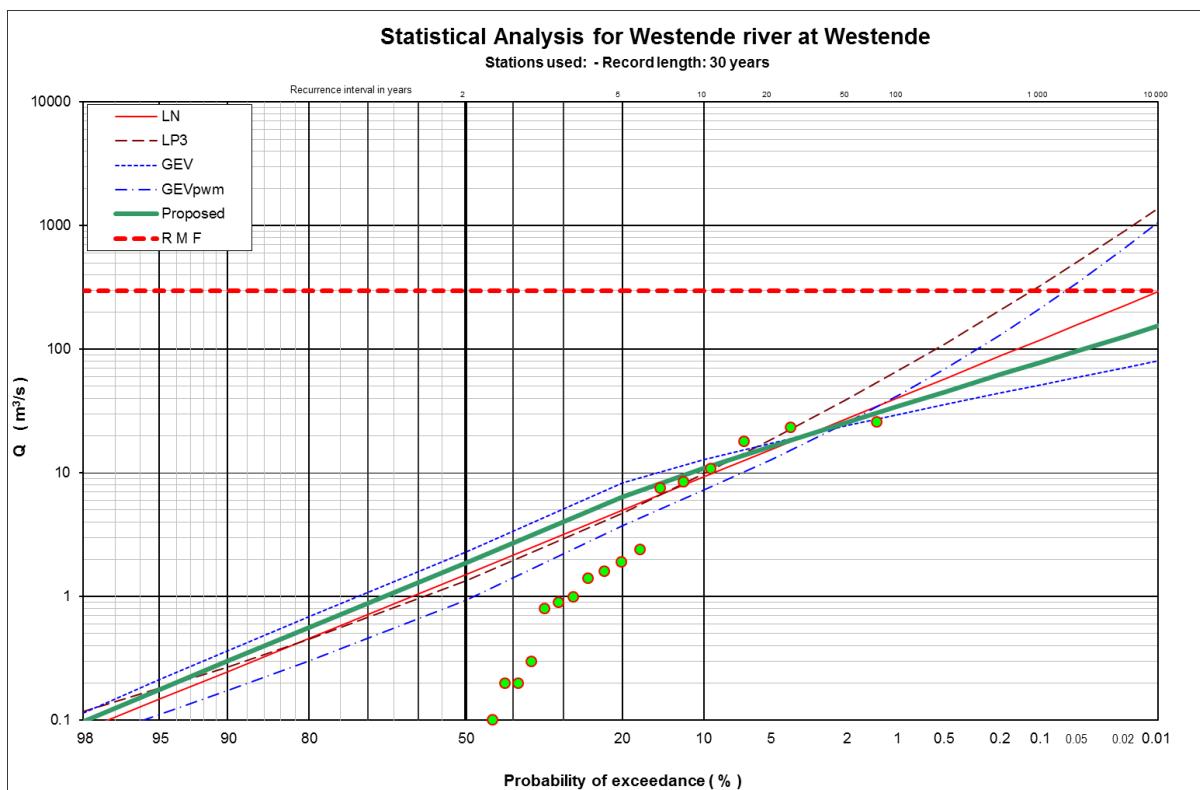
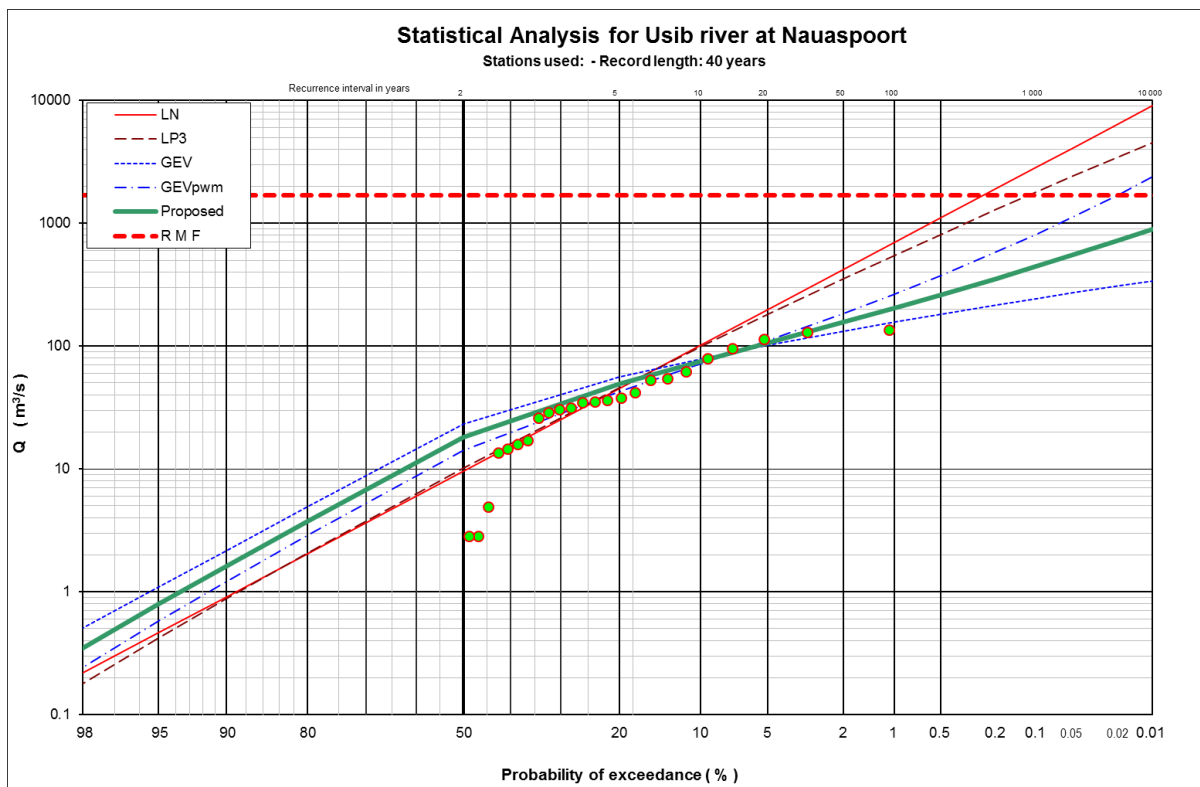
Appendix N: Flood peak distributions for the available flow gauging station data



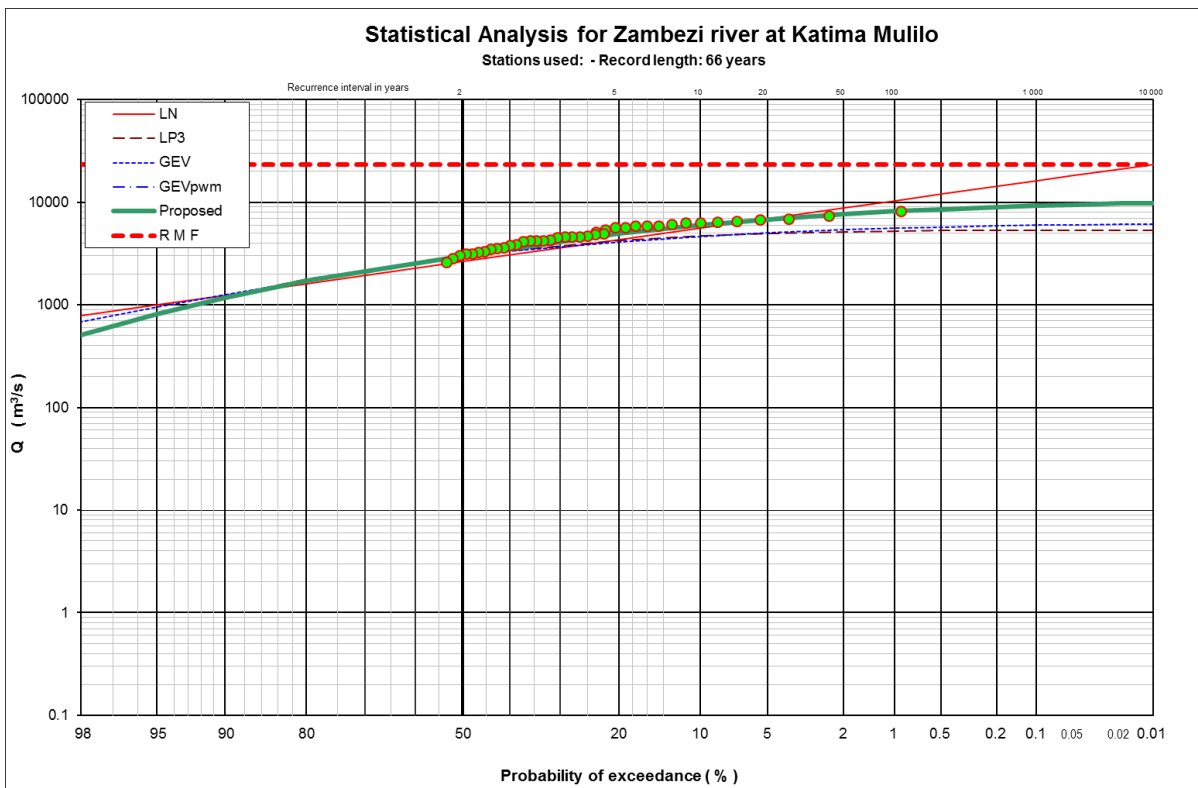
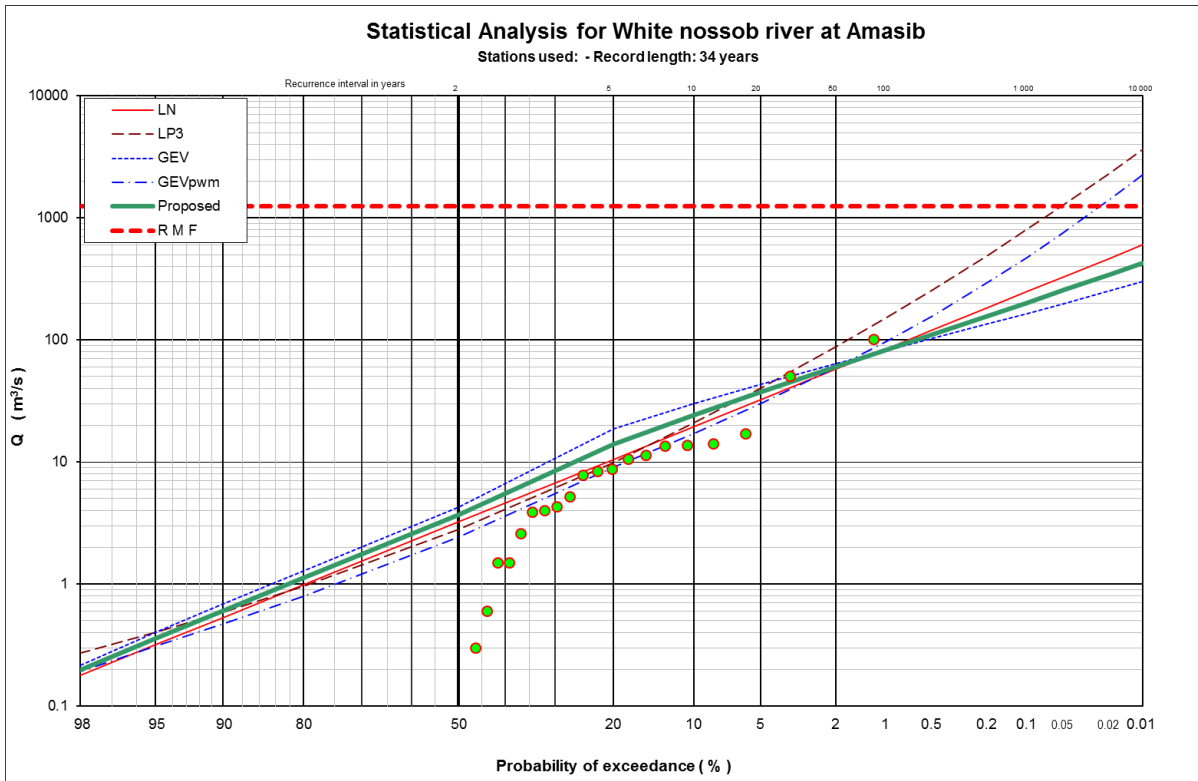
Appendix N: Flood peak distributions for the available flow gauging station data



Appendix N: Flood peak distributions for the available flow gauging station data



Appendix N: Flood peak distributions for the available flow gauging station data



Appendix O: Namibia annual flood peak data

NORTH EAST										
River & station	Zambezi Katima Mulilo		Kwando Kongola		Okavango Rundu		Okavango Mukwe		Omatoko Ousema	
Area km ²	334 000		170 000		97 300		26 000		4 970	
Year	Month	Peak (m ³ /s)	Month	Peak (m ³ /s)	Month	Peak (m ³ /s)	Month	Peak (m ³ /s)	Month	Peak (m ³ /s)
1943	Apr	2 053								
1944	Apr	3 129								
1945	Apr	4 573								
1946	May	1 909			Jan	432				
1947	Apr	5 378			Feb	778				
1948	Mar	6 711			Mar	620				
1949	May	920			Apr	454				
1950	Mar	5 627			Apr	673	Apr	716		
1951	Mar	4 882			May	866	May	1010		
1952	Mar	6 851			Mar	464	Mar	569		
1953	Mar	6 532			Apr	551	May	677		
1954	Apr	4 187			Apr	878	Apr	1110		
1955					Feb	166	Mar	383		
1956					Feb	494	Mar	644		
1957					Apr	417	Apr	534		
1958					Apr	309	Apr	465		
1959					Feb	350	Apr	461		
1960					Mar	417	Mar	509		
1961					Apr	751	Apr	864	Apr	16
1962					Jan	738	Feb	827	Nov	7
1963					Mar	950	Mar	1316	Jan	435
1964					Mar	397	Apr	569	Nov	14
1965	Mar	3 230			Apr	639	Apr	750	Feb	182
1966	Apr	5 864			Apr	641	Apr	852	Feb	113
1967	Apr	4 118			May	341	May	499	Feb	44
1968	Apr	5 901			Feb	922	Feb	1473	Apr	47
1969	Apr	8 152	May	121	Apr	962	Apr	1159	Feb	31
1970	Mar	5 645	Oct	87	Apr	645	Apr	821	Feb	59
1971	Mar	3 803	Sep	52	Mar	415	Mar	633	Feb	77
1972	May	2 518	Oct	45	May	177	Apr	392	Mar	112
1973	Apr	1 686	Nov	34	Apr	309	May	419	Mar	46
1974	Mar	3 322	Apr	71	Apr	401	May	559	Mar	217
1975	Apr	6 051	Jun	102	Mar	755	Mar	997	Mar	9
1976	Apr	6 279	Oct	81	May	571	Apr	750	Feb	169
1977	May	3 532		0	Apr	563	May	705	Feb	30
1978	Apr	7 284		0	Apr	450	May	665	Jan	161
1979	Apr	6 434		0	Apr	809	Apr	1166	Feb	74
1980	Apr	3 869	Jun	82	Mar	395	Mar	617	Mar	38
1981	Apr	4 260	Jul	83	Apr	729	Apr	1010	Feb	21
1982	Apr	1 996	Oct	59	Mar	500	Mar	622	Feb	29
1983	Mar	1 427	Jan	32	Apr	348	Apr	649	Dec	20
1984	Apr	2 527	Sep	33	Apr	798	Apr	1050	Apr	112
1985	May	2 582	Feb	34	Apr	437	May	575	Jan	126
1986	Apr	4 222	Mar	34	Apr	600	Apr	756	Jan	30
1987	Apr	3 039	Dec	34	Apr	357	Apr	451	Feb	106
1988	Apr	3 585	Apr	31	Apr	456	Apr	575	Jan	91
1989	May	4 589	Sep	44	Feb	428	Feb	595	Feb	65
1990	May	1 264	Feb	43	Apr	475	May	569	Mar	14
1991	Mar	3 139	Apr	30	Jan	289	Feb	419	Feb	141
1992	Mar	1 087	Mar	26	Mar	629	Apr	727	Dec	4
1993	Apr	4 800	Feb	30	Mar	267	Apr	379	Apr	38
1994	Mar	2 806	Mar	33	Jan	186	Feb	383		0
1995	Apr	2 086	Feb	21	Apr	397	Apr	475	Feb	5
1996	May	1 112	Mar	20	Apr	291	Apr	370	Jan	23
1997	Apr	2 070	Feb	21	Apr	280	Apr	437	Dec	1
1998	Apr	4 541	Mar	17	Mar	447	Apr	595	Dec	20
1999	Apr	4 222	Mar	21	Apr	677	Apr	874	Feb	15
2000	Apr	4 653	Mar	29	Apr	392	May	492	Dec	241
2001	Apr	4 589	Aug	50	Apr	650	May	931	May	13
2002	May	2 289	Oct	43	Apr	485	Apr	597		0
2003	Apr	5 101	Feb	24	Mar	492	Mar	575	Apr	15
2004	Apr	5 864			Feb	738	Mar	1090		
2005	May	1 512			Apr	650	Apr	833		
2006	Apr	3 447			May	374	May	569		
2007	Mar	6 279			Mar	727	Apr	997		
2008	Oct	286			Mar	417	Apr	615		
2009					Jan	419				

Appendix O: Namibia annual flood peak data

River & station	EAST FLOWING RIVERS																	
	Arrebusch Monravia		Black Nossob Henopsrus		Black Nossob Mentz		White Nossob Amasib		Swart-modder at Swart-modder		Usib Nauaspr		Auob Gochas		Auob Stampriet		Seelis Ondekermba	
Area km ²	49.3	4530	8160	9250	240.2	727	19600	19200	326									
Year	Month	Peak (m ³ /s)	Month	Peak (m ³ /s)	Month	Peak (m ³ /s)	Month	Peak (m ³ /s)	Month	Peak (m ³ /s)	Month	Peak (m ³ /s)	Month	Peak (m ³ /s)	Month	Peak (m ³ /s)	Month	Peak (m ³ /s)
1971																		
1972																		
1973																		
1974																		
1975																		
1976																		
1977																		
1978																		
1979																		
1980																		
1981																		
1982																		
1983																		
1984																		
1985																		
1986																		
1987																		
1988																		
1989																		
1990																		
1991																		
1992																		
1993																		
1994																		
1995																		
1996																		
1997																		
1998																		
1999																		
2000																		
2001																		
2002																		
2003																		
2004																		
2005																		
2006																		
2007																		
2008																		
2009																		

Appendix O: Namibia annual flood peak data

River & station	Ham Tsamab		Hutub Rietkuil		Hutub Breckhorn		Fish Seeheim		Fish Tses		Loewen Altdorn		Loewen Geduld		Konklep Bethanien		Konklep Moofontein		Fish Ai-Ais		Gab Hologg	
	Area km ²	2470	5850	4780	46400	37600	7000	3200	4140	2070	63300	2510										
1961																						
1962																						
1963																						
1964																						
1965																						
1966																						
1967																						
1968																						
1969																						
1970																						
1971																						
1972																						
1973																						
1974																						
1975																						
1976																						
1977																						
1978																						
1979																						
1980																						
1981																						
1982																						
1983																						
1984																						
1985																						
1986																						
1987																						
1988																						
1989																						
1990																						
1991																						
1992																						
1993																						
1994																						
1995																						
1996																						
1997																						
1998																						
1999																						
2000																						
2001																						
2002																						
2003																						
2004																						
2005																						
2006																						
2007																						
2008																						
2009																						
2010																						

Appendix O: Namibia annual flood peak data

River & station	WEST FLOWING RIVERS																		
	Kuiseb Us		Bismark Stanco		Simminau Wasserval		Heunis Heunis		Tsauchab Sesriem		Djab KosTower		Huis Kos		Kuiseb Gobabeb		Kuiseb Roobibank		
Area km ²	1900		276		266		38.4		1480		231		20.1		11700		14700		
Year	Month	Peak (m ³ /s)	Month	Peak (m ³ /s)	Month	Peak (m ³ /s)	Month	Peak (m ³ /s)	Month	Peak (m ³ /s)	Month	Peak (m ³ /s)	Month	Peak (m ³ /s)	Month	Peak (m ³ /s)	Month	Peak (m ³ /s)	
1975									Feb	1.5									
1976										0					Mar		85.8		
1977	Apr	44.4							Mar	13.5								0	
1978	Jan	77.6	Jan	26.3	Mar	11				0				Feb	28.1			0	
1979	Feb	41.8		0	Feb	29.4	Feb	56.6		0				Mar	9.3			0	
1980	Mar	36.2	Mar	13.2	Mar	12.1	Mar	2.2	Mar	151.6					0			0	
1981	Dec	7.1		0	Dec	51.4		0	Apr	29.4					0			0	
1982	Mar	17.6	Feb	8.2	Mar	1.2	Mar	12.8	Jan	222.2				Apr	8.7			0	
1983	Jan	16.6	Mar	8.2	Jan	10.5	Jan	2.8	Apr	75.8					0			0	
1984	Feb	12.3	Dec	62.5	Dec	97.5	Dec	34.5	Jan	30.7				Mar	19.7			0	
1985	Mar	88	Feb	27	Feb	87.4	Feb	36.1	Feb	69.6				Feb	97.2			29.5	
1986	Feb	333	Mar	20.1		0	Mar	3.4	Mar	118.8				Apr	70.4			9.6	
1987	Oct	78.4	Feb	40.9	Feb	51.6	Dec	4.4		0				Feb	24.9			0.3	
1988	Feb	98.1	Jan	60.3	Jan	15.1	Jan	18.4		0				Apr	53.3			16.7	
1989	Feb	72.6	Feb	8.2	Feb	43.4	Dec	1.2	Jan	5				Feb	69.9			12.6	
1990	Feb	88	Feb	114.6	Mar	13.9	Feb	37.8	Feb	48.3				Feb	59.1			10.8	
1991	Jan	130.2	Jan	1.4	Jan	18.5	Jan	0	Mar	64.9				Jan	9.9			0	
1992	Apr	10.3	Feb	1	Oct	22.4	Feb	1.3	Jan	33.5				Mar	3.3			0	
1993	Feb	59.2	Feb	114.6	Mar	30	Feb	54.4	Jan	360.2				Feb	27.3			13.5	
1994	Jan	80.1	Feb	18.9	Mar	0	Feb	13.8	Mar	36.2				Jan	51.3			0	
1995	Mar	1.1	Feb	15.8	Feb	48.4	Feb	30.7	Mar	11.2				Feb	27.3			7.2	
1996	Jan	84.5	Jan	47.2	Jan	23.1	Mar	0.8	Mar	204.4				Jan	23.9			0	
1997	Jan	174	Feb	120.9	Mar	23.9	Mar	9.9	Apr	17.2				Jan	88.2			0	
1998	Dec	22.6	Feb	0.5	Jan	35.4	Dec	15.6	Apr	33.1				Jan	21.1			0	
1999		0		0		0	Mar	5.7	Jan	0				Jan	4.8			0	
2000	Feb	180.6	Mar	65.9	Apr	28.5		0	Feb	6.1				Mar	4.1			0	
2001	Apr	1.3	Feb	18.2	May	0	Feb	0.7	Feb	0				Mar	594.2			0	
2002	Mar	22.9	Mar	31.6	Jan	12.7		0	Feb	17.4				Apr	137.4			222.3	
2003	Apr	114.7		0	Mar	61.4		0		0					0			0	
2004	Jan	106.1		0	Jan	9.2		0		0				Apr	56			0	
2005	Mar	37.7	Nov	25.7	Mar	0.4		0		0				Mar	33.8			0	
2006	Feb	114.2		0	Jan	32.7		0		0				Feb	142.1			0	
2007	Jan	19.7		0		0	Jan	0.5		0					0			0	
2008	Feb	62.2		0	Feb	13	Feb	1.4		0				Jan	47.9			0	
2009	Dec	32.3	Feb	39.5	Dec	10.7	Feb	3.1		0				Mar	0.1			0	
2010			Feb	30.5															

Appendix O: Namibia annual flood peak data

WEST FLOWING RIVERS																	
River & station Area km ²	Tsauchab Sesriem		Nausgomab Changns		Westende		Katros Tweespruit		Gaub Greyings		Kuiseb Schlesian Tower						
	Month	Peak (m ³ /s)	Month	Peak (m ³ /s)	Month	Peak (m ³ /s)	Month	Peak (m ³ /s)	Month	Peak (m ³ /s)	Year	Month	Peak (m ³ /s)	Year	Month	Peak (m ³ /s)	
	1480		690		17.3		81.6		2490		6530						
1975	Feb	1.5										1962	Mar	0	1996	Jan	16.2
1976		0										1963	Jan	841.4	1997	Jan	230.2
1977	Mar	13.5										1964		0	1998		0
1978		0	Mar	71.3	Mar	8.5						1965	Apr	308.9	1999	Jan	22.8
1979		0	Jan	69.3	Feb	0.2						1966	Apr	168.8	2000	Feb	150.2
1980	Mar	151.6	Feb	2.1	Mar	1.6						1967	Mar	456	2001	Apr	159.4
1981	Apr	29.4		0	Dec	1.4						1968	Nov	20.6	2002	Apr	117.9
1982	Jan	222.2		0	Mar	0.3						1969	Mar	71.4	2003	Apr	113.4
1983	Apr	75.8	Jan	20.1	Dec	0.2						1970	Mar	122.1	2004	Jan	56.7
1984	Jan	30.7	Apr	29.9	Dec	2.4						1971	Feb	98.7	2005		0
1985	Feb	69.6	Feb	139.9	Feb	10.9						1972		0	2006	Feb	367.2
1986	Mar	118.8	Jan	21.8	Jan	7.5						1973	Mar	218.8	2007	Jan	150
1987		0	Apr	6.5	Oct	23.4						1974	Feb	396.6	2008		0
1988		0	Apr	30.4		0						1975	Mar	133.9			
1989	Jan	5	Feb	111.4	Feb	25.8						1976	Jan	133.9			
1990	Feb	48.3	Mar	18.2	Jan	0.8						1977	Mar	267.3			
1991	Mar	64.9		0	Jan	1.9						1978	Feb	71.5			
1992	Jan	33.5	Nov	76.4		0						1979	Jan	73			
1993	Jan	360.2	Feb	58.3	Mar	0.9						1980	Nov	8.9			
1994	Mar	36.2	Jan	44.2		0						1981	Mar	73			
1995	Mar	11.2	Feb	92		0						1982	Mar	1.8			
1996	Mar	204.4	Jan	1.9	Jan	1						1983	Jan	0.5			
1997	Apr	17.2	Feb	121.9	Jan	17.9						1984	Mar	58.1			
1998	Apr	33.1	Dec	30		0						1985	Feb	123.6			
1999		0	Feb	26.8		0						1986	Feb	151.3			
2000	Feb	6.1	Apr	14.6		0						1987	Feb	29.1			
2001		0	Apr	17.5		0						1988	Apr	138.7			
2002	Feb	17.4	Feb	101		0						1989	Feb	175.9			
2003		0	Feb	6.2		0						1990	Feb	121.4			
2004			Jan	1.7	Jan	0.1						1991	Jan	13.2			
2005			Mar	80.7		0						1992	Nov	16.2			
2006			Mar	0.7		0						1993	Apr	92.6			
2007				0		0						1994	Jan	111.7			
2008			Mar	11.5								1995	Mar	52.5			

Appendix O: Namibia annual flood peak data

River & station	NORTH-NORTHWEST FLOWING RIVERS												
	Ondova Mimi mahoro Area km ² 117		Omuhonga Ombuku 1620		Hoanib Sesfontein 11000		AbaHuab Rooiberg 1570		Huab Vrede 10600		Kunene Ruacana 89500		
Year	Month	Peak (m ³ /s)	Month	Peak (m ³ /s)	Month	Peak (m ³ /s)	Month	Peak (m ³ /s)	Month	Peak (m ³ /s)	Year	Month	Peak (m ³ /s)
1975											1962	Jan	1028.2
1976											1963	Mar	1524.2
1977											1964	Apr	416.3
1978											1965	Mar	1386.4
1979											1966	Apr	585.7
1980	Feb	90.3	Mar	189.7	Mar	104.5	Mar	38.7	Mar	23	1967	Apr	418.6
1981	Apr	9.5	Mar	74.6	Mar	176.5	Mar	0	May	0	1968	Jan	1396.7
1982	Jan	3.6	Mar	232.5	Mar	523.7	Apr	70.6	Jun	0	1969	Mar	1269.5
1983	Feb	0	Feb	0	Mar	53.6	Jan	258.8	Mar	0	1970	Mar	1227
1984	Mar	246	Apr	146.9	Mar	308.7	Apr	48	Mar	0	1971	Mar	483.1
1985	Feb	0	Dec	28.1	Mar	61.1	Mar	89.6	Feb	0.4	1972	Apr	151.3
1986	Feb	0	Oct	106.2	Jan	85.5	Jan	68	Mar	1.3	1973	Apr	418.6
1987	Mar	0	Mar	12.8	Feb	27.4	Mar	175.9	Mar	7.2	1974	Apr	681.7
1988	Apr	3.6	Jan	35.1	Jan	39.9	Jan	110.7	Jan	2.3	1975	Apr	198
1989	Jan	30.9	Jan	39.5	Dec	281.8	Dec	66.7	Mar	0	1976	Apr	319.5
1990	Jan	87.5	Jan	31	Feb	85.5	Feb	125.4	Jul	0	1977	Apr	555.7
1991	Mar	10.7	Dec	24.5	Mar	185.6	Feb	91.1	Jul	0	1978	May	303.3
1992	Jun	0	Dec	60.5	Dec	3.2	Sep	1	Jun	0	1979	Mar	1383.1
1993	May	0	Mar	16	Mar	87.5	Apr	50.2	May	0			
1994	Dec	63.6	Feb	457.4	Feb	248.2	Dec	88.2	Apr	0			
1995	Mar	39.7	Apr	13.4	Feb	747.7	Apr	120.4	Apr	0.2			
1996	Mar	0	Mar	12.8	Jan	28.1	Jan	0	Mar	0			
1997	Feb	0	Mar	139.6	Mar	366.6	Mar	158.8	Mar	0.1			
1998	Dec	102	Jan	161.2	Dec	202.1	Dec	24.3	Apr	0			
1999	Feb	41.9	Feb	275.6	Jan	85.5	Feb	10.4	Jun	0			
2000	Mar	52.7	Apr	0	Mar	338.6	Jan	18.8	Aug	0			
2001	Apr	46.4	Mar	81	Mar	111.8	Mar	87.8	Mar	22.4			
2002	Mar	0	May	0	Feb	228.7	Mar	179.5	Mar	198.4			
2003	Apr	23	Apr	100	Jan	4	Jan	0	Apr	12.3			
2004	Feb	8.1	Mar	74.4	Feb	199.4	Apr	13.3	Feb	1.3			
2005	Feb	33			Mar	183.1	Feb	0	Mar	22.7			
2006	Mar	30.7			Jan	49	Mar	146.9	Mar	184.8			
2007	Dec	0			Feb	13.5	Apr	34.2					
2008					Feb	299.9	Mar	123					
2009							Feb	289.6					
2010							Jan	20.5					

Appendix P: Partial Duration Time Series

